Potential of Lactic Acid Bacteria in Antibacterial Therapy

A Thesis

Submitted in Partial Fulfillment of the Requirements for the Degree of

DOCTOR OF PHILOSOPHY

by

SANDIPAN MUKHERJEE

Department of Biosciences and Bioengineering
Indian Institute of Technology Guwahati
Guwahati-781039, Assam, India

March 2018

Potential of Lactic Acid Bacteria in Antibacterial Therapy

A Thesis

Submitted in Partial Fulfillment of the Requirements for the Degree of

DOCTOR OF PHILOSOPHY

by

SANDIPAN MUKHERJEE

Department of Biosciences and Bioengineering
Indian Institute of Technology Guwahati
Guwahati-781039, Assam, India

March 2018

ॐ असतो मा सद्गमय ।

तमसो मा ज्योतिर्गमय ।

मृत्योर्मा अमृतं गमय ।

ॐ शान्तिः शान्तिः शान्तिः ॥

Bṛhadāraṇyakopaniṣat 1.3.28

From untruth lead us to Truth.

From darkness lead us to Light.

From death lead us to Immortality.

Peace, Peace, Peace.

Brihadaranyaka Upanishad, 1.3.28

INDIAN INSTITUTE OF TECHNOLOGY GUWAHATI

DEPARTMENT OF BIOSCIENCES AND BIOENGINEERING

STATEMENT

I do hereby declare that the research findings of this thesis is the result of research work carried out by me in the Department of Biosciences and Bioengineering, Indian Institute of Technology Guwahati, Guwahati, India, under the supervision of Professor Aiyagari Ramesh.

As per the general norms of reporting research findings, due acknowledgements have been made, wherever the research findings of other researchers have been cited in this thesis.

Date: **Sandipan Mukherjee**

INDIAN INSTITUTE OF TECHNOLOGY GUWAHATI

DEPARTMENT OF BIOSCIENCES AND BIOENGINEERING

CERTIFICATE

It is certified that the work described in this thesis entitled "***Potential of Lactic Acid Bacteria in Antibacterial Therapy***" by Mr. Sandipan Mukherjee for the award of degree of Doctor of Philosophy is an authentic record of the results obtained from the research work carried out under my supervision in the Department of Biosciences and Bioengineering, Indian Institute of Technology Guwahati, India, and this work has not been submitted elsewhere for the award of any other degree.

CERTIFIED

Sandipan Mukherjee

(Candidate)

Roll No: 126106018

Aiyagari Ramesh, Ph.D.

(Thesis Supervisor)

Date:

ACKNOWLEDGEMENT

I would like to take this opportunity to offer my heartfelt gratitude to my family members and teachers who have made my journey all the more worthwhile.

First and foremost, I would like to acknowledge the pivotal role played by my PhD thesis supervisor, Professor Aiyagari Ramesh in my PhD tenure. I am grateful to have spent my formative years in academics under such a learned person, who inculcated in me an appreciation of science and a unique outlook towards research. The association with Prof. Aiyagari Ramesh has been inspiring; motivating me to scale critical issues during my PhD thesis work. Amongst his various features, his dedication towards the subject and tremendous breadth of knowledge stand out as commendable qualities. Furthermore, his inimitable support, moral guidance and steadfast resolve has helped me in completing this work. Most importantly, his enduring compassion and empathy throughout my stay at IIT Guwahati has enabled my growth as a student of science and as a person.

I am grateful to my doctoral committee members, Professor Kannan Pakshirajan, Professor Gurvinder Kaur Saini and Dr. Bhubaneswar Mandal for their insightful suggestions and motivation, which has led to an improvement in the quality of my research work.

I would like to acknowledge Professor Gopal Das, Department of Chemistry, for giving me an opportunity to learn the fundamentals of the interfacial science. Under his tutelage, I acquired a different perspective to resolve problems pertaining to my PhD. I owe him my sincere gratitude for his insights, patience and never-ending kindness, which has made my stay at IIT Guwahati all the more meaningful.

My sincere gratitude goes towards Professor Kannan Pakshirajan, Head of the Department of Biosciences and Bioengineering, IIT Guwahati, and Professor V.V. Dasu and Professor Arun Goyal, Former Heads of the Department Biosciences and Bioengineering, IIT Guwahati for providing me the necessary facilities that helped me to pursue my research at IIT Guwahati.

I am grateful to Professor Siddhartha Sankar Ghosh, Professor Pranab Goswami, Professor Lingaraj Sahoo and Dr. Biplab Bose for providing a state-of-the-art facility and an academic environment which enabled me to develop my skills and complete my Ph.D. work.

I am also grateful to all faculty members and staff of the Department of Biosciences and Bioengineering for supporting me throughout the Ph.D. tenure. I would like to thank Department of Biosciences and Bioengineering for providing infrastructural facility for my research work. I would also like to thank Central Instruments Facility (CIF) of IIT Guwahati for providing ambient atmosphere of research and high-end equipments to execute my experiments. I would also like to

acknowledge Department of Chemistry and Centre of Nanotechnology, IIT Guwahati for providing high-end equipment for my experiments.

I acknowledge the state-of-art facility at the Center for Excellence under the aegis of Program Support Grant provided by Department of Biotechnology (DBT), Government of India. I am grateful to Department of Biotechnology (DBT) and Science and Engineering Board (SERB), Department of Science & Technology (DST) for supporting my research through grants. I am also grateful to Ministry of Human Resource Department (MHRD) and IIT Guwahati for providing research fellowship.

I would like to extend sincere gratitude to Dr. Chirantan Kar, Dr. Barun Kumar Dutta and Dr. Abhijit Gogoi, Department of Chemistry, IIT Guwahati for the scientific collaboration.

I would like to acknowledge my B. Tech thesis supervisor Dr. Arun Kumar Maity, Department of Biotechnology, Haldia Institute of Technology for providing me an opportunity to explore the field of microbiology, which was an initial glimpse for me into this subject. Further, I sincerely thank Prof. Nandan Bhattacharyya, Department of Biotechnology, Haldia Institute of Technology for his constant support and encouragement.

I would also like to acknowledge my school teachers, Dr. Kajol Gupta, Dr. Kotikalpudi Sharada and Dr. Sandip Sen for their dedication towards teaching, which served as a primer for my curiosity and in-turn helped me to develop an inclination towards science at school level.

I am indebted to Dr. Atul Kumar Singh, for his contribution and motivation which enabled the realization of this thesis. It has been my privilege to have worked with my seniors, Dr. Manab Deb Adhikari, Dr. Sudeep Goswami and Dr. Thiyagarajan Durairaj. It is my pleasure to thank my current lab members Poulomi, Priya, Basu, Barlina, Narahari and Shrihari. I am also thankful to my former lab members Umakanth, Pallavi, Vidushi, Rajanikant, Preeti, Tabassum, Nikhil, Tushar, Abhay and Suraj for their support during my PhD tenure.

I also wish to thank my departmental seniors, Dr. Pallab Sanpui, Dr. Aditi Bannerjee, Dr. Asim Bikash Das, Dr. Kohila Vellaichamy, Dr. Vinod Yata, Dr. Amit Jaiswal, Dr. Sagarika Mishra and Dr. Amaresh Sahoo. I would also like to acknowledge Mr. Bablu Das, for all the elevating discussions and knowledge he has passed on to me.

I stand grateful and indebted to Dr. (Prof.) Rupa Vedantam, Department of Ear, Nose and Throat, Christian Medical Hospital and College. Her tenacity, grace and kindness has enabled me to surmount difficult challenges and continues to inspire me.

I wish to thank my friends, Dr. Mohitosh Dey, Shiv, Payel, Nilanjan, Manishekhar, Mahesh, Ziauddin, Ashif, Rwivoo, Bandhan, Babina, Upashi, Bibhas, Dooradarshi, Rana, Poulami, Angkana, Sanjeev, Subbi, Amarto, Sujoy, Subhodeep,

Soumita, Anand, Sreya, Sayan, Joyobroto, Anubhav, Basundhara, Avichal, Rajarshi, Anamika, Poulomi, Shayan, Suvodeep and Gourav, for having enriched me as a person.

Lastly, and also most importantly, I am extremely grateful to my parents, Mrs. Samata Mukherjee and Mr. Ashim Kumar Mukherjee. They have filled my life with their love and blessings. I am also thankful to my brother and sister-in-law, Mr. Arindam Mukherjee and Mrs. Sanhita Mukherjee for their unconditional love and affection during the course of my education at every level.

Sandipan Mukherjee

CONTENTS

ABBREVIATIONS

µg	Microgram
µL	Microliter
µM	Micromolar
A_{600}	Absorbance at 600 nm
AMPs	Antimicrobial peptides
ANOVA	Analysis of variance
AU	Arbitrary unit
BHI	Brain-heart infusion broth
BLAST	Basic local alignment search tool
bp	Base pair
bsh	Bile salt hydrolase gene
BSH	Bile salt hydrolase enzyme
CDRA	*Dahi* isolate
cFDA-SE	5(and 6)-carboxyfluorescein diacetate succinimidyl ester
CFU	Colony forming unit
cps	Counts per second
CR	Congo red
CRA	Salt-fermented cucumber isolate
CV	Crystal violet
DF	Dried fish isolate
$DiSC_35$	3,3′-dipropylthiadicarbocyanine iodide
DLS	Dynamic light scattering
DMEM	Dulbecco's modified eagles medium
DMSO	Dimethyl sulfoxide
DNA	Deoxyribonucleic acid
dNTP	Deoxynucleoside triphosphate
ECM	Extracellular matrix
EE	Encapsulation efficiency
ELISA	Enzyme-linked immunosorbent assay
e_m	Maximum number of adhered bacteria
FBS	Fetal bovine serum
FCM	Flow cytometry
FDA	Food and Drug Administration

Abbreviations

FESEM	Field emission scanning electron microscope
FSC	Forward-angle light scatter
GI	Gastrointestinal
GIT	Gastrointestinal tract
GRAS	Generally Regarded As Safe
HCA	Hierarchical cluster analysis
HEK	Human embryonic Kidney
HEPES	N-2-Hydroxyethyl Piperazine N-2 Ethane Sulphonic acid
HNPs	Human serum albumin (HSA)-based nanoparticles
HSA	Human serum albumin
K_a	Association constant
k_d	Dissociation constant
kDA	Kilo Dalton
LAB	Lactic acid bacteria
LC	Loading capacity
LPS	Lipopolysaccharide
MBC	Minimum bactericidal concentration
MIC	Minimum inhibitory concentration
mL	Milliliter
mM	Millimolar
MRS	de Man, Rogosa and Sharpe
MRSA	Methicillin resistant *Staphylococcus aureus*
MSCRAMMs	Microbial surface component recognizing adhesive matrix molecules
MTCC	Microbial Type Culture Collection, Institute of Microbial Technology (IMTECH), Chandigarh, India
MTT	3-(4,5-Dimethylthylthiazol-2-yl)-2,5-diphenyltetrazolium bromide
MWCO	Molecular weight cut-off
NCIM	National Collection of Industrial Microorganism, National Chemical Laboratory (NCL), Pune, India
NK	Not known
nm	Nanometer
NPs	Nanoparticles
NRRL	Northern Regional Research Laboratory, Peoria, IL, USA
OD_{600}	Optical density at 600 nm
PBS	Phosphate buffered saline
PCA	Principal component analysis
PI	Propidium iodide
rpm	Revolutions per minute

Abbreviations

SD	Standard deviation
SEM	Scanning electron microscope
SGF	Simulated gastric fluid
SIF	Simulated intestinal fluid
SSC	Side scatter
TAMRA-SE	5-carboxy-tetramethylrhodamine N-succinimidyl ester
λ_{Em}	Emission wavelength
λ_{Ex}	Excitation wavelength

भारतीय प्रौद्योगिकी संस्थान गुवाहाटी
Indian Institute of Technology Guwahati

LIST OF TABLES

List of Tables

LIST OF FIGURES

CHAPTER 1 **Page No.**

Nil

CHAPTER 2

CHAPTER 3

Chapter 1

Introduction and Literature Review

Introduction and Literature Review

Introduction

The emergence of drug-resistant pathogenic bacteria fueled by indiscriminate use of antibiotics has led to the rise of one of the critical challenges in modern healthcare regime. This fact coupled with a depleting armory of therapeutic antibiotics has escalated the challenge associated with the mitigation of several life-threatening bacterial infections. Since antibiotics have a broad spectrum of activity, their excessive use has led to the evolution and dissemination of antibiotic resistance in pathogens. Furthermore, the broad-spectrum nature of conventional antibiotics has been observed to cause severe collateral damage to the human commensal gut microbiota. This fact has led to the need to develop alternate therapeutic antibacterial agents, which are remarkably different from conventional antibiotics. In this regard, bacteriocins from lactic acid bacteria may constitute a viable alternative towards targeted mitigation of pathogens.

Lactic acid bacteria (LAB) constitute a group of beneficial microbes, which hold a GRAS status (Generally Regarded As Safe), have a long history of extensive and safe use in food systems for human consumption and are promising candidates for bacteria-based therapy. LAB are widely acknowledged as probiotics that impart significant benefits to the host, such as improved nutrition and microbiome function of the gut, primarily through their ability to colonize the gut and exclude pathogens and through immunomodulation. Probiotic LAB can render an inherent favourable safety profile in conjunction with an ability to tolerate bile, gastric and intestinal fluids as well as bind to extracellular matrix (ECM) and gut cells. As a consequence, probiotic LAB can persist in the intestinal environment and thus prevent pathogen colonization. LAB are also known to elaborate bacteriocins, which are natural secreted antimicrobial peptides (AMPs) that hold considerable merit as alternatives to conventional antibiotics. In contrast to antibiotics, LAB bacteriocins represent promising therapeutics, given their restricted activity spectra against specific Gram-positive pathogenic bacteria and thus ensure minimal collateral damage to human commensal microbiota, which in turn is anticipated to curtail the threat of infections by opportunistic pathogens. Bacteriocins display potent activity on key targets such as the bacterial membrane and are expected to flout resistance development in target strains.

Bacteriocins from LAB have been shown to be effective against various bacterial pathogens such as *Listeria monocytogenes*, *Staphylococcus aureus*, *Enterococcus faecalis* and *Clostridium difficile*. Apart from their conventional food applications, there is a vast and unexplored healthcare potential of LAB and their secreted metabolites such as bacteriocins, which remains to be harnessed. The FDA approved bacteriocin nisin is being explored in preclinical trials against vancomycin-resistant Enterococci (VRE). The exciting prospect of exploring probiotic LAB and their secreted bacteriocins as new prophylactic or therapeutic agents against human pathogens has received impetus with emerging reports that demonstrate their potential in either bacteria-based therapy or antibacterial-based mitigation of gastro-intestinal pathogens. To harness the true potential of LAB and their bacteriocins as antibacterial therapeutics, it is imperative to identify candidate probiotic LAB strains and develop judicious delivery systems that would be biocompatible, render stability and provide the bacteriocin in a bioactive form.

The proposed research project is essentially based on the above-mentioned rationale. The initial endeavor would be to identify promising probiotic native LAB strains that display tolerance to bile salts, gastric and intestinal fluids, demonstrate significant adhesion potential onto ECM and cultured model intestinal cells and can prevent pathogen adhesion. A major emphasis in the study would be on the generation of a non-toxic proteinaceous nanocarrier loaded with bacteriocins from LAB and test its potential against pathogenic bacteria. In essence, the proposed research project aims to demonstrate the potential and merit of the GRAS microbe LAB in bacteria-based prophylactic approaches to prevent pathogen colonization as well as develop safe and novel antibacterial nanocomposites using LAB secreted bacteriocins as an antibacterial payload. In the age of unbridled antibiotic-resistance and at a time when several therapeutic antibiotics are rendered ineffective against life-threatening infections, this study, which strives to generate potent therapeutic antibacterial agents, addresses a very important and contemporary global healthcare problem. The following section provides a detailed literature review pertinent to the research area of the present investigation.

Literature Review

1.1. Lactic acid bacteria (LAB)

Lactic acid bacteria (LAB) are a group of Gram-positive bacteria, which are non-sporulating, non-respiring aerotolerant, either cocci or rods, and which produce lactic acid as one of the major end-products after fermentation of carbohydrates. LAB strains can belong to five classes of families namely *Aerococcaceae*, *Carnobacteriacea*, *Enterococcaceae*, *Lactobacillaceae*, *Leuconostocaceae* and *Streptococcaceae* (Holzapfel and Wood, 2014). LAB have the distinction of being generally regarded as safe (GRAS) microorganisms that have a significant role in food product development and fermentation processes (Kleerebezem *et al.*, 2017; Barbosa *et al.*, 2014; Gaggia *et al.*, 2011; Jimenez *et al.*, 2013; Delavenne *et al.*,, 2013; Coolbear *et al.*, 2008). The ability of LAB strains to produce antimicrobial peptides such as bacteriocins, which are antagonistic to food-borne pathogens is well documented (Hegarty *et al.*, 2016; Alvarez-Seiro *et al.*, 2016; O'Connor *et al.*, 2015). LAB are also designated as probiotic strains that can significantly influence the microbial composition and host metabolism and this tenet has led to a renewed interest in the healthcare potential of LAB (Ruggiero, 2014; Andermann *et al.*, 2016; Bischoff *et al.*, 2014; Ghosal *et al.*, 2016; Pamer, 2016).

Amongst various LAB, *Lactobacillus* occupies an important niche and bears significant technological, commercial and healthcare implications. Further, *Lactobacillus* is a heterogeneous group of more than 170 recognized LAB species possessing low G + C content, being facultative anaerobes and a catalase negative phenotype (Goldstein *et al.*, 2015; Salvetti *et al.*, 2012; Claesson *et al.*, 2007). *Lactobacillus* sp. continue to be used for the preservation of food products, considering their beneficial attributes such as facile production of organic acids, ability to synthesize bacteriocins and in general augmentation of food essence (Stiles, 1996). *Lactobacillus* are known to exist in diverse environments, such as dairy environments, mucosal surfaces in host habitats, as well as in plants and soil (Wood and Holzapfel, 1995; Mujagic *et al.*, 2017; van Baarlen *et al.*, 2013; Claesson *et al.*, 2009). Considering that *Lactobacillus* strains are uniquely positioned to lend a beneficial effect in the healthcare regime and serve the role of a probiotic, the following section elaborates the expanded definition of a probiotic.

1.2. Definition of probiotics

Probiotics is defined as "live microorganisms which when administered in adequate amounts confer a health benefit on the host" (FAO/WHO, 2002). This definition has been revisited by the International Scientific Association for Probiotics and Prebiotics in a consensus meeting, wherein the term probiotic has been defined as "live microorganisms that, when administered in adequate amounts, confer a health benefit on the host" (Hill *et al.*, 2014). The distinction between microbes and probiotics is deduced from this definition, as clear demonstration of health benefit is paramount in considering a microbe as a probiotic strain. In this context, countries such as Canada and Italy have a set of guidelines for claiming probiotics, such as, a minimum number of viable cells (1×10^9 CFU) administered per day, genetic characterization, history of safe use (Hill *et al.*, 2014). Further, these countries also expect probiotics to contribute a core benefit, which is towards supporting a healthy gut (Hill *et al.*, 2014). This tenet was tested in a meta-analysis, wherein it was found that, in general, probiotics lend a beneficial effect in the treatment of gastrointestinal infections and can also play a preventive role (Ritchie and Romanuk, 2012). To designate any strain as probiotic, FAO/WHO has given a set of *in vitro* screening tests to be conducted, after which the strains are considered for *in vivo* testing. The following sections describe the various *in vitro* tests as mandated by FAO/WHO.

1.3. Probiotic attributes

1.3.1. Bile acid resistance

In order to influence the gut microbiota, probiotic lactobacilli should be able to reach the colon in sufficiently viable numbers. One of the major roadblocks towards the viability of probiotic lactobacilli is the presence of bile acids in the descending part of the small intestine (Ruiz *et al.*, 2012). Under normal physiological conditions, bile acids concentration ranges from 0.05% to 2.0%, facilitating fat adsorption by the epithelial cells (Islam *et al.*, 2011). The bile acids possess detergent-like properties, leading to disruption of bacterial membranes, and this leads to bile functioning as a potent antimicrobial agent in the gut, profoundly shaping the microbial composition of the gut (Begley *et al.*, 2005; Islam *et al.*, 2011). Thus, bile tolerance forms one of the major cornerstones of probiotic virtues of *Lactobacillus* strains. In this context, it has been observed that bile-resistant strains can display tolerance to multiple factors implicated in inducing gastrointestinal stress (Margolles *et al.*, 2003). Some of the

mechanisms behind bile tolerance in probiotic lactobacilli is active efflux of bile acids, hydrolysis of bile salts, and changes in the composition of cell membranes (Bustos *et al.*, 2011; Kumar *et al*., 2006; Ruiz *et al*., 2007).

1.3.2. Bile salt hydrolase activity

One of the mechanisms behind bile tolerance in probiotic LAB is the hydrolysis of the amide bond, leading to de-conjugation of glycine and taurine in bile salts. This reaction is catalyzed by the bile salt hydrolase (BSH) enzyme that releases free amino acid and free bile acids (Begley *et al.*, 2006). BSHs belong to the choloylglycine hydrolase family of enzymes that also contains penicillin amidases (EC 3.5.1.11), enzymes that hydrolyse penicillin to yield 6-aminopenicillinic acid (6-APA) (Begley *et al.*, 2006; Patel *et al.*, 2010). Since BSHs can alleviate the deleterious effects of bile, a role for these enzymes in survival of probiotic LAB within the gastrointestinal tract is anticipated. In this context, BSH activity has been observed to be inducible in presence of bile, indicating that exposure to bile salt enriched environment is a prerequisite for expression of these enzyme (Duary *et al.*, 2012). Thus, it can be conceived that possession of such enzymes can increase the chances of survival and persistence in the gastrointestinal tract (Begley *et al.*, 2006; Ruiz *et al.*, 2012).

1.3.3. Resistance to gastric acidity

Another major obstruction in the gut is the presence of gastric fluids, having low pH and being rich in proteases, such as pepsin (Charteris *et al.*, 1998). These are acute stress factors and are known to negatively impact the viability of ingested probiotics (Liong and Shah, 2005). It has been observed that presence of acidic pH leads to a lowering of the intracellular pH, leading to a reduction in the transmembrane pH difference, which is an important factor in generating proton motive force (Corcoran *et al.*, 2005). Internal acidification also reduces the activity of acid-sensitive enzymes and results in damage to proteins and DNA (van de Guchte *et al.*, 2002). Thus, it is imperative that probiotic *Lactobacillus* demonstrate sufficient viability in the presence of gastric fluid to exert any beneficial effect in the gastrointestinal tract. In this context, it has been observed that the probiotic strain *Lactobacillus rhamnosus* GG can survive in an acidic niche in the presence of glucose, indicating the role of carbohydrates in tolerance to gastric niche (Charalampopoulos *et al.*, 2003).

1.3.4. Adhesion to mucus and epithelial cells

One of the critical probiotic attributes of LAB is the ability to adhere onto mucus proteins and epithelial cells, which form a major component in the gastrointestinal tract (Arena *et al.*, 2017). Further, it is universally acknowledged that adhesion of probiotic LAB is a prelude to persistence and sustained colonization in the gastric niche and is a pivotal mechanism behind its ability to exert beneficial effects on the host gut microflora (Rivera-Espinoza and Gallardo-Navarro, 2010; Arena *et al.*, 2017). Since a major thrust of the present thesis is on adhesion of *Lactobacillus* strains, a detailed discussion is provided in a subsequent section.

1.3.5. Antimicrobial activity against pathogenic bacteria

The antimicrobial activity of lactobacilli in inhibiting pathogenic bacteria is exerted through various mechanisms such as competitive utilization of a common substrate, reduction of pH in the vicinity through the production of organic acids or through expression of specific antibacterial molecules such as bacteriocins or hydrogen peroxide (Gänzle, 2009). The faster consumption of an important substrate by probiotic LAB reduces its bioavailability for growth of the pathogen, leading to its inhibition (O'Toole and Cooney, 2008). Further, the end-product of the carbohydrate metabolism in lactobacilli are composed of weak acids such as lactic acid or acetic acid. These organic acids render a lowering of the pH, leading to the inhibition of metabolism and growth of the pathogenic bacteria. Considering that a major portion of the present thesis is on application of bacteriocins to mitigate pathogenic bacteria, a detailed discussion is provided in a subsequent section.

1.3.6. Ability to reduce pathogen adhesion to surfaces

The potential of probiotic lactobacilli to inhibit adhesion of pathogenic bacteria onto surfaces, such as mucus and epithelial cells is an important probiotic attribute. The ability of probiotic LAB to inhibit pathogen adhesion is correlated with its own proclivity to form cellular auto-aggregates and adhering onto surfaces in high numbers with strong affinity (Kos *et al.*, 2003; Lee *et al.*, 2000). Further, prior adhesion of LAB cells is also anticipated to hinder the interaction of pathogen with mucus or receptors on epithelial cell. Additionally, intestinal injury renders exposure of basal extracellular matrix (ECM) proteins such as collagen and fibronectin, which can be an anchoring site for pathogen adhesion (Chagnot *et al.*, 2012; Foster *et al.*, 2014). Thus, it is imperative

that lactobacilli, which are anticipated to be endowed with probiotic virtues, should display potent adhesion inhibition of pathogenic bacteria on ECM molecules. In line with this tenet, bacteriocin production renders a competitive edge for colonization and clearance of pathogen in the gastric niche (Arena *et al.*, 2017). This fact has been highlighted in a seminal study wherein bacteriocin-producing *Lactobacillus salivarius* UCC 118 has been found to reduce *Listeria monocytogenes* infection in murine gut (Corr *et al.*, 2007). In the context of pathogen adhesion inhibition, it has been reported that *Lactobacillus acidophilus* is capable of producing a heat-stable small molecule, which reduced the transcription of the genes responsible for colonization and quorum sensing in *E. coli* (Medellin-Peña and Griffiths, 2009).

1.4. Models for determination of adhesion potential of probiotic LAB

The ability of probiotic LAB to beneficially impact human health is usually brought about by three main mechanisms (Lebeer *et al.*, 2010). First, the propensity of probiotic LAB to compete for binding sites in the gastric niche and thereby exclude pathogen colonization (Lebeer *et al.* 2008; Zhang *et al*, 2013). Second, augmentation of the intestinal barrier function by probiotic LAB through various mechanisms, such as production of extracellular proteins, enhancing tight junction functions, induction of defensin production, and protection against xenobiotics (Schlee *et al.*, 2008; Sańchez *et al.*, 2010; Jones *et al.*, 2015; Jariwala *et al.*, 2017). A third mechanism is through immunomodulation of the host immune responses, leading to upregulation of anti-inflammatory genes (Rieu *et al.*, 2014). In the context of probiotic LAB, the critical step is its interaction and adhesion onto host cells (Lievin-Le Moal and Servin, 2014; Nishiyama *et al.*, 2016). Thus, it is paramount to develop assays for quantitative determination of the adhesion potential of LAB strains onto host cells. An initial step towards estimation of adhesion of probiotic LAB onto host cells is screening the adhesion of a range of strains on *in vitro* models, which closely mimic the *in vivo* conditions. A few classical models for studying LAB adhesion are discussed in the following sections.

1.4.1. Adhesion on immobilized extracellular matrix model

The extracellular matrix (ECM) is a protein complex, whose primary function is to support and link the cells and tissues (Chagnot *et al.*, 2012). Further, ECM performs an important function as a platform for microbial adhesion and colonization

(Chagnot *et al.*, 2012). Probiotic LAB express proteins on the cell surface, such as adhesins, or S-layer proteins, which specifically interact with the domains of ECM (Lievin-Le Moal and Servin, 2014; Nishiyama *et al.*, 2016) The principal components of ECM are collagen, laminin and fibronectin, which are occasionally shed into the mucus from the epithelial cells (Chagnot *et al.*, 2012, Vélez *et al.*, 2007). An alarming fact associated with ECM is that damage to the mucosa is often a prelude to pathogen adhesion of ECM, subsequent colonization and infection (Brandl *et al.*, 2008; Petersson *et al.*, 2011). The ability of LAB to adhere to these ECM molecules and occlude the receptors can perhaps be exploited for targeted pathogen elimination (Pamer, 2016). In this regard, probiotic LAB has been found to adhere onto ECM components and their adhesive ability has been demonstrated to inhibit pathogen colonization on ECM proteins such as collagen (Prince *et al.*, 2012). The adhesion of probiotic LAB to mucin has also been probed in detail and reported to be pivotal in influencing pathogen colonization onto mucin (MacKenzie *et al.*, 2010; Zhang *et al.*, 2013; Arena *et al.*, 2017; Campana *et al.*, 2017; Celebioglu *et al.*, 2017). A representative list of models used for ascertaining adhesion of probiotic LAB on ECM has been provided in Table 1.1.

1.4.2. Adhesion o*n epithelial cell line model*

In vitro cell culture can be considered as close to realistic depiction of host-microbe interactions. In this context, human adenocarcinoma cell line (HT-29) and human colorectal adenocarcinoma cell line (Caco-2) have been extensively used to study host-LAB interactions (Brito *et al.*, 2013; Van Tassell and Miller, 2011; Celebioglu *et al.*, 2017). These models are also used to study the prospect of LAB in inhibiting the adhesion of pathogens as well as in maintain the tight junction function against the pathogen-induced damages (Walsham *et al.*, 2016, Zhang *et al.*, 2013; Jariwala *et al.*, 2017). For example, *Lactobacillus* strains were found to inhibit adhesion of enterotoxicogenic *E. coli* on polarized cells of porcine jejunal epithelial IPEC-J2 (Liu *et al.*, 2015). Interestingly, HT-29 cells treated with methotrexate were observed to differentiate into mucin-secreting goblet cells (called HT29-MTX cell line), which is considered to replicate the surface of mucus-producing goblet cells present in the gastric niche (González-Rodríguez *et al.*, 2012; Lukić *et al.*, 2012). This cell line has been pivotal in providing insights in the adhesion process of probiotic LAB onto host cells, as well as in attenuation of *Campylobacter jejuni* infection on exposure to

Table 1.1. Studies on the adhesion of LAB on ECM

Serial no.	ECM	Method for estimating adhesion	LAB strain	Reference
1.	Mucin	Plating on selective media	*Lactobacillus mucosae* LM *Lactobacillus plantarum* CIF17A2	Valeriano *et al.*, 2014 Buntin *et al.*, 2017
		Crystal violet staining	*Lactococcus lactis* BGKP1 *Lactobacillus casei* BL23 *L. plantarum* 299v	Lukić *et al.*, 2012 Munoz-Provencio *et al.*, 2009
		Fluorescence labelling	*L. acidophilus* NCFM	Celebioglu *et al.*, 2017
		Radiolabeling	*L. rhamnosus* GG	von Ossoswski *et al.*, 2010
2.	Collagen	Plating on selective media	*L. plantarum* Lp5276	Yadav *et al.*, 2013
		Crystal violet staining	*L. plantarum* 299v *L. casei* BL23	Muňoz-Provencio *et al.*, 2011
3.	Fibronectin	Crystal violet staining	*L. casei* BL23 *L. plantarum* Lp5276	Muňoz-Provencio *et al.*, 2011; Yadav *et al.*, 2015

probiotic LAB (Lukić *et al.*, 2012; Alemka *et al.*, 2010). A representative list of models used for ascertaining adhesion of probiotic LAB in cell culture has been provided in Table 1.2.

1.4.3. Adhesion in animal model

Animal models offer an immense scope to probe host-microbe interactions over the entire landscape of gastrointestinal tract (GIT). In this regard, germ-free mice or gnotobiotic mice have played a vital role in revealing the fundamentals of bacterial adhesion and subsequent colonization of the GIT (Verdú *et al.*, 2009; Jones *et al.*, 2015). Several seminal articles report the pivotal role played by probiotic LAB in augmenting intestinal host defense, displaying immune-modulatory effects, attenuating antibiotic-caused hypersensitivity, and reducing pro-inflammatory signals in gastrointestinal tract in mouse model (Verdú *et al.*, 2006, Choi, 2011, Lin *et al.*, 2008,

Table 1.2. Studies on the adhesion of LAB in cell culture model

Serial no.	Cell culture model	Method for estimation	Bacterial strain tested	Reference
1.	Caco-2 cells	Plating method	*L. rhamnosus* GG	Deepika *et al.*, 2012
			L. salivarius W24	Deepika *et al.*, 2009
			L. casei W56	Campana *et al.*, 2017
			L. acidophilus W37	Calasso *et al.*, 2013
			L. plantarum W21	
		Fluorescence labelling	*Bifidobacterium bifidum* S17	Grimm *et al.*, 2014
2.	HT-29 cells	Plating method	*L. plantarum* NCDO 5276	Yadav *et al.*, 2013
			Pediococcus pentosaceus 9.1	Turpin *et al.*, 2012
			Pediococcus acidilactici 12.6	
		Fluorescence labelling	*L. acidophilus* NCFM	Celebioglu *et al.*, 2017
3.	HT 29-MTX cells	Plating method	*L. plantarum* 5.8	Turpin *et al.*, 2012
			L. lactis BGKP1	Lukić *et al.*, 2012

Natividad *et al.*, 2012; van Beek *et al.*, 2016). Other models such as *Caenorhabditis elegans*, drosophila and zebrafish have also been utilized to reveal the beneficial effects imparted by the presence of probiotic LAB in gastrointestinal tract (Kim and Mylonakis, 2012; Jones *et al.*, 2015; Rieu *et al.*, 2014).

1.5. Methods to estimate adhesion of LAB

Considering that the adhesion of LAB is a pivotal step in subsequent colonization, it is necessary to be able to measure the amount of the bacterial load on the host tissue. In this regard, various quantitative methods have been used. They are discussed as follows:

1.5.1. Plating method

One of the earliest methods to study adhesion has been plating of the bacteria on agar containing selective growth medium (Vesterlund *et al.*, 2005). In this process, the principal steps involve separation of adhered bacteria in *in vitro* cell culture model,

followed by serial dilution in sterile PBS and plating in selective media. It may also be mentioned here that plating is often the preferred method to ascertain the number of colonizing LAB in *in vivo* experiments (involving either mice, rabbit or human subjects) as the method is sensitive and does not entail any modification of the bacterial physiology, genetics or metabolism (Grimm *et al.*, 2014; Jones *et al.*, 2015; Bendali *et al.*, 2011). However, the method can be cumbersome in nature and necessitates the use of specific media for growth of probiotic LAB.

1.5.2. Radiolabelling

In this method, radioactive thymidine is added to metabolically active bacteria and incubated for a certain period of time (Vesterlund *et al.*, 2005). For example, *L. rhamnosus* GG, the standard probiotic, was radiolabeled using radioactive thymidine and subsequently subjected to adhesion experiments on isolated mucus (von Ossoswski *et al.*, 2010). With the advent of non-radioactive tools for estimating adhesion, the use of radiolabelled LAB cells prior to adhesion assays is on the decline.

1.5.3. Bacterial cell staining

In this method, the LAB cells are allowed to adhere onto ECM coated well, followed by removal of non-adhered and weakly adhered cells and subsequent staining with crystal violet. Subsequently, the stain bound to the adhered bacterial cells is released by incubating in citrate buffer and the released stain is quantified spectrophotometrically to acquire a measure of the adhered cells (Munoz-Provencio *et al.*, 2009). Although this method is easy to perform, it is not used to study adhesion of probiotic LAB onto mammalian cells.

1.5.4. Fluorescence-based method

In recent times, labelling of probiotic LAB either using fluorochromes, or through expression of a fluorescent protein has led to a deeper insight in the field of bacteria-host interactions (Grimm *et al.*, 2014; Rieu *et al.*, 2014; Jones *et al.*, 2015). For labelling of with a fluorochrome, cFDA-SE or TAMRA-SE is incubated with LAB cells prior to performing an adhesion assay (Fuller *et al.*, 2000). Expression of a fluorescent protein in bacteria is an attractive option and it has been leveraged to study the host-bacteria interaction at the transcriptional level (Coombes and Robey, 2010, Bumann and Valdivia, 2007). Fluorescent labelling of LAB also allows the

visualization of host-adhered bacteria and thereby provides an insight with regard to the spatial distribution of the bacteria on the host cell (Grimm *et al.*, 2014).

1.6. Implications of antibiotic usage on the beneficial gut microflora

It has been estimated that antibiotics are consumed by ~ 3% of patients in developed countries to alleviate symptoms associated with infectious diseases (Costello *et al.*, 2012). However, the spread of antibiotic resistance gene amongst the pathogenic bacteria and a concomitant decline in antibacterial agents is of great concern in the healthcare regime. In recent times, the eradication of the beneficial microflora due to the consumption of antibiotics has come to focus (Schulfer and Blaser, 2016; Blaser, 2016; Looft and Allen, 2012). The human gut microbiome is composed of a variety of microorganisms, which interact with each other and with the host cells, leading to expression of host genes, production of metabolites and modulation of the host immune system, in a local as well as systemic range (Blaser, 2016). Use of antibiotic has been reported to alter the microbial composition in the gastrointestinal niche, leading to an abrogation of susceptible microorganisms and proliferation of antibiotic-resistant pathogenic bacteria (Pham and Lawley, 2014; Langdon *et al.*, 2016; Browne, 2016). Further, it has also been reported that using antibiotics in children leads to a shift in the gut microbiota over an extended period, which is causally related to an increased risk for metabolic and immunological diseases (Schulfer and Blaser, 2016; Korpela *et al.*, 2016). The shift includes a change in the population of various microbial species such as in Actinobacteria, Bacteroidetes and Proteobacteria, as well as a decrease in bile-salt hydrolase-producing microbes and an increase in macrolide resistance. Further, the ramifications of antibiotic-mediated perturbation of gut microbiota or a dysbiosis-like condition often entails repeated cycles of infection, chronic medication and prolonged care (Lawley *et al.*, 2012).

Development of an antibacterial therapy, which encompasses selective elimination of gastrointestinal pathogenic bacteria may serve as better for reduction in the development of antimicrobial resistance. In this regard, some of therapeutic approaches include the use of natural products, antimicrobial peptides, antibacterial polypharmacology entailing multiple targeting of pathogenic sites, small molecules as antibiotic adjuvants and using a bacteria-based approach to selectively target pathogenic strains and expel them from host system (Maxson and Mitchell, 2016, Defoirdt, 2013, Hancock *et al.*, 2012, Kalan and Wright, 2011, Hwang *et al.*, 2016,

Brötz-Oesterhelt and Brunner, 2008, Butler *et al.*, 2014, Fernebro, 2011). Amongst the above possibilities, the use of selective commensal microbes to combat pathogenic strains may serve as an attractive option (Lemon *et al.*, 2012, Fischbach *et al.*, 2013). In this context, the potential of probiotic LAB has recently come into the forefront for mitigation of gastrointestinal pathogenic bacteria (Pamer, 2016; Andermann *et al.*, 2016). To this end, the following section describes the healthcare potential of probiotic LAB as a whole-cell approach in mitigating gastrointestinal pathogenic bacteria.

1.7. Probiotic LAB as a whole-cell approach to mitigate gastrointestinal pathogens

A serious disadvantage with antibiotics is the collateral damage to the beneficial microflora, and the concomitant proliferation and invasion of the gastric niche by antibiotic-resistant pathogenic bacteria. In this regard, targeting the key step of pathogenesis, which is, adhesion of pathogenic bacteria onto gastrointestinal cells, may be conceived as a safe antibacterial therapy (Chagnot *et al.*, 2012; Foster *et al.*, 2014; Prince *et al.*, 2012; Krachler and Orth, 2013). Deploying probiotic LAB to counter adhesion of pathogenic bacteria is a viable option considering the seminal literature reports on probiotic LAB, which provide compelling evidence of their beneficial impact on human intestinal function (Vitetta *et al.*, 2014; Haleja *et al.*, 2012; Salminen *et al.*, 2010; Buffie and Pamer, 2013; Gutierrez-Castrellon *et al.*, 2014; Lievin-Le Moal and Servin, 2014). It may be mentioned here that damage to the intestinal mucosa leads to the exposure of ECM, which allows pathogen adhesion and subsequent bloodstream infections (Chagnot *et al.*, 2012; Brandl *et al.*, 2008; Singh *et al.*, 2012b). Thus, the propensity of probiotic LAB to prevent pathogen adhesion onto ECM molecules is a critical property for mitigating gastrointestinal pathogenic bacteria (Lebeer *et al.*, 2010; Reid *et al.*, 2011). In line with this tenet, a study reported that application of *Lactobacillus ruminis* ATCC 25644 led to a competitive inhibition of *Yersinia enterocolitica* and enterotoxicogenic *E. coli* on fibronectin and collagen-coated wells (Yu *et al.*, 2017). In a separate study, the inhibition of adhesion of *Staphylococcus aureus* or *E. coli* O157:H7 onto collagen-coated wells was correlated with the ability of *Lactobacillus* strains to aggregate and adhere onto collagen molecules (Miljkovic *et al.*, 2015). Likewise, the higher affinity of *Lactobacillus fermentum* to mucin molecules has been found to be the key for preventing *E. coli* adhesion onto mucin-coated wells (Chatterjee *et al.*, 2017). The source of LAB isolation may also play a role, as reported

in a study wherein *L. plantarum* isolated from infant feces was found to cause higher adhesion inhibition of *E. coli* O157:H7 on mucin molecules (Buntin *et al.*, 2017). In a separate study, the higher number of pili in *L. rhamnosus* GG has been reported to be pivotal in preventing the adhesion of *Enterococcus faecium* onto intestinal mucus (Tytgat *et al.*, 2016).

The ability of probiotic LAB cells to counter gastrointestinal pathogen adhesion onto intestinal cells is a key beneficial attribute of probiotic LAB. It has been reported that *L. reuteri* and *L. salivarius* strains expressing S-layer protein could render higher inhibition of *E. coli* K88 and *Salmonella enteritidis* 50335 adhesion onto Caco-2 cells (Zhang *et al.*, 2013). In a separate study, the efficiency of *L. rhamnosus* W71 to inhibit *L. monocytogenes* adhesion in exclusion mode and competition mode on Caco-2 cell line has been correlated with the ability of LAB cells to co-aggregate with gastrointestinal pathogens (Campana *et al.*, 2017). In that same study, *L. salivarius* W24 demonstrated adhesion inhibition only in exclusion mode, implying that there were more than one mechanism behind prevention of pathogen adhesion on cultured cells (Campana *et al.*, 2017). Separately, the propensity of *L. acidophilus* to produce small molecules that inhibit adhesion of enterohaemorrhagic *E. coli* was considered as the basis for preventing the adhesion of *E. coli* cells on cultured Caco-2 cells (Tabasco *et al.*, 2014). In a separate study, the higher number of adhered cells of *L. plantarum* AS1 led to a decline in the number of *Vibrio parahaemolyticus* adhering onto HT-29 cells (Kumar *et al.*, 2011). Further, in another study, the auto-aggregation efficacy of *L. plantarum* Tennozu-SU2 was correlated with a higher adhesion inhibition of *Salmonella typhimurium* onto HT-29 cells (Hirano *et al.*, 2016). A representative list of additional examples that demonstrate the ability of LAB strains in mitigation of pathogen adhesion in cell culture models is provided in Table 1.3.

The potential of probiotic LAB to impede pathogen adhesion onto host cells has been reported to thwart biofilm formation by the pathogen in the intestinal lumen (Woo and Ahn, 2013). In a separate investigation, it was observed that the prevalence of large numbers of *Lactobacillus* cells in mice gut could support colonization by the commensal strain *Lactobacillus reuteri* and reduce invasion by *Salmonella enterica* cells (Stecher *et al.*, 2010). In a mice model, it was shown that exposure to *Pediococcus pentosaceus* JWS 939 led to a higher survival of the animals following *Listeria monocytogenes* infection (Choi *et al.*, 2011). In another study, *L. reuteri* 55730 prevents *S. aureus*-mediated cytotoxicity in a human cell culture model (Prince *et al.*,

Table 1.3. Use of probiotic LAB in the mitigation of gastrointestinal pathogens in a cell culture model

Serial no.	Cell culture model	LAB Bacterial strain tested	Target pathogen	Reference
1.	Caco-2 cells	*L. rhamnosus* W71	*L. monocytogenes* ATCC 7644	Campana *et al.*, 2017
		L. acidophilus ATCC 4356	*C. jejuni* ATCC 33291	Campana *et al.*, 2012
2.	HT-29 cells	*L. plantarum* CS24.20	*E. coli* O26:H11	Dhanani and Bagchi, 2013
		L. plantarum ULAG11	*S. enterica* LT2	Oguntoyinbo and Narbad, 2015
		L. lactis L3A21M1	*L. monocytogenes* ATCC 7466	Ribeiro *et al.*, 2016
		L. plantarum LB95	*S. enterica* subsp. *enterica* serovar Enteritidis	Dutra *et al.*, 2016
3.	HT29-MTX cells	*L. paraplantarum* BGCG11	*L. monocytogenes*	Zivkovic *et al.*, 2015
		L. salivarius SMXD51	*C. jejuni*	Saint-Cyr *et al.*, 2017

2012). The inherent ability of probiotic LAB to prevent pathogen adhesion has also been demonstrated in animal models to counter *S. aureus*-induced intestinal and colonic injury, recurrent *Clostridium difficile* infection, and colonization by vancomycin-resistant *Enterococcus faecalis* (Bendali *et al.*, 2014; Ghosal *et al.*, 2016; Manley *et al.*, 2007). The potential of probiotic LAB has been also demonstrated in clinical trials, wherein it has been observed that strains such as *L. plantarum* TIFN101 led to an enhanced repair process in the compromised intestine of human subjects (Mujagic *et al*., 2017). In another study, prophylactic use of *L. reuteri* DSM 17938 during the first three months of life in an infant led to a reduction in the number of infants having gastrointestinal disorders (Indrio *et al.*, 2014). The regular consumption of *Lactobacillus casei* strain shirota has also been linked to a reduction in acute

diarrhea in a human trial (Sur *et al.*, 2011), reiterating the promise of probiotic LAB in preventing gastrointestinal disorders.

1.8. Bacteriocins from LAB

Bacteriocins are ribosomally-synthesized antimicrobial peptides (AMPs), which are secreted to the extracellular medium (Cotter *et al*., 2005). Further, bacteriocins from LAB are currently under renewed focus due to the GRAS status of LAB and long history of their use in food and fermentation process. Bacteriocins may possess an advantage over conventional antibiotics, as they can be active at nanomolar range and are less likely to have toxic implications as compared to antibiotics (Cotter *et al.*, 2013; Hassan *et al.*, 2012). Most importantly, bacteriocins have a restricted antimicrobial spectrum, unlike conventional antibiotics, which is anticipated to cause minimal collateral damage to the beneficial microflora in the human gastrointestinal tract. Based on this rational, bacteriocins from probiotic LAB are uniquely positioned as safe and targeted antibacterial molecules for mitigating gastrointestinal pathogens. The following sections describes the classification of bacteriocins produced by LAB.

1.9. Bacteriocin classification

1.9.1. Class I: Small post-translationally modified peptides (less than 10 kDa)

This class is composed of those peptides that undergo enzymatic modification while being synthesized, leading to the presence of unique amino acids and structures, that has an influence on their properties. The bacteriocin is made up of a leader peptide, which plays a role in transport and renders the molecule inactive when it is fused with the peptide (Alvarez-Sieiro *et al*., 2016; Arnison *et al.*, 2013). This class is further subdivided into Ia (lanthipeptides), Ib (head-to-tail cyclized peptides), Ic (sactibiotics), Id (linear azoline-containing peptides- LAC), Ie (glycoins) and If (lasso peptides) (Alvarez-Sieiro *et al*., 2016). One of the well-known bacteriocins from this group is nisin A, which is a FDA approved bacteriocin for application in food packaging materials.

1.9.2. Class II: Unmodified bacteriocins (less than 10 kDa)

These bacteriocins have no unique amino acids and hence do not require any unusual modification during their biosynthesis. However, they still require a leader peptidase and/ or a transporter. This class is further subdivided into IIa (pediocin-like

bacteriocins), IIb (two-peptide bacteriocins), IIc (leaderless bacteriocins) and IId (non-pediocin like, single-peptide bacteriocins) (Alvarez-Sieiro *et al*., 2016). Pediocin PA-1 is a widely studied molecule from this group of bacteriocins. Considering that the major thrust of the present thesis is on class IIa bacteriocins, an elaborate discussion on these bacteriocins is provided in a subsequent section.

1.9.3. Class III

The Class III bacteriocins are larger than 10 kDa in size and are sensitive to heat. These generally act by lytic (enterolysin A) or non-lytic (caseicin) mechanism (Alvarez-Sieiro *et al*., 2016). When these bacteriocins act by non-lytic mechanisms, either blockage of biosynthesis or membrane leakage is found to occur.

1.10. Class IIa bacteriocins (pediocin-like bacteriocins)

The designation of these class of bacteriocins as pediocin-like bacteriocins refers to the molecule pediocin PA-1/ AcH, which was the first class IIa bacteriocin characterized for its antibacterial properties (Biswas *et al.*, 1991, Nieto Lozano *et al.*, 1992; Cleveland *et al.*, 2001, Ennahar *et al.*, 2000, Klaenhammer, 1993). In recent times, class IIa bacteriocins produced by LAB have emerged as a group of antimicrobial peptides for use in food preservation and in medicine, as antibiotic adjuvants in treating infectious diseases (Alvarez-Sieiro *et al*., 2016, Umu *et al.*, 2016). Class IIa bacteriocins act on gram-positive food spoilage and pathogenic bacteria such as *Bacillus cereus*, *Clostridium perfringens*, *C. difficile*, *E. faecalis*, *S. aureus* and *L. monocytogenes* (Cotter *et al.*, 2005; O'Connor *et al.*, 2015). These bacteriocins are often described as anti-listerial, have a molecular weight of less than 10 kDa, are heat-stable, unmodified peptides having a net positive charge, with pI values ranging from 8 to 10 (Umu *et al.*, 2016). Further, class IIa bacteriocins possess a highly conserved, and hydrophilic region, having the consensus motif YGNGV(X)C (X denotes any amino acid) which is known as the pediocin box (Alvarez-Sieiro *et al*., 2016; Perez *et al.*, 2014). The C-terminal region is more flexible in terms of amino acid composition and is primarily hydrophobic and/or amphiphilic in nature (Alvarez-Sieiro *et al*., 2016). Pediocin PA-1 is a classical molecule of this class and its mode of action has been elucidated in previous studies. The bacteriocin was found to render a loss of K^+ ions in sensitive cells (Bhunia *et al.*, 1991). It also led to a decline in the concentration of intracellular ATP, dissipation of the membrane potential ($\Delta\psi$) and caused the

Table 1.4. Examples of class IIa bacteriocins

Serial no.	Name	Producer	Target pathogen	Reference
1.	Pediocin PA-1	*P. pentosaceus* NCDC 273	*E. faecalis* NCDC 114	Verma *et al.*, 2017
2.	Plantaricin ZJ008	*L. plantarum* ZJ008	*M. luteus* 10209 *S. carnosus* LTH1502 *S. aureus* D48 *S. epidermidis* Z80 *L. monocytogenes* LM1	Zhu *et al.*, 2014
3.	Enterocin K1	*E. lactis* Q1	*E. faecium* MMT21 *E. faecalis* JH22 *S. aureus* ATCC 6538	Braïek *et al.*, 2018
4.	Sakacin P	*L. sake* C2	*L. monocytogenes* CMCC 54002	Gao *et al.*, 2015
5.	Leucocin A	*L. gelidum* UAL187	*L. monocytogenes* FSL C1-056 *C. divergens* UAL9	Balay *et al.*, 2017

breakdown of the pH gradient (ΔpH) in target cells of *L. monocytogenes* (Christensen and Hutkins, 1992; Chikindas *et al.*, 1993). Based on studies with pediocin and pediocin-like bacteriocins, it is proposed that class IIa bacteriocins trigger membrane permeabilization in the target bacterial cell, probably by the formation of ion selective pores, which lead to a dissipation of the proton motive force and a decline in the concentration of intracellular ATP. A list of representative Class IIa bacteriocins and their salient features is indicated in Table 1.4.

1.11. Healthcare applications of LAB bacteriocins

Bacteriocins from LAB are considered as safe and promising antibacterial molecules considering that they are produced from LAB, their ability to act on a select group of pathogenic bacteria, lack of host-directed toxicity and their propensity to be stable molecules. Of the various classes of bacteriocins, nisin and pediocin PA-1 have been commercialized as food additives (Alvarez-Sieiro *et al.*, 2016). However, their unique

properties of possessing a restricted antimicrobial spectrum of pathogenic bacteria and being non-toxic to mammalian cells, renders them amenable for mitigation of pathogens in the healthcare regime. Further, it is anticipated that utilization of bacteriocins for the mitigation of gastrointestinal pathogens will lead to their removal from the gastrointestinal tract. This tenet was elucidated in a study wherein consumption of a purified formulation of nisin in broiler chickens led to a reduced number of *Bacteroides* and *Enterobacteriacae* in ileal region of gastrointestinal tract (Jozefiak *et al.*, 2013). In a similar study, application of the bacteriocin OR-7 encapsulated in polyvinylpyrrolidone led to a one-million-fold reduction in the population of the human gastroenteritis pathogen *C. jejuni* in chicken (Stern *et al.*, 2006). LAB bacteriocins can also function as antibiotic synergists to potentiate the antimicrobial efficacy of conventional antibiotics. Recently, the combination of nisin with ceftriaxone or cefotaxime led to membrane permeabilization in tested strains of *Salmonella* spp. (Singh *et al.*, 2013). Interestingly, the application of the combinatorial regime of nisin and β-lactam antibiotics led to a direct immunomodulatory effect in mice infected with *Salmonella* (Singh *et al.*, 2014).

In the context of targeting pathogens in the gastric niche, bacteriocin-producing LAB can be deployed and the anti-adhesion propensities of such bacteriocinogenic LAB can also be exploited in tandem. It may be hypothesized such LAB strains can lead to an effective abrogation of gastrointestinal pathogens with minimal effect on the beneficial microflora. The role played by bacteriocin production towards increasing the probiotic effectiveness of the *Lactobacillus* sp. in the gastric niche has been brought out through various seminal studies (van Hemert *et al.*, 2010; Meijerink *et al.*, 2010; Gotteland *et al.*, 2008). In particular, colonization of mouse gut by the bacteriocinogenic *L. salivarius* UCC118 has been correlated with protection from *L. monocytogenes* infection (Corr *et al.*, 2007). Interestingly, in a related study, adhesion of *L. salivarius* UCC118 to epithelium cells was found to lead to an induction of the genes expressing bacteriocins, highlighting the probable mechanism for its protective effect on *L. monocytogenes* infection in murine gut (van Pijkeren *et al.*, 2006). In a seminal study, it was found that conjugation defective *E. faecalis* cells harboring the plasmid for production of bacteriocin 21 led to the clearance of vancomycin resistant *E. faecalis* cells from the gastric niche, underscoring the fact that deployment of bacteriocinogenic LAB can be an effective therapeutic regimen to achieve selective clearance of gastrointestinal pathogens (Kommineni *et al.*, 2015).

MOTIVATION AND OBJECTIVES OF THE PRESENT INVESTIGATION

MOTIVATION AND OBJECTIVES OF THE PRESENT INVESTIGATION

Mitigation of gastrointestinal infections using therapeutic antibiotics can be counterproductive since their administration is likely to cause a significant collateral damage to the gut microflora. Based on the existing literature reports as highlighted in Chapter 1 of the thesis, it is quite evident that probiotic lactic acid bacteria (LAB) and its metabolites, specifically bacteriocins, has come to the forefront as potential therapeutic agents for selective elimination of pathogens along with minimal effect on the beneficial gut microbes. Notably, the high adhesion propensity of probiotic LAB to host intestinal cells can prevent pathogen adhesion by occluding host cell receptors or extracellular matrix (ECM) molecules. The origin of the present research investigation and the salient motivating factors stem from the following considerations:

1. Administration of therapeutic antibiotics can impart significant collateral eradication of beneficial gut microbiome and lead to occupation of niches by antibiotic-resistant pathogens such as vancomycin-resistant *E. faecalis* (VRE). This is an alarming fact, considering that occupation is followed by chronic colonization and systemic infections such as antibiotic-associated diarrhea. Given this backdrop, there is an urgent need to conceive alternate therapeutic approaches, which could adequately address the dual issue of the development of a selection pressure that favors resistance development in pathogens and minimize collateral damage towards the commensal microbes.

2. LAB have a long history of safe use in food and agriculture. The recent unraveling of the biomedical potential of LAB has positioned them as potential candidates for anti-pathogen therapy. The inherent propensity of probiotic LAB to survive in the harsh gastro-intestinal niche in combination with their ability to adhere onto ECM and host intestinal cells and prevent pathogen adhesion offer an exciting prospect of developing a LAB-based anti-bacterial therapeutic regime.

3. Bacteriocins, which are natural antimicrobial peptides (AMPs) secreted by LAB are promising therapeutic antibacterial molecules. In contrast to antibiotics, the restricted antimicrobial spectrum of bacteriocins is likely to ensure minimal collateral damage on commensal microbiota. Thus, it can be conceived that combinatorial deployment of probiotic LAB and its secreted bacteriocin may constitute a safe therapeutic antibacterial and an anti-adhesion agent.

4. Applications of bacteriocins as therapeutic antibacterial agents demand the development of a robust delivery system that would render stability and retention of bacteriocin activity during gastric transit. To this end, nanocarriers can be conceived as rational vehicles for generating suitable payload delivery modules. Further, the combination of probiotic LAB and bacteriocin-loaded nanocomposite can be harnessed in tandem to selectively reduce colonization of host cells by gastrointestinal pathogens.

In the light of the enormous scope of exploring probiotic LAB and its bacteriocin for niche-specific antibacterial therapy, the essential objectives of the Ph.D. thesis encompassed the following:

1. Selection of candidate LAB strains based on quantitative appraisal of probiotic attributes.
2. Determination of the potential of probiotic LAB to prevent pathogen adhesion onto extracellular matrix (ECM).
3. Evaluation of the potential of probiotic LAB to prevent pathogen adhesion in an *in vitro* cell culture model.
4. Generation of bacteriocin-loaded nanocomposite for mitigation of gastrointestinal pathogenic bacteria.
5. Evaluation of the combinatorial effect of bacteriocin-loaded nanocomposite and probiotic LAB for potential anti-adhesion intervention in an *in vitro* model.

Chapter 2

Quantitative Appraisal of Probiotic Attributes of Native Lactic Acid Bacteria

In this chapter the native LAB strains, which were previously isolated from various indigenous source were characterized for salient probiotic attributes. A quantitative comparison of these attributes using various in vitro assays are presented in detail.

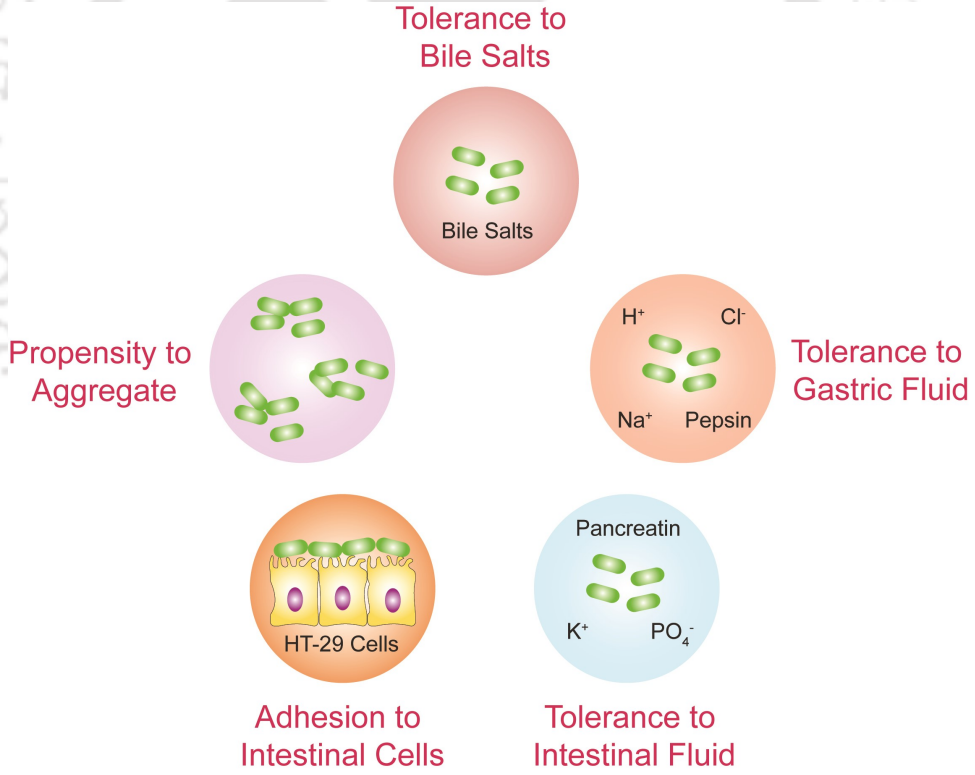

ABSTRACT

The aim of the present study was to ascertain the probiotic potential of anti-listerial bacteriocin-producing LAB strains isolated from indigenous sources such as *dahi*, dried fish and salt-fermented cucumber. Eleven anti-listerial bacteriocin producing natural LAB isolates were screened for bile tolerance. All the native isolates exhibited tolerance towards bile salt as their viability was virtually unaffected over 24 h. The presence of bile salt hydrolase gene (*bsh*) was determined through PCR in *Lactobacillus plantarum* strains. Further, presence of collagen-binding protein (*cnbp*) and fibronectin-binding protein (*fbp*) gene was also detected through PCR in *L. plantarum* strains. Upon testing tolerance to simulated gastric fluid (SGF), the native isolates *Lactobacillus* sp. CDRA60, *L. plantarum* CRA38 and *P. pentosaceus* CRA51 demonstrated less than one log decrease in cell viability and this result was found to be comparable to that observed for the standard probiotic *L. rhamnosus* GG. An overwhelming majority of the native LAB demonstrated resilience to simulated intestinal fluid (SIF), akin to *L. rhamnosus* GG. A sensitive fluorescence-based adhesion assay indicated that the native isolates, *Lactobacillus* sp. DF3, *L. plantarum* DF9 and *E. faecium* DF14 displayed adhesion comparable to that observed for *L. rhamnosus* GG. It was also interesting to observe that *Lactobacillus* sp. DF3, *L. plantarum* DF9 and *E. faecium* DF14 displayed auto-aggregation akin to *L. rhamnosus* GG. Finally, antibiogram assays revealed that the native LAB strains were sensitive to conventional therapeutic antibiotics used for mitigation of gastrointestinal pathogens. It is conceived that these anti-listerial bacteriocinogenic LAB strains may find niche application in the healthcare domain.

2.1. Introduction

Lactic acid bacteria (LAB) have the distinction of being generally regarded as safe (GRAS) microorganisms that play a crucial role in food product development and fermentation processes (Coolbear *et al.,* 2008; Rhee *et al.,* 2011; Leroy and De Vuyst, 2004; Angmo *et al.,* 2016). LAB may also enhance food safety by producing antimicrobial peptides such as bacteriocins, which are antagonistic to pathogens such as *Listeria monocytogenes*, *Enterococcus faecalis*, *Staphylococcus aureus* and *Clostridium difficile* (Cotter *et al.*, 2013; O'Connor *et al.*, 2015; Umu *et al.*, 2016; Cavera *et al.*, 2015; Schillinger *et al.,* 2014; Chikindas *et al.,* 2018). Recently, LAB have come to the forefront as probiotic candidates, which can largely impact the activity and composition of the intestinal microbiota, and this fact, has led to emerging healthcare applications (Lebeer *et al.,* 2008; Vitetta *et al.*, 2014; Pamer, 2016; Yan and Polk, 2010; Ghosal *et al.*, 2016; Nishiyama *et al.*, 2016). Considering the fact that probiotic LAB need to colonize and persist in the intestine, it is critical that such LAB strains have a protective mechanism to survive in extremely low pH of the gastric fluid and the harsh digestive enzymes and bile encountered during gastrointestinal transit. Thus, tolerance to gastric and intestinal fluid and bile constitutes a key selection criterion for probiotic LAB strains. With regard to other cardinal attributes of probiotic LAB, the ability to adhere to intestinal cells is considered to be vital in the context of persistence (Alander *et al.*, 1999; Jensen *et al.*, 2014), enhanced healing of the damaged mucosa (Verdu *et al.*, 2009; van Beek *et al.,* 2016), antagonism against pathogens (Collado *et al.,* 2007; Reid and Burton 2002) and immunomodulation (Paginini *et al.,* 2010; Zhou and Gill, 2005).

Evaluation of desirable probiotic attributes in native LAB isolates through rigorous assays is vital prior to establishing the probiotic traits in the strains. Further, the assays should be insightful and quantitative that would enable a comparative analysis and selection of the potential strains thereof. To ascertain bile tolerance as well as transit tolerance of LAB in the upper human gastrointestinal tract (GIT), well-established *in vitro* models have been described in the literature (Nueno-Palop and Narbad, 2011; Charteris *et al.,* 1998; Huang and Adams, 2004). A number of *in vitro* models have been routinely employed to ascertain adhesion of probiotic LAB to epithelial cells, of which cell culture-based experiments are routinely used (Bermudez-Brito *et al.*, 2013). Previous research work has demonstrated the utility of model intestinal cell lines such as the human colon adenocarcinoma cells Caco-2 and HT-29

in evaluating the adhesion potential of potent probiotic LAB strains (Bermudez-Brito *et al.*, 2013; Sambuy *et al.,* 2005; Walsham *et al.,* 2016). Adhesion of LAB to epithelial cells has been studied by visualizing the adhered cells by Gram staining (Tuomola and Salminen, 1998) or Giemsa staining (Forestier *et al.,* 2001). Quantitative estimation of LAB adhesion has been accomplished by using radio-labeled probe, enzyme-linked immunosorbent assay (ELISA), culture dependent plating techniques and fluorescence-based assays (Gopal *et al.,* 2001; Binachi *et al.,* 2004; Blay *et al.,* 2004; Lee *et al.,* 2004). In this context, the propensity of LAB cells to form aggregates has been implicated in their ability to adhere onto intestinal cells (García-Cayuela *et al.,* 2014; Botta *et al.,* 2014). It has been presumed that formation of bacterial clumps leads to an increased bacterial surface area for interaction with intestinal cells leading to an enhanced ability to adhere and colonize (Younes *et al.,* 2012; MacKenzie *et al.,* 2010).

Considering the fact that probiotic LAB largely constitutes the human gut microbiota, isolation of putative probiotic LAB has been largely accomplished from human intestinal source (Guinane *et al.,* 2015; Zheng *et al.,* 2016). However, in the light of reports, which highlight interesting probiotic attributes in LAB isolated from non-intestinal source (Chang *et al.,* 2010; Vitali *et al.,* 2012; Angmo *et al.,* 2016; Botta *et al.,* 2014), there is a growing interest in probing unique ecological niches as alternate source of isolating novel probiotics. In the present study, several native LAB strains, which were isolated previously from diverse indigenous sources and produced bacteriocin was found to demonstrate potent activity against the intestinal pathogen *Listeria monocytogenes* (Singh *et al.,* 2012a). Given the potency of these LAB strains against a gastrointestinal pathogen, the initial endeavor of the present investigation was to probe some of the characteristic probiotic attributes such as bile tolerance, survival potential in simulated gastric and intestinal fluids and *in vitro* adhesion to model human intestinal cells. It was envisaged that apart from bacteriocinogenic potential, the presence of other probiotic traits may significantly enhance the scope of these native LAB strains in the mitigation of intestinal pathogens.

2.2. Materials and Methods

2.2.1. Growth media and chemicals

5 (and 6) carboxyfluorescein diacetate succinimidyl ester (cFDA-SE), pepsin, pancreatin, penicillin and streptomycin were obtained from Sigma Aldrich, USA. For cell culture experiments, Dulbecco's Modified Eagle Medium (DMEM) was procured from Sigma-Aldrich (USA) and fetal bovine serum (FBS) was procured from PAA Laboratories, USA. de Man, Rogosa and Sharpe (MRS) broth, oxgall bile salts and antibiogram octadiscs (G-IV-minus) were procured from HiMedia, Mumbai, India.

2.2.2. Bacterial strains and culture condition

The reference and native LAB in this investigation are indicated in Table 2.1. All LAB strains were grown and maintained as stock cultures as described in a previous investigation (Singh and Ramesh, 2009).

2.2.3. Bile salt tolerance of native LAB

To study the survival of native LAB isolates in presence of oxgall bile salt, 1.0 mL of cells from an overnight grown culture (7.0 $\log_{10}$ CFU/mL) was harvested by centrifugation, washed and resuspended in 1.0 mL sterile MRS broth. Subsequently, 0.1 mL of cells was added to 0.9 mL of MRS broth containing 0.3% (w/v) oxgall bile (final cell number of 6.0 $\log_{10}$ CFU/mL), vortexed thoroughly and incubated at 37 °C under static condition. To determine viability in presence of oxgall bile, aliquots of 0.1 mL were periodically withdrawn (6 h, 12 h and 24 h) and cell viability ($\log_{10}$ CFU/mL) was ascertained by pour plating in sterile MRS agar medium.

2.2.4. PCR-based detection of bile salt hydrolase gene (bsh), fibronectin-binding protein gene (fbp) and collagen-binding protein gene (cnbp) in native isolates of Lactobacillus plantarum

Template DNA was isolated from native isolates of *L. plantarum* (isolates CRA21, CRA38, CRA52 and DF9 in case of *bsh* and *fbp* gene; isolates CRA21, CRA38, CRA49, CRA52 and DF9 in case of *cnbp* gene) by following the method described in an earlier work (Singh and Ramesh, 2009). Detection of *bsh*, *cnbp* and *fbp* genes was accomplished using the primers indicated in Table 2.2. The PCR reaction mix consisted of PCR buffer (diluted from a 10X stock), 200 µM of each deoxynucleoside triphosphate (dNTP), 1U of Taq DNA polymerase (Sibenzyme, Novosibirsk, Russia)

Table 2.1. Bacterial strains used in present study

Bacteria	Strain
Standard LAB	
Lactobacillus gasseri	NRRL B4240
Lactobacillus helveticus	NCIM 2126
Lactobacillus johnsonii	NRRL B2178
Lactobacillus plantarum	MTCC 1407
Lactobacillus plantarum	MTCC 1746
Lactobacillus plantarum	NCIM 2592
Lactobacillus rhamnosus	GG
Bacteriocin producing LAB isolates	
Lactobacillus plantarum	CRA21
Lactobacillus plantarum	CRA38
Lactobacillus plantarum	CRA49
Lactobacillus plantarum	CRA52
Lactobacillus plantarum	DF9
Non-LAB strain	
Staphylococcus aureus	MTCC 96
Listeria monocytogenes	Scott A
Enterococcus faecalis	MTCC 439

NRRL: Northern Regional Research Laboratory, Peoria, IL, USA; MTCC: Microbial Type Culture Collection, Institute of Microbial Technology (IMTECH), Chandigarh, India; NCIM: National Collection of Industrial Microorganism, National Chemical Laboratory (NCL), Pune, India; Native *L. plantarum* strains CRA21, CRA38, CRA49, CRA52, DF9 were isolated as described previously (Singh and Ramesh, 2008; Singh *et al.*, 2012); *L. rhamnosus* GG and *L. monocytogenes* Scott A were obtained from Dr. Prakash Halami, Central Food Technological Research Institute (CFTRI), Mysuru, India.

and 50 pmol each of forward and reverse primer. The template DNA was initially subjected to denaturation at 94 °C for 2 min followed by a total of 35 amplification cycles in a programmable thermal cycler (Gene Amp Gold PCR System, Applied Biosystems, USA). Each cycle included denaturation for 1 min at 94 °C, primer annealing for 1 min at 56 °C (for *bsh* and *fbp*) or 55 °C (for *cnbp*) and extension for 1 min at 72 °C. A final extension at 72 °C for 10 min followed the last cycle. The PCR products were subjected to agarose (1%) gel electrophoresis.

Table 2.2. Primers used in the present investigation

Primer	Nucleotide sequence (5'-3')	PCR target	Reference
1F	CACCAGTCCTAAGCGACCAT	*bsh* gene	Present work
1R	GTTGTTCGTGACCAGTCGTG		
2F	GCTTCCTAGTGACGATCCAATC	*fbp* gene	Present work
2R	GTAAGGTCCGAGACCAGATGAC		
3F	CGCTATTTATGCTGGGGAGTAC	*cnbp* gene	Present work
3R	GCCCTAGCGTATCTGTAACCAC		

2.2.5. Survival in simulated gastric fluid (SGF) and simulated intestinal fluid (SIF)

Simulated gastric fluid (SGF) was prepared as described in a previous work (Charteris *et al.,* 1998). SGF was prepared fresh prior to assay and was composed of pepsin (3.0 g/L) suspended in 0.5% w/v sterile saline. The pH of SGF was adjusted to 2.0 using 0.2 N HCl. Simulated intestinal fluid (SIF) was prepared fresh as per the composition mentioned in US Pharmacopeia and consisted of 6.8 g/L of monobasic potassium phosphate and 10 g/L of pancreatin in sterile water. Pancreatin was used as an ingredient of SIF based on a previous literature report (Charteris *et al.,* 1998). The pH of SIF was adjusted to 8.0 using 0.1 M NaOH. To study the tolerance of native LAB isolates to SGF and SIF, 1.0 mL of cells from an overnight grown culture (consisting of 7.0 $\log_{10}$ CFU/mL) was harvested by centrifugation, washed twice in sterile phosphate buffered saline (PBS) and resuspended in 1.0 mL sterile PBS. Subsequently, 0.1 mL of cells was added to 0.9 mL of SGF or SIF (final cell number of 6.0 $\log_{10}$ CFU/mL), vortexed thoroughly and incubated at 37 °C under static condition. To determine tolerance in SGF, aliquots of 0.1 mL were periodically withdrawn (40 min, 80 min and 120 min) and cell viability ($\log_{10}$ CFU/mL) was ascertained by pour plating in MRS agar medium. In case of tolerance to SIF, samples were withdrawn intermittently (2 h, 4 h and 6 h) and cell viability ($\log_{10}$ CFU/mL) was ascertained by pour plating in MRS agar medium. For both SGF and SIF tolerance, control experiments consisted of untreated cells. Triplicate samples were analyzed for both SGF and SIF tolerance and the mean cell numbers and standard deviations were calculated (Microsoft Office Excel 2007, Microsoft Corporation, USA). The viable cell

counts obtained at 0 min in the respective simulated fluids was compared to the counts obtained at other periods of exposure (40 min, 80 min and 120 min for SGF and 2 h, 4 h and 6 h for SIF) and subjected to statistical analysis using one-way analysis of variance (ANOVA) performed on Sigma Plot version 11.0.

2.2.6. In vitro adhesion assay

For adhesion studies, HT-29 cells (human colon adenocarcinoma cells) were procured from National Animal Cell Repository, National Centre of Cell Sciences (NCCS) Pune, India. HT-29 cells were grown in 25 cm^2 tissue culture flasks in DMEM supplemented with 10% (v/v) FBS, 2.0 mM glutamine, 1.0 mM sodium pyruvate, 100 units/mL penicillin, and 50 mg/mL streptomycin at 37 °C in a humidified 5% CO_2 incubator until the cells were approximately 90% confluent. Prior to the adhesion experiments with LAB strains, the HT-29 monolayer was washed twice with sterile PBS, trypsinized and transferred to a 24-well multi-dish (final cell concentration 1×10^4 cells per well) having fresh DMEM medium (without antibiotics) and incubated at 37 °C in 5% CO_2. Subsequently, the monolayer of HT-29 cells was propagated for 7 days, with a periodic change of medium every 2 days and used at late post-confluence stage for carrying out adhesion assays. The LAB strains were grown overnight in MRS broth and harvested by centrifugation at 3,000 x g for 10 min. The cell pellet was washed twice with sterile PBS and resuspended in 1.0 mL of sterile PBS. The LAB were then labelled with cFDA-SE (final concentration of 50 µM) at 37 °C for 20 min. The labelling reaction was terminated by centrifugation of the cells at 3,000 x g for 10 min and the excess dye molecules were removed by washing the cell pellet twice with sterile PBS. The solution fluorescence of a 100 µL (6.0 $\log_{10}$ CFU/mL) aliquot of the cFDA-SE-labelled LAB strains was measured in a multiplate reader (Infinite M200, Tecan, Austria) and considered as total fluorescence (F_T). A 100 µL aliquot of cFDA-SE labelled LAB cells (6.0 $\log_{10}$ CFU/mL in antibiotic-free DMEM medium) was then added in different sets to 24-well multi-dish containing HT-29 cells in antibiotic-free DMEM medium and incubated at 37°C in 5% CO_2 atmosphere for 2 h. Following incubation, non-adhered LAB cells were aspirated and washed twice with sterile PBS. Subsequently, the non-adhered LAB, as cell pellet, was resuspended in sterile PBS and its fluorescence intensity was measured (F_{NA}). A quantitative measure of LAB adhesion (F_A) to HT-29 cells was calculated as per the following expression:

$$F_A = F_T - F_{NA} \quad .....2.1.$$

To quantify the adhesion potential of the selected LAB strains as compared to *L. rhamnosus* GG, the following expression was used:

$$\text{Adhesion potential (\%)} = \frac{F_A}{F^*} \times 100 \quad .....2.2.$$

where F* represents the quantitative measure of adhered cells of *L. rhamnosus* GG on HT-29 cells (corresponding to F_A for *L. rhamnosus* GG ascertained by using the expression indicated in equation 2.1). All the experiments were performed in triplicates and mean and standard deviation was calculated (Microsoft Office Excel 2007, Microsoft Corporation, USA).

2.2.7. Autoaggregation assay

Autoaggregation assays were performed by essentially following the method described previously (Kos *et al*., 2003). Initially, 1.0 mL of cells from an overnight grown culture of the LAB strains (7.0 $\log_{10}$ CFU/mL) was harvested by centrifugation, washed twice with sterile PBS and resuspended in 1.0 mL of sterile PBS. Subsequently, 0.1 mL of cells was added to 0.9 mL of sterile PBS (final cell number of 6.0 $\log_{10}$ CFU/mL), vortexed thoroughly and incubated for 2 h at 37 °C under static condition. Following incubation, 0.1 mL of the upper layer of the suspension was added to 0.9 mL of sterile PBS and the absorbance (A_T) was measured at 600 nm.

Autoaggregation was determined by the following expression:

$$\text{Autoaggregation (\%)} = \frac{A_0 - A_T}{A_0} \times 100 \quad .....2.3.$$

where, A_0 refers to absorbance of the initial bacterial suspension, which was used to set up the auto-aggregation assay. All the experiments were performed in triplicates and mean and standard deviation was calculated (Microsoft Excel 2007, Microsoft Corporation, USA).

2.2.8. Antibiogram assay

Antibiogram assay was performed by a standard disc diffusion method. Briefly, overnight grown cells of LAB (8.0 $\log_{10}$ CFU/mL) were grown as a lawn on MRS agar plates. Subsequently, antibiogram discs containing ampicillin (10 µg), cephalothin (5.0 µg), colistin sulphate (25 µg), gentamicin (10 µg), streptomycin (200 µg), sulphatriad (200 µg), tetracycline (25 µg) and co-trimoxazole (25 µg) were placed on the MRS plates and incubated at 37 °C for 48 h. Following incubation, the diameter of zone of inhibition around the antibiotic discs was measured and the LAB strains were classified as susceptible or resistant as per the manufacturer's instruction.

2.2.9. Nucleic acid sequence

The PCR generated amplicon for *bsh* and *cnbp* gene of *L. plantarum* CRA38 was purified using GenElute PCR Cleanup kit (Sigma Aldrich, USA) and subsequently subjected to nucleic acid sequencing (Delhi University, South Campus). The partial coding sequence was subjected to BLAST analysis (http://blast.ncbi.nlm.nih.gov/Blast.cgi) and deposited in GenBank with accession number JN831152 (*bsh*) and JQ231230.1 (*cnbp*).

2.3. Results and Discussion

2.3.1. Survival in presence of bile salt

Probiotic LAB are in great demand owing to their special attributes such as acid and bile tolerance, antagonism towards certain gastrointestinal pathogens and their favorable influence on the activity and composition of the intestinal microbiota (Haleja *et al.,* 2012, Ghosal *et al.*, 2016; Ohland and MacNaughton, 2010). Although probiotic strains isolated from human gastrointestinal tract hold special interest, it is worthwhile to probe the functional characteristics of LAB, which exist as intrinsic microbiota in diverse niche. This fact motivated us to undertake the present study, wherein potent bacteriocin producing LAB isolated previously from dahi, dried fish and salt fermented cucumber (Singh *et al.,* 2012a) were selected to ascertain tolerance to bile salt, simulated gastric and intestinal fluid and *in vitro* adhesion potential. It is conceivable that prior to exerting any health promoting benefits, probiotic LAB need to endure gastrointestinal (GI) transit and remain viable in adequate numbers. In the course of GI passage, LAB cultures are required to overcome a number of impediments of which tolerance to bile remains a formidable challenge. The detergent like property of bile

Table 2.3. Viability of LAB in presence of oxgall bile salts

Strain	[a] Viable count (log_{10} CFU/mL) ± SD			
	0 h	**6 h**	**12 h**	**24 h**
L. rhamnosus GG	6.11 ± 0.03	6.59 ± 0.06	7.03 ± 0.05	8.97 ± 0.02
Lactobacillus sp. CDRA60	6.13 ± 0.05	6.81 ± 0.05	7.05 ± 0.08	9.0 ± 0.2
L. plantarum CRA21	6.16 ± 0.01	6.94 ± 0.02	7.10 ± 0.1	9.05 ± 0.05
P. acidilactici CRA28	6.12 ± 0.03	6.71 ± 0.01	7.08 ± 0.06	9.01 ± 0.03
L. plantarum CRA38	6.11 ± 0.01	6.91 ± 0.02	7.26 ± 0.1	9.1 ± 0.12
Lactobacillus sp. CRA39	6.03 ± 0.06	6.80 ± 0.02	6.97 ± 0.02	7.95 ± 0.06
L. plantarum CRA49	6.15 ± 0.05	5.5 ± 0.02*	5.1 ± 0.07*	5.04 ± 0.06*
P. pentosaceus CRA51	6.06 ± 0.1	6.75 ± 0.03	7.01 ± 0.03	9.00 ± 0.02
L. plantarum CRA52	6.07 ± 0.08	6.86 ± 0.11	7.03 ± 0.04	9.0 ± 0.1
Lactobacillus sp. DF3	6.0 ± 0.02	6.9 ± 0.07	7.97 ± 0.05	9.95 ± 0.06
L. plantarum DF9	6.12 ± 0.01	6.8 ± 0.1	7.06 ± 0.06	9.0 ± 0.04
E. faecium DF14	6.10 ± 0.1	6.88 ± 0.02	7.02 ± 0.2	9.0 ± 0.1

[a] Viable cell numbers are expressed as mean cell count (log_{10} CFU/mL) followed by standard deviation (SD) value. * indicates p value < 0.05 obtained in a one way ANOVA

may lead to disruption of bacterial membranes and this fact renders bile as a potent antimicrobial agent (Begley *et al.,* 2005). Bile tolerance is thus a critical parameter for screening probiotic LAB. Interestingly, all the bacteriocin producing LAB strains exhibited tolerance towards bile salt as their cell viability proliferated over a period of 24 h (Table 2.3). This attribute of bile tolerance could also be observed for the standard probiotic strain *L. rhamnosus* GG (Table 2.3) as well as the other reference LAB strains used in these experiments (Table A2.1 in Appendix). It is to be noted that the bile tolerant bacteriocin producing LAB isolates were obtained from various indigenous source (Singh *et al.,* 2012a). Considering the fact that the native LAB isolates in the present study were essentially non-human in origin, the bile tolerance observed in these isolates is a rather interesting functional attribute. This finding is also analogous to earlier reports on the isolation of bile-tolerant LAB of non-intestinal origin

(Burns *et al.,* 2008). Although the tolerance of LAB strains to oxgall bile incorporated MRS broth may not strictly represent their ability to tolerate bile *in vivo*, the inherent resistance to physiological concentrations of bile displayed by the native LAB strains may stand in good stead for increasing their survival in the intestinal environment. In the human GIT, bile salt conjugates are present in high concentrations and some of the resident indigenous microflora, which belong to the genera of lactobacilli and bifidobacteria, have acquired the capacity to deconjugate bile salts. This ability to tolerate bile salts in the intestine has been attributed to the presence of the enzyme bile salt hydrolase (BSH; EC 3.5.1.24) that aids in the hydrolysis of glycine- and/or taurine-conjugated bile salts into amino acid residue and bile acid and thus contributes to the detoxification mechanism (Begley *et al.,* 2005). Evidence for relevance of bile salt hydrolysis in conferring bile tolerance to LAB strains has been provided in an earlier study (Grill *et al.,* 2000).

2.3.2. Detection of bile salt hydrolase gene (bsh) in native L. plantarum

In the present study, the high bile salt tolerance exhibited by the native LAB strains suggested the presence of bile salt hydrolase enzyme in these isolates. Application of *bsh* gene specific primers enabled PCR-based detection of *bsh* gene in native LAB strains of *L. plantarum* CRA21, CRA38, CRA52 and DF9 (Figure 2.1), which suggested that these LAB strains were potential BSH producers. Evidently, all the native *L. plantarum* strains yielded amplicons of 365 bp (Figure 2.1, lane nos. 6-9), which coincided with the expected size of *bsh* gene based on primer design. This was corroborated by the fact that the standard *L. plantarum* strains also produced amplicons of the same size (Figure 2.1, lanes nos. 1-4). The *bsh* gene amplicon of *L. plantarum* CRA38 was sequenced and assigned a GenBank accession number JN831152. BLAST analysis of the nucleotide sequence indicated a ~ 99% homology with earlier deposited *bsh* gene sequence (Table A2.2 in Appendix). The presence of *bsh* gene in *L. plantarum* has been reported earlier (Kaushik *et al.,* 2009; Lambert *et al.,* 2008). It may be mentioned here that the putative BSH producing native strains of *L. plantarum* also revealed high bile salt tolerance (Table 2.3), suggesting the probable role of BSH in conferring bile tolerance trait.

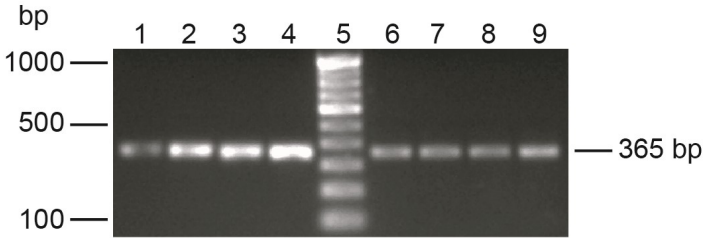

Figure 2.1. Agarose gel electrophoresis of PCR amplicons obtained with *bsh* specific primer for *L. plantarum* strains. Lanes: (1) *L. plantarum* MTCC 1407, (2) *L. plantarum* MTCC 1746, (3) *L. plantarum* NCIM 2083, (4) *L. plantarum* NCIM 2592, (5) 100 bp DNA ladder marker, (6) *L. plantarum* CRA21, (7) *L. plantarum* CRA38, (8) *L. plantarum* CRA52, (9) *L. plantarum* DF9.

2.3.3. Detection of collagen binding protein gene (cnbp) and fibronectin binding protein gene (fbp) in native L. plantarum

All the *L. plantarum* strains yielded amplicons of expected size in PCR using *cnbp* gene-specific primers (Figure 2.2A). The size of the amplicons obtained from the *L. plantarum* strains coincided with that of the standard *L. plantarum* strains (Figure 2.2A). The *cnbp* gene amplicon of *L. plantarum* CRA38 was sequenced and assigned a GenBank accession number JQ231230.1. BLAST analysis of the nucleotide sequence indicated ~ 99% homology with earlier deposited *cnbp* gene sequence of *L. plantarum* strains (Table A2.3 in Appendix). The presence of *cnbp* suggested the potential of *L. plantarum* strains to adhere onto collagen. It may be mentioned that collagen binding protein of *L. plantarum* has been previously reported to be instrumental in adhesion and in reducing the binding of gut pathogen to collagen (Yadav *et al.,* 2013).

Interestingly, amplicons of expected size in PCR were also obtained using *fbp* gene-specific primer in all of the tested native *L. plantarum* isolates (Figure 2.2B). The size of the amplicons obtained from the native *L. plantarum* strains were found to coincide with that of the standard *L. plantarum* strains (Figure 2.2B). On performing BLAST analysis of the nucleotide sequence, ~ 99% homology could be observed with earlier deposited *fbp* gene sequences of *L. plantarum* strains (Table A2.4 in Appendix). It has been reported previously that binding to fibronectin protein is correlated with higher adhesion in *in vitro* mammalian cells and resected tissues (Kaushik *et al.,* 2009; Munoz-Provencio *et al.,* 2009).

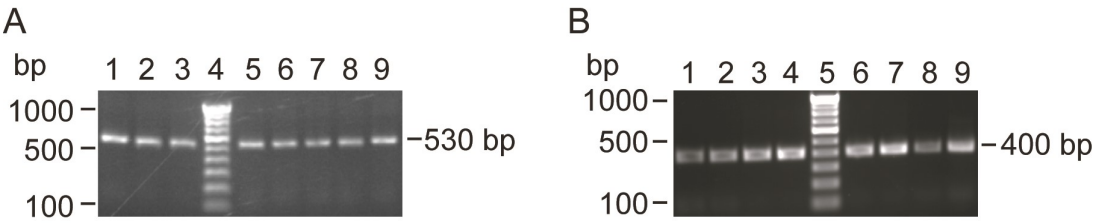

Figure 2.2. (A) Agarose gel electrophoresis of PCR amplicons obtained with *cnbp* specific primer for *L. plantarum*. Lanes: (1) *L. plantarum* MTCC 1746, (2) *L. plantarum* MTCC 1407, (3) *L. plantarum* NCIM 2592, (4) 100 bp DNA ladder marker, (5) *L. plantarum* CRA21, (6) *L. plantarum* CRA38, (7) *L. plantarum* CRA49, (8) *L. plantarum* CRA52, (9) *L. plantarum* DF9. (B) Agarose gel electrophoresis of PCR amplicons obtained with *fbp* specific primer for *L. plantarum*. Lanes: (1) *L. plantarum* MTCC 1407, (2) *L. plantarum* MTCC 1746, (3) *L. plantarum* NCIM 2083, (4) *L. plantarum* NCIM 2592, (5) 100 bp DNA ladder marker, (6) *L. plantarum* CRA21, (7) *L. plantarum* CRA38, (8) *L. plantarum* CRA52, (9) *L. plantarum* DF9.

2.3.4. Viability of native LAB in simulated gastric fluid (SGF) and simulated intestinal fluid (SIF)

Potential probiotic LAB strains have to survive the harsh environment during gastrointestinal transit. In this context, it is imperative that the probiotic LAB are able to withstand exposure to gastric and intestinal fluids, which constitute a profound environmental stress and are known to have deleterious effect on the viability of ingested probiotics (Liong and Shah, 2005). Hence, it is pertinent to determine the tolerance of potential probiotic LAB to gastric and intestinal fluids in order to ascertain their functionality and their robustness. In the present study, the survival potential of native LAB isolates were determined in SGF and SIF by following well established protocols (Charteris *et al.,* 1998). The growth of bile salt tolerant native LAB strains exposed to SGF and SIF for various time periods was ascertained by a conventional plating method. Amongst the tested LAB strains, four native LAB isolates (CRA28, CRA52, DF3 and DF9) and the standard LAB strains, *L. plantarum* MTCC 1407, *L. plantarum* MTCC 1746 and *L. gasseri* NRRL B4240 exhibited a progressive loss of cell viability with increasing exposure to SGF (Table 2.4, Table A2.5 in Appendix). On the basis of statistical analysis, this phenomenon was observed to be significant (p value <0.05) and explicit in every time period (Table 2.4, Table A2.5 in Appendix). It may also be noted that the LAB isolate DF9 was particularly susceptible as evident from the dramatic decrease in viable cells from 0 minute (6.02 ± 0.08 $\log_{10}$ CFU/mL)

Table 2.4. Viability of native LAB in simulated gastric fluid (SGF)

Strain	[a] Viable count (log_{10} CFU/mL) ± SD			
	0 min	**40 min**	**80 min**	**120 min**
L. rhamnosus GG	6.10 ± 0.09	6.06 ± 0.05	6.01 ± 0.01	5.78 ± 0.03*
Lactobacillus sp. CDRA60	6.12 ± 0.03	6.01 ± 0.01	5.9 ± 0.01	5.4 ± 0.03*
L. plantarum CRA21	6.06 ± 0.04	6.01 ± 0.01	5.2 ± 0.07*	5.23 ± 0.04*
P. acidilactici CRA28	6.08 ± 0.02	5.04 ± 0.02*	4.57 ± 0.15*	4.47 ± 0.02*
L. plantarum CRA38	6.07 ± 0.04	6.01 ± 0.01	6.00 ± 0.06	5.31 ± 0.1*
Lactobacillus sp. CRA39	6.00 ± 0.04	5.94 ± 0.05	5.54 ± 0.05*	5.4 ± 0.08*
L. plantarum CRA49	6.15 ± 0.05	6.0 ± 0.3	5.71 ± 0.02	5.14 ± 0.03*
P. pentosaceus CRA51	6.02 ± 0.13	6.01 ± 0.07	5.86 ± 0.06	5.77 ± 0.03*
L. plantarum CRA52	6.02 ± 0.13	6.00 ± 0.05	4.94 ± 0.05*	3.91 ± 0.02*
Lactobacillus sp. DF3	6.05 ± 0.05	5.45 ± 0.05*	5.1 ± 0.1*	3.81 ± 0.07*
L. plantarum DF9	6.02 ± 0.08	3.55 ± 0.05*	2.74 ± 0.03*	1.94 ± 0.02*
E. faecium DF14	6.00 ± 0.17	5.45 ± 0.06*	5.39 ± 0.05*	5.22 ± 0.08*

[a] Viable cell numbers are expressed as mean cell count (log_{10} CFU/mL) followed by standard deviation (SD) value. * indicates p value < 0.05 obtained in a one way ANOVA

to 120 min incubation (1.94 ± 0.02 log_{10} CFU/mL) in SGF as compared to the other native LAB strains (Table 2.4). Amongst the native LAB isolates, the strains CRA21, CRA39, CRA52 and DF14 exhibited significant reduction in viable cell population, when the LAB strains were treated with SGF for 80 min and 120 min. It was also evident that for isolate CRA21 and CRA39, there was a one log reduction in cell number following 120 min incubation in SGF, whereas for isolate CRA52, the effect of SGF on cell viability was more pronounced resulting in 2.0 log reductions in cell number (3.91 log_{10} CFU/mL) (Table 2.4). The bacteriocin producing native LAB isolates CDRA60, CRA38 and CRA51 did not reveal any dramatic decrease in cell viability when the cells were exposed to SGF up to 80 min. However, upon prolonged incubation in SGF for 120 min a significant reduction in cell viability was observed for these LAB isolates (Table 2.4). It may be mentioned here that the native LAB isolates

Table 2.5. Viability of native LAB in simulated intestinal fluid (SIF)

Strain	[a] Viable count (log_{10} CFU/mL) ± SD			
	0 h	**2 h**	**4 h**	**6 h**
L. rhamnosus GG	6.10 ± 0.09	6.07 ± 0.1	6.00 ± 0.1	6.00 ± 0.1
Lactobacillus sp. CDRA60	6.12 ± 0.03	6.10 ± 0.04	6.00 ± 0.1	5.98 ± 0.1
L. plantarum CRA21	6.06 ± 0.04	6.04 ± 0.05	5.95 ± 0.12	5.95 ± 0.08
P. acidilactici CRA28	6.08 ± 0.02	6.01 ± 0.04	6.00 ± 0.05	6.00 ± 0.05
L. plantarum CRA38	6.07 ± 0.04	6.03 ± 0.06	6.00 ± 0.14	6.00 ± 0.1
Lactobacillus sp. CRA39	6.00 ± 0.04	6.00 ± 0.07	6.00 ± 0.04	6.00 ± 0.04
L. plantarum CRA49	6.15 ± 0.05	6.1 ± 0.03	6.02 ± 0.01	6.0 ± 0.07
P. pentosaceus CRA51	6.02 ± 0.13	6.02 ± 0.06	6.00 ± 0.07	6.00 ± 0.07
L. plantarum CRA52	6.02 ± 0.13	6.00 ± 0.1	5.93 ± 0.06	5.14 ± 0.2*
Lactobacillus sp. DF3	6.05 ± 0.05	6.03 ± 0.05	5.98 ± 0.03	5.97 ± 0.04
L. plantarum DF9	6.02 ± 0.08	6.00 ± 0.2	5.96 ± 0.1	5.95 ± 0.1
E. faecium DF14	6.00 ± 0.17	5.95 ± 0.05	5.12 ± 0.3*	5.10 ± 0.3*

[a] Viable cell numbers are expressed as mean cell count (log_{10} CFU/mL) followed by standard deviation (SD) value. * indicates p value < 0.05 obtained in a one way ANOVA.

CDRA60, CRA38 and CRA51 are non-human in origin. *Lactobacillus* sp. CDRA60 was isolated from dahi, which is an acidic fermented milk product, whereas *L. plantarum* CRA38 and *P. pentosaceus* CRA51 were isolated from salt fermented cucumber (Singh *et al.,* 2012a). It is plausible that the inherent adaptation of these LAB strains to an acidic niche enhanced their survival capacity in SGF.

In contrast to the results obtained in SGF, when the tolerance of native LAB isolates to SIF was determined, an overwhelming majority of the strains displayed appreciable survival in SIF up to 6 h, with a viable cell number comparable with the standard LAB strains (Table 2.5, Table A2.6 in Appendix). In case of *L. plantarum* CRA52, cell viability was affected upon extended incubation in SIF for 6 h, with a one log reduction in cell number (5.14 log_{10} CFU/mL) (Table 2.5). It was also evident that the native LAB *E. faecium* DF14 appeared to be most susceptible to SIF

treatment. While the cell viability of this strain remained unaffected up to 2 h, an extended incubation in SIF (4 h and 6 h treatment) resulted in a one log reduction in cell viability (Table 2.5). The present study also revealed that certain native LAB strains, which were susceptible to SGF (CRA28, DF3, and DF9) could survive in the intestinal fluid (Table 2.4 and Table 2.5). This fact suggested that the LAB strains with poor gastric tolerance may recover during intestinal transit. The survival capacity of non-intestinal native LAB bacteria in a simulated intestinal environment suggested that characteristic functional properties of LAB isolated from the intestine may also be present in certain LAB strains isolated from fermented foods. On the basis of bile tolerance and survival in simulated fluids (Table 2.3, 2.4 and 2.5), it is to be noted that amongst the native LAB strains, the dahi isolate *Lactobacillus* sp. CDRA60, cucumber isolates *L. plantarum* CRA38, *Lactobacillus* sp. CRA39 and *P. pentosaceus* CRA51 and the dried fish isolate *E. faecium* DF14 are potential probiotics as they demonstrated considerable bile tolerance and ability to survive in SGF and SIF. The results obtained in the present study through *in vitro* tolerance tests provide a comparative assessment of the probiotic potential of native LAB strains and assist in selection of promising strains, which can perhaps be subjected to *in vivo* studies in future to ascertain potential health benefits.

2.3.5. In vitro adhesion to HT-29 cells

One of the key prerequisites of a probiotic LAB strain is the ability to adhere to mucus and intestinal epithelial cells. This intestinal adherence of LAB holds significant implications with regard to persistence, refurbishment of damaged mucosa, antagonism against pathogens colonizing the intestine and in immunomodulation (Campana *et al.,* 2017; van Beek *et al.,* 2016; Arena *et al.*, 2017; Lebeer *et al.,* 2010). A number of *in vitro* models have been used to evaluate the adhesion of probiotic LAB to epithelial cells. Of these, the colon adenocarcinoma cells Caco-2 and HT-29 have been extensively used in cell culture experiments (Bermudez-Brito *et al.*, 2013). In the present study, HT-29 cells were used to ascertain *in vitro* adhesion of potential native probiotic LAB. These cells have been advocated as an *in vitro* model of the host condition and has been considered as a useful tool for understanding bacteria-mammalian cell interactions (Langerholc *et al.,* 2011). *L. rhamnosus* GG was used as a positive control strain based on the well documented strong adhesion potential of this strain on enterocytes (Ossowski *et al.,* 2010). Adhesion potential of anti-listerial LAB

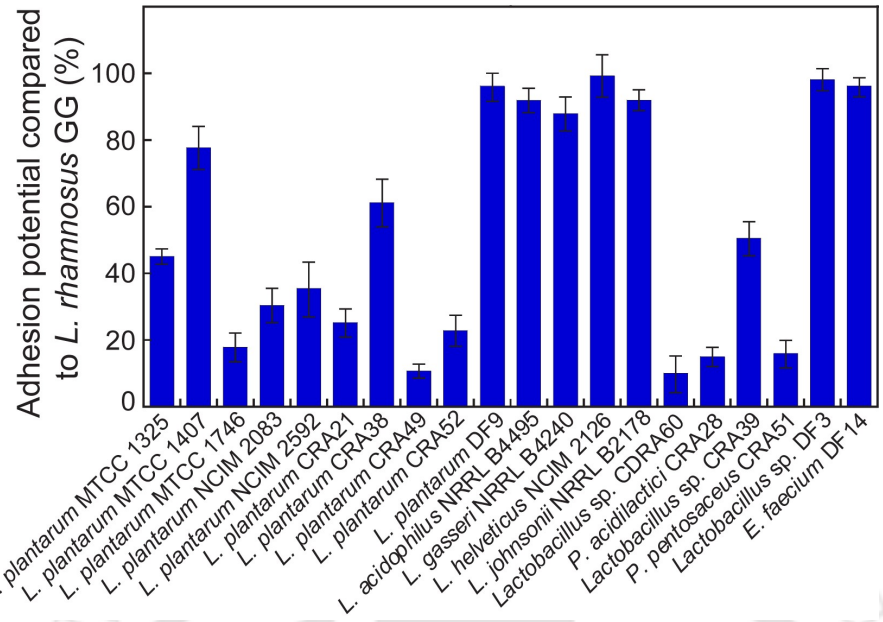

Figure 2.3. Fluorescence-based adhesion assay of LAB strains onto HT-29 cells.

strains was investigated through fluorescence-based method, in which the LAB cells were stained with the dye cFDA-SE followed by the adhesion assay. Amongst the native LAB, the dried fish isolates *Lactobacillus* sp. DF3, *L. plantarum* DF9, and *E. faecium* DF14 demonstrated highest adhesion capacity, which was found to be comparable to that observed for *L. rhamnosus* GG. An interesting observation was that the adhesion ability of the dried fish isolates was far superior to that observed for other LAB strains (Figure 2.3). Further, the adhesion potential of the native LAB isolates CDRA60, CRA21, CRA28, CRA38, CRA39, CRA51 and CRA52 to HT-29 cells were found to be variable (Figure 2.3). It has been suggested earlier that adhesion can be a strain-dependent phenomenon and may be influenced by the specific matrix (Jensen *et al.,* 2012; Tallon *et al.,* 2007).

2.3.6. Auto-aggregation ability in native LAB

The LAB strains investigated in the present study were found to demonstrate varying levels of adhesion onto HT-29 cells. It may be mentioned that bacterial adhesion to mammalian cells is considered to be a multistep process, which involves interaction between the bacterial cell membrane and interacting surfaces (Chagnot *et al.,* 2012). Previous investigations have reported that bacterial adhesion to host cells may be correlated to the autoaggregation behavior of LAB strains and is implicated in the

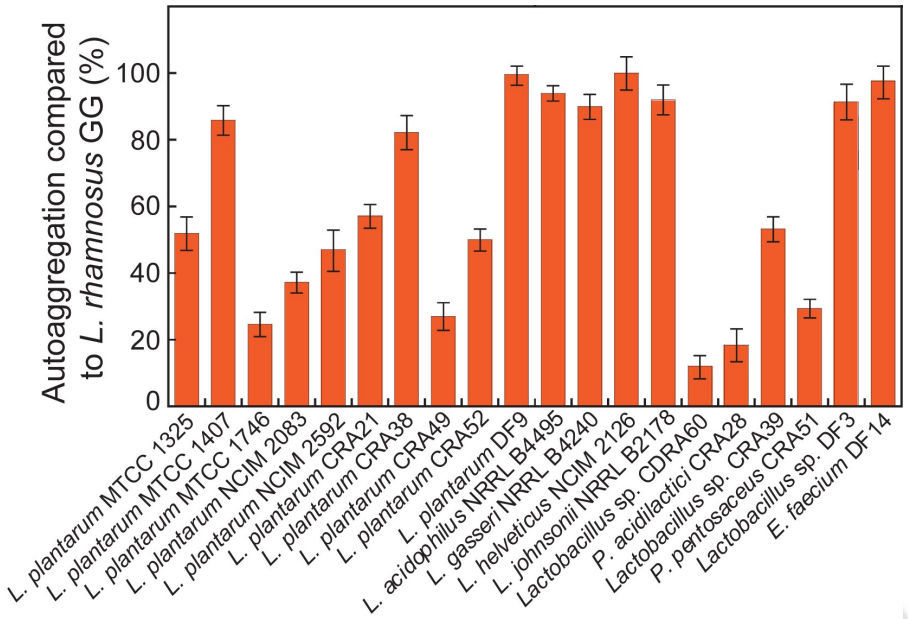

Figure 2.4. Auto-aggregation assay of LAB strains.

formation of a protective biofilm layer as well as co-aggregation with pathogens (MacKenzie *et al.,* 2010; García-Cayuela *et al.,* 2014; Nader-Marcias *et al.,* 2008; Younes *et al.,* 2012). To this end, the propensity of native LAB strains to autoagrregate was tested using a standard spectrophotometric method. A primary observation was that native LAB isolates, such as *L. plantarum* DF9, *L. plantarum* CRA38 and *E. faecium* DF14 demonstrated high autoaggregation comparable to *L. rhamnosus* GG (Figure 2.4). It may be mentioned here that these LAB strains were also found to possess *in vitro* adhesion comparable to that of *L. rhamnosus* GG (Figure 2.3). It is anticipated that *L. plantarum* DF9 which possess high adhesion potential and high autoaggregation would be a suitable candidate for the mitigation of pathogen from the intestinal niche. The autoaggregation behavior of other native LAB (CDRA60, CRA21, CRA28, CRA38, CRA39, CRA51 and CRA52) were found to be highly variable and substantially less as compared to *L. plantarum* DF9 or *L. plantarum* CRA38 (Figure 2.4).

2.3.7. Antibiogram assay

The native LAB strains were found to be susceptible to all tested antibiotics with the exception of sulphatriad and colistin sulphate in an antibiogram assay (Table 2.6). An Antibiogram assay provides qualitative evidence of sensitivity of a bacterial strain to

Table 2.6. Antibiogram assay

Strains	Antibiotic							
	AMP (10 µg)	**COL (25 µg)**	**GEN (10 µg)**	**STR (10 µg)**	**TET (25 µg)**	**CTR (25 µg)**	**SUL (200 µg)**	**CEP (5.0 µg)**
L. plantarum CRA21	+	-	+	+	+	+	-	+
L. plantarum CRA38	+	-	+	+	+	+	-	-
L. plantarum CRA49	+	-	+	+	+	+	-	+
P. pentosaceus CRA51	+	-	+	+	+	+	-	+
L. plantarum CRA52	+	-	+	+	+	+	-	+
Lactobacillus sp. DF3	+	-	+	+	+	+	-	+
L. plantarum DF9	+	-	+	+	+	+	-	-

AMP: Ampicillin; COL: Colistin sulfate; GEN: Gentamicin; STR: Streptomycin; TET: Tetracycline; CTR: Co-trimixazole; SUL: Sulphatriad; CEP: Cephalothonin
+ Sensitive; - Resistant.

the tested antibiotics (Reller *et al.,* 2009). Interestingly, the native LAB isolates were found to be susceptible to antibiotics such as tetracycline, ampicillin and gentamicin (Table 2.6), which are known to be used clinically for the mitigation of gastrointestinal pathogens (Fouhy *et al.,* 2012; Francino, 2015). Further, the native LAB strains were found to be susceptible to cephalothin, an antibiotic belonging to the cephalosporin family, which is often used as animal feed (Francino, 2015). Importantly, all of the tested LAB strains demonstrated susceptibility to co-trimoxazole, a combinatorial antibiotic, underpinning the safety of these LAB strains. The lack of resistance trait in the LAB strains against these clinically relevant antibiotics is a beneficial attribute as it implies that these LAB strains are unlikely to disseminate the resistance trait to opportunistic pathogens residing in the gut. This tenet is particularly encouraging considering that these LAB strains can be used as therapeutic interventions in combination with antibacterial molecules for mitigation of gastrointestinal pathogens.

2.4. Significant Findings

The salient findings of the present study can be enlisted as follows:

1. In the present investigation, native bacteriocin–producing LAB strains were subjected to *in vitro* experiments to evaluate certain quintessential probiotic features. The revelations of the *in vitro* tests were interesting since native LAB isolates obtained from non-human source such as dahi, dried fish and fermented cucumber displayed functional traits, which are typically associated with potential probiotics.
2. The native LAB strains were found to demonstrate tolerance to the presence of oxgall bile salt, simulated gastric fluid and simulated intestinal fluid. It is anticipated that these native LAB isolates may be able to survive during gastrointestinal transit.
3. On performing *in vitro* adhesion assay on HT-29 cells, *L. plantarum* DF9 and *L. plantarum* CRA38 were found to demonstrate adhesion comparable to that observed for other standard LAB strains. Interestingly, these native LAB isolates were also found to possess high auto-aggregating ability, indicating a probable cause for their high adhesion potential to model intestinal cells.
4. The native LAB were also found to be sensitive to some of the clinically relevant therapeutic antibiotics, emphasizing their safety for healthcare applications.

Based on the leads obtained in the study, it was evident that certain LAB strains such as *L. plantarum* CRA21, CRA38, CRA52 and DF9 displayed characteristic attributes associated with standard probiotic strains such as *L. rhamnosus* GG. Further, these native LAB isolates were also found to possess bile salt hydrolase (*bsh*) gene, collagen-binding protein (*cnbp*) gene and fibronectin-binding protein (*fbp*) gene. It is anticipated that the presence of these genes may enhance their ability to interact with the components of extracellular matrix (ECM). On the basis of this tenet, the next chapter highlights the detailed study on the adhesion potential of these bacteriocinogenic LAB strains on extracellular matrix protein (ECM) molecules, collagen and mucin and illustrates their ability to inhibit adhesion of model pathogens on ECM.

Chapter 3

Inhibition of Pathogen Adhesion onto Extracellular Matrix (ECM) by Native LAB

This chapter essentially describes the ability of native LAB strains to inhibit the adhesion of model pathogens onto extracellular matrix (ECM). The nuances of the adhesion process and inhibition of pathogen adhesion on ECM by LAB are illustrated in detail.

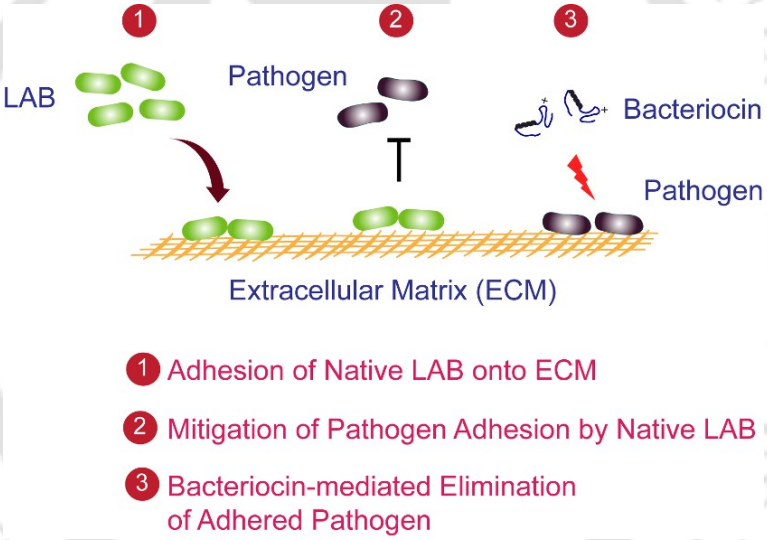

ABSTRACT

In the present study, the adhesion of bacteriocin producing native strains of *Lactobacillus plantarum* onto extracellular matrix (ECM) proteins such as collagen and mucin and their potential to prevent pathogen adhesion onto ECM was evaluated. Fluorescence-based *in vitro* assays indicated that the *L. plantarum* CRA21, *L. plantarum* CRA38 and *L. plantarum* CRA52 displayed considerable adhesion onto ECM molecules, which was found to be comparable to that observed for the probiotic *L. rhamnosus* GG. Flow cytometry-based quantitative assessment of the adhesion suggested that *L. plantarum* CRA21 exhibited superior adhesion onto ECM as compared to other native LAB strains. Estimation of the adhesion process parameters indicated that, on collagen-coated wells, the dissociation constant (k_d) for *L. plantarum* CRA21, *L. plantarum* CRA38 and *L. plantarum* CRA52 was more or less similar, while *L. plantarum* CRA21 displayed the highest value for maximum number of adhered bacteria (e_m) (2.43 $\log_{10}$ CFU per well). On mucin-coated wells, *L. plantarum* CRA52 demonstrated lowest k_d (7.58 $\log_{10}$ CFU per well) indicating a superior binding affinity as compared to the other native *L. plantarum* strains. Further, *L. plantarum* CRA21 was found to possess the highest e_m (1.32 log10 CFU/mL) on mucin-coated wells. Furthermore, fluorescence-based assays suggested that the highest inhibition of *S. aureus* MTCC 96 adhesion onto collagen and mucin by *L. plantarum* strains was observed in the exclusion mode as compared to competition and displacement mode. This observation was also supported by the higher binding affinity (k_d) for ECM exhibited by the *L. plantarum* strains as compared to *S. aureus* strain. Further, *L. plantarum* CRA21 demonstrated the highest inhibition (83.61% ± 1.74) as compared to the other native *L. plantarum* strains. Interestingly, a crude plantaricin A extract obtained from the native *L. plantarum* strains displayed potent antibacterial activity on ECM-adhered *S. aureus* MTCC 96 cells. It is envisaged that the *L. plantarum* isolates displaying bacteriocinogenic and ECM-adhering traits can perhaps be leveraged to develop safe antibacterial therapeutic agents.

3.1. Introduction

Lactic acid bacteria (LAB) play a pivotal role in food fermentation processes and have been traditionally employed to develop a wide range of fermented food products owing to their significant contributions towards flavor, aroma, and texture (Coolbear *et al.,* 2008; Leroy and De Vuyst, 2004). In recent times, LAB have also emerged as safe candidates for food safety applications and pathogen mitigation as literature reports have demonstrated the inherent ability of LAB strains to produce antimicrobial peptides such as bacteriocins, which are known to act against pathogenic bacteria (Cotter *et al.,* 2005; Cotter *et al.,* 2013; Drider *et al.,* 2006; Jones *et al.,* 2008; O'Connor *et al.,* 2015; Umu *et al.*, 2016; Chikindas *et al.*, 2018). In addition, LAB have also drawn attention as probiotic candidates, which can significantly influence the activity and composition of the gut microbiota (Pamer, 2016). In particular, *Lactobacillus rhamnosus* GG has been extensively studied and is being marketed as a probiotic under the names- ActifitPlus®, Gefilus®, LGG®, Onaka He GG®, VifitThus® (Doron *et al.,* 2005; Saxelin *et al.,* 2005). Several literature reports have suggested that LAB strains exhibit traits such as tolerance to low pH, digestive enzymes and bile (Begley *et al.,* 2006; De Vries *et al.,* 2006; Ouwehand *et al.,* 2002; Rastall *et al.,* 2005). These traits are likely to enhance the resilience of LAB strains during gastrointestinal (GI) transit. Furthermore, the ability of probiotic LAB to prevail in the intestinal milieu and render significant health benefits is vindicated by their inherent ability to adhere to intestinal cells, their antagonistic activity against pathogens known to invade the GI tract and their significant role in healing of damaged mucosa and immunomodulation (Alander *et al.,* 1999; Collado *et al.,* 2007; Elliott *et al.,* 1998; Pagnini *et al.,* 2010; Reid and Burton, 2002; Zhou and Gill, 2005; Mujagic *et al*., 2017).

Apart from their conventional food applications, LAB are heavily sought as compelling scientific evidence seems to suggest that they can significantly impact the activity and composition of human intestinal microbiota (Priedis *et al.,* 2011; Shanahan, 2010; Patel and DuPont, 2015; Guandalini, 2011). Based on this premise, probiotic LAB have been positioned in the vanguard of healthcare applications. Probiotic LAB can prevent pathogen colonization in the intestine by occupying sites and producing bacteriocins and other metabolites (Gopal *et al.,* 2001; Lee *et al.,* 2003; Millette *et al.,* 2008; O'Shea *et al.,* 2012; Vitetta *et al,.* 2014). Several reports describe the beneficial effects of *Lactobacillus* species on the gastrointestinal tract (GIT) (Bernbom *et al.,* 2009; Guarner and Malagelada, 2003; O'Callaghan *et al.,* 2012;

Walter, 2008; Hungin *et al.*, 2013). Adhesion to extracellular matrix (ECM) and intestinal cells is a key attribute of probiotic strains (Lebeer *et al.,* 2010; Lee *et al.,* 2004; Ouwehand and Salminen, 2003; Reid and Burton, 2002, Prince *et al.,* 2012). Certain lactobacilli have been shown to have an inclination to adhere to ECM molecules such as collagen and mucin and can thus be applied for inhibition of pathogen adhesion (Lorca *et al.,* 2002; Miyoshi *et al.,* 2005; Ouwehand *et al.,* 2001; Munoz-Provencio *et al.,* 2009; Velez *et al.*, 2007; Vesterlund *et al.,* 2005; Yadav *et al.,* 2013, García-Cayuela *et al.,* 2014). Furthermore, mucin binding lactobacilli have been shown to inhibit attachment of opportunistic pathogens and this is noteworthy since several enteric pathogens have evolved mechanisms to breach the mucosal barrier (McGuckin *et al.,* 2011; Shanahan, 2010).

Amongst the gut-colonizing pathogens, emerging literature reports have elucidated the detrimental implications of colonization by *S. aureus* (Acton *et al.,* 2009; Yan *et al.,* 2014). *S. aureus* is known to be equipped with adhesins known as microbial surface component recognizing adhesive matrix molecules (MSCRAMMs) for binding to ECM molecule such as collagen (Foster *et al.,* 2014). On the other hand, reports also suggest that binding to mucin is perhaps critical for *S. aureus* pathogenesis and persistence in intestine (Gries *et al.,* 2005; Vesterlund *et al.,* 2006). Given this backdrop, there is a need to conceive alternate therapeutic approaches, which could adequately combat colonization of ECM by *S. aureus*. Although LAB have a long history of safe use in food and agriculture industry, food isolates of LAB having probiotic traits also offer an exciting prospect of developing a safe LAB-based anti-bacterial regime, given their inherent propensity to survive in the harsh gastrointestinal niche and their ability to adhere onto ECM and host intestinal cells and thereby prevent pathogen adhesion. Further, it can be conceived that a bacteriocin producing probiotic LAB may acquire a competitive advantage and constitute a dual armament. The LAB strain itself can be explored as an anti-adhesion agent, while the bacteriocin produced by the strain may serve as a safe therapeutic antibacterial. Based on this premise, herein we report the adhesion of bacteriocin producing native isolates of *L. plantarum* and their potential to inhibit the adhesion of model pathogen, *S. aureus* MTCC 96, onto ECM molecules, collagen and mucin in an *in vitro* model.

3.2. Materials and Methods

3.2.1. Reagents and growth media

5 (and 6) carboxyfluorescein diacetate succinimidyl ester (cFDA-SE), sodium dodecyl sulphate (SDS), Tween 20, collagen type I derived from human placenta, mucin derived from porcine stomach were obtained from Sigma Aldrich, USA. Brain-Heart Infusion (BHI) broth, de Man, Rogosa and Sharpe (MRS) broth, urea, sodium hydroxide and crystal violet were procured from HiMedia, Mumbai, India.

3.2.2. Bacterial strains

The standard LAB and the bacteriocinogenic native LAB used in this investigation is listed in Table 2.1 indicated in Chapter 2. The strains were grown as per the conditions described previously in section 2.2.2. in Chapter 2. The target pathogens used in the present investigation comprised of *Listeria monocytogenes* Scott A (*L. monocytogenes* Scott A), *Enterococcus faecalis* MTCC 439 (*E. faecalis* MTCC 439) and *Staphylococcus aureus* MTCC 96 (*S. aureus* MTCC 96). Prior to experiments, the bacterial strains were propagated in BHI broth at 37 °C and 180 rpm for 12 h.

3.2.3. Adhesion of L. plantarum strains onto collagen and mucin

Collagen and mucin binding was performed as described in a previous report (Munoz-Provencio *et al.,* 2009). Stock solution of collagen was prepared in filter sterilized PBS (pH 5.5) to a final concentration of 1.0 mg/mL and stored at -20 °C prior to experiments. Stock solution of mucin was prepared in 0.1 M acetate buffer (pH 5.0) to a final concentration of 1.0 mg/mL and stored at 4 °C prior to experiments. Briefly, 96-well microtitre plates (Maxisorp, Nunc) were coated with collagen and mucin overnight at 4 °C at a concentration of 50 µg/mL and 500 µg/mL, respectively. Following coating, the wells were washed with sterile PBS thrice and blocked with 0.1 % (v/v) Tween 20 for 1 h. The adhesion potential of *L. plantarum* strains to collagen and mucin was studied by crystal violet staining, fluorescence-based adhesion assay and flow cytometry as described in the following sections.

3.2.3.1. Crystal violet staining

The standard LAB strains and natural LAB strains were grown overnight, harvested by centrifugation, washed and resuspended in sterile PBS to an OD_{600} of 1.0. Subsequently, 100 µL of cells was added to the collagen- or mucin-coated well and

incubated overnight at 4 °C. Non-adhered cells were aspirated from the wells and the wells were washed thrice with sterile PBS having 0.05% (v/v) Tween 20 and air dried in a laminar hood. Crystal violet was then added to the wells at a final concentration of 1.0 mg/mL and incubated for 45 min. The dye solution was aspirated, followed by three PBS washes and subsequently, 50 mM citrate buffer (pH 4.0) was added to the wells and incubated for 45 min. The absorbance of the solution was measured at 595 nm in a multiplate reader (Infinite M200, Tecan, Austria). To quantify the adhesion ability of the selected LAB strains as compared to *L. rhamnosus* GG, the absorbance obtained for the tested strain was compared with that obtained in case of *L. rhamnosus* GG and expressed as percentage adhesion potential as compared to *L. rhamnosus* GG. All the experiments were performed in triplicates and mean and standard deviation was calculated. Statistical analysis was performed by a one-way analysis of variance (ANOVA) using Sigma Plot version 11.0.

3.2.3.2. Fluorescence-based adhesion assay

The reference and native LAB strains were grown overnight, harvested by centrifugation, washed and resuspended in sterile PBS to OD_{600} of 1.0. Fluorescence labelling of LAB strains with cFDA-SE was accomplished as described previously (Singh *et al.*, 2012a). The solution fluorescence of a 100 µL aliquot of the cFDA-SE-labelled LAB strains was measured in a multiplate reader (Infinite M200, Tecan, Austria) and considered as total fluorescence (F_T). Subsequently, 100 µL aliquot of cFDA-SE-labelled LAB cells were added to collagen or mucin-coated wells and incubated overnight at 4 °C. Following incubation, non-adhered LAB cells were aspirated and their fluorescence intensity was measured (F_{NA}).

A quantitative measure of LAB adhesion (F_A) to collagen and mucin was calculated from the following expression:

$$F_A = F_T - F_{NA} \quad .....3.1.$$

To quantify the adhesion potential of the selected LAB strains as compared to *L. rhamnosus* GG, the following expression was used:

$$\text{Adhesion potential (\%)} = \frac{F_A}{F^*} \times 100 \quad .....3.2.$$

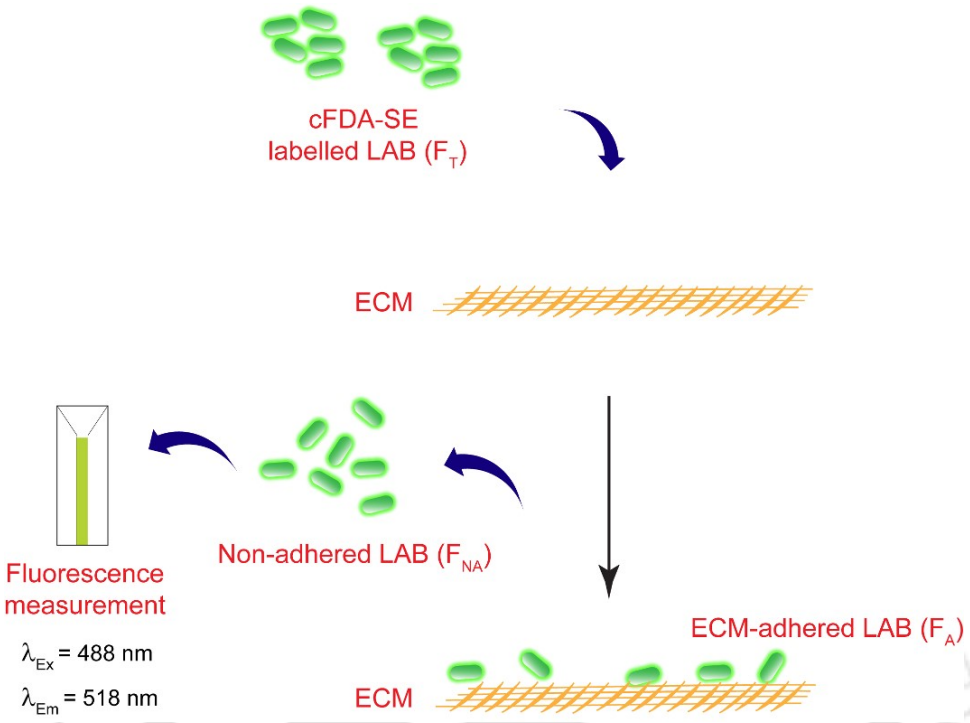

Figure 3.1. Schematic representation of the experimental protocol for fluorescence-based adhesion assay on ECM.

Where F* represents the quantitative measure of adhered cells of *L. rhamnosus* GG on ECM molecules. All the experiments were performed in triplicates and mean and standard deviation was calculated. The adhered cells were also observed under fluorescence microscope (Eclipse Ti-U, Nikon, USA) with a filter that allowed blue light excitation at 465 nm to 495 nm for cFDA-SE stained cells. A schematic for the protocol for fluorescence-based adhesion assay is indicated in Figure 3.1.

3.2.3.3. Flow cytometry analysis of adhesion to ECM

The adhesion of *L. rhamnosus* GG and the strains of *L. plantarum* to collagen and mucin was evaluated by flow cytometry (FCM), which was performed on a FACS Calibur flow cytometer (Becton-Dickinson Immunocytometry Systems, San Jose, CA, USA) equipped with a 15-mW, 488 nm, air-cooled argon ion laser. LAB cells were grown for 6 h, harvested and labelled with cFDA-SE as mentioned in an earlier study (Singh *et al.,* 2012a). A 100 µL aliquot of cFDA-SE labelled bacterial cells (10^8 CFU/mL) was then incubated overnight at 4 °C in microtitre plate wells coated with collagen or mucin. In another set of microtitre plate wells devoid of collagen or mucin,

cFDA-SE labelled bacteria was incubated for the same period of time and was considered as control cells. Subsequently, the supernatant containing non-adhered LAB cells were aspirated from both sets of wells and diluted in 1.0 mL filter-sterilized PBS (pH 7.4). The aspirated cells were subjected to FCM analysis at a low flow rate setting and the instrument was adjusted to acquire 30,000 events. Unlabelled cells were used to compensate for cellular autofluoresence and to set the appropriate voltage and threshold parameters. Forward-angle light scatter (FSC) vs. side scatter (SSC) plot were analyzed to detect bacterial cells. Detection of green fluorescence of cFDA stained cells was accomplished through FL1 channel (band pass filter of 530 nm). Data acquisition was performed with CellQuest Pro software (BD CellQuestTM Pro Version 6.0, Becton-Dickinson, USA). Data analysis was performed with the assistance of FCS Express 5.0 (DeNovo Software Inc.).

3.2.4. Dose-dependent adhesion of L. plantarum strains to collagen and mucin

L. rhamnosus GG, *L. plantarum* strains CRA21, CRA38 and CRA52 and *S. aureus* MTCC 96 were grown overnight, harvested and labelled with cFDA-SE as described earlier. To ascertain the dose-dependent adhesion of the strains, 100 µL aliquot of cFDA-SE labelled cells of the bacterial strains were added in the range of 2.0 $\log_{10}$ CFU per well to 8.0 $\log_{10}$ CFU per well to collagen- or mucin-coated 96-well microtitre plate wells and a fluorescence-based adhesion assay for each cell concentration was performed as described in section 3.2.2.2. The solution fluorescence of a 100 µL aliquot of the cFDA-SE-labelled LAB strains of varying cell number (2.0 $\log_{10}$ CFU per well to 8.0 $\log_{10}$ CFU per well) was measured in a multiplate reader (Infinite M200, Tecan, Austria) and considered as total fluorescence (F_T). For each LAB strain, the dose-dependent adhesion onto collagen- or mucin-coated wells was quantified by determining F_A using the following expression:

$$F_A = F_T - F_{NA} \quad .....3.3.$$

Subsequently, for every LAB strain and at each cell number, adhesion onto collagen- or mucin-coated wells was ascertained by the following expression:

$$\text{Adhesion (\%)} = \frac{F_A}{F^*} \times 100 \quad .....3.4.$$

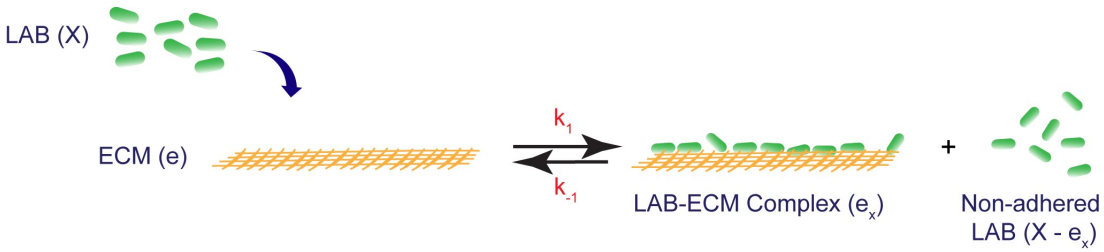

Figure 3.2. Schematic representation of the adhesion process of LAB cells on ECM molecule, collagen or mucin.

The adhesion percentage was considered to represent the LAB-ECM complex (e_x). Each experiment was performed in triplicate and the result was represented as mean ± standard deviation. Subsequently, the maximum number of adhered bacteria (e_m) and the dissociation constant (k_d) for the adhesion process was essentially ascertained by the method described previously (Lee *et al*., 2000) and is as follows:

A schematic for the interaction between bacterial cells and ECM molecules is indicated in Figure 3.2. There are two assumptions in the adhesion of bacteria on ECM molecules:

1. The adhesion process between the bacterial cells and ECM molecules is in equilibrium. This condition may be met if the tested strain do not penetrate ECM molecules during the duration of the experiment.
2. Additionally, it is assumed that the concentration of the bacterial culture remained the same during the course of the study, which implies that the concentration of the bacterial culture could be considered to be equal to the initial bacterial concentration. This condition can be met if the total number of bacterial cells far exceed the number of bacterial cells adhering onto the ECM molecules.

In the simple adhesion model illustrated in Figure 3.2, if X is the concentration of the bacterial culture added, e is the initial ECM molecule concentration and e_x is the concentration of the LAB-ECM complex, then the concentration of free ECM molecule will be ($e - e_x$). Considering that the interaction between LAB and ECM is in equilibrium, the dissociation constant for the adhesion process, k_d, can be expressed as follows:

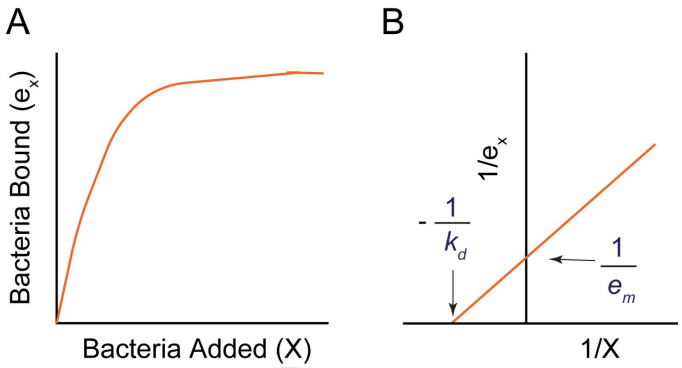

Figure 3.3. (A) Representative plot of bacteria bound to ECM against the total bacteria used for the assay (B) Double reciprocal plot for (A).

$$k_d = \frac{k_{-1}}{k_1} \quad .....3.5.$$

On inserting the variables for the forward and reverse rate constants in equation 3.5:

$$k_d = \frac{(e - e_x).X}{e_x} \quad .....3.6.$$

On rearrangement of equation 3.6,

$$e_x = \frac{e.X}{(k_d + X)} \quad .....3.7.$$

When the number of total bacterial cells (X) far exceed the dissociation constant (k_d), e_x approaches e and is considered as maximum number of adhered bacterial cells (e_m).

On replacing e with e_m in equation 3.7:

$$e_x = \frac{e_m.X}{(k_d + X)} \quad .....3.8.$$

On plotting bacteria bound (e_x) against total concentration of bacteria (X) used for the assay, a rectangular hyperbolic curve is obtained (Figure 3.3A).

The reciprocal of equation 3.8 yields:

$$\frac{1}{e_x} = \frac{1}{e_m} + \frac{k_d}{e_m.X} \quad .....3.9.$$

On plotting $1/e_x$ against 1/X, the intercept on the ordinate ($1/e_m$) and the abscissa ($-1/k_d$) can be used to ascertain the adhesion process parameters e_m and k_d, respectively (Figure 3.3B).

3.2.5. Inhibition of S. aureus MTCC 96 adhesion onto ECM by L. plantarum

Cells of *L. plantarum* strains CRA21, CRA38, CRA52 and *L. rhamnosus* GG were grown in MRS and cells of *S. aureus* MTCC 96 were grown in BHI broth for 6 h each. The cells were then harvested by centrifugation, washed and resuspended in sterile PBS to an OD_{600} of 1.0. Cells of *S. aureus* MTCC 96 were then labelled with cFDA-SE following the protocol described in an earlier study (Singh *et al.,* 2012a) and its fluorescence intensity was measured (F_T) using a multi-well plate reader (Infinite M200, Tecan, Austria). To determine the ability of LAB strains to inhibit *S. aureus* adhesion, three experimental models namely exclusion, competition and displacement were adopted. In case of exclusion, cells of LAB (6.0 $\log_{10}$ CFU per well) were first added to 96-well microtitre plates (Maxisorp, Nunc) coated with either collagen (50 µg/mL) or mucin (500 µg/mL) and incubated for 1 h, followed by washing and removal of non-adherent LAB by sterile PBS. Subsequently, cFDA-SE labelled cells of *S. aureus* MTCC 96 (6.0 $\log_{10}$ CFU per well) were added to collagen- or mucin-coated wells bearing adherent LAB and further incubated for 1 h. In competitive inhibition assays, LAB cells as well as cFDA-SE labelled cells of *S. aureus* MTCC 96 (6.0 $\log_{10}$ CFU per well for each) were added simultaneously to ECM-coated wells and incubated for 2 h. In the displacement mode, cFDA-SE labelled *S. aureus* MTCC 96 cells in PBS (6.0 $\log_{10}$ CFU per well) were added to ECM-coated wells and incubated for 1 h. The wells were then washed with sterile PBS to remove the non-adherent bacteria. Subsequently, cells of LAB (6.0 $\log_{10}$ CFU per well) were added to the wells and incubated for 1 h. The non-adherent *S. aureus* cells from all the experimental samples were aspirated from ECM-coated wells and their fluorescence intensity (F_{NA}) was measured using a multi-well plate reader (Infinite M200, Tecan, Austria). Adhesion of *S. aureus* for each experimental setup in collagen and mucin coated wells was determined by calculating the difference between F_T and F_{NA}, respectively. The results were represented as percentage inhibition by comparing the adhesion obtained for each mode of inhibition with that obtained without addition of any *L. plantarum* cells. Each experiment was performed in triplicate and the result was represented as mean ±

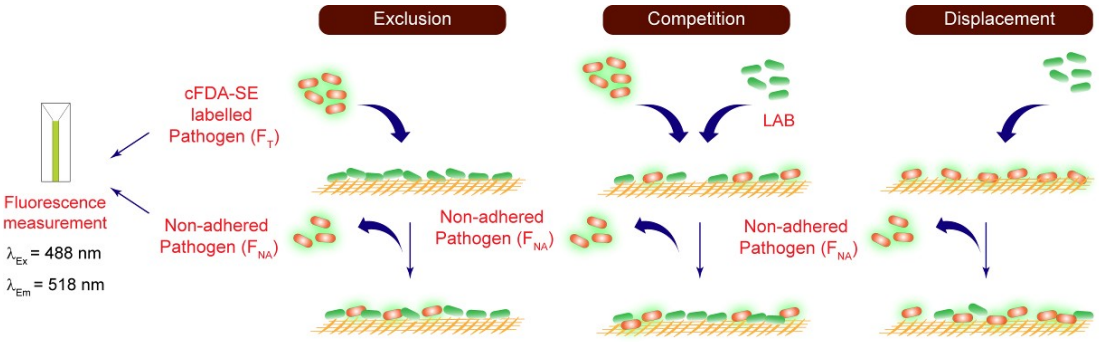

Figure 3.4. Schematic representation for the experimental protocol of the adhesion inhibition of model pathogen by LAB cells on ECM.

standard deviation. The adhered cFDA-SE labelled *S. aureus* cells in the three adhesion modes were also observed under fluorescence microscope (Eclipse Ti-U, Nikon, USA) with a filter that allowed blue light excitation for cFDA-SE. A schematic for the protocol of LAB cell-mediated adhesion inhibition is indicated in Figure 3.4.

3.2.6. Effect of plantaricin A extract on S. aureus MTCC 96 cells adhering on collagen and mucin

Initially, bacteriocin producing *L. plantarum* strains CRA21, CRA38 and CRA52 were grown overnight in 10.0 mL sterile MRS broth, followed by centrifugation to separate the bacterial cells. The supernatant was then extensively dialyzed in a 1.0 kDa MWCO dialysis bag, followed by freeze drying and reconstitution in 1.0 mL of sterile PBS. The reconstituted fraction was considered as a crude plantaricin A extract. The bacteriocin activity in this extract was ascertained by spot-on-lawn method and expressed as arbitrary units per mL (AU/mL) as described in a previous study (Singh *et al.*, 2012a). Prior to testing the effect of plantaricin A extract on *S. aureus* cells adhering onto collagen and mucin, the target cells were labelled with cFDA-SE following the protocol described in an earlier study (Singh *et al.*, 2012a) and its fluorescence intensity was measured (F_T) using a multi-well plate reader (Infinite M200, Tecan, Austria). Subsequently, the cells were allowed to adhere onto collagen or mucin coated wells for 2 h followed by aspiration of non-adhered cells and washing to remove sparsely adhered cells. To each well, a crude plantaricin A extract obtained from the *L. plantarum* strains was added at a final concentration of 400 AU/mL. Following incubation for 2 h, the supernatant was gently aspirated, centrifuged to remove any cells and the fluorescence intensity of the collected supernatant (F_S) was measured

using a multi-well plate reader (Infinite M200, Tecan, Austria). The results were expressed as percentage leakage by comparing F_S to F_T in the experiments involving plantaricin A extract from each *L. plantarum* strain. Each experiment was performed in triplicate and the result was represented as mean ± standard deviation. The adhered cFDA-SE labelled *S. aureus* cells following treatment with plantaricin A extract were also observed under fluorescence microscope (Eclipse Ti-U, Nikon, USA) with a filter that allowed blue light excitation for cFDA-SE.

3.3. Results and Discussion

3.3.1. Adhesion to collagen and mucin by L. plantarum strains

In an earlier study, *L. plantarum* strains were isolated from various indigenous sources and were characterized as potent bacteriocin producers (Singh *et al.,* 2012a). Further in the present study, the LAB strains were also observed to possess archetypical probiotic attributes (Chapter 2). With an aim to expand the prospect of these strains, it was envisaged that estimation of the adhesion potential of the strains to extracellular matrix (ECM) would be important, as adhesion to ECM molecules such as collagen and mucin is considered as a cardinal feature of probiotic strains (Lebeer *et al.,* 2008). The propensity of the pathogen *S. aureus* to colonize the intestine in conjunction with its ability to adhere onto ECM molecules is a serious healthcare concern and can be implicated in various ailments (Acton *et al.,* 2009; Bhalla *et al.,* 2007; Foster *et al.,* 2014; Gries *et al.,* 2005; Hansen *et al.,* 2006). In this context, probiotic LAB strains having an ability to adhere onto ECM such as collagen and mucin could emerge as an interesting therapeutic intervention to prevent invasion of ECM by *S. aureus*. In order to vindicate the potential of the *L. plantarum* strains to adhere onto ECM, conventional *in vitro* binding assays with collagen and mucin were pursued. Prior to the binding assays, the *L. plantarum* strains were labelled with the fluorescent dye cFDA-SE, based on previous investigations, which established that cFDA-labelling of LAB strains retained the viability of the cells and did not affect their adhesion in *in vitro* cell culture models (Fuller *et al.,* 2000; Singh *et al.,* 2012). It may be mentioned that for the adhesion assays, *L. rhamnosus* GG was selected as a standard probiotic strain (Doron *et al.,* 2005) for comparative evaluation. Collagen binding assay revealed that the native LAB strains *L. plantarum* CRA21, CRA38 and CRA52 displayed high *in vitro* adhesion to human collagen type I (95%-97% adhesion potential) and was on par with the standard probiotic strain *L. rhamnosus* GG whose adhesion potential was

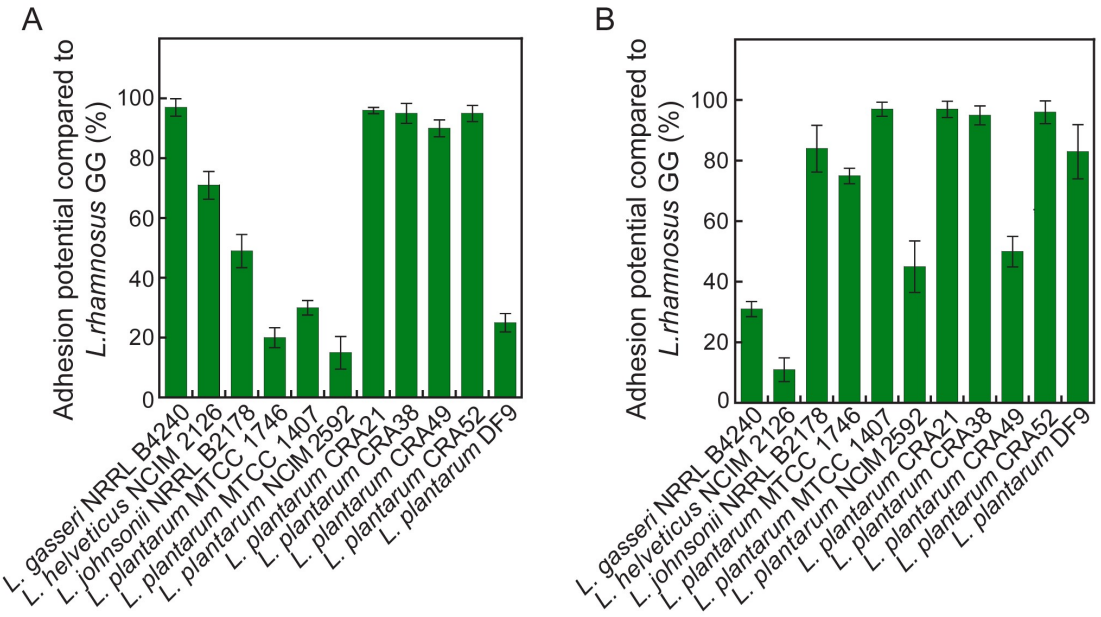

Figure 3.5. Fluorescence-based adhesion assay of *L. plantarum* strains onto (A) collagen and (B) mucin.

considered to be 100% (Figure 3.5A). Comparative analysis also indicated that *L. plantarum* DF9 demonstrated considerably lower adhesion potential to collagen (Figure 3.5A). Interestingly, the trend of *in vitro* adhesion to collagen demonstrated by the *L. plantarum* strains was also observed with crystal violet staining (Figure A3.1A in Appendix). Further, the native LAB isolates, *L. plantarum* CRA21, CRA38 and CRA52, which had earlier displayed considerable adhesion to collagen, were also observed to exhibit high *in vitro* adhesion potential to mucin, which was comparable to that observed for *L. rhamnosus* GG and *L. plantarum* MTCC 1407 (Figure 3.5B). It may be mentioned that amongst the *L. plantarum* strains, CRA49 and DF9 revealed lower adhesion potential to mucin. The trend of adhesion potential of *L. plantarum* strains to mucin observed by fluorescence-based method was also corroborated by crystal violet staining (Figure A3.1B in Appendix). In the context of collagen and mucin adhesion potential, the minor variations in the results obtained in the fluorescence-based assay and crystal violet staining method could perhaps be attributed to the variations in the sensitivity of the methods as well as the inherent differences in ECM binding amongst the strains. In the present study, cFDA-SE labelling rendered a convenient analytical tool and enabled tracking of the adhesion of *L. plantarum* strains onto collagen and mucin. The manifestation of bright green fluorescent cells of the

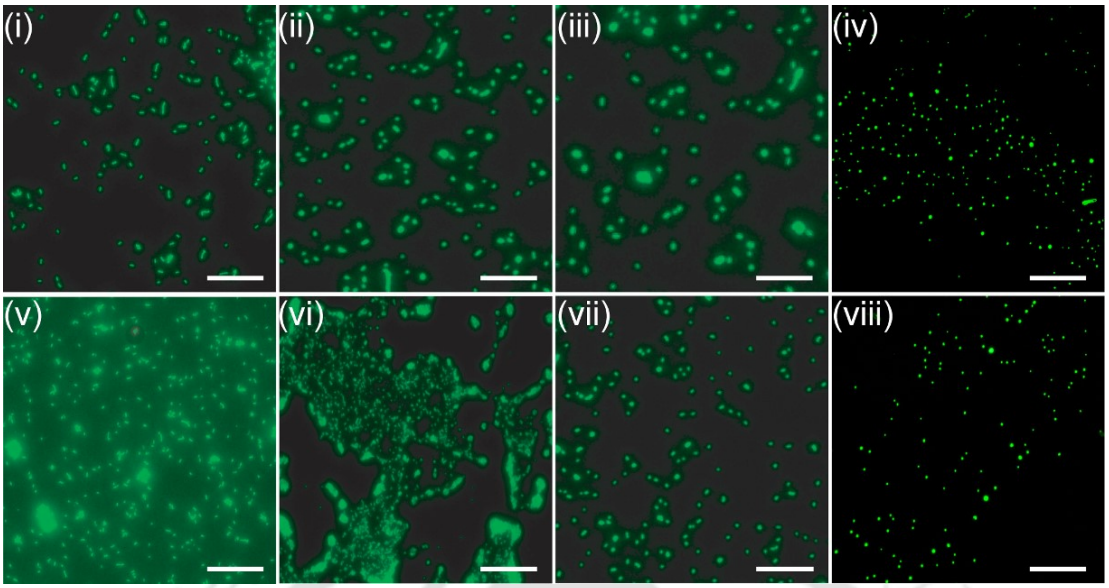

Figure 3.6. Fluorescence microscope analysis of cFDA-labelled LAB adhered onto (i-iv) collagen and (v-viii) mucin. Panels: (i and v) *L. rhamnosus* GG (ii and vi) *L. plantarum* CRA21, (iii and vii) *L. plantarum* CRA38, (iv and viii) *L. plantarum* CRA52. Scale bar for the images is 200 µm.

L. plantarum cells adhering onto the selected ECM (Figure 3.6, panels i-viii) provided additional qualitative evidence for their adhesion.

The adhesion of LAB strains onto collagen and mucin was also investigated by flow cytometry. In these experiments, the LAB strains were labelled with cFDA-SE prior to adhesion assays. From the contour plots obtained in flow cytometry, the essential observation was that the median of the cell population shifted when the non-adhered cells were analyzed as compared to the initial cells (total cells) that were subjected to adhesion on collagen and mucin (Figure 3.7). This observation was unequivocal across all the LAB strains tested and was quantitatively verified by statistical analysis through comparison of the median for the cell populations (Table 3.1). Collectively, the shift in the median in contour plots (Figure 3.7) in conjunction with quantitative analysis of the median (Table 3.1) reflected the propensity of the native *L. plantarum* strains to adhere onto collagen and mucin and corroborated the earlier results (Figure 3.5A-3.5B).

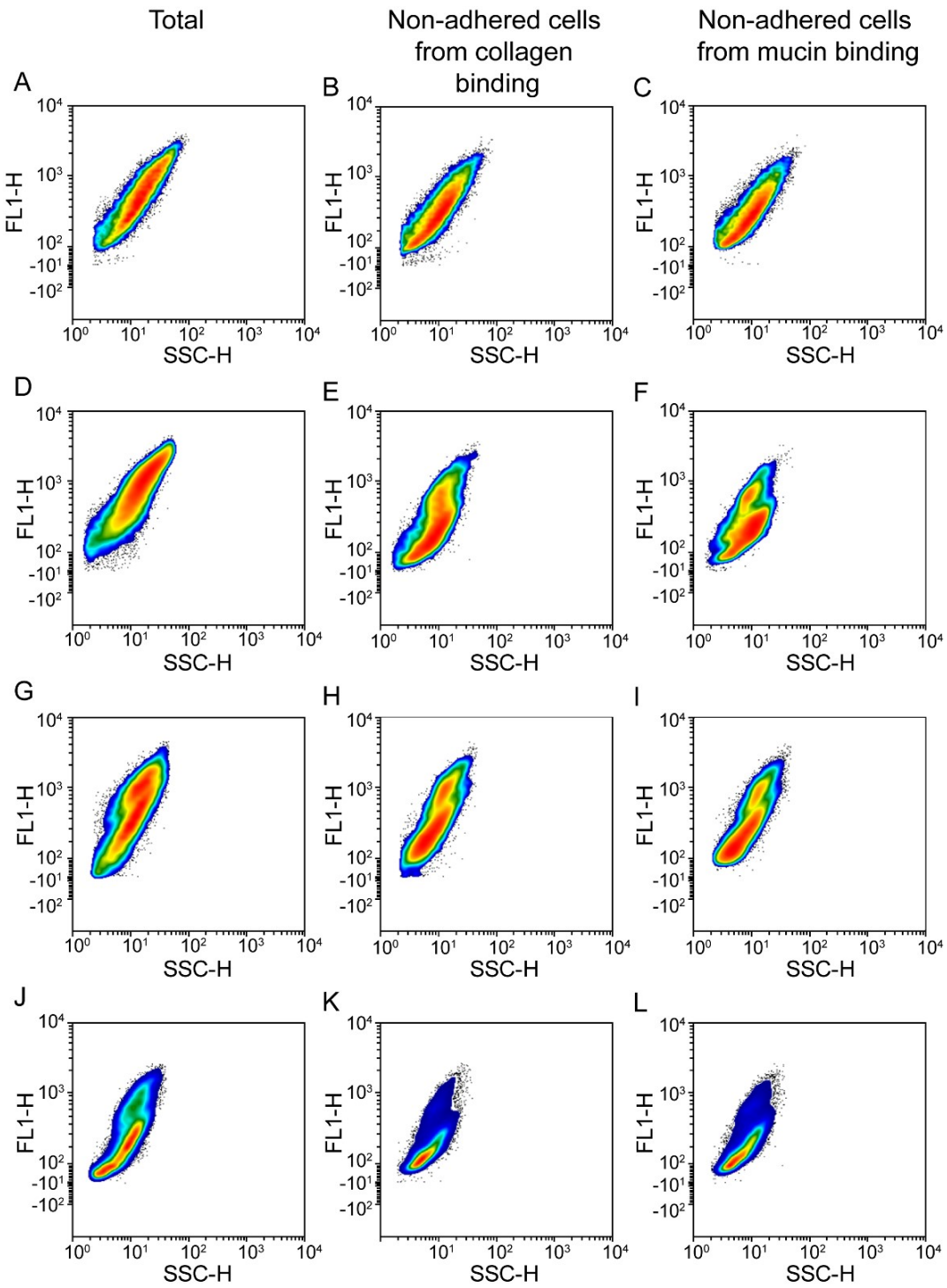

Figure 3.7. Flow cytometry analysis of adhesion of LAB strains onto collagen and mucin adhesion assay. Panels: (A-C) *L. rhamnosus* GG, (D-F) *L. plantarum* CRA21, (G-I) *L. plantarum* CRA38 and (J-L) *L. plantarum* CRA52.

Table 3.1. Analysis of median for various cell populations used in flow cytometry to study adhesion of LAB strains onto collagen and mucin.

LAB strain	Cell population	Median
L. rhamnosus GG	Cells labelled with cFDA-SE	523.3
	Non-adhered cells from collagen binding	321.97
	Non-adhered cells from mucin binding	294.27
L. plantarum CRA21	Cells labelled with cFDA-SE	736.53
	Non-adhered cells from collagen binding	264.16
	Non-adhered cells from mucin binding	268.96
L. plantarum CRA38	Cells labelled with cFDA-SE	513.97
	Non-adhered cells from collagen binding	299.61
	Non-adhered cells from mucin binding	261.8
L. plantarum CRA52	Cells labelled with cFDA-SE	276.32
	Non-adhered cells from collagen binding	165.48
	Non-adhered cells from mucin binding	182.69

3.3.2. Quantitative analysis of binding to collagen and mucin

The subsequent endeavor was to accomplish a comparative and quantitative appraisal of the *in vitro* adhesion of *L. plantarum* strains onto ECM and to determine their binding affinities. On the basis of their adhesion potential on ECM, *L. plantarum* strains CRA21, CRA38 and CRA52 were selected for these experiments along with the reference probiotic *L. rhamnosus* GG. A fluorescence-based adhesion assay on collagen and mucin indicated a systematic increase in adhesion for all the tested strains, with increasing cell concentrations up to 6.0 $\log_{10}$ CFU per well (Figure 3.8). At higher cell concentrations (7.0 and 8.0 $\log_{10}$ CFU per well), the increase in adhesion was

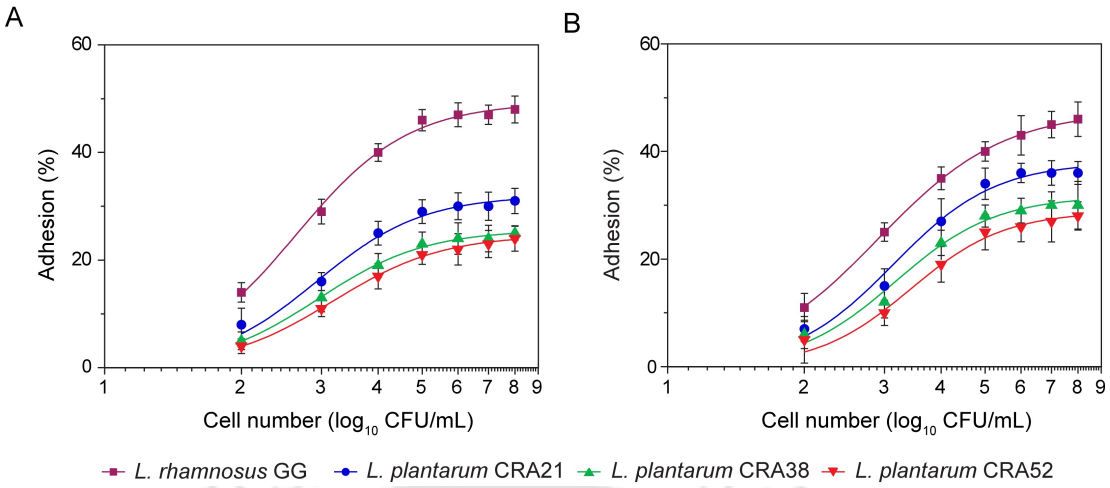

Figure 3.8. Concentration-dependent adhesion of LAB strains onto (A) collagen and (B) mucin.

minimal, indicating a saturation effect (Figure 3.8). At the highest initial cell concentration of 8.0 $\log_{10}$ CFU per well, the maximum adhesion on collagen was demonstrated by *L. rhamnosus* GG (48%) followed by the *L. plantarum* strains CRA21 (31%), CRA38 (25%) and CRA52 (24%), respectively (Figure 3.8A). A similar trend was also observed in case of adhesion on mucin (Figure 3.8B).

When the reciprocal plots were analyzed, a linear relationship emerged in case of *L. rhamnosus* GG (Figure 3.9A-B). However, in case of the *L. plantarum* strains, two distinct linear sections could be discerned (Figure 3.9C-H). This observation suggested that the *L. plantarum* strains perhaps display two exclusive modes of binding to collagen and mucin. Presumably, one of them represents adhesion for a high bacterial cell number, which may be attributed to non-specific interactions such as van der Waals and hydrophobic interactions. On the other hand, the other linear region of the plot accounts for adhesion to collagen and mucin at lower cell concentrations, which is represented by a specific adhesion mechanism. This bimodal phenomenon of adhesion onto ECM by LAB strains has been described in earlier studies (Lee *et al.,* 2000; Vesterlund *et al.,* 2006). The comparative adhesion potential of the LAB strains onto ECM was also ascertained through estimation of quantitative parameters such as maximum number of bacteria bound to ECM (e_m) and the dissociation constant (k_d). In case of adhesion to collagen, the essential observation was that the maximum number of adhered cells for all the LAB strains was comparable (Table 3.2). Further, the dissociation constant of the tested LAB strains for the adhesion process onto collagen

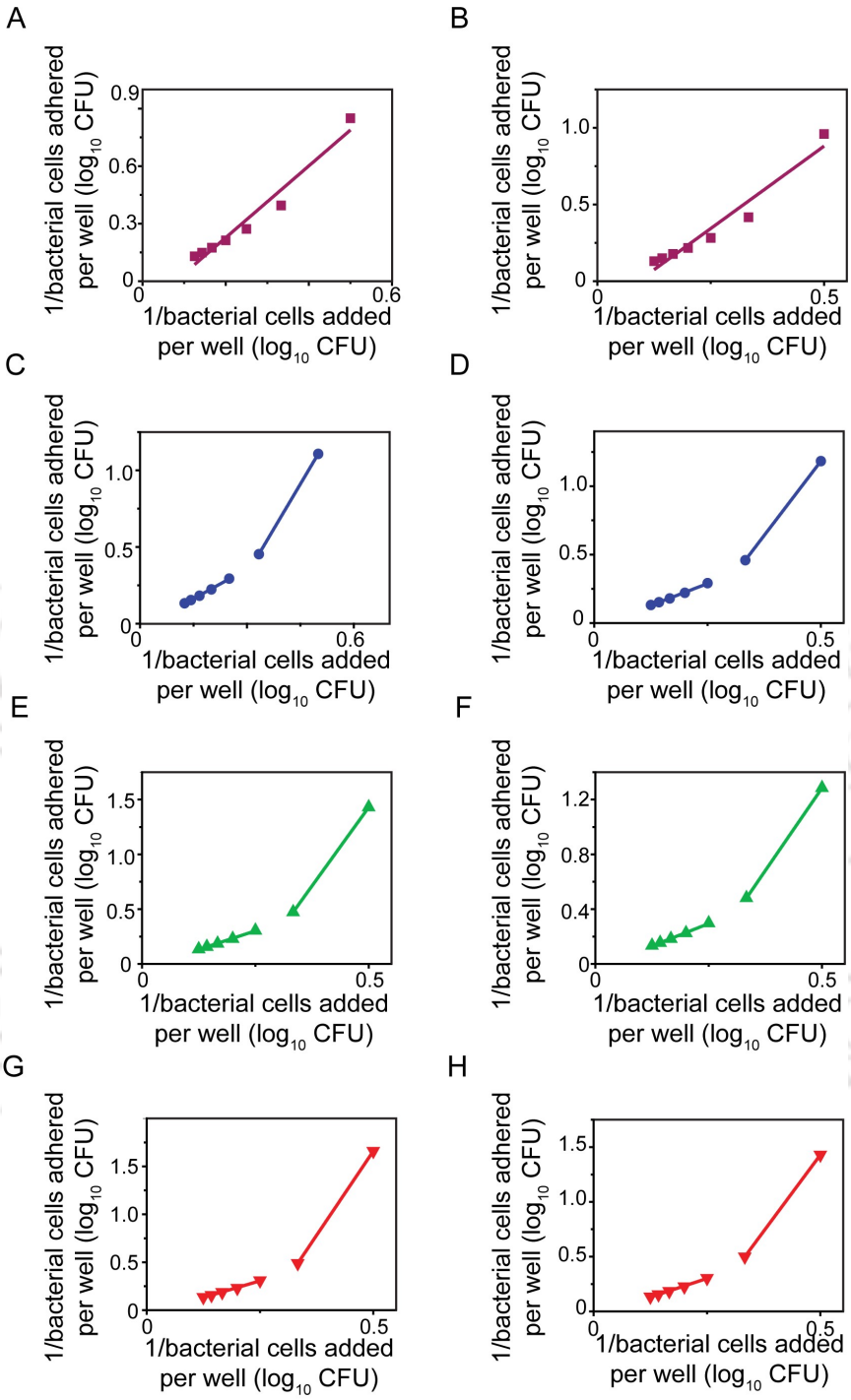

Figure 3.9. Double reciprocal plot for concentration-dependent adhesion of LAB strains onto (A, C, E and G) collagen and (B, D, F and H) mucin. Panels: (A and B) *L. rhamnosus* GG, (C and D) *L. plantarum* CRA21, (E and F) *L. plantarum* CRA38, (G and H) *L. plantarum* CRA52.

Table 3.2. Quantitative parameters for the adhesion process of LAB strains on collagen and mucin

LAB strains	Adhesion on collagen		Adhesion on mucin	
	Maximum number of adhered bacteria (e_m) $\log_{10}$ CFU per well	Dissociation constant (k_d) $\log_{10}$ CFU per well	Maximum number of adhered bacteria (e_m) $\log_{10}$ CFU per well	Dissociation constant (k_d) $\log_{10}$ CFU per well
L. rhamnosus GG	2.26	9.25	1.78	8.48
L. plantarum CRA21	2.43	9.97	1.32	7.97
L. plantarum CRA38	2.22	9.9	1.16	7.83
L. plantarum CRA52	2.02	9.94	1.00	7.58

was also observed to be equivalent and was on par with the standard *L. rhamnosus* GG strain (Table 3.2). In case of mucin, the maximum number of adhered cells was observed to be highest for *L. rhamnosus* GG (1.78 $\log_{10}$ CFU per well), while it decreased progressively for the *L. plantarum* strains. Interestingly, the dissociation constant for the adhesion process to mucin was observed to be lowest for *L. plantarum* CRA52 (k_d = 7.58 $\log_{10}$ CFU per well), which suggested that this strain exhibited superior adhesion to mucin as compared to the other tested LAB strains. The adhesion process parameters for the tested model pathogens were also ascertained (Table A3.1 in Appendix).

3.3.3. In vitro inhibition of S. aureus adhesion to ECM by L. plantarum strains

Colonization of the intestine by *S. aureus* due to its ability to adhere onto ECM molecules has serious healthcare implications and is responsible for chronic infections (Senn *et al.*, 2016; Lin *et al.*, 2010; Boyce *et al.*, 2005). The results obtained in the comparative adhesion assays were encouraging (Figure 3.8) and suggested that the *L. plantarum* strains could perhaps be explored in inhibiting adhesion of model gut pathogens onto ECM. To this end, standard *in vitro* adhesion assays on collagen and mucin were conducted in the three formats viz. exclusion, competition and displacement. A fluorescence-based method revealed that *L. rhamnosus* GG, *L. plantarum* CRA21, *L. plantarum* CRA38 and *L. plantarum* CRA52 strains could exclude *S. aureus* MTCC 96 from binding to collagen (Figure 3.10A). Amongst the LAB strains, *L. plantarum* CRA21 rendered significant inhibition of adhesion of

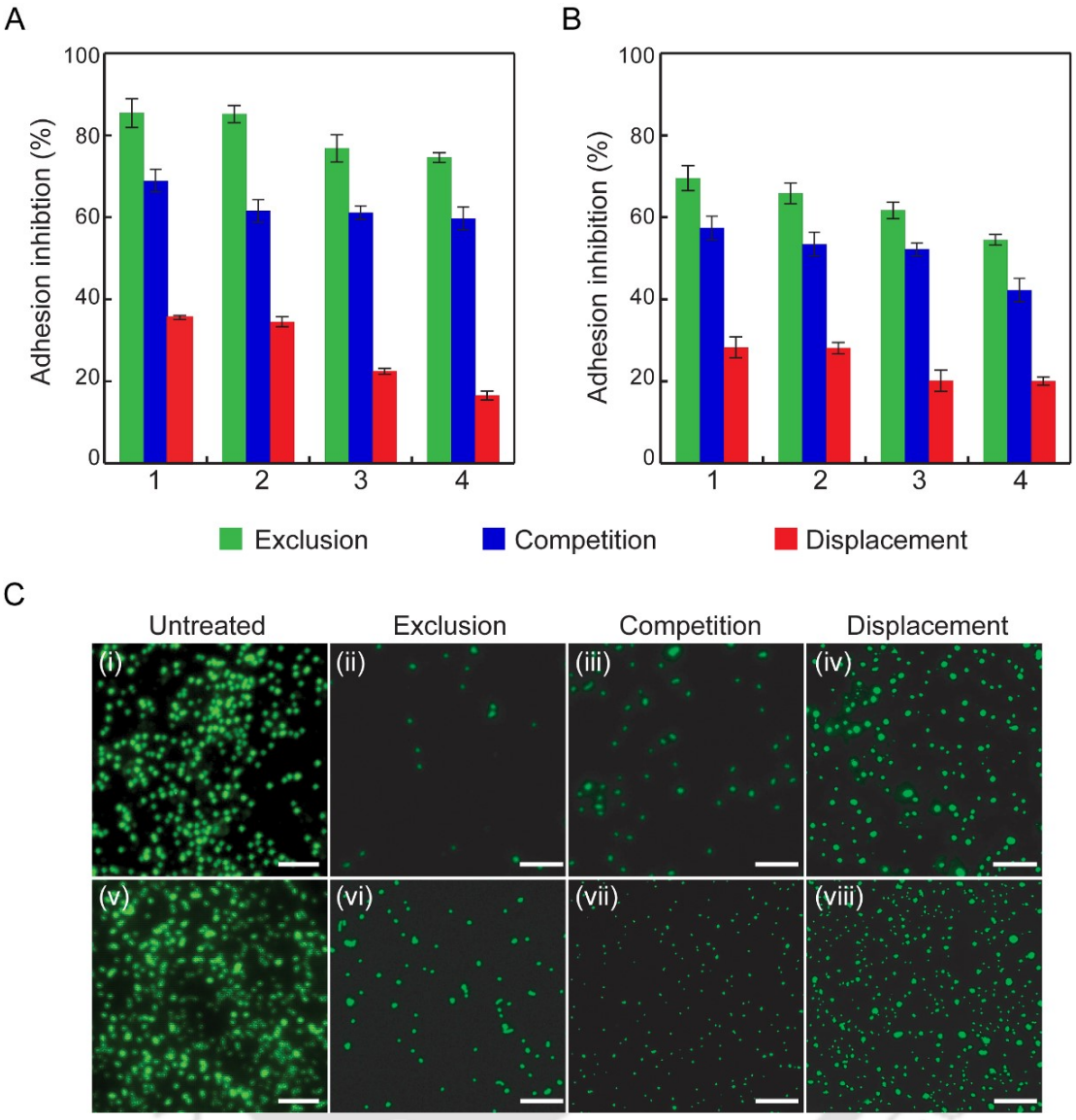

Figure 3.10. Inhibition of *S. aureus* MTCC 96 adhesion onto (A) collagen and (B) mucin by *L. plantarum* strains. LAB strains: 1. *L. rhamnosus* GG, 2. *L. plantarum* CRA21, 3. *L. plantarum* CRA38, 4. *L. plantarum* CRA52. (C) Fluorescence microscope analysis to study the inhibition of *S. aureus* MTCC 96 adhesion onto (i-iv) collagen and (v-viii) mucin by *L. plantarum* CRA21. Scale bar for the images is 200 µm.

S. aureus cells (85%), which was on par with that of the standard probiotic *L. rhamnosus* GG. In the exclusion mode of adhesion assay, addition of LAB onto collagen coated wells precedes addition of *S. aureus* cells. Based on the strong adhesion parameters of *L. plantarum* strains onto collagen (Table 3.2), it is expected that these strains would exhibit efficient colonization of ECM, which perhaps resulted in the reduced ability of *S. aureus* cells to adhere onto collagen. It can be presumed that

the ability of the *L. plantarum* strains to prevent adhesion of *S. aureus* cells onto collagen is also likely to be influenced by a combined effect of the adhesion process parameters (e_m and k_d). In the exclusion model, it can be conceived that the initial strong adhesion of LAB cells onto collagen as indicated by the low dissociation constant (k_d) of the adhesion process could be critical for efficient exclusion of *S. aureus* cells added subsequently. The differences observed in the ability to exclude *S. aureus* adhesion onto collagen by the bacteriocin producing *L. plantarum* strains may be attributed to the differences in their inherent binding parameters (e_m and k_d), which could be captured in the experiments (Table 3.2 and Table A3.1 in Appendix). Further, in the exclusion mode, the probability of *S. aureus* cells adhering onto collagen would be largely governed by the ability to displace initially colonizing LAB, which, in turn, would depend on the magnitude of the binding affinity of *S. aureus* with collagen (k_d). To this end, it was observed that in case of collagen, the dissociation constant for *S. aureus* MTCC 96 binding with collagen (k_d = 12.85 $\log_{10}$ CFU per well), was distinctly higher (Table A3.1 in Appendix) than that obtained in case of the *L. plantarum* strains (Table 3.2). This perhaps provides a probable explanation for the strong inhibition of *S. aureus* adhesion on collagen initially colonized by LAB strains. A similar phenomenon was also observed in case of inhibition of *S. aureus* MTCC 96 adhesion onto mucin by LAB strain in the exclusion mode (Figure 3.10B). However, the inhibition of *S. aureus* MTCC 96 adhesion onto mucin was comparatively less than that observed in case of collagen in the exclusion mode of assay (Figure 3.10B).

In the competitive mode of adhesion inhibition, the magnitude of inhibition of *S. aureus* MTCC 96 adhesion was observed to be highest for *L. rhamnosus* GG (69%) followed by *L. plantarum* CRA21 (62%), *L. plantarum* CRA38 (60%) and *L. plantarum* CRA52 (58%), respectively (Figure 3.10A). In case of competition, the dissociation constant (k_d) is perhaps critical as it determines the binding affinity of the cells with the ECM molecules collagen and mucin. Notwithstanding the higher e_m values for *S. aureus* as compared to LAB strains (Table A3.1 in Appendix and Table 3.2), the significant difference in the dissociation constant (k_d) obtained for the LAB strains as compared to *S. aureus* cells (Table 3.2 and Table A3.1 in Appendix) perhaps has an overriding effect and renders the *L. plantarum* strains to outcompete *S. aureus* in the adhesion assays conducted in competition mode. A similar phenomenon was observed in the competition mode in case of mucin (Figure 3.10B). In the displacement mode of adhesion assay, it was observed that the inhibition of adhesion of *S. aureus*

MTCC 96 cells to ECM-coated wells was considerably lower than that of the other tested interactions (Figure 3.10A-3.10B). Initial colonization of ECM by *S. aureus* is effective as the bacterium is able to occupy majority of the binding sites. Subsequent addition of LAB strains is less effective in overcoming the high surface coverage of the ECM by *S. aureus* cells owing to the reduced ability of the added LAB cells to displace *S. aureus* cells, a phenomenon, which can be largely ascribed to the inferior e_m obtained for the LAB strains as compared to *S. aureus* MTCC 96 (Table 3.2 and Table A3.1 in Appendix).

Fluorescence microscope analysis revealed that a large number of cFDA-SE labelled *S. aureus* MTCC 96 cells could adhere onto ECM (Figure 3.10C, panel i and panel v). However, in presence of *L. plantarum* CRA21, adhesion of *S. aureus* MTCC 96 cells onto ECM was observed to be reduced in the three tested models of adhesion assay (Figure 3.10C, panels ii-iv, panels vi-viii). It may be mentioned here that a similar trend of inhibition of adhesion by the *L. plantarum* strains in the three tested formats was also observed in case of model target bacteria *L. monocytogenes* Scott A and *E. faecalis* MTCC 439 (Figure 3.11).

3.3.4. Effect of bacteriocin extract from L. plantarum strains on ECM-adhering target bacteria

The native isolates of *L. plantarum* used in the present study were earlier characterized as potent plantaricin A producers displaying activity against the target bacteria *S. aureus* MTCC 96, *L. monocytogenes* Scott A and *E. faecalis* MTCC 439 (Singh *et al.,* 2012a). Literature reports suggest that these target bacteria are known to colonize ECM and are implicated in disruption of ECM-related barrier functions (Gries *et al.,* 2005; Flemming and Ackermann 2007). Hence it was envisaged that treatment with plantaricin A is likely to result in a significant loss of viability of these bacterial strains, which in turn, would curtail their ability to adhere and colonize ECM. To this end, the model strains were allowed to adhere onto collagen or mucin-coated wells in separate sets, followed by addition of a crude sample of plantaricin A extract (400 AU/mL) from the *L. plantarum* strains CRA21, CRA38 and CRA52. In these experiments, the target bacterial cells were pre-labelled with the fluorescent dye cFDA-SE, which enabled us to pursue a fluorescence-based dye leakage assay to ascertain the effect of the bacteriocin on ECM-adhered cells.

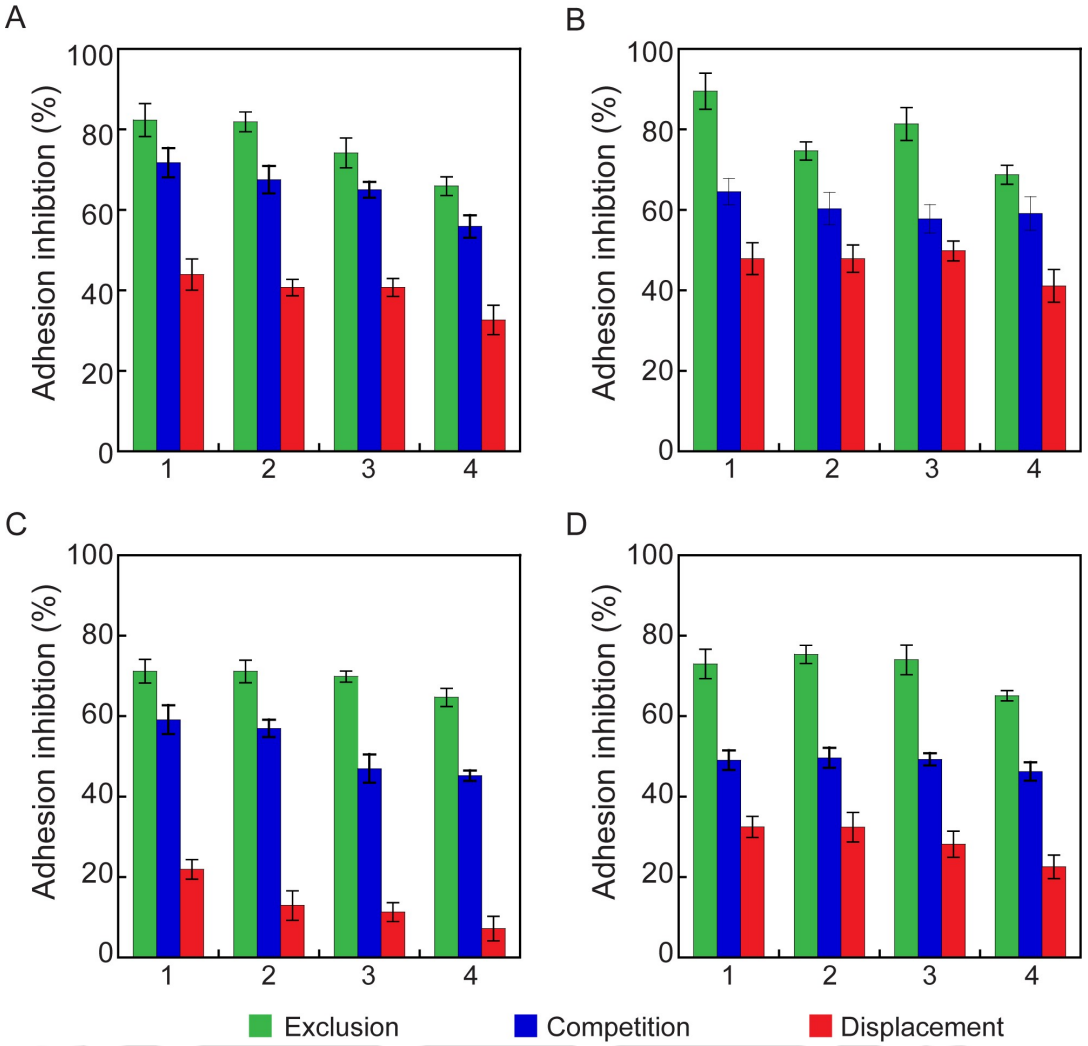

Figure 3.11. Inhibition of adhesion of target bacteria onto (A and C) collagen and (B and D) mucin by *L. plantarum* strains. Panels: (A-B) Target bacteria is *L. monocytogenes* Scott A and (C-D) Target bacteria is *E. faecalis* MTCC 439. LAB strains: 1. *L. rhamnosus* GG, 2. *L. plantarum* CRA21, 3. *L. plantarum* CRA38 and 4. *L. plantarum* CRA52.

Interestingly, exposure of collagen-adhering bacterial cells to plantaricin A extracts resulted in notable leakage of cFDA-SE (Figure 3.12A), which can perhaps be attributed to the signature membrane-directed activity of plantaricin A (Singh *et al.,* 2012a). Upon treatment with the plantaricin A extract obtained from the LAB strains, the maximum extent of dye leakage was observed for *L. monocytogenes* Scott A, given the strong anti-listerial activity associated with the bacteriocin (Singh *et al.,* 2012a). Amongst the LAB strains, plantaricin A extract obtained from *L. plantarum* CRA52 displayed the highest anti-listerial activity on collagen-adhered cells as evident from the

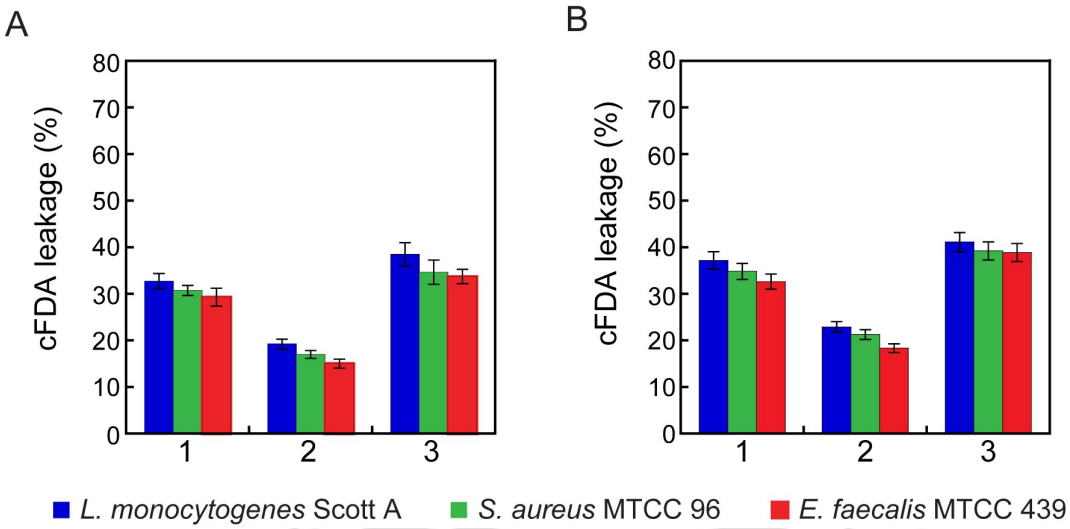

Figure 3.12. cFDA-SE leakage assay on (A) collagen- and (B) mucin-adhered target bacteria treated with plantaricin A extract (400 AU/mL) from *L. plantarum* strains. LAB strains: 1. *L. plantarum* CRA21, 2. *L. plantarum* CRA38 and 3. *L. plantarum* CRA52.

high dye-leakage (38.52%) as compared to the results obtained with plantaricin A extracts from *L. plantarum* CRA21 and CRA38, wherein the dye leakage amounted to 32.77% and 19.26%, respectively (Figure 3.12A). The overall trend of plantaricin A-mediated abrogation of target bacterial cells adhering onto collagen could also be captured in experiments conducted with mucin (Figure 3.12B). Fluorescence microscope analysis of cFDA-SE labelled target bacterial cells adhering onto ECM and treated with plantaricin A extracts from *L. plantarum* strains indicated a reduction in number of adhered target cells in case of bacteriocin-treated sample (Figure 3.13 and Figure A3.2 in Appendix) and these results were consistent with the trend observed in the dye-leakage assays (Figure 3.12). The results obtained in the aforementioned experiments is particularly encouraging considering a previous report, which describes the critical role of plantaricin A as a pheromone that promotes biofilm formation and adhesion of *L. plantarum* strains onto Caco-2 cell line and thereby prevent pathogen adhesion onto the cells (Calasso *et al.,* 2013). Based on the leads obtained in this study, it would perhaps be interesting in future to determine the biofilm forming potential of plantaricin A producing *L. plantarum* strains and their effect in precluding adhesion of target pathogens onto ECM.

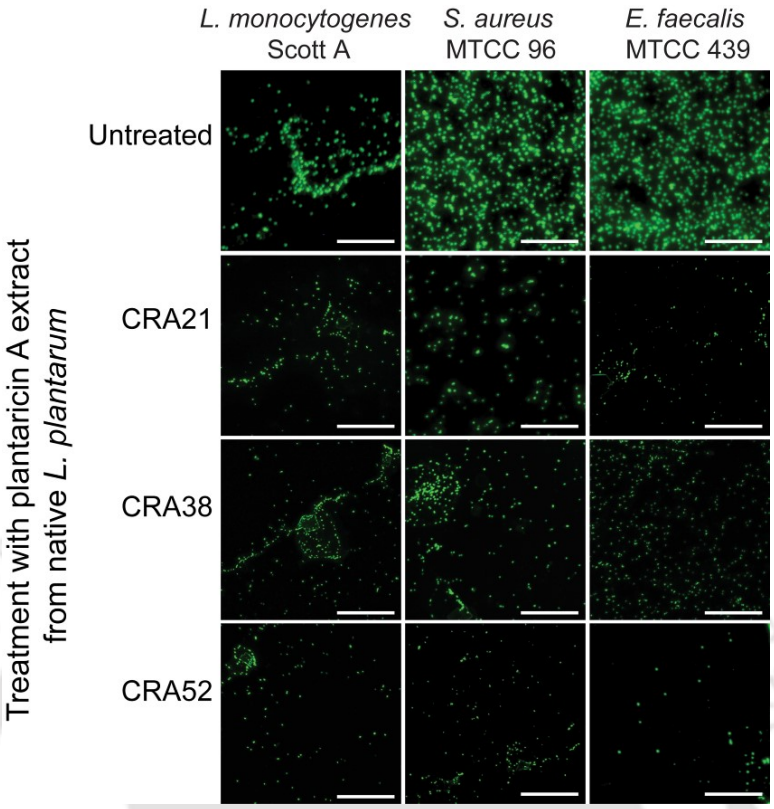

Figure 3.13. Fluorescence microscope analysis to study the effect of plantaricin A extract (400 AU/mL) from *L. plantarum* strains on collagen-adhered target bacteria. Scale bar for the images is 200 µm.

3.4. Significant Findings

The salient findings of the present study are as follows:

1. Fluorescence-based *in vitro* assays indicated that amongst the various LAB strains, the *L. plantarum* strains CRA21, CRA38 and CRA52 displayed adhesion on the ECM molecules collagen and mucin, which was comparable to the standard probiotic *L. rhamnosus* GG.

2. On the basis of flow cytometry-based quantitative assessment of the adhesion potential, *L. plantarum* CRA21 demonstrated the highest adhesion onto the ECM as compared with other native LAB strains.

3. Dose-dependent adhesion assays suggested that amongst the native LAB, *L. plantarum* CRA21 displayed the highest e_m on collagen. On the other hand, *L. plantarum* CRA52 demonstrated strongest binding to mucin amongst the

native LAB strains, as evidenced by the low value of the dissociation constant, k_d.

4. Adhesion inhibition assays suggested that the highest inhibition of *S. aureus* adhesion onto collagen and mucin by bacteriocin-producing *L. plantarum* strains was observed in the exclusion mode as compared with the competition and displacement modes. Perhaps the higher binding affinity for the ECM exhibited by the *L. plantarum* strains as compared with *S. aureus* led to the aforementioned observation.

5. Addition of plantaricin A extract from the bacteriocinogenic *L. plantarum* strains displayed potent antibacterial activity on ECM-adhered model pathogens.

In the present investigation, the prominent ECM adhering and bacteriocin producing *L. plantarum* isolates emerge as promising strains having a competitive edge, whose potential can perhaps extend from the conventional domain of food fermentation to healthcare applications. In particular, it would be interesting to validate this scope of the native isolates for niche specific antibacterial therapy. In line with this rational, the next chapter describes the ability of these LAB strains to adhere onto model human intestinal cells and thereby inhibit pathogen colonization in an *in vitro* cell culture model.

Chapter 4

Inhibition of Pathogen Adhesion in Cell Culture Model by Native LAB

This chapter essentially describes the ability of native LAB to inhibit the adhesion of model pathogens on cultured human intestinal cells. The mechanistic insights from the adhesion inhibition of model pathogens on host cells by LAB are discussed in detail.

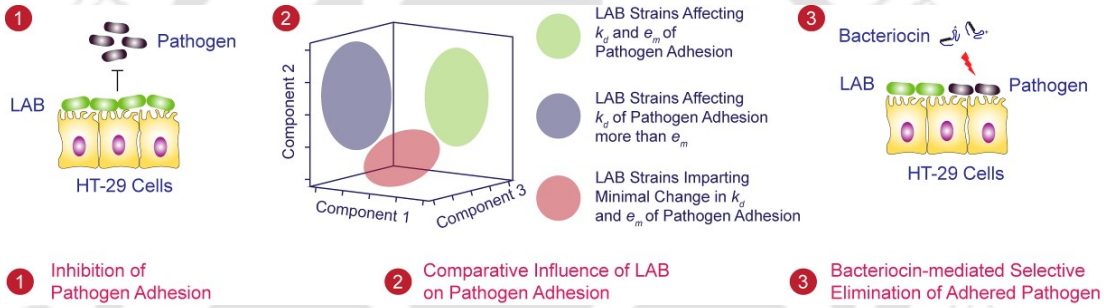

ABSTRACT

The use of antibiotics to mitigate gastrointestinal pathogenic bacteria can lead to profound damage to the beneficial gut microbes and a concomitant proliferation of antibiotic-resistant bacteria. To this end, deployment of LAB strains to target the critical step of adhesion of the pathogens to intestinal cells can be conceived as a viable approach towards developing a safe and niche-specific therapeutic intervention. The present chapter reports the potential of native isolates of *L. plantarum* to inhibit adhesion of model gastrointestinal pathogens, *Enterococcus faecalis* and *Staphylococcus aureus* in an *in vitro* cell culture model using HT-29 cells. Amongst the native *L. plantarum* strains, *L. plantarum* DF9 displayed highest adhesion to HT-29 cells (29.94%), and it was comparable to that observed for *L. rhamnosus* GG (31.18%). Dual-color flow cytometry (FCM) of cFDA-SE labelled *L. plantarum* DF9 and TAMRA-SE labelled *E. faecalis* MTCC 439 indicated that exclusion mode of adhesion inhibition demonstrated highest pathogen adhesion inhibition as compared to competition and displacement mode of adhesion inhibition. Hierarchical cluster analysis (HCA) indicated that the anti-adhesion efficacy of *L. plantarum* DF9 was on par with the probiotic *L. rhamnosus* GG. The quantitative analysis of the adhesion process parameters indicated the dissociation constant (k_d) for *L. plantarum* DF9 was 0.224×10^{-6} $\log_{10}$ CFU/mL, while the maximum number of adhered bacteria (e_m) was estimated to be 3.09 $\log_{10}$ CFU/mL per 10,000 HT-29 cells. Combination of FCM with principal component analysis (PCA) captured the relative influence of LAB strains on adhesion process parameters k_d and e_m wherein it was observed that the native *L. plantarum* DF9 and *L. plantarum* CRA38 could impart a significant change in both the adhesion process parameters k_d and e_m of the model pathogens adhering onto HT-29 cells. Interestingly, the potential of LAB bacteriocin was captured in host cell adhesion assays, which revealed the selective elimination of adhered pathogen while having minimal effect on adhered LAB, in contrast to the effect observed with therapeutic antibiotics. It is envisaged that the native *L. plantarum* strains may be used in conjunction with bacteriocins as safe anti-adhesion therapeutic agents against gastrointestinal pathogens.

4.1. Introduction

The use of antibiotics to mitigate bacterial infections in the gastrointestinal tract can be counterproductive owing to eradication of the beneficial gut microbes and subsequent colonization by antibiotic-resistant opportunistic pathogenic strains (Ferrer *et al.*, 2014). This necessitates the development of a therapeutic intervention, which does not trigger a selection pressure and favor the persistence of antibiotic resistant strains. Conceivably, adhesion inhibition therapy can be an efficient strategy to counter gastrointestinal infections as adhesion of the pathogen to intestinal cells is considered to be a critical step in pathogenesis (Chagnot *et al.*, 2012; Foster *et al.*, 2014; Prince *et al.*, 2012; Krachler and Orth, 2013). Amongst the various approaches, bacteria-based therapy using probiotic lactic acid bacteria (LAB) has come to the forefront (Paton *et al.*, 2006; Salminen *et al.*, 2010; Quigley, 2012; Shanahan *et al.*, 2012; Buffie and Pamer, 2013; Gutierrez-Castrellon *et al.*, 2014; Lievin-Le Moal and Servin, 2014). Probiotic LAB not only endure the harsh environment of the intestinal niche, but can also prevent pathogen colonization by occluding host cell receptors, producing antimicrobial peptides such as bacteriocins and other metabolites (Lee *et al.*, 2003; Ingrassia *et al.*, 2005; Millette *et al.*, 2008; Maudsotter *et al.*, 2011; O'Shea *et al.*, 2012). Adhesion to extracellular matrix (ECM) and intestinal cells is a key attribute of probiotic LAB strains (Lebeer *et al.*, 2010; Reid *et al.*, 2011; Rendueles *et al.*, 2012). Further, such LAB strains, which exhibit high adhesion propensity and produce bacteriocin are likely to sustain and colonize the intestine effectively (Millette *et al.*, 2008; Dobson *et al.*, 2012; Cotter *et al.*, 2013) and thus hold considerable potential in anti-adhesion therapy. This premise is further validated in studies that demonstrated the potential of probiotic LAB as an effective treatment regimen for gastrointestinal ailments (Ruszczynski *et al.*, 2008; Huynh *et al.*, 2009; Miele *et al.*, 2009; Rautava *et al.*, 2009; Lonnermark *et al.*, 2010).

In order to leverage the potential of probiotic LAB as an anti-adhesion agent, it is important to develop a fast, reliable and reproducible host cell adhesion assay, which can simultaneously probe the relative adhesion of LAB and pathogens onto host cells. It may be conceived that such an assay would provide a fundamental understanding of the adhesion process, lead to quantification of the adhesion of LAB and pathogens onto host cells, unravel the influence of LAB on the adhesion process of pathogens onto host cells and provide a guideline to select an appropriate probiotic LAB, that can be explored for anti-adhesion therapy. Further, it is also envisaged that the developed host

cell adhesion assay can perhaps be used to ascertain the prospect of antimicrobial agents such as therapeutic antibiotics and LAB bacteriocins to counter adhesion of gastrointestinal pathogens and also quantify collateral damage by probing the relative adhesion of LAB vis-a-vis pathogen onto host cells.

In the context of probing and quantifying various physiological aspects of host-microbe interactions, flow cytometry (FCM) is emerging as a powerful tool as exemplified in the detection of malaria, tuberculosis or polio virus infection and studying bacterial endotoxin mediated acceleration of metastatic colorectal cancer (Shapiro and Perlmutter, 2008; Sivaraman *et al.*, 2013; Killeen *et al.*, 2009). FCM-based assays have provided insights on bacterial adhesion such as adhesion of *Streptococcus pyogenes* to epithelial cells and role of fibrinogen binding protein to host cell adhesion of group A *Streptococcus* (Hytonen *et al.*, 2006; Anderson *et al.*, 2014). FCM can analyze and quantify cell populations on a real-time basis and thus offers an exciting prospect to study adhesion of probiotic LAB onto host cells and their ability to impede pathogen adhesion. Based on this rationale, in the present study, a dual dye-based FCM analysis is described in order to assess the ability of native strains of *L. plantarum* to inhibit adhesion of pathogenic bacteria *Enterococcus faecalis*, *Listeria monocytogenes* and *Staphylococcus aureus* onto model human intestinal cells (HT-29 cells). The FCM-based assay in conjunction with principal component analysis (PCA) was used to compare the potency of native *L. plantarum* strains in inhibiting pathogen adhesion as well as to probe the mechanistic aspects of the adhesion inhibition process on HT-29 cells. The application potential of the adhesion assay was finally validated by measuring the relative abrogation of adhered LAB vis-a-vis pathogen, upon exposure to either LAB bacteriocins or conventional therapeutic antibiotics.

4.2. Materials and Methods

4.2.1. Reagents and growth media

5 (and 6) carboxyfluorescein diacetate succinimidyl ester (cFDA-SE), 5-carboxy-tetramethylrhodamine N-succinimidyl ester (TAMRA-SE), 2-(4-amidinophenyl)-6-indolecarbamidine dihydrochloride (DAPI), Triton X-100, Dulbecco's modified Eagle medium (DMEM), penicillin, streptomycin and trypsin-EDTA solution were obtained from Sigma-Aldrich Chemicals, USA. Brain-Heart infusion (BHI) broth, de Man, Rogosa and Sharpe broth (MRS) were procured from HiMedia, Mumbai, India.

4.2.2. Bacterial strains and growth conditions

The standard LAB and the bacteriocinogenic native LAB used in this investigation is listed in Table 2.1 indicated in Chapter 2. The strains were grown as per the conditions described previously in section 2.2.2. The target pathogens used in the present investigation comprised of *Listeria monocytogenes* Scott A (*L. monocytogenes* Scott A), *Enterococcus faecalis* MTCC 439 (*E. faecalis* MTCC 439) and *Staphylococcus aureus* MTCC 740 (*S. aureus* MTCC 740). Prior to experiments, the bacterial strains were propagated in BHI broth at 37 °C and 180 rpm for 12 h.

4.2.3. HT-29 cell culture

HT-29 cells were grown and maintained as previously described in Section 2.2.6. in Chapter 2. Prior to adhesion experiments, the HT-29 monolayer was washed twice with sterile phosphate buffered saline (PBS), trypsinized and transferred to a 24-well multi-dish (1×10^4 cells per well) having fresh DMEM medium and incubated at 37 °C in 5% CO_2. Subsequently, the monolayer of HT-29 cells was propagated for 7 days, with a change of medium every 2 days and used at late post-confluence stage for the adhesion assays.

4.2.4. Analysis of bacterial adhesion onto HT-29 cells by single color flow cytometry (FCM) and plating method

A stock solution of cFDA-SE and TAMRA-SE (500 µM each) was prepared in ethanol and stored at -20 °C. The selected LAB and non-LAB bacterial strains were grown overnight and harvested by centrifugation at 3,000 x g for 10 min. The cell pellet was washed twice with sterile PBS and resuspended in the same. The LAB and the non-LAB strains were then labelled with cFDA-SE or TAMRA-SE, respectively (final

concentration of 50 µM) at 37 °C for 20 min. The labelling reaction was terminated by pelleting the cells and the excess dye molecules were removed by washing twice with sterile PBS. A 100 µL aliquot of cFDA-SE labelled LAB cells or TAMRA-SE pathogen cells (8.0 $\log_{10}$ CFU/mL in DMEM medium) were then added in separate sets to 24-well multi-dish containing HT-29 cells in DMEM medium and incubated at 37 °C in 5% CO_2 atmosphere for 2 h. Subsequently, the supernatant was aspirated and HT-29 cells were washed twice with 1.0 mL of sterile PBS. In order to enumerate the adhered bacteria by flow cytometry (FCM), 1.0 mL of 0.05% Triton X-100 was added to each well and incubated for 10 min to specifically lyse the mammalian cells. The lysates were then subjected to FCM on a FACS Calibur flow cytometer (Becton-Dickinson Immunocytometry Systems, San Jose, CA, USA) equipped with a 15 mW, 488 nm, air-cooled argon ion laser. FCM was performed at a low flow rate and the instrument was adjusted to acquire 30,000 events. Unlabeled cells were used to compensate for cellular autofluoresence and to set the appropriate voltage and threshold parameters. Forward-angle light scatter (FSC) vs. side scatter (SSC) plots were analyzed to detect bacterial cells. Detection of green fluorescence of cFDA stained cells was accomplished through FL1 channel (band pass filter of 530 nm/30 nm), while red fluorescence of TAMRA stained cells was detected through FL2 channel (band pass filter of 630 nm/40 nm). Data acquisition was performed with CellQuest Pro software (BD CellQuestTM Pro Version 6.0, Becton-Dickinson, USA). Data analysis was performed with FCS Express 5.0 (DeNovo Software Inc.). Following FCM analysis, the median fluorescence intensity observed in the dot plot for the labelled bacteria (LAB or pathogen) adhered onto HT-29 cells (F_A) was compared to the median fluorescence intensity obtained for the total labelled bacterial cells (LAB or pathogen), which was used initially for the adhesion assay (F_T). All the experiments were performed in triplicates and mean and standard deviation was calculated. A schematic for the protocol of FCM-based estimation of bacterial adhesion onto HT-29 cells is indicated in Figure 4.1.

For each bacterial strain, adhesion was estimated by the FCM method using the following expression:

$$\text{Adhesion (\%)} = \frac{F_A}{F_T} \times 100 \quad .....4.1.$$

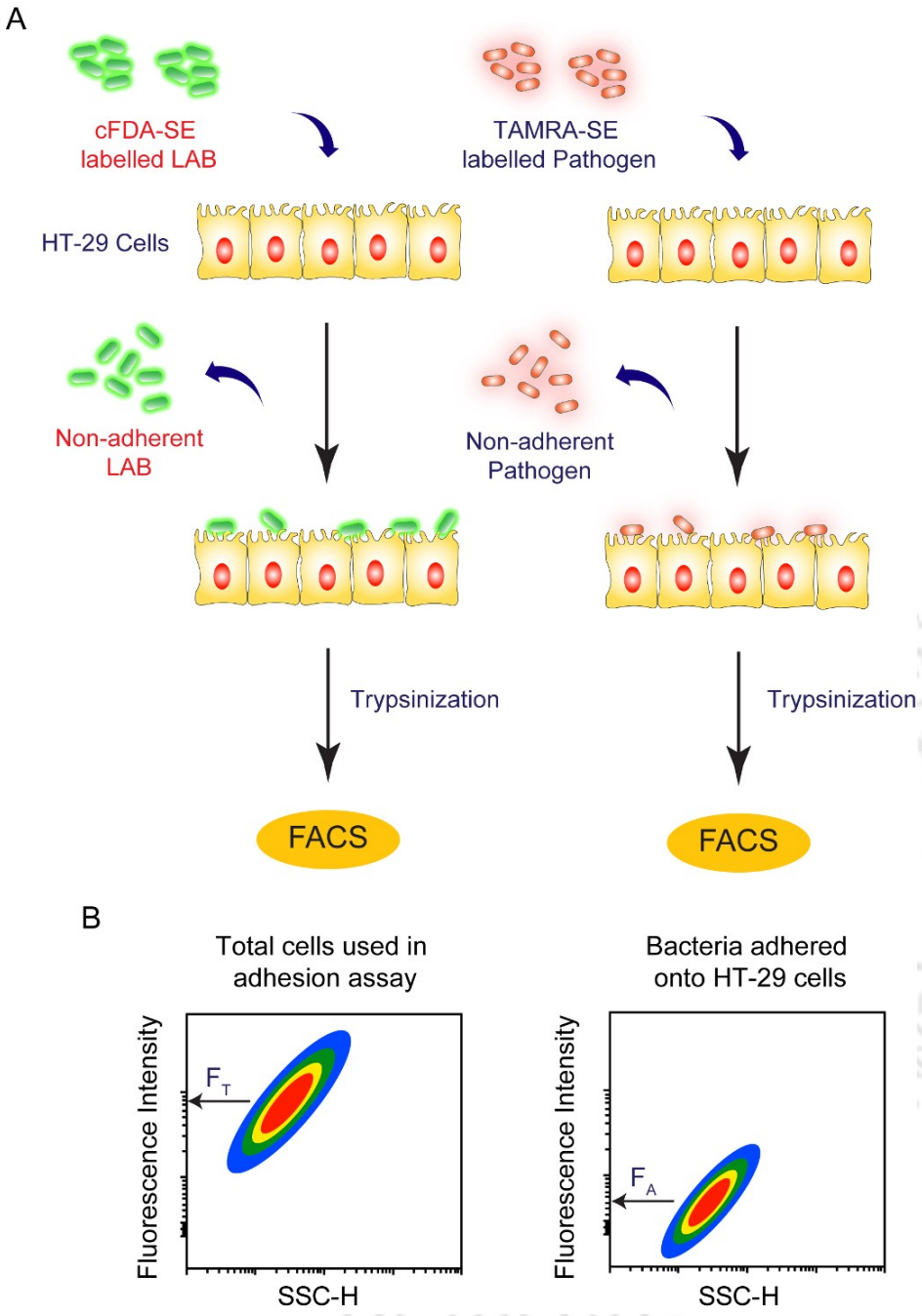

Figure 4.1. (A). Schematic representation of the experimental protocol of bacterial adhesion onto model intestinal cells. (B) Representative dot plots for estimation of bacterial adhesion onto model intestinal cells.

Estimation of bacterial adhesion onto HT-29 cells was also carried out by plating method as described previously (Yadav *et al.*, 2013). For each bacterial strain, adhesion was estimated by the plating method using the following expression:

$$\text{Adhesion (\%)} = \frac{F}{I} \times 100 \quad .....4.2.$$

Where, I and F refer to initial number of cells used for the adhesion assay and final number of cells obtained after adhesion assay, respectively. All the experiments were performed in triplicates and mean and standard deviation was calculated.

4.2.5. Dual color FCM to study inhibition of pathogen adhesion on HT-29 cells by L. plantarum strains

Initially the LAB and non-LAB strains (*E. faecalis* MTCC 439 and *S. aureus* MTCC 740) were labelled with cFDA-SE and TAMRA-SE, respectively as described previously. To ascertain the potential of the LAB strains in inhibiting pathogen adhesion onto HT-29 cells, adhesion assays were conducted in exclusion, competition and displacement modes by using varying concentration of pathogen (4.0 $\log_{10}$ CFU/mL, 6.0 $\log_{10}$ CFU/mL and 8.0 $\log_{10}$ CFU/mL). In case of exclusion, cFDA-SE labelled LAB were first added in separate sets to confluent HT-29 cells grown in 24-well multi-dish and incubated for 1 h, followed by washing and removal of non-adherent LAB by sterile PBS. Subsequently, TAMRA-SE labelled *E. faecalis* MTCC 439 or *S. aureus* MTCC 740 were added in separate sets to the wells bearing the adhered LAB and further incubated for 1 h. In competition mode, LAB as well as the pathogens were added simultaneously to HT-29 cells and incubated for 2 h. The non-adherent cells from the experimental samples were aspirated and the cells were washed twice with sterile PBS. In the displacement mode, the pathogens were initially added to HT-29 cells in a 24-well multi-well plates and incubated for 1 h. The wells were then washed with sterile PBS to remove the non-adherent bacteria and cFDA-labelled LAB were added to the wells and incubated for 1 h. Subsequently, HT-29 cells containing the adhered bacterial cells from all three modes of adhesion assay were treated with 0.05 % Triton X-100 to selectively lyse the mammalian cells and the suspension containing the bacterial cells were then analyzed using FCM. Detection of fluorescence signal, data acquisition and data analysis were accomplished as mentioned for single color FCM in section 4.2.4. To estimate adhesion inhibition of pathogen by FCM analysis, the ratio of the population in percentage obtained from upper left and lower right quadrant, which represent the percentage of TAMRA-labelled pathogen and cFDA-labelled LAB adhered onto HT-29 cells, respectively, were ascertained.

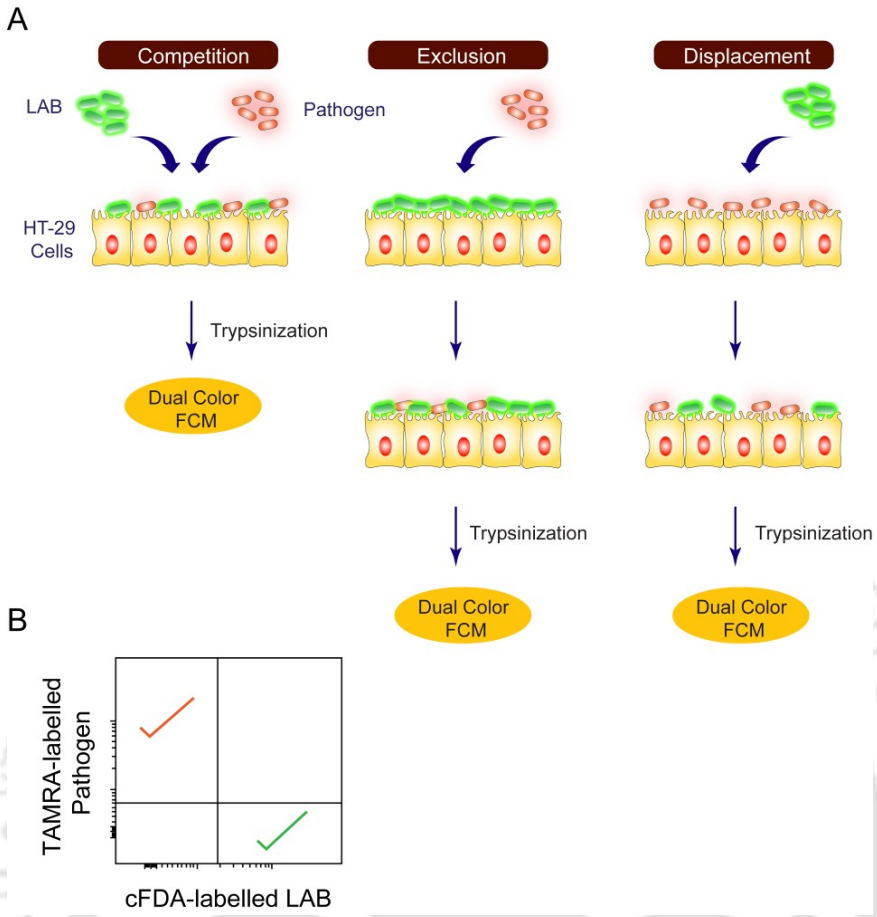

Figure 4.2. (A) Schematic representation of the experimental protocol for measuring the adhesion inhibition of pathogen by LAB cells on model intestinal cells. (B) Representative quadrant plot analysis for quantification of the adhesion of pathogen (indicated by a red tick mark on upper left quadrant) and LAB (indicated by a green tick mark on lower right quadrant).

All the experiments were performed in triplicates and mean and standard deviation was calculated. A schematic for the protocol of the assays used to ascertain adhesion inhibition of pathogens on model intestinal cells is indicated in Figure 4.2.

4.2.6. Estimation of process parameters for adhesion inhibition

To estimate the parameters of the adhesion inhibition process, varying concentrations of TAMRA-labelled pathogens (4.0 $\log_{10}$ CFU/mL, 6.0 $\log_{10}$ CFU/mL and 8.0 $\log_{10}$ CFU/mL) were used in the exclusion, competition and displacement mode of adhesion assay. Subsequently, FCM analysis was performed and the results were acquired as quadrant plots as mentioned previously. The quadrant plots were subjected to statistical analysis and the number of events obtained from upper left quadrant (for

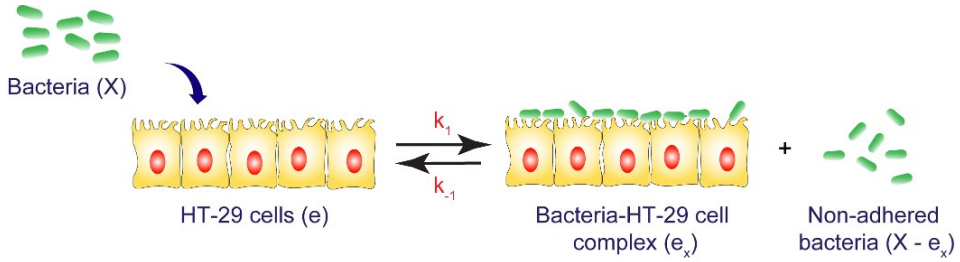

Figure 4.3. Schematic representation of the interaction between bacterial cells and HT-29 cells.

pathogens) and lower right quadrant (for LAB strains) was considered to assess the number of bacterial cells adhered onto HT-29 cells. Each experiment was performed in triplicate and the result was represented as mean ± standard deviation.

The obtained number of events was considered to represent bacteria-host cell complex (e_x). Subsequently, the maximum number of adhered bacteria (e_m) and the dissociation constant (k_d) for the adhesion process was essentially ascertained by the method described previously (Lee *et al.* 2000; Lee, 2004) and is briefly discussed below:

A schematic for the interaction between bacterial cells and host intestinal cell is indicated in Figure 4.3. There are two assumptions in the adhesion of bacteria on host intestinal cell:

1. The adhesion process between the bacterial cells and host intestinal cells is in equilibrium. This condition may be met if the tested strain do not penetrate the host cells during the duration of the experiment.
2. Additionally, it is assumed that the concentration of the bacterial culture remained the same during the course of the study, which implies that the concentration of the bacterial culture could be considered to be equal to the initial bacterial concentration. This condition can be met if the total number of bacterial cells far exceed the number of bacterial cells adhering onto the host intestinal cells.

In the simple adhesion model (Figure 4.3), if X is the concentration of the bacterial culture added, e is the initial model intestinal cells (HT-29 cells) and e_x is the concentration of the bacterium-HT-29 cell complex, then the concentration of free HT-29 cells will be ($e - e_x$). Considering that the interaction between bacteria and HT-29

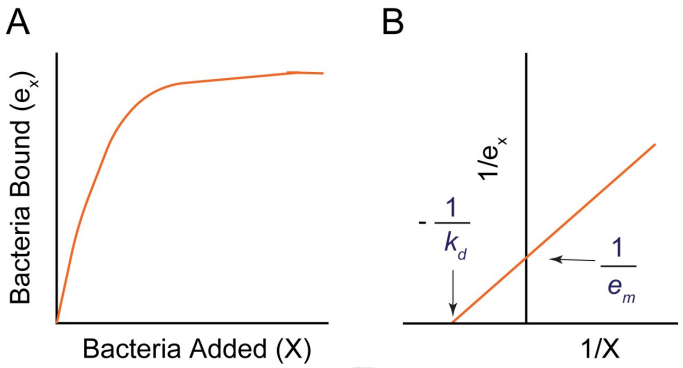

Figure 4.4. (A) Representative plot of bacteria bound to host cells against the total bacteria used for the assay. (B) Double reciprocal plot for (A).

cells is in equilibrium, the dissociation constant for the adhesion process, k_d, can be expressed as follows:

$$k_d = \frac{k_{-1}}{k_1} \quad .....4.3.$$

On inserting the variables for the forward and reverse rate constants in equation 4.3:

$$k_d = \frac{(e - e_x).X}{e_x} \quad .....4.4.$$

On rearrangement of equation 4.4,

$$e_x = \frac{e.X}{(k_d + X)} \quad .....4.5.$$

When the number of total bacterial cells (X) far exceed the dissociation constant (k_d), e_x approaches e and is considered as maximum number of adhered bacterial cells (e_m).
On replacing e with e_m in equation 4.5:

$$e_x = \frac{e_m.X}{(k_d + X)} \quad .....4.6.$$

On plotting bacteria bound (e_x) against total concentration of bacteria (X) used for the assay, a rectangular hyperbolic curve is obtained as indicated in Figure 4.4A.
The reciprocal of equation 4.6 yields:

$$\frac{1}{e_x} = \frac{1}{e_m} + \frac{k_d}{e_m.X} \quad .....4.7.$$

On plotting $1/e_x$ against 1/X, the intercept on the ordinate ($1/e_m$) and the abscissa ($-1/k_d$) can be used to ascertain the adhesion process parameters e_m and k_d, respectively (Figure 4.4B).

4.2.7. Application of dual color FCM to study the effect of antibacterials in an in vitro adhesion model

The therapeutic antibiotics selected for these experiments comprised of vancomycin, gentamicin, ampicillin and ciprofloxacin. The bacteriocins used in these studies included plantaricin A, pediocin and enterocin, which were purified from *L. plantarum* DF9, *Pediococcus pentosaceus* CRA51, and *Enterococcus faecium* DF14, respectively, by following the cell-adsorption method described previously (Singh *et al.*, 2012a). Initially, cFDA-labelled *L. plantarum* DF9 and TAMRA-labelled *E. faecalis* MTCC 439 (8.0 $\log_{10}$ CFU/mL each) were added onto a monolayer of HT-29 cells and incubated for 30 min. Subsequently, the non-adhered cells were aspirated and HT-29 cells bearing adherent bacteria were treated with the individual antibiotics (final concentration of 100 µg/mL each) in separate sets for 30 min. In another independent experiment, the adherent bacteria were treated with the individual bacteriocins (final concentration of 800 AU/mL each) in separate sets for 30 min. Subsequently, the HT-29 cells bearing adherent bacteria were lysed and dual color FCM analysis was pursued to ascertain the number of adherent LAB and pathogen, which was compared to the control (number of adherent LAB and pathogen in the absence of antibiotic or bacteriocin treatment) to estimate the change in host adhered bacterial cells (%). All the experiments were performed in triplicates and the mean and standard deviation was calculated.

4.2.8. Imaging studies

Prior to cell imaging studies, HT-29 cells were seeded onto a 24-well multidish plate and grown in DMEM medium at 37 °C till 90% confluency under 5.0 % CO_2. Subsequently, the cells were washed thrice with sterile PBS and incubated with 5.0 µM DAPI for 30 min. Following DAPI-labelling, HT-29 cells were washed with sterile PBS and incubated in separate sets with either cFDA-labelled *L. plantarum* DF9

(8.0 $\log_{10}$ CFU/mL) or cFDA-labelled *L. rhamnosus* GG (8.0 $\log_{10}$ CFU/mL) or TAMRA-labelled *E. faecalis* MTCC 439 (8.0 $\log_{10}$ CFU/mL) for 2 h each. Subsequently, HT-29 cells were gently washed with sterile PBS to remove any non-adherent or weakly adherent bacteria, and observed under a fluorescence microscope (Eclipse Ti-U, Nikon, USA) using appropriate filters (UV filter for DAPI: Excitation: 360/20 nm, Emission: 460/25 nm; Blue filter for cFDA-SE: Excitation: 480/15 nm, Emission: 535/20 nm; Green filter for TAMRA-SE: Excitation: 540/25 nm, Emission: 605/55 nm). To study adhesion inhibition, *E. faecalis* MTCC 439 and *L. plantarum* DF9 were labelled with TAMRA-SE and cFDA-SE, respectively, while HT-29 cells were labelled with DAPI. Subsequently, the three modes of adhesion inhibition were performed with 8.0 $\log_{10}$ CFU/mL of the pathogen and LAB as described previously in section 4.2.5. Following adhesion, the cells were washed with sterile PBS and the image was captured using appropriate filters as mentioned previously.

4.2.9. *Statistical analysis*

In Bland-Altman analysis, the adhesion percentage of all of the bacterial strains obtained through plating method and FCM method were compared and the differences of the two paired measurements were plotted against the mean (Martin-Bland and Altman, 1986). The agreement levels (95% confidence) were calculated and Bland-Altman analysis was depicted as a plot (Graphpad Prism Software Version 5.0). Hierarchical cluster analysis (HCA) of quadrant plot obtained in FCM was accomplished by following a previously described method (Marchant and Moreno, 2013). Principal component analysis (PCA) of the adhesion inhibition assays was performed using a standard method (Fernandes *et al.*, 2014).

4.3. Results and Discussion

4.3.1. In vitro adhesion potential of LAB onto HT-29 cells

Pathogenic bacteria such as *E. faecalis* and *S. aureus* have been shown to trigger gastrointestinal infections (Steck *et al.*, 2011; Shogan *et al.*, 2015; Kernbauer *et al.*, 2015; Senn *et al.*, 2016). This premise has been reported previously wherein it was shown that antibiotic treatment can potentially abrogate intestinal commensal flora, leading to enhanced pathogen colonization, which can subsequently cause systemic bloodstream infections and antibiotic-associated diarrhea (Brandl *et al.*, 2008; Mahrshak *et al.*, 2015; Lin *et al.*, 2010; Boyce and Havill, 2005).

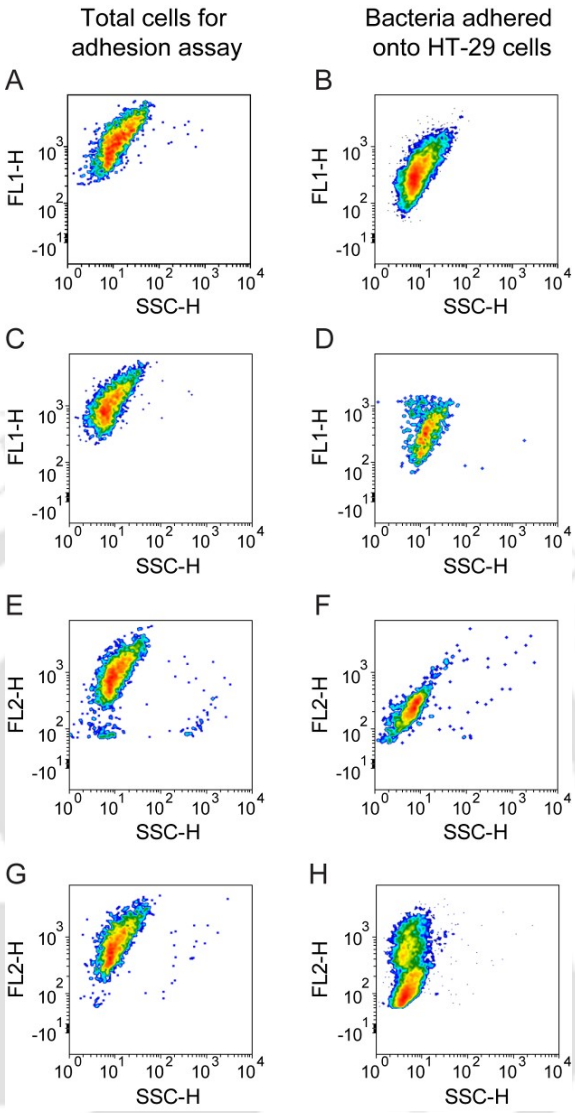

Figure 4.5. Dot plots from FCM analysis to study adhesion of LAB and pathogens onto HT-29 cells. (A-B) *L. plantarum* DF9, (C-D) *L. rhamnosus* GG, (E-F) *E. faecalis* MTCC 439, (G-H) *S. aureus* MTCC 740.

In order to prevent colonization of the intestinal niche by *E. faecalis* and *S. aureus*, targeting the key step of pathogen adhesion onto gastrointestinal cells can be considered as a viable option (Foster *et al.*, 2014; Ribet and Cossart, 2015). Given the strong adhesion potential and bacteriocinogenic trait of previously isolated *L. plantarum* strains (Chapter 2 and Chapter 3), it was envisaged in the present study that these native LAB strains can perhaps be explored to mitigate adhesion of *E. faecalis* and *S. aureus* onto intestinal cells. To strengthen this notion, it was pertinent to develop a facile adhesion assay that can emulate the gastro-intestinal niche, provide

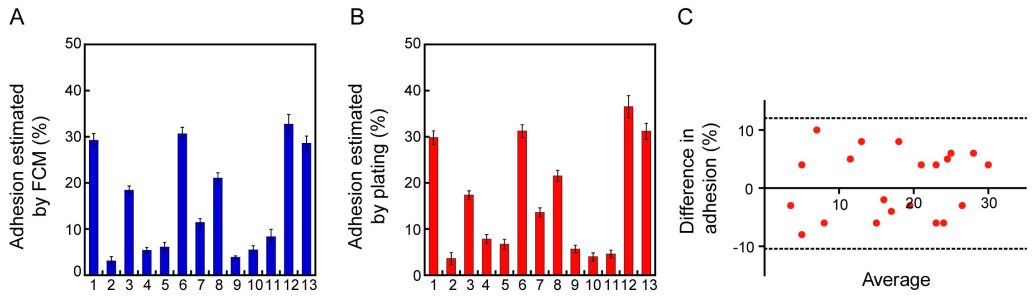

Figure 4.6. Quantification of bacterial adhesion based on (A) single-color FCM based assay and (B) plating method. 1. *L. plantarum* DF9, 2. *L. plantarum* CRA21, 3. *L. plantarum* CRA38, 4. *L. plantarum* CRA49, 5. *L. plantarum* CRA52, 6. *L. rhamnosus* GG, 7. *L. plantarum* MTCC 1325, 8. *L. plantarum* MTCC 1407, 9. *L. plantarum* MTCC 1746, 10. *L. plantarum* NCIM 2592, 11. *L. monocytogenes* Scott A, 12. *S. aureus* MTCC 740 and 13. *E. faecalis* MTCC 439. (C) Bland-Altman statistics for comparison between FCM-and plating-based method.

a fundamental understanding and insight on the adhesion of native LAB onto intestinal cells and ascertain their potential as anti-adhesion agents. To this end, the *in vitro* adhesion of cFDA-SE labelled LAB strains and TAMRA-SE labelled model pathogens onto HT-29 cells (intestinal cells) was initially ascertained by a single color-based FCM analysis. Dot plots for the LAB strains and the pathogens indicated that the median of the cell population shifted for the adhered cells as compared to the total cells used in the adhesion assay (Figure 4.5, Figure A4.1-A4.3 in Appendix). In case of *L. plantarum* DF9, the adhered cell population was 29.94% and was on par with the standard probiotic *L. rhamnosus* GG, wherein the adhered cell population was 31.18% (Figure 4.6A). The dot plots in conjunction with quantification of adhesion on the basis of the shift of the median also indicated that *L. plantarum* CRA21, *L. plantarum* CRA38, *L. plantarum* CRA49 and *L. plantarum* CRA52 could adhere onto HT-29 cells, albeit on a lesser magnitude as compared to *L. plantarum* DF9 and *L. rhamnosus* GG (Figure A4.1 in Appendix, Figure 4.6A). The adhesion of *L. plantarum* and *L. rhamnosus* GG onto host cells can perhaps be attributed to the presence of adhesin proteins (Lebeer *et al.*, 2012; von Ossowski *et al.*, 2010; Tallon *et al.*, 2007; Garcia-Cayuela *et al.*, 2014). Amongst the standard *L. plantarum* strains, *L. plantarum* MTCC 1407 and *L. plantarum* MTCC 1325 demonstrated relatively higher adhesion onto HT-29 cells (Figure A4.2 in Appendix, Figure 4.6A). In case of pathogens, adhesion of *S. aureus* MTCC 740 and *E. faecalis* MTCC 439 onto HT-29 cells was superior as compared to *L. monocytogenes* Scott A (Figure 4.5, Figure A4.3 in Appendix and

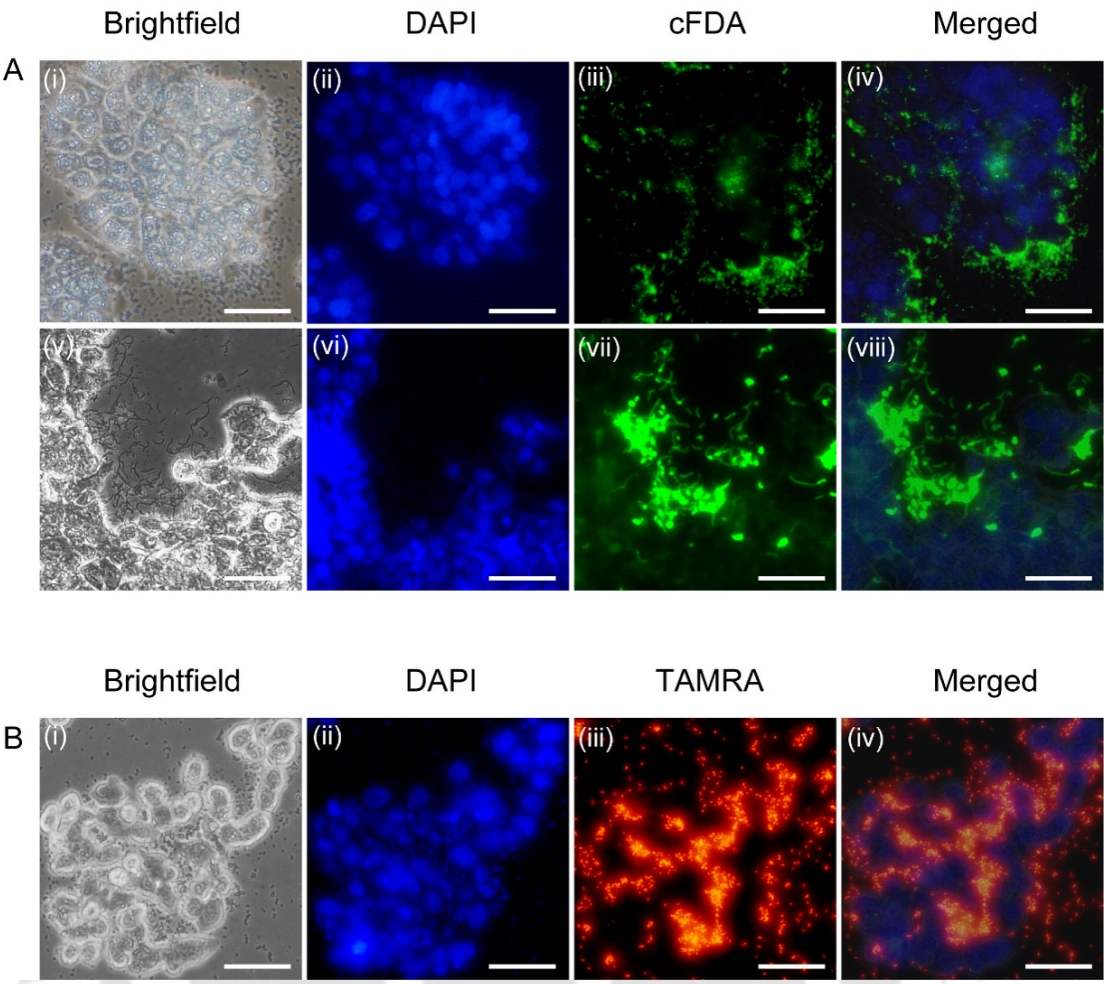

Figure 4.7. Fluorescence microscopic analysis to determine adhesion of (A) *L. plantarum* DF9, panels (i-iv) and *L. rhamnosus* GG, panels (v-viii) and (B) *E. faecalis* MTCC 439, panels (i-iv) onto DAPI-labelled HT-29 cells. Scale bar for the images is 100 µm.

Figure 4.6A). The adhesion of bacterial strains estimated by FCM was also in agreement with the standard plating method (Figure 4.6B), vindicating the reliability of FCM-based adhesion assay. This correspondence was also evident in a Bland-Altman plot (Giavarina, 2015), wherein most of the independently measured values were within the limits of agreement and there was an even distribution of data points in positive and negative regions of the plot (Figure 4.6C). In addition to FCM analysis, the use of cFDA-SE or TAMRA-SE as cell labelling dyes also enabled selective visualization of adhered LAB or the model pathogens onto HT-29 cells by fluorescence microscopy (Figure 4.7).

4.3.2. Potential of native L. plantarum strains to inhibit pathogen adhesion

Based on the encouraging results obtained in the single color FCM analysis, it was envisaged that simultaneous deployment of the differentially labelled bacterial cells in an adhesion assay can yield distinct signals in FCM and provide a measure of adhesion inhibition of pathogens by the LAB strains. To this end, cFDA-SE labelled LAB (8.0 $\log_{10}$ CFU/mL) and varying concentrations of TAMRA-SE labelled model pathogens (4.0 $\log_{10}$ CFU/mL, 6.0 $\log_{10}$ CFU/mL and 8.0 $\log_{10}$ CFU/mL) were subjected to exclusion, competition and displacement modes of *in vitro* adhesion assay followed by FCM. Analysis of the quadrant plot in the exclusion assay indicated that adhesion of *E. faecalis* MTCC 439 onto HT-29 cells was 1.03%, 2.29% and 3.94%, when the initial number of the pathogen used in the assay was 4.0 $\log_{10}$ CFU/mL, 6.0 $\log_{10}$ CFU/mL and 8.0 $\log_{10}$ CFU/mL, respectively (Figure 4.8A-4.8C, upper left quadrant), suggesting that *L. plantarum* DF9 could significantly prevent invasion of *E. faecalis*.

In contrast to the pathogen, adhesion of *L. plantarum* DF9 onto HT-29 cells was manifold higher, although a reduction was observed in presence of increasing number of *E. faecalis* cells (Figure 4.8A-4.8C, lower right quadrant). It may be mentioned here that the dual-label FCM could measure low levels of pathogen adhesion even in presence of high number of LAB adhered onto HT-29 cells (Figure 4.8A-4.8C, upper left quadrant and lower right quadrant). The significantly higher numbers of *L. plantarum* DF9 adhering onto HT-29 cells evident in fluorescence microscopy also suggested the potential of the LAB to inhibit adhesion of *E. faecalis* onto HT-29 cells in the exclusion mode (Figure 4.9, panels i-v). Presumably, the inherently high propensity of *L. plantarum* DF9 cells to adhere onto HT-29 cells resulted in a high niche occupancy, which perhaps hampered the adhesion of *E. faecalis* MTCC 439 onto HT-29 cells in the exclusion mode. It may also be mentioned here that *L. plantarum* DF9 is known to secrete the bacteriocin plantaricin A (Singh *et al.*, 2012a). Hence, in future it would perhaps be interesting to probe whether the host cell adhered *L. plantarum* DF9 can secrete plantaricin A and thereby hinder adhesion of *E. faecalis* onto HT-29 cells. In the competition mode, the degree of inhibition of the pathogen's adhesion onto HT-29 cells rendered by *L. plantarum* DF9 was diminished (Figure 4.8D-4.8F, upper left quadrant) compared to the effect observed in the exclusion mode (Figure 4.8A-4.8C, upper left quadrant). Although the dual color FCM analysis indicated that the number of *L. plantarum* DF9 adhered onto HT-29 cells was

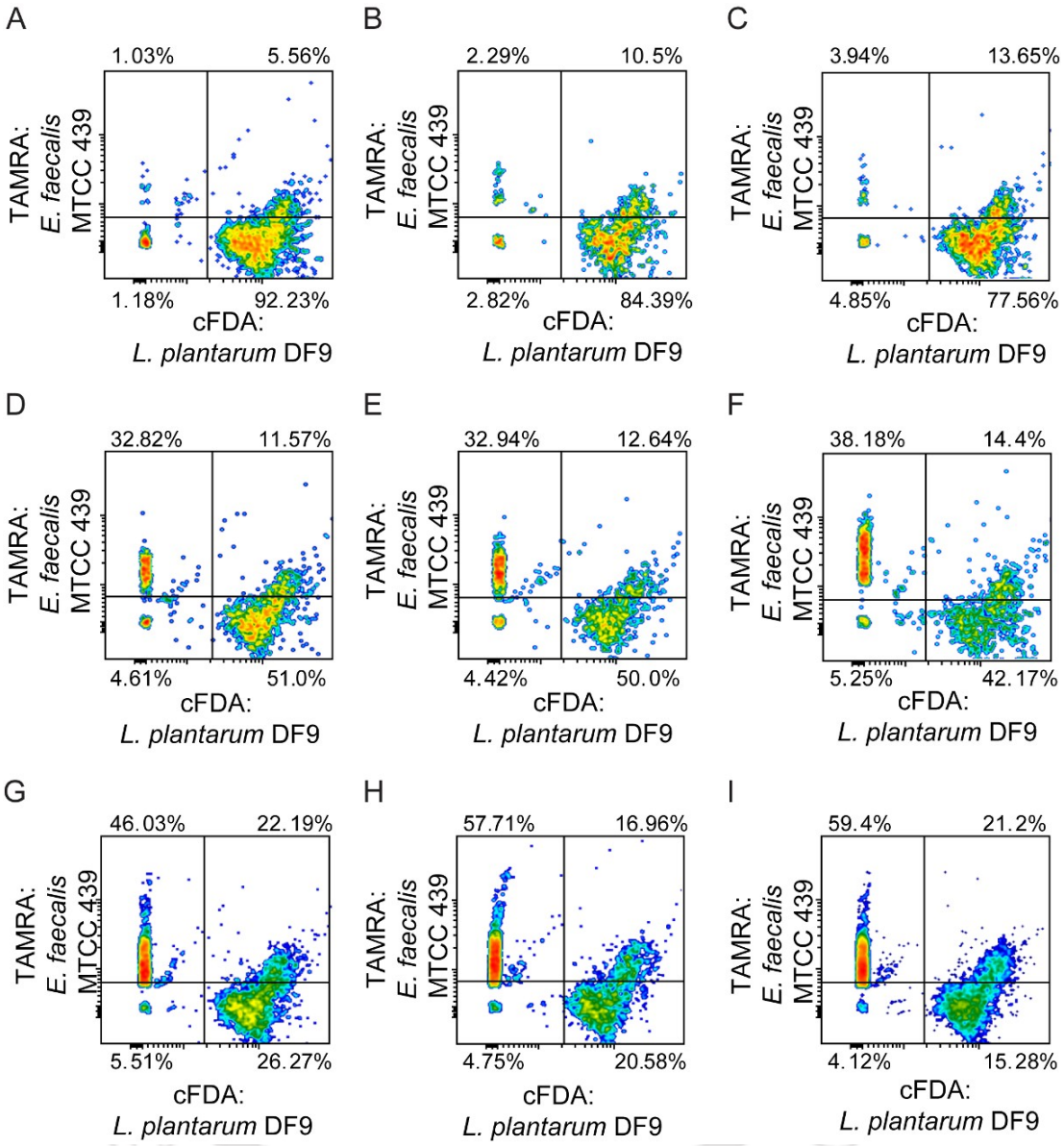

Figure 4.8. Quadrant plots for dual-color FCM based adhesion assay on HT-29 cells. (A-C) represents exclusion mode of adhesion inhibition, and (D-F) represents competition mode of adhesion inhibition and (G-I) represent displacement mode of adhesion inhibition of 4.0 $\log_{10}$ CFU/mL, 6.0 $\log_{10}$ CFU/mL, and 8.0 $\log_{10}$ CFU/mL of *E. faecalis* MTCC 439, respectively, by *L. plantarum* DF9.

higher than the adhered pathogen (Figure 4.8D-4.8F, upper left quadrant and lower right quadrant), there was a reduction in the adhesion of *L. plantarum* DF9 with increasing number of *E. faecalis* cells (Figure 4.8D-4.8F, lower right quadrant). In the

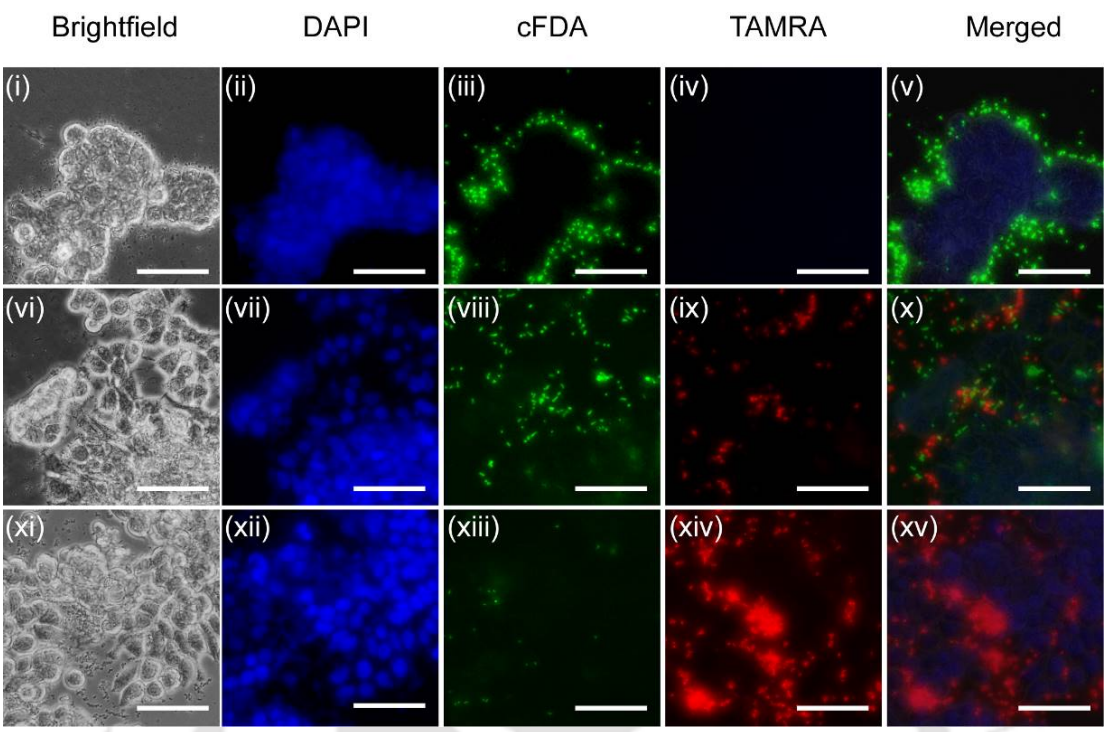

Figure 4.9. Fluorescence microscopic analysis to determine (i-v) exclusion mode of adhesion inhibition, (vi-x) competition mode of adhesion inhibition and (xi-xv) displacement mode of adhesion inhibition of *E. faecalis* MTCC 439 by *L. plantarum* DF9 on DAPI-labelled HT-29 cells. Scale bar for the images is 100 µm.

displacement mode, *L. plantarum* DF9 was less effective in mitigating the adhered pathogen, as a significant population of *E. faecalis* MTCC 439 cells (46.03%, 57.71% and 59.4%) was observed to adhere onto HT-29 cells (Figure 4.8G-4.8I, upper left quadrant). The essential features of adhesion inhibition of *E. faecalis* rendered by *L. plantarum* DF9 in the competition and displacement modes evidenced in FCM analysis was also observed in fluorescence microscopy (Figure 4.9, panels vi-xv). In a similar experiment, the dual label FCM analysis also indicated the propensity of *L. plantarum* DF9 to impede adhesion of *S. aureus* MTCC 740, albeit of a lesser magnitude as compared to *E. faecalis* MTCC 439 (Figure A4.4 in Appendix).

From the quadrant plots, a measure of the ratio of adhered pathogen and LAB (ratio of percentage obtained from upper left and lower right quadrant of the quadrant plots) indicated that the efficiency of inhibiting pathogen adhesion onto HT-29 cells varied amongst the LAB, with *L. plantarum* DF9 and *L. rhamnosus* GG displaying the highest efficiency as evident in the low values of the estimated ratio (Figure 4.10A). In

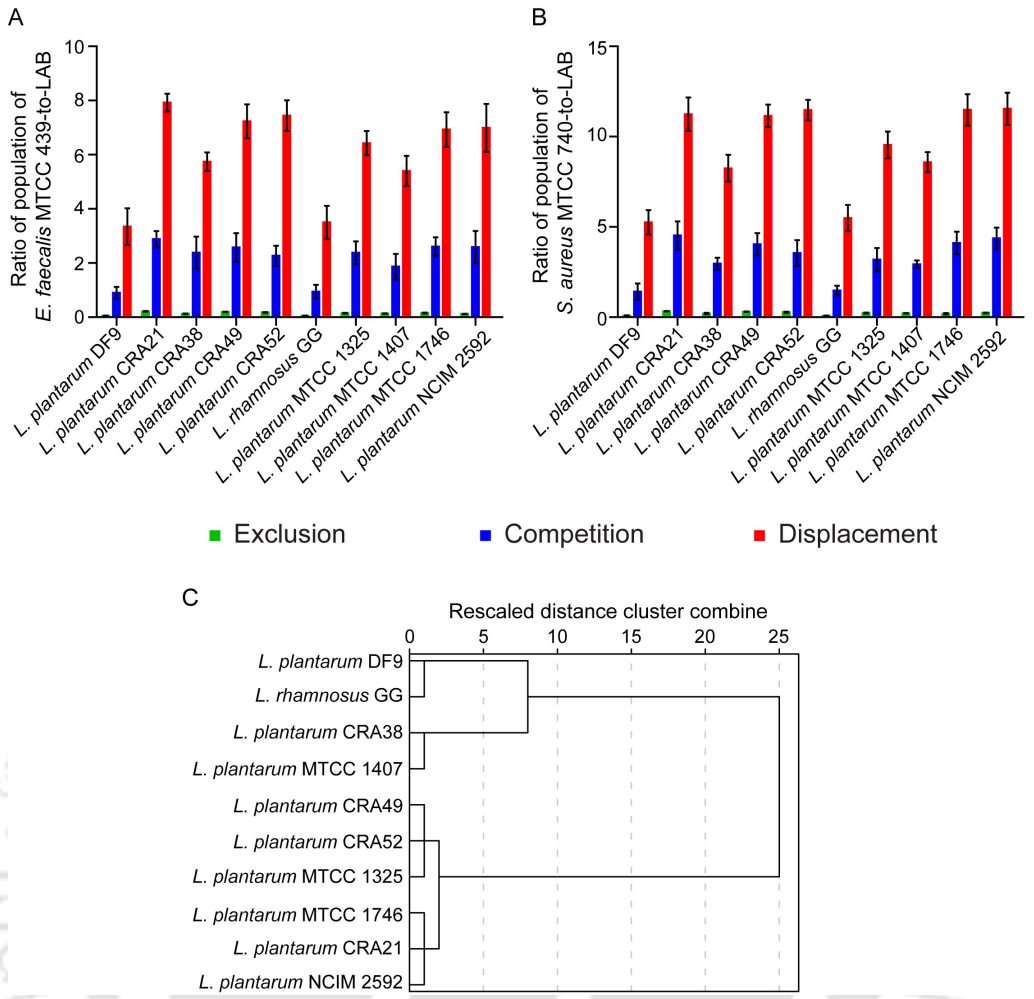

Figure 4.10. (A-B) Relative adhesion of LAB strains and pathogens on HT-29 cells ascertained by dual-color FCM analysis. (C) Hierarchical cluster analysis to group LAB strains based on their adhesion inhibition potential.

case of *S. aureus* MTCC 740, the ratio was found to be comparatively high, indicating lower inhibition of *S. aureus* MTCC 740 adhesion by the LAB strains (Figure 4.10B).

The estimated ratios were subsequently used to perform a hierarchical cluster analysis (HCA), which enabled us to categorize the LAB strains based on their ability to inhibit adhesion of *E. faecalis* and *S. aureus*. Notably, the cluster comprising of *L. plantarum* CRA49, *L. plantarum* CRA52 and *L. plantarum* MTCC 1325 was separated from the cluster of *L. plantarum* CRA21, *L. plantarum* MTCC 1746, *L. plantarum* NCIM 2592 by a distance of only 2.25 units, suggesting that the LAB strains belonging to these two clusters exhibit similar adhesion inhibition potential (Figure 4.10C). On the other hand, the cluster comprising of *L. plantarum* DF9 and *L. rhamnosus* GG was

Table 4.1. Quantitative parameters for the adhesion process of LAB and pathogens on HT-29 cells

Bacterial Strains	Dissociation constant (k_d) ($\times 10^{-6}$ $\log_{10}$ CFU/mL)	Maximum number of adhered cells (e_m) ($\log_{10}$ CFU/mL per 10,000 HT-29 cells)
L. plantarum DF9	0.224 ± 0.005	3.09 ± 0.16
L. plantarum CRA21	0.898 ± 0.082	2.28 ± 0.3
L. plantarum CRA38	0.30 ± 0.046	2.95 ± 0.15
L. plantarum CRA49	0.58 ± 0.09	2.51 ± 0.12
L. plantarum CRA52	0.62 ± 0.02	2.37 ± 0.02
L. rhamnosus GG	0.12 ± 0.08	3.16 ± 0.24
L. plantarum MTCC 1325	0.60 ± 0.019	2.59 ± 0.24
L. plantarum MTCC 1407	0.27 ± 0.02	2.72 ± 0.14
L. plantarum MTCC 1746	0.84 ± 0.042	2.32 ± 0.116
L. plantarum NCIM 2592	0.88 ± 0.06	2.18 ± 0.16
E. faecalis MTCC 439	0.48 ± 0.025	2.89 ± 0.28
S. aureus MTCC 740	0.80 ± 0.054	3.67 ± 0.42

separated from the cluster of *L. plantarum* MTCC 1407 and *L. plantarum* CRA38 by a large distance of 7.5 units, indicating that there was a considerable difference in adhesion inhibition potential between the LAB strains of these two clusters (Figure 4.10C).

4.3.3. Quantitative analysis of adhesion inhibition of pathogens by native L. plantarum

To gain further insight, assessment of adhesion inhibition of varying concentrations of *E. faecalis* MTCC 439 and *S. aureus* MTCC 740 by the LAB strains was pursued using the dual dye FCM, and the dissociation constant (k_d) and the maximum number of adhered cells (e_m) of the pathogen were ascertained as mentioned previously in section 4.2.6. In the absence of any pathogen, *L. plantarum* DF9 and *L. rhamnosus* GG

demonstrated the lowest k_d and highest e_m indicating their high affinity to host cell receptors and their ability to adhere in large numbers onto host cells, while *L. plantarum* CRA38 and *L. plantarum* MTCC 1407 demonstrated inferior adhesion process parameters (Table 4.1). Further, in the absence of any LAB, *E. faecalis* MTCC 439 displayed a lower k_d as compared to *S. aureus* MTCC 740, implying a superior interaction with HT-29 cells (Table 4.1). Subsequently, the three modes of adhesion inhibition of *E. faecalis* MTCC 439 and *S. aureus* MTCC 740 were pursued with different LAB strains and the variables from the dose-dependent adhesion of the pathogen was used to derive k_d and e_m. In the exclusion mode, there was an increase in k_d and decrease in e_m for *E. faecalis* MTCC 439, and this trend was unequivocally observed in presence of all the LAB strains (Figure 4.11A-4.11B). The differences observed in the change in k_d and e_m of *E. faecalis* MTCC 439 in presence of the LAB strains can perhaps be attributed to the inherent variations in the adhesion of the tested LAB strains onto HT-29 cells. In presence of *L. plantarum* DF9 and *L. rhamnosus* GG, the increase in k_d was highest and the e_m was markedly less (Figure 4.11A-4.11B). In the exclusion model, the initial strong adhesion of *L. plantarum* DF9 or *L. rhamnosus* GG onto HT-29 cells as evident in the lower k_d of these LAB strains as compared to *E. faecalis* MTCC 439 (Table 4.1) could be critical for efficient exclusion of the pathogen. Further, *L. plantarum* DF9 and *L. rhamnosus* GG rendered a comparable change in the adhesion process parameters (k_d and e_m) for *E. faecalis* MTCC 439 in the exclusion mode of assay (Figure 4.11A-4.11B), which can perhaps be ascribed to the comparable adhesion of *L. plantarum* DF9 and *L. rhamnosus* GG onto HT-29 cells as observed in the FCM analysis using a single dye (Figure 4.6A). In competition mode, the adhesion process parameters of *E. faecalis* MTCC 439 was observed to change based on the LAB strain (Figure 4.11C-4.11D). For instance, in presence of *L. plantarum* DF9, the k_d and e_m for *E. faecalis* MTCC 439 were observed to be $7.26 \pm 0.2 \times 10^{-6}$ $\log_{10}$ CFU/mL and 1.95 ± 0.12 $\log_{10}$ CFU/mL per 10,000 HT-29 cells, respectively (Figure 4.11C-4.11D). Presumably, the higher binding affinity of *L. plantarum* DF9 as compared to that of *E. faecalis* MTCC 439 (Table 4.1) rendered *L. plantarum* DF9 to prevail over *E. faecalis* MTCC 439 in the adhesion assays conducted in competition mode. In the displacement mode, the inhibition of adhesion of *E. faecalis* MTCC 439 cells onto HT-29 cells was considerably lower (Figure 4.11E-4.11F), wherein an increase in k_d was observed only in the case of *L. plantarum* DF9

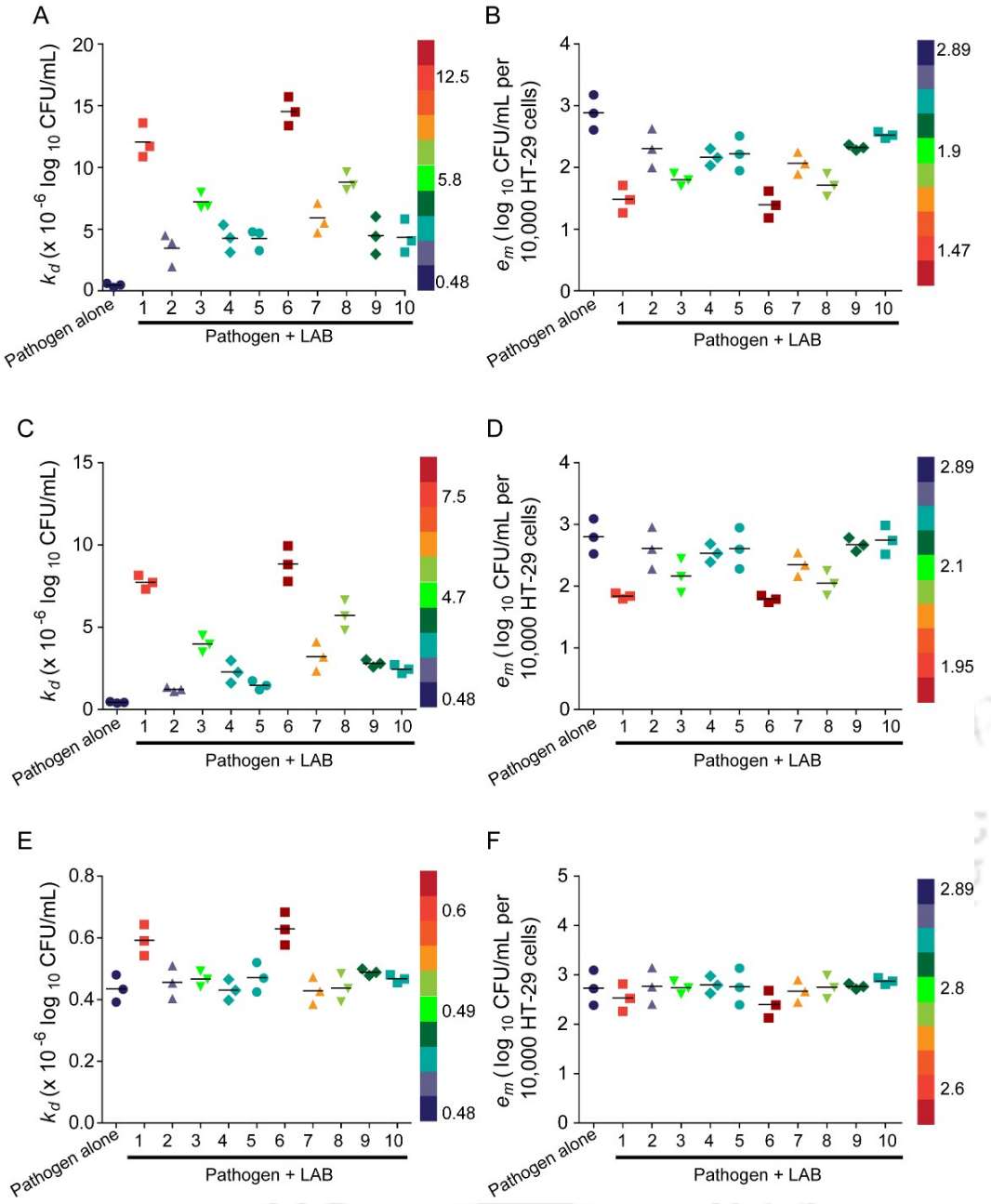

Figure 4.11. Change in adhesion process parameters of *E. faecalis* MTCC 439 imparted by LAB strains. (A-B) exclusion mode of adhesion inhibition, (C-D) competition mode of adhesion inhibition, (E-F) displacement mode of adhesion inhibition. 1. *L. plantarum* DF9, 2. *L. plantarum* CRA21, 3. *L. plantarum* CRA38, 4. *L. plantarum* CRA49, 5. *L. plantarum* CRA52, 6. *L. rhamnosus* GG, 7. *L. plantarum* MTCC 1325, 8. *L. plantarum* MTCC 1407, 9. *L. plantarum* MTCC 1746, 10. *L. plantarum* NCIM 2592.

and *L. rhamnosus* GG. Presumably, the LAB strains had a minimal effect in the displacement mode owing to prior occupation of HT-29 cells by *E. faecalis* MTCC

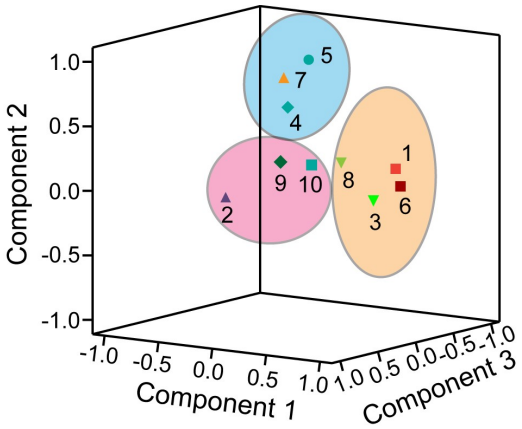

Figure 4.12. Principal component analysis to determine the relative influence of various LAB strains on the k_d and/or e_m of pathogen adhesion onto HT-29 cells. 1. *L. plantarum* DF9, 2. *L. plantarum* CRA21, 3. *L. plantarum* CRA38, 4. *L. plantarum* CRA49, 5. *L. plantarum* CRA52, 6. *L. rhamnosus* GG, 7. *L. plantarum* MTCC 1325, 8. *L. plantarum* MTCC 1407, 9. *L. plantarum* MTCC 1746, 10. *L. plantarum* NCIM 2592.

439. It may also be mentioned here that in case of adhesion inhibition of *S. aureus* MTCC 740 by *L. plantarum* DF9, a similar trend was observed and the adhesion process parameters were observed to decrease albeit to a lesser magnitude as compared to *E. faecalis* MTCC 439 (Figure A4.5 in Appendix).

4.3.4. Principal component analysis (PCA) for inhibition of pathogen adhesion by LAB

A nuanced understanding of the change in adhesion process parameters i.e. k_d and/or e_m of the pathogen by the LAB strains could perhaps provide a better selection guideline for identifying promising LAB strains, that hold potential in inhibiting pathogen adhesion onto intestinal cells. To this end, a principal component analysis (PCA) was performed (Fernandes *et al.*, 2014; Ringner, 2008) based on the relative change in k_d and e_m of the pathogens in presence of various LAB strains. It was interesting to observe that *L. rhamnosus* GG, *L. plantarum* DF9, *L. plantarum* CRA38 and *L. plantarum* MTCC 1407 exhibited a high value for component 1 (Figure 4.12 and Table A4.1 in Appendix), which implied that these strains imparted a significant effect on both k_d and e_m of pathogen and consequently had a strong propensity to inhibit pathogen adhesion on HT-29 cells. Multiple kinds of receptors present on host cells may play a role in the adhesion of LAB as well as gastrointestinal pathogens (Hartlova *et al.*, 2010; Cho *et al.*, 2012; Svensson *et al.*, 2006). Based on PCA, it may be

presumed that the strong adhesion of these LAB strains is likely driven by their efficient interactions with high affinity receptors on HT-29 cells. However, it is also possible that these LAB strains may additionally bind to receptors critical for pathogen adhesion and diminish their accessibility. Consequently, the competing pathogen may be able to bind to other available receptors having low affinity, which is perhaps manifested as an increase in the k_d and decrease of the adhesion process in case of the pathogen (Figure 4.11 and Figure A4.5 in Appendix). Secondly, since these LAB strains inherently display strong adhesion potential onto HT-29 cells and adhere in high numbers (Table 4.1), the pathogens *E. faecalis* and *S. aureus* thus adhere in lesser numbers, leading to a decrease in their e_m. Thus, the PCA results suggest that these LAB strains, which significantly deter pathogen adhesion onto the host cell (evidenced by the large change in k_d and e_m of the pathogen) perhaps qualify as probiotic strains that may be suitable in therapeutic interventions meant for imparting long-term effects in the gastro-intestinal niche, such as in eliciting immunomodulatory responses in intestinal cells.

L. plantarum CRA52, *L. plantarum* MTCC 1325 and *L. plantarum* CRA49 displayed a high value for component 2 (Figure 4.12 and Table A4.1 in Appendix), reflecting that these strains imparted a larger change on k_d as compared to e_m of pathogen. Since these LAB strains display superior affinity (k_d) to HT-29 cells as compared to the pathogens (Table 4.1), they were perhaps able to hinder the pathogen's adhesion, as captured in the change in the k_d in case of the pathogens (Figure 4.11 and Figure A4.5 in Appendix). However, it is to be noted that the adhesion potential of these LAB strains is relatively less as compared to *L. rhamnosus* GG and *L. plantarum* DF9 (Figure 4.6A and Table 4.1). Consequently, obstruction of the host cell receptors for adhesion of the pathogen is perhaps comparatively less, enabling pathogen adhesion in larger numbers thereof, which is reflected as a minimal change in the e_m of pathogen (Figure 4.11 and Figure A4.5 in Appendix). In terms of the potential of *L. plantarum* CRA52, *L. plantarum* MTCC 1325 and *L. plantarum* CRA49 in anti-adhesion intervention, PCA seems to suggest that these LAB strains need to be used in large numbers in order to overwhelm and inhibit adhesion of the pathogen.

Finally, *L. plantarum* CRA21, *L. plantarum* 1746 and *L. plantarum* NCIM 2592 score high on component 3 (Figure 4.12 and Table A4.1 in Appendix), which implies that these strains failed to impart any notable change in either the k_d or e_m of pathogen (Figure 4.11 and Figure A4.5 in Appendix). This observation can perhaps be attributed

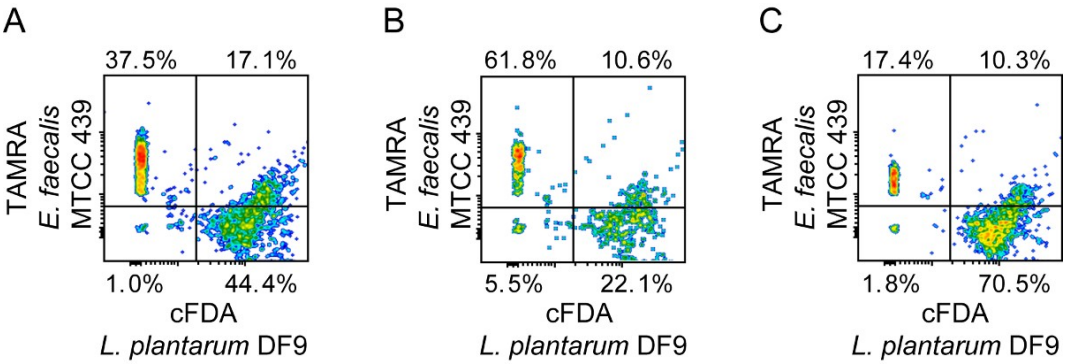

Figure 4.13. Dual color FCM-based adhesion assay to ascertain the effect of antibiotics or bacteriocins on *L. plantarum* DF9 and *E. faecalis* MTCC 439 cells adhered onto HT-29 cells. (A) Adhered cells of LAB and pathogen (untreated), (B) Adhered cells of LAB and pathogen treated with gentamicin, (C) Adhered cells of LAB and pathogen treated with plantaricin A.

to their weak adhesion propensity onto HT-29 cells as evidenced previously (Figure 4.6A and Table 4.1). Collectively, PCA analysis of the dual color FCM data rendered an insightful and quantitative tool to study the mechanistic facets of LAB vis-à-vis pathogen adhesion onto host cells and provided a guideline for selecting appropriate LAB strains that may hold promise in anti-adhesion therapy against gastro-intestinal pathogens.

4.3.5. Effect of antibacterial agents on host-adhered LAB and Pathogen

Administration of therapeutic antibiotics can impart significant collateral eradication of beneficial gut microbiome, leading to ailments such as antibiotic-associated diarrhea (Baumler and Sperandio, 2016; Langdon *et al.*, 2016). Given this predicament, there is an urgent need for therapeutic arsenals, which can selectively target the pathogen, causing minimal damage to the beneficial gut microbes. In this context, bacteriocins secreted by LAB are promising, owing to their selective activity towards gastrointestinal pathogens such as *L. monocytogenes*, *E. faecalis* and *S. aureus* (Cotter *et al.*, 2013; Drider *et al.*, 2006). However, a facile and an accurate screening tool is critical to verify the potential of bacteriocins in selective antimicrobial therapy. In order to simulate the gastro-intestinal niche in a pathogen infection model, an *in vitro* adhesion assay was set up with both *L. plantarum* DF9 and *E. faecalis* MTCC 439 and the effect of extraneously added LAB bacteriocins and model therapeutic antibiotics on both the LAB as well as the pathogen were evaluated by the dual color FCM analysis. In the absence of any antimicrobial agent, FCM indicated that percentage of

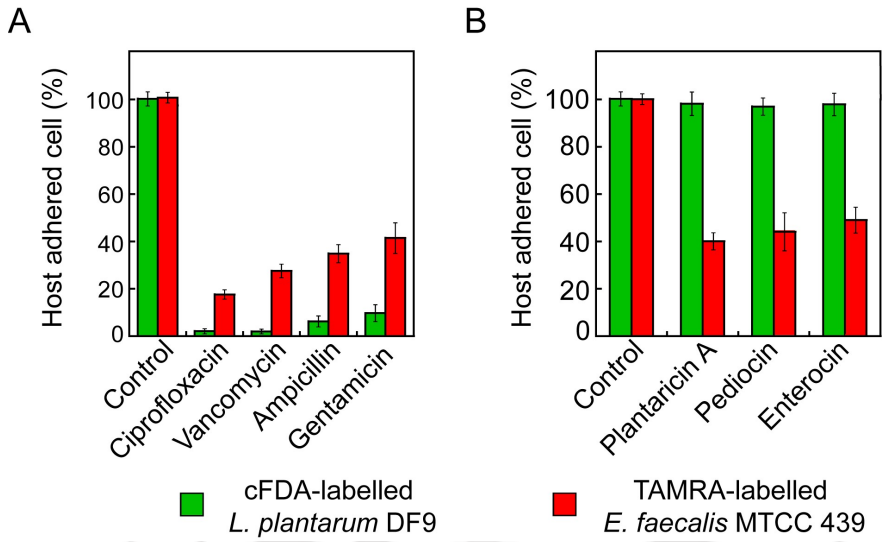

Figure 4.14. (A) and (B) refer to relative change in the number of adhered cells upon treatment with antibiotics or bacteriocins, respectively.

L. plantarum DF9 and *E. faecalis* MTCC 439 adhered onto HT-29 cells were 44.4% and 37.5%, respectively (Figure 4.13A). In an independent experiment, when the adhered cells were treated with gentamicin (100 µg/mL), there was a sharper reduction in the population of *L. plantarum* DF9 (22.1%) as compared to *E. faecalis* MTCC 439 (61.8%) (Figure 4.13B), implying that elimination of *E. faecalis* by gentamicin was associated with a high collateral damage to *L. plantarum* DF9. In a separate experiment, addition of plantaricin A (800 AU/mL) on the adhered population of LAB and the model pathogen led to a sharper reduction in the adhered population of *E. faecalis* MTCC 439 (17.4%) as compared to *L. plantarum* DF9 (70.5%), suggesting that the bacteriocin was selective and could render a preferable eradication of adhered *E. faecalis* MTCC 439, with minimal effect on the adhered population of *L. plantarum* DF9 (Figure 4.13C).

The analytical merit of the dual color FCM analysis in distinguishing collateral damage associated with the use of antibiotics as opposed to selective abrogation of pathogenic bacteria using LAB bacteriocins was further substantiated in experiments with other antibiotics and bacteriocins as well (Figure 4.14A-4.14B). The observations of FCM analysis (Figure 4.13) was also corroborated in cell imaging studies, which indicated the presence of relatively higher numbers of either *E. faecalis* MTCC 439 or *L. plantarum* DF9 adhered onto HT-29 cells following treatment with either the antibiotic or the bacteriocin, respectively (Figure 4.15, panels i-xv).

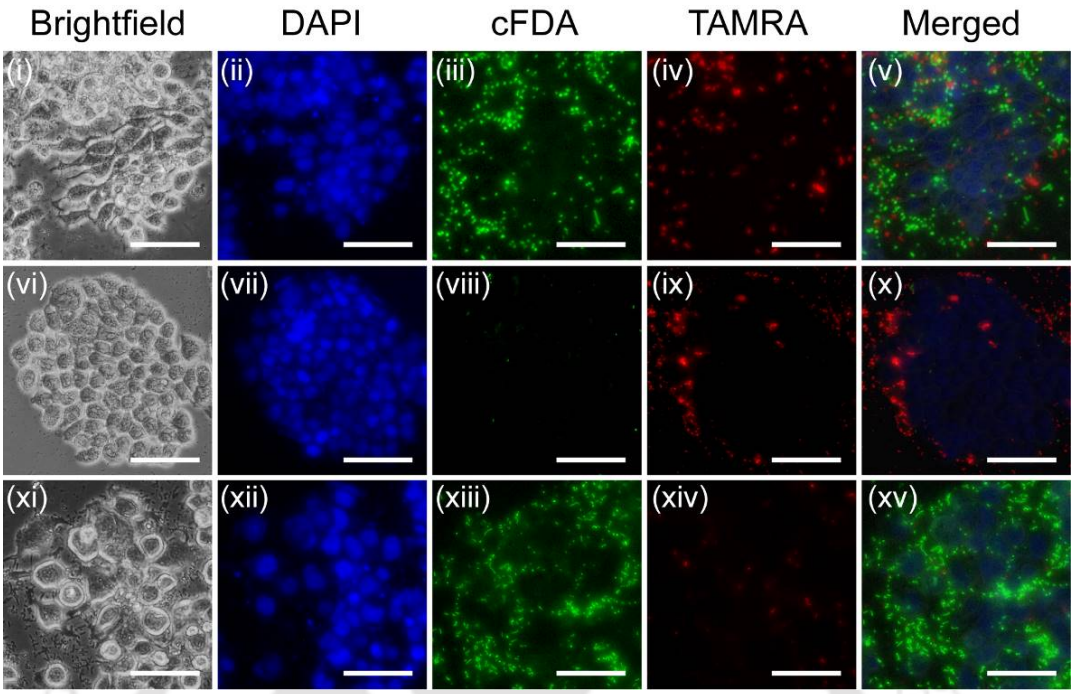

Figure 4.15. Fluorescence microscopic analysis to ascertain the effect of antibiotics and bacteriocins on *L. plantarum* DF9 and *E. faecalis* MTCC 439 cells adhered onto HT-29 cells. Panels i-v: untreated adhered cells, Panels vi-x: adhered cells treated with gentamicin and Panels xi-xv: adhered cells treated with plantaricin A, respectively. Scale bar for the images is 100 µm.

4.4. Significant Findings

The salient findings of this chapter are as follows:

1. The present study suggested that FCM-based analysis of differentially labelled LAB and pathogens can be effectively used to study their relative adhesion onto HT-29 cells.

2. The reliability of the FCM-based analysis was established as the Bland-Altman analysis indicated that quantification of adhered bacterial cells by FCM analysis was on par with the conventional plating method.

3. Adhesion inhibition assays using dual color FCM-based experiments suggested that in the exclusion mode a higher level of adhesion inhibition of *E. faecalis* MTCC 439 onto HT-29 cells was observed as compared to competition and displacement mode. On performing a comparative assessment of adhesion inhibition potential of LAB strains using hierarchical cluster

analysis (HCA), *L. plantarum* DF9 clustered closely with the standard probiotic *L. rhamnosus* GG.

4. Estimation of the adhesion process parameters (k_d and e_m) in conjunction with a principal component analysis provided a mechanistic insight on the comparative adhesion propensities of LAB and the model pathogen and rendered a means to screen and select LAB strains that may hold potential in anti-adhesion therapy.

5. Encouragingly, bacteriocins from LAB were found to selectively abrogate the adhered cells of *E. faecalis* MTCC 439, while having no effect on adhered *L. plantarum* DF9, and this phenomenon was in contrast to the significant elimination of the adhered LAB strain upon exposure to antibiotic treatment.

In the present study, native LAB were found to demonstrate potent adhesion inhibition of gastrointestinal pathogens onto HT-29 cells chosen as model intestinal cells. It is envisaged that the promising native isolates of LAB may find application in niche-specific therapeutic interventions. In this context, it was interesting to observe in the present study that bacteriocins from LAB could selectively abrogate adhered cells of gastrointestinal pathogens. In order to leverage this potential and expand the scope of LAB bacteriocins in mitigation of gastro-intestinal pathogens, it is pertinent to develop a delivery system that would render favorable sustained delivery of the bacteriocin and preserve its activity in the harsh niche during gastric transit. In line with this rational, the next chapter describes the development of a robust nanocarrier for sustained delivery and retention of antibacterial activity of bacteriocin during gastric transit.

Chapter 5

Bacteriocin-loaded Nanocomposite for Mitigation of Gastrointestinal Pathogenic Bacteria

This chapter describes the development of pediocin-loaded milk protein nanocomposite (Ped-MNC) that renders retention of antibacterial activity of the bacteriocin through gastric transit in presence of simulated gastric fluid (SGF) and simulated colonic fluid (SCF).

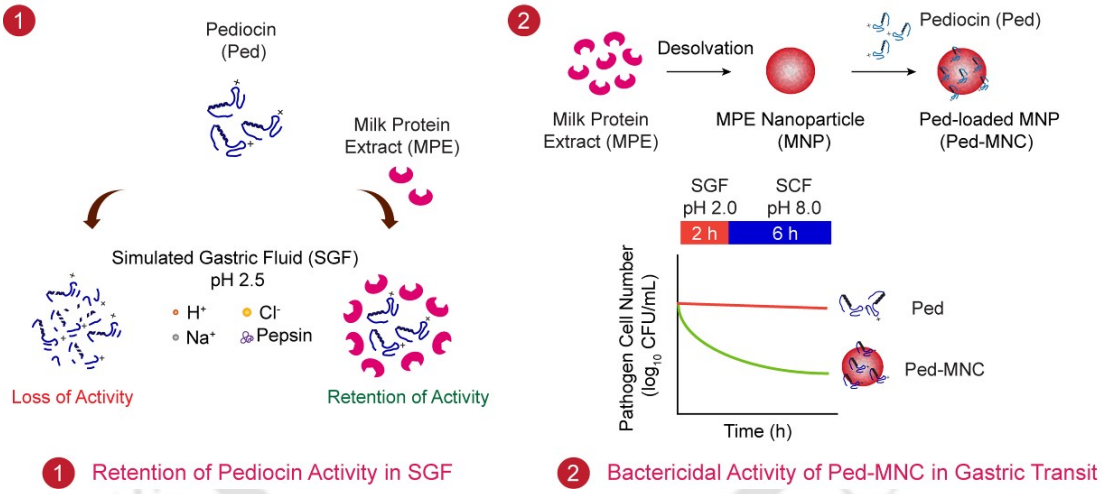

1 Retention of Pediocin Activity in SGF

2 Bactericidal Activity of Ped-MNC in Gastric Transit

ABSTRACT

Bacteriocins secreted by lactic acid bacteria (LAB) are promising therapeutic antibacterials against gastrointestinal pathogens considering their narrow spectrum of antimicrobial activity and minimal effect on the beneficial gut microflora. A major bottleneck for application of LAB bacteriocins is their susceptibility to proteolytic inactivation by enzymes during gastric transit. In an effort to address this issue, the present chapter describes the generation of a milk protein nanoparticle (MNP), wherein the activity of the encapsulated LAB bacteriocin pediocin is protected against proteolytic inactivation by pepsin present in simulated gastric fluid (SGF). Pasteurized cow milk was decaseinated by acid treatment followed by lyophilization to yield a milk protein extract (MPE). Subsequent incubation of pediocin in presence of MPE in SGF indicated nearly 72% retention of pediocin activity against the target pathogen *L. monocytogenes* Scott A. On performing isothermal calorimetry (ITC), the binding between MPE and pepsin present in SGF was found to be efficient and exothermic. Circular dichroism spectroscopy indicated that the β-sheet content of pepsin present in SGF decreased from 74% to 45.8% in presence of MPE. This perturbation in the secondary structure of pepsin could be further correlated with the competitive inhibition of pepsin in presence of MPE. Subsequently, MNP were prepared from MPE by desolvation and pediocin was loaded onto it to generate pediocin-loaded milk protein nanocomposite (Ped-MNC). Encouragingly, Ped-MNC demonstrated nearly 64% retention of anti-listerial activity in SGF. Interestingly, akin to MPE, MNPs exhibited strong binding with pepsin, rendered distortion of the secondary structure of the enzyme as captured in the decrease in the β-sheet content of pepsin present in SGF from 74% to 57.2% and emerged as a competitive inhibitor of the enzyme. In a simulated gastric transit experiment, Ped-MNC was found to render 3.0 log reduction in the cell viability of model gastrointestinal pathogens *L. monocytogenes*, *E. faecalis* and *S. aureus*. *In vitro* cytotoxicity assays revealed that the developed nanocomposite Ped-MNC was non-toxic at bactericidal concentrations. It is envisaged that the developed nanocomposite can be used as rational therapeutic agent against gastrointestinal pathogens.

5.1. Introduction

Bacterial infections in the gastrointestinal tract have been reported to be responsible for morbidity and mortality worldwide (Gibson and Barrett, 2010; Rodriguez *et al.*, 2011; Humphries *et al.*, 2015; Kirk *et al.*, 2015). In this context, *Listeria monocytogenes*, *Enterococcus faecalis* and *Staphylococcus aureus* have been implicated in intestinal infections (Allen *et al.*, 2016; Barbuddhe and Chakraborty, 2009; Steck *et al.*, 2011; Shogan *et al.*, 2015; Kernbauer *et al.*, 2015). Further, the prevalence of antibiotic resistance genes in *E. faecalis* and their possible dissemination to other pathogens present in the gut (Werner *et al.*, 2012) is a cause of concern. Mitigation of pathogenic bacteria by antibiotic treatment has been counterproductive, leading to an abrogation of the beneficial microbes and consequent proliferation of opportunistic pathogenic bacteria (Ferrer *et al.*, 2014; Lin *et al.*, 2010). Commensal gut microflora are known to hinder pathogen invasion by a phenomenon termed as "colonization resistance" (Buffie and Pamer, 2013, Abt and Pamer, 2014). Hence, the absence of a healthy microbiota can lead to enhanced susceptibility to infections (Fukuda *et al.*, 2011). Antibiotic use is known to change the composition of the gut bacterial community, killing susceptible organisms, and thus allowing resistant ones to propagate leading to community disruption or dysbiosis (Pham and Lawley, 2014). For example, it has been reported that upon exposure to a combination of ampicillin and gentamicin, there was a profound loss of beneficial bacteria such as *Lactobacillus* and Bifidobacterium and an increase in the population of Enterobacteriaceae, presumably owing to the loss in overall diversity of the beneficial microflora (Fouhy *et al.*, 2012). Further, the propensity of enterococci to produce β-lactamase, which can render resistant trait against β-lactam based therapeutic antibiotics is a serious concern in the healthcare regime (Bush, 2010; Weisser *et al.*, 2012).

Based on the above mentioned rational, there is a distinct need for therapeutic arsenals, which can selectively target the gastrointestinal pathogen and render minimal damage to the beneficial gut microbes. In this context, antibacterial agents, which possess a narrow spectrum of activity towards gastrointestinal pathogens such as *L. monocytogenes*, *S. aureus* and *E. faecalis* are emerging as viable therapeutic agents (Drider *et al.*, 2006; Cotter *et al.*, 2013; Eckert *et al.*, 2006; Fosgreau and Torsten, 2015). In particular, bacteriocins, which are natural membrane-acting antimicrobial peptides (AMPs) secreted by LAB have come to the forefront. Encouragingly, the optimism associated with bacteriocins from LAB has gained momentum with emerging

reports on their potential as new therapeutic agents against human pathogens, apart from their conventional food applications (Drider *et al.*, 2006; Cotter *et al.*, 2005; Cotter *et al*., 2013; Cavera *et al.*, 2015; Chikindas *et al.*, 2018).

LAB bacteriocins have been demonstrated to be effective against potential gastrointestinal pathogens such as *L. monocytogenes*, *S. aureus* and *E. faecalis* (Rodríguez *et al.*, 2002; Umu *et al.*, 2016; Singh *et al*., 2012a). In particular, the LAB bacteriocin pediocin from Pediococci is an important candidate bacteriocin considering its potent activity against several gastrointestinal pathogens (Drider *et al.*, 2006; Blay *et al.*, 2007; Dabour *et al.*, 2009; Umu *et al.*, 2016). The dual properties of pediocin-like bacteriocins, which includes their potent antibacterial activity against a narrow spectrum of gram-positive pathogens and the absence of a collateral damage towards the commensal microflora highlights their therapeutic potential (Dobson *et al.*, 2012; Porto *et al.*, 2017). However, a major bottleneck in the application of LAB bacteriocins for the mitigation of gastro-intestinal pathogen is their susceptibility to proteolytic inactivation in the gastric milieu. This necessitates the development of a bacteriocin delivery system which renders protection against proteolytic cleavage, supports a favorable release kinetics of the payload and retains the activity of the bacteriocin during gastric transit. Based on this rational, this chapter describes the generation of a pediocin-loaded milk protein nanocomposite for protection of the bacteriocin against proteolytic inactivation in gastric fluid as well as for sustained release of the bacteriocin molecule. Finally, the therapeutic potential of the developed nanocomposite is demonstrated during a simulated gastric transit experiment on model gastrointestinal pathogens *L. monocytogenes* Scott A, *E. faecalis* MTCC 439 and *S. aureus* MTCC 96.

5.2. Materials and Methods

5.2.1. Growth media and chemicals

5 (and 6)-carboxyfluorescein diacetate succinimidyl ester (cFDA-SE), pepsin, human serum albumin (HSA), 3,3'-dipropylthiadicarbocyanine iodide ($DiSC_35$), 12.0 kDa cut-off dialysis bag, 1.0 KDa cut-off dialysis bag, Dulbecco's modified Eagle's Medium (DMEM), penicillin-streptomycin and MTT (3-(4,5-dimethylthiazol-2-yl)-2,5-diphenyltetrazolium bromide) reagent were obtained from Sigma-Aldrich Chemicals, USA. Glutaraldehyde was purchased from Merck, Mumbai, India. HEPES buffer was procured from Sisco Research Laboratories (SRL), Mumbai, India. Brain-Heart infusion (BHI) broth, deMan, Rogosa and Sharpe (MRS) broth and trichloroacetic acid (TCA) were purchased from Himedia, Mumbai, India.

5.2.2. Bacterial strains and growth conditions

The target pathogens used in the present investigation comprised of *Listeria monocytogenes* Scott A (*L. monocytogenes* Scott A), *Enterococcus faecalis* MTCC 439 (*E. faecalis* MTCC 439) and *Staphylococcus aureus* MTCC 96 (*S. aureus* MTCC 96). Prior to experiments, the bacterial strains were propagated in Brain-Heart Infusion (BHI) broth at 37 °C and 180 rpm for 12 h. *Pediococcus pentosaceus* CRA51 (*P. pentosaceus* CRA51) was propagated in MRS broth at 37 °C in static condition for 24 h.

5.2.3. Purification of pediocin

The steps involved in the purification of pediocin from *P. pentosaceus* CRA51 were as follows:

1. *P. pentosaceus* CRA51 was initially grown in 5.0 mL MRS medium at 37°C for 24 h in static condition. The grown culture was then used to inoculate 25 mL MRS medium (1% v/v) taken in a conical flask and grown again at 37°C for 24 h in static condition. Subsequently, this culture was used to inoculate 1.0 L MRS medium (2% v/v) taken in a 2.0 L conical flask and grown at 37°C for 24 h in static condition.
2. The culture broth was then heat inactivated at 70°C for 30 min and the pH of the culture broth was adjusted to 6.0 with 10 N NaOH and stirred for 2 h to facilitate adsorption of pediocin present in the culture broth onto the producer

cells. The cell-adsorbed pediocin was recovered by centrifugation (Centrifuge 5810R, Eppendorf, Germany) at 8000 x g for 15 min at 4°C.

3. The cells were washed twice by resuspending in 25 ml of 10 mM phosphate buffer (pH 6.0), followed by centrifugation at 8000 x g for 15 min at 4°C and the buffer washings were discarded.
4. Subsequently the cells were resuspended in 25 ml of 100 mM NaCl solution and the pH of the solution was adjusted to 2.0 by gradual addition of 5.0% orthophosphoric acid. The mixture was then stirred at 4°C for 18 h and then centrifuged at 10,000 x g for 15 min at 4°C.
5. The supernatant was filtered through 0.22 µm sterile disposable filter (Millipore, USA) and dialyzed for 24 h against deionized water using a 1.0 KDa cut-off dialysis bag (Sigma-Aldrich, USA).
6. The dialysate was freeze-dried in a lyophilizer (Scanvac Coolsafe 100-9 Pro, Labogene ApS, Denmark). The lyophilized dialysate was referred to as purified pediocin (Ped).
7. The pediocin activity in this purified sample was ascertained by spot-on-lawn method and expressed as arbitrary units per mL (AU/mL) as described in a previous study (Singh *et al.*, 2012a).

5.2.4. Purification of milk protein extract (MPE)

Purification of the milk protein extract (MPE) encompassed the following steps:

1. Ten cartons of 500 mL of pasteurized homogenized milk (Amul Taaza) was procured from a local retail store (Amul Parlour).
2. The milk sample from the carton was distributed into sterile 50 mL oakridge tubes and defatted by centrifugation (Centrifuge 5810R, Eppendorf, Germany) at 1000 × g for 10 min at 4 °C.
3. The supernatant was collected in a sterile conical flask and the pH was adjusted to 4.0 by dropwise addition of 2.0 M acetic acid.
4. Subsequently, the solution was centrifuged (Optima Max-XP Ultracentrifuge, Beckman Coulter, USA) at 26,000 × g for 30 min at 4 °C and the supernatant was collected in a sterile conical flask.
5. The pH of the supernatant was adjusted to pH 7.0 by dropwise addition of 1.0 N NaOH and centrifuged again at 1000 × g for 10 min at 4°C to obtain a clear solution.

6. The supernatant was then dialyzed extensively at 4ºC in a 12.0 kDa cut-off dialysis bag (Sigma-Aldrich, USA) against deionized water with a change of water every 1 h. The dialysate was then lyophilized and labelled as milk protein extract (MPE) and stored at -80 °C until further use.

5.2.5. Preparation of pediocin-milk protein extract (Ped-MPE) complex

Initially, a stock solution of purified pediocin (Ped) having a protein concentration of 155 µg/mL, which corresponded to bacteriocin activity of 1600 AU/mL, was prepared in sterile MilliQ water. A 10 mg/mL stock of MPE and HSA were also prepared in sterile MilliQ water. To initiate the formation of pediocin-milk protein extract (Ped-MPE) complex, the respective stock solutions of Ped and MPE were mixed in appropriate proportions to yield a solution wherein the final pediocin concentration was 9.8 µg/mL (100 AU/mL), 19.5 µg/mL (200 AU/mL) and 38.3 µg/mL (400 AU/mL), respectively, while the MPE concentration was 1.0 mg/mL. Likewise, formation of pediocin-HSA (Ped-HSA) complex was also initiated so as to achieve an equivalent concentration of Ped and HSA in the complex as mentioned for Ped-MPE complex. For one set of samples, the pH of the solution was then adjusted to 2.0 with 0.1 N HCl. In a separate set, the pH of the solution containing either Ped and MPE or Ped and HSA was not adjusted for performing control experiments. Subsequently, the contents of the solution were allowed to mix thoroughly in a shaking incubator at 37°C for 12 h to facilitate formation of Ped-MPE complex and Ped-HSA complex. The Ped-MPE and Ped-HSA complex was always prepared fresh prior to experiments unless stated otherwise.

5.2.6. In vitro digestion of Ped-MPE in simulated gastric fluid (SGF)

SGF consisted of pepsin (3.0 g/L) suspended in 0.5 % w/v sterile saline and the pH of SGF was adjusted to 2.0 using 0.1 N HCl (Charteris *et al.*, 1998). Subsequently, in separate sets, solution of either Ped or Ped-MPE, each having a pediocin activity of 400 AU/mL were taken. Subsequently, the pH of these solutions were adjusted to 2.0 using 0.1 N HCl and the solutions were then added to equal volume of double strength SGF (2X SGF) and incubated for 2 h. Likewise, in separate sets, solution of either pediocin or Ped-MPE having a pediocin activity of 400 AU/mL were taken. The pH of these solutions were adjusted to 7.0 and then the solutions were added to equal volume of 10 mM phosphate buffer (pH 7.0) and incubated for 2 h. All the experiments were

performed in three independent sets and every set consisted of three replicates. Following incubation, pediocin activity in the samples was ascertained by agar well diffusion assay and cFDA-SE based fluorescence assay as follows:

5.2.6.1. Agar well diffusion assay

The assay plates had a bottom layer of BHI agar (1.5% agar), which was overlaid with BHI soft agar (0.8% agar) seeded separately with 10^6 cells of freshly grown target cells of *L. monocytogenes* Scott A. Requisite number of holes of 6.0 mm diameter was punched in all the assay plates. To each well, 30 µL of test sample was added. The plates were pre-incubated at 4 °C for 3 h to facilitate diffusion of the sample followed by incubation at 37°C for 24 h. The bactericidal activity of the samples was determined by observing the zone of inhibition produced around the wells.

5.2.6.2. Fluorescence-based cFDA-SE leakage assay

Target cells of *L. monocytogenes* Scott A were labelled with cFDA-SE as described previously in section 3.2.5 of Chapter 3. The labelled cells (approximately 10^6 CFU/mL) were treated with either pediocin or Ped-MPE, which were subjected to *in vitro* digestion in either SGF (pH 2.0) or 10 mM phosphate buffer (pH 7.0). The treatment of the cells was pursued at 37ºC and 180 rpm for 3 h. Subsequently, all the samples were centrifuged at 8,000 × g for 10 min. Leakage of carboxyfluorescein from cells was determined by measuring fluorescence of the cell free supernatant at an excitation wavelength of 488 nm and emission wavelength of 518 nm in a spectrofluorimeter (FluoroMax-4, HORIBA, Japan). The fluorescence measurements were recorded after subtracting the fluorescence of effluxed dye from control samples. The fluorescence intensity (F_T) of leaked cFDA obtained for cells treated with pure pediocin (200 AU/mL) incubated in 10 mM phosphate buffer (pH 7.0) was considered as maximum pediocin activity (100%). The fluorescence intensity (F_A) of cFDA obtained for cells treated with either Ped or Ped-MPE were then compared with that obtained for pediocin incubated in 10 mM phosphate buffer (pH 7.0) for ascertaining the relative pediocin activity. Pediocin activity was calculated as follows: $[(F_A/F_T) \times 100]$. Fluorescence measurements were taken for three independent experimental samples having three replicates each. A schematic representation of the cFDA-SE leakage assay is indicated in Figure 5.1.

5.2.7. Characterization of MPE-SGF interaction

5.2.7.1. Dynamic light scattering (DLS) analysis

For DLS analysis, MPE (1.0 mg/mL) was incubated in SGF for 2 h. Subsequently, the solution was diluted twentyfold in sterile milliQ water (pH 2.0) and subjected to DLS analysis (Zeta Sizer, Malvern, UK). Independently, MPE (1.0 mg/mL) and SGF were also diluted twentyfold in sterile milliQ water (pH 2.0) and subjected to DLS analysis (Zeta Sizer, Malvern, UK). All the experiments were performed in three independent sets and every set consisted of three replicates.

5.2.7.2. Isothermal calorimetry (ITC)

ITC measurements were made at 37 °C using a VP-ITC device (MicroCal, Northampton, USA). To prevent the formation of air bubbles, the buffers were degassed under vacuum prior to experiment. MPE and pepsin were dissolved in 0.5% NaCl sterile solution pH 2.0 so as to minimize heats of dilution. To study the binding of pepsin and MPE, pepsin (0.3%) was dissolved in 0.5% NaCl solution pH 2.0 and loaded onto the cell and titrated against MPE (0.5 mg/mL). Integrated heat effects, after correction for heats of dilution, were analyzed by non-linear regression using a single site-binding model (Microcal Origin, version 5.0).

5.2.7.3. Circular dichroism (CD)

For CD spectra analysis, MPE solution (0.5 mg/mL) was added to SGF, and incubated for 2 h. The CD spectra of SGF, MPE and MPE (incubated in SGF) were recorded between 240 and 190 nm on a spectropolarimeter (JASCO, J-815) with a 2.0 mm path length cuvette at 25°C. CD spectra of the respective buffers were also recorded and subtracted from the sample readings to eliminate the background signal. For every sample, three scans were recorded and averaged in order to improve the signal-to-noise ratio. Data were digitally acquired every 1 nm and the obtained spectra was smoothed using the instruments in-built program.

5.2.7.4. Enzyme kinetics

Simulated gastric fluid (SGF) consisted of pepsin (3.0 g/L) suspended in 0.5 % w/v sterile saline and the pH of SGF was adjusted to 2.0 using 0.1 N HCl (Charteris *et al.*, 1998). Subsequently, in separate sets, solution of either Ped or Ped-MPE (pH adjusted

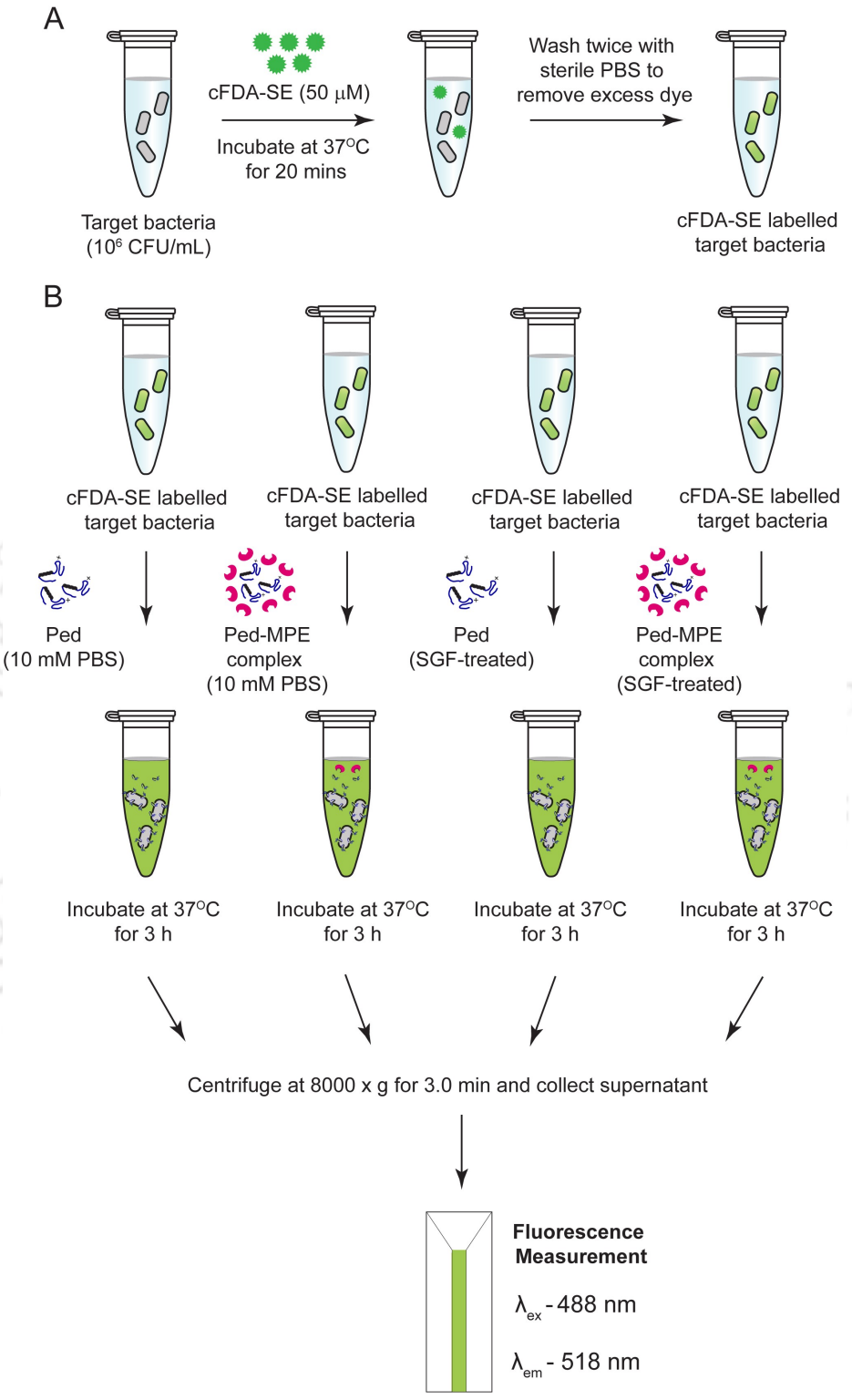

Figure 5.1. Schematic representation of experimental protocol of fluorescence-based cFDA-SE leakage assay to ascertain the pediocin activity.

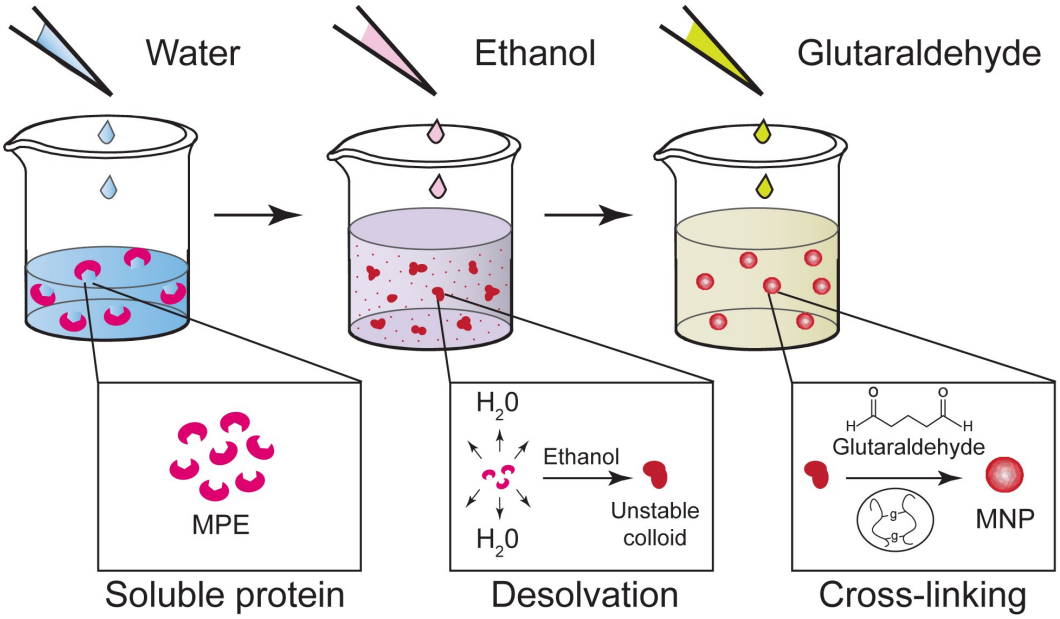

Figure 5.2. Schematic representation of the experimental protocol for preparation of milk protein nanoparticle (MNP).

to 2.0) having pediocin concentration from 10 µg/mL to 80 µg/mL were added to SGF. Subsequently, 0.5 mL of either Ped in SGF or Ped-MPE in SGF was aspirated and mixed with 0.5 mL TCA (10% w/v) and incubated at 37 °C for 15 min. Following incubation, the solution was centrifuged at 9,000 x g for 20 min and the absorbance of the supernatant was measured at 280 nm. All the experiments were performed in triplicates and the mean and standard deviations was calculated.

5.2.8. Preparation of milk protein nanoparticle (MNP)

Briefly, 200 mg of MPE was dissolved in 2.0 mL of Milli-Q water (pH adjusted to 8.2). The protein solution was then stirred for 2 h in room temperature to obtain a clear solution. Subsequently, methanol was added at a rate of 1.0 mL/min to a final volume of 10 mL, leading to the formation of a colloidal solution. The colloidal solution was then stirred at room temperature for another 15 min. Finally, 100 µL of 8.0 % glutaraldehyde was added and the solution was stirred overnight at room temperature. Subsequently, the solution was centrifuged at 10,000 × g for 15 min. The supernatant was discarded and the pellet was washed twice using MilliQ water (pH adjusted to 8.2). The washings were discarded and the pellet, which was referred to as milk protein nanoparticle (MNP) was lyophilized and stored in -80 °C until further use. A schematic representation of the protocol for preparation of MNP is indicated in Figure 5.2.

5.2.9. Generation of pediocin-loaded milk protein nanocomposite (Ped-MNC)

An aqueous solution of MNP was prepared initially by adding 2.0 mg of lyophilized MNP powder to 1.0 mL of 10 mM phosphate buffer (pH 7.4). To this, purified pediocin (Ped) was added at a concentration of 155 µg/mL corresponding to a bacteriocin activity of 1600 AU/mL and the pediocin and MNP solution were incubated at 37°C for 18 h. Subsequently, the solution was centrifuged at 10,000 × g for 15 min at 4°C to recover the pellet, which was referred to as pediocin-loaded milk protein nanocomposite (Ped-MNC). The generated nanocomposite (Ped-MNC) was lyophilized and stored in -80°C until further use.

5.2.10. Characterization of MNP and Ped-MNC

5.2.10.1. FESEM analysis

Aliquots of MNP (2.0 mg/mL) and Ped-MNC (2.0 mg/mL MNP loaded with 800 AU/mL pediocin) were added on a clean sterile cover slip. The samples were then air-dried in a laminar hood and examined in a field emission scanning electron microscope (Zeiss Sigma, USA). The particle size of MNP and Ped-MNC was determined using ImageJ software (http://rsb.info.nih.gov/ij).

5.2.10.2. Dynamic light scattering analysis of MNP and Ped-MNC

For particle size estimation, a sample of MNP (2.0 mg/mL in sterile MilliQ water, pH adjusted to 8.2) was diluted tenfold in sterile MilliQ water (pH adjusted to 8.2) and subjected to DLS analysis (Zeta Sizer, Malvern, UK). Ped-MNC (2.0 mg/mL MNP loaded with a final concentration of 800 AU/mL Ped) was dispersed in 1.0 mL sterile MilliQ water (pH adjusted to 8.2). A 0.2 mL aliquot of this solution was further diluted to 1.0 mL in sterile MilliQ water (pH adjusted to 8.2) and subjected to particle size estimation by DLS. The DLS experiments were performed in three independent sets and every set consisted of three replicates.

5.2.10.3. Differential scanning calorimetry and thermogravimetric analysis (DSC-TGA)

For ascertaining the thermal stability of MNP and Ped-MNC (lyophilized powder ~ 8.0 mg each), the developed nanomaterials were subjected to DSC-TGA (Libra TG 209, NETZSCH, Germany). The temperature range was fixed from 0 °C to 1200 °C with a

heating rate of 10 °C per minute under an inert atmosphere. The collected raw data was subjected to fitting using the instruments built-in program.

5.2.10.4. Estimation of loading capacity (LC) and encapsulation efficiency (EE)

For estimation of LC and EE, MNPs (2.0 mg/mL in sterile 10 mM phosphate buffer, pH 7.4) were interacted with varying concentrations of Ped (4.8 µg/mL to 97.93 µg/mL) for 18 h on a rocker at 37 °C. Following incubation, the solution was centrifuged at 10,000 × g for 5 min. The pellet, which represents Ped-MNC was resuspended in sterile 10 mM phosphate buffer (pH 7.4). The level of free Ped in the supernatant (in AU/mL) was determined using a standard curve obtained from the cFDA-SE leakage assay by following the method described previously (Singh *et al.*, 2012a). The loading capacity (LC) and encapsulation efficiency (EE) of MNP was calculated as follows:

$$LC = \frac{W_{\text{Total Ped}} - W_{\text{Free Ped}}}{W_{np}} \times 100\ \%$$

$$EE = \frac{W_{\text{Total Ped}} - W_{\text{Free Ped}}}{W_{\text{Total Ped}}} \times 100\ \%$$

where $W_{\text{Total Ped}}$ is the concentration of Ped (in mg/mL) used initially for preparing Ped-MNC, $W_{\text{Free Ped}}$ is the concentration of free Ped (in mg/mL) recovered after formation of Ped-MNC and W_{np} is the weight of MNP (in mg).

5.2.10.5. In vitro release kinetics of pediocin from Ped-MNC

To study the *in vitro* release kinetics of pediocin, Ped-MNC loaded with 800 AU/mL of pediocin was dispersed in separate sets in 1.0 mL of 10 mM HEPES buffer (pH 7.4) and 100 mM citrate buffer (pH 3.0), respectively. The samples were incubated in an orbital shaker at 180 rpm at 37 °C. At specific time intervals (3 h, 6 h, 9 h, 12 h and 24 h) the samples were withdrawn and centrifuged at 10,000 × g for 15 min. The supernatant from various samples were transferred into a fresh microcentrifuge tube, and pediocin activity based on cFDA-based leakage assay was measured at 518 nm in a spectrofluorometer. The fluorescence intensity value at 518 nm and a previously generated calibration curve for pediocin levels (AU/mL) was used to measure the

quantity of pediocin released from Ped-MNC at specific time periods and expressed as %-cumulative release.

5.2.11. In vitro digestion of Ped-MNC in simulated gastric fluid (SGF)

In separate sets, solution of either Ped (800 AU/mL) or Ped-MNC (2.0 mg/mL MNP loaded with 800 AU/mL pediocin, pH adjusted to 2.0) were added to SGF and incubated for 2 h. Likewise, in separate sets, solution of either Ped (800 AU/mL) or Ped-MNC (2.0 mg/mL MNP loaded with 800 AU/mL pediocin, pH adjusted to 7.4) were added to 10 mM phosphate buffer (pH 7.4) and incubated for 2 h. All the experiments were performed in three independent sets and every set consisted of three replicates. Following incubation, pediocin activity in the samples was ascertained by agar well diffusion assay and cFDA-SE based fluorescence assay by essentially following the methods described in section 5.2.6.1. and 5.2.6.2.

5.2.12. Membrane depolarization assay

L. monocytogenes Scott A cells were grown till mid-logarithmic phase (A_{600} = 0.4-0.5). The cells were harvested by centrifugation, washed with a buffer solution (5.0 mM HEPES buffer, 5.0 mM glucose, pH 7.2) and suspended in the same buffer (A_{600} of 0.05). The cell suspensions were incubated with 0.4 µM $DiSC_35$ for 1 h at 37 °C followed by the addition of 100 mM KCl. Subsequently, the labelled cells were harvested by centrifugation at 8,000 × g for 5 min, and resuspended in 5.0 mM HEPES, 5.0 mM glucose, pH 7.2. The cell suspension (1.0 mL) was placed in separate cuvettes and was treated with either pediocin or Ped-MNC, which were subjected to *in vitro* digestion in either SGF (pH 2.0) or 10 mM phosphate buffer (pH 7.4). The fluorescence readings were monitored periodically (1 min interval) in a spectrofluorimeter (FluoroMax-4, HORIBA, Japan) at an excitation wavelength of 622 nm and emission wavelength of 670 nm.

5.2.13. FESEM analysis

Target cells of *S. aureus* MTCC 96 (approximately 6.0 $\log_{10}$ CFU/mL suspended in sterile PBS) was treated with Ped-MNC, which was prior exposed to in vitro digestion in SGF (pH 2.0). A 5.0 µL aliquot of cells treated with SGF-treated Ped-MNC was spotted on a clean sterile glass cover slip, air-dried in laminar hood and examined in a field emission scanning electron microscope (Zeiss Sigma, USA).

5.2.14. Characterization of MNP-SGF interaction

5.2.14.1. Isothermal calorimetry (ITC)

ITC measurements were made at 37 °C using a VP-ITC device (MicroCal, Northampton, USA). To prevent the formation of air bubbles, the buffers were degassed under vacuum prior to experiment. MNP and pepsin were dissolved in 0.5% NaCl sterile solution pH 2.0 so as to minimize heats of dilution. To study the binding of pepsin and MNP, pepsin (0.3%) was dissolved in 0.5% NaCl solution pH 2.0 and loaded onto the cell and titrated against MNP (0.5 mg/mL). Integrated heat effects, after correction for heats of dilution, were analyzed by non-linear regression using a single site-binding model (Microcal Origin, version 5.0).

5.2.14.2. Circular dichroism (CD)

For CD spectra analysis, MNP solution (0.5 mg/mL) was added to SGF, and incubated for 2 h. The CD spectra of SGF, MNP and MNP (incubated in SGF) were recorded between 240 and 190 nm on a spectropolarimeter (JASCO, J-815) with a 2.0 mm path length cuvette at 25 °C. CD spectra of the respective buffers were also recorded and subtracted from the sample readings to eliminate the background signal. For every sample, three scans were recorded and averaged in order to improve the signal-to-noise ratio. Data were digitally acquired every 1 nm and the obtained spectra was smoothed using the instruments in-built program.

5.2.14.3. Enzyme kinetics

Simulated gastric fluid (SGF) consisted of pepsin (3.0 g/L) suspended in 0.5 % w/v sterile saline and the pH of SGF was adjusted to 2.0 using 0.1 N HCl (Charteris *et al.*, 1998). In separate sets, solution of either Ped (pH adjusted to 2.0) or Ped along with MNP (1.0 mg/mL and pH adjusted to 2.0) having pediocin concentration from 10 µg/mL to 80 µg/mL were added to SGF. Subsequently, 0.5 mL of either solution was aspirated at regular intervals, mixed with 0.5 mL TCA (10% w/v) and incubated at 37 °C for 15 min. Following incubation, the solution was centrifuged at 9,000 × g for 20 min and the absorbance of the supernatant was measured at 280 nm. All the experiments were performed in triplicates and the mean and standard deviations was calculated.

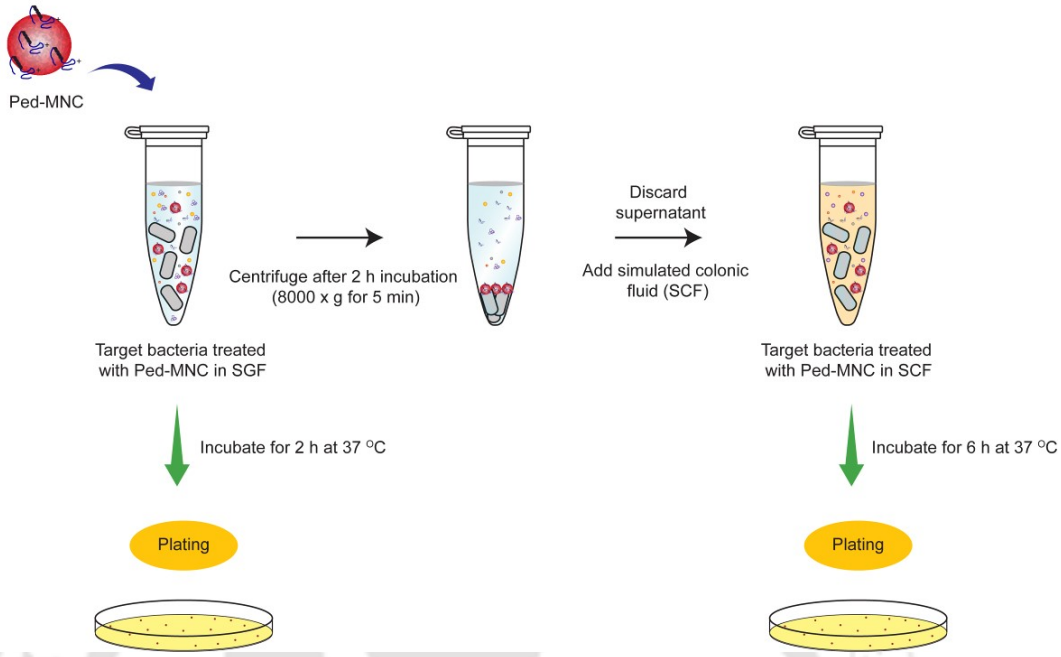

Figure 5.3. Schematic representation of the protocol for ascertaining the activity of Ped-MNC in a simulated gastric transit experiment.

5.2.15. Activity of Ped-MNC in simulated gastric transit experiment

SGF was prepared fresh as described previously in section 5.2.6. The simulated colonic fluid (SCF) was formulated as mentioned previously (Marques *et al.,* 2011). In one set, approximately 6.0 $\log_{10}$ CFU/mL of target bacteria *L. monocytogenes* Scott A, *E. faecalis* MTCC 439 and *S. aureus* MTCC 96 were incubated with Ped-MNC (corresponding to pediocin levels of 800 AU/mL) in SGF for 2 h at 37 ºC and 180 rpm. Viable cell numbers ($\log_{10}$ CFU/mL) were determined at regular intervals by serial dilution and plating. In a separate set, Ped-MNC (corresponding to pediocin levels of 800 AU/mL) was incubated in SGF for 2 h at 37 ºC and 180 rpm. The samples were then centrifuged at 8000 × g for 5 min and the supernatant was discarded. The SGF-treated Ped-MNC was resuspended in simulated colonic fluid (SCF) containing approximately 6.0 $\log_{10}$ CFU/mL of target bacteria *L. monocytogenes* Scott A, *E. faecalis* MTCC 439 and *S. aureus* MTCC 96 in separate sets and further incubated for 6 h at 37ºC and 180 rpm. Viable cell numbers ($\log_{10}$ CFU/mL) of the treated target bacteria were then determined at regular intervals by serial dilution and plating. All the experiments were performed in triplicates and the mean and standard deviations was

calculated. A schematic representation of the protocol for the gastric transit experiment is indicated in Figure 5.3.

5.2.16. In vitro cytotoxicity assay

The cytotoxic effect of purified pediocin, Ped-MPE complex, Ped-MNC, MPE, and MNPs was tested on human embryonic kidney (HEK 293) cell lines and human colon adenocarcinoma (HT-29) cell lines by an MTT assay following the manufacturer instruction (Sigma-Aldrich, MO, USA). HEK 293 cells and HT-29 cells were initially propagated in Dulbecco's Modified Eagle Medium (DMEM) supplemented with 10% fetal calf serum (FCS), penicillin (100 µg/mL) and streptomycin (100 µg/mL) at 37 °C in a humidified atmosphere of 5% CO_2. The cells were subsequently seeded in 96 well plates (10^4 cells/well) and purified pediocin (10-80 µg/mL), Ped-MPE complex (corresponding to pediocin concentration of 10-80 µg/mL and MPE concentration of 1.0 mg/mL), Ped-MNC (corresponding to a loaded pediocin concentration of 10-80 µg/mL and MNP concentration of 1.0 mg/mL), MPE (1.0 mg/mL), and MNPs (1.0 mg/mL) made in DMEM were added to the cells in separate sets and incubated for 24 hours under 5% CO_2 at 37°C. Following incubation, the media was aspirated and fresh DMEM containing MTT solution was added to the wells and incubated for 4 h at 37°C. Subsequently, the supernatant was removed and the insoluble formazan product was solubilized in DMSO and its absorbance was measured in a microtitre plate reader (Infinite M200, Tecan, Austria) at 550 nm. The absorbance obtained for solvent control samples (cells treated with PBS alone) was considered to represent 100% cell viability, whereas the absorbance for treated cells were compared to the solvent control cells to determine % cell viability. MTT assay was performed in six independent sets and each set consisted of three replicates. Data analysis and determination of standard deviation was performed with Microsoft Excel 2010 (Microsoft Corporation, USA).

5.3. Results and Discussion

5.3.1. Bactericidal activity of pediocin-MPE complex in SGF

Gastrointestinal infections due to *L. monocytogenes*, *E. faecalis* and *S. aureus* have emerged as serious healthcare concern. The ability of *L. monocytogenes* to survive in extreme niches such as low pH or in high salt concentration exacerbates its pathogenicity (Cossart *et al.*, 2011). *E. faecalis* and *S. aureus* are especially known to harbor antibiotic resistance genes, which may be implicated in prolonged infection and

enhanced mortality (van Harten *et al.*, 2017; Nikaido, 2009; Rubenstein and Keynan, 2013). A further cause of concern is that *E. faecalis* and *S. aureus* have been detected in healthcare settings, indicating a prospective opportunistic infection in antibiotic-treated or immune-compromised patients (Murray, 2000; Richards *et al.*, 2000). In particular, vancomycin-resistant *E. faecalis* (VRE) has been observed to colonize the gastrointestinal (GI) tract, and cause systemic bloodstream infections (Brandl *et al.*, 2008; Ubeda *et al.*, 2010; Maharshak *et al.*, 2015). In this context, antibiotic treatment has been found to be counterproductive as they can lead to elimination of commensal flora, thereby enabling invasion of previously occupied niches by VRE (Brandl *et al.*, 2008; Ubeda and Pamer, 2012). Likewise, *S. aureus* has been implicated in causing antibiotic-associated diarrhea (Lin *et al.*, 2010; Boyce and Havill, 2005). Bacteriocins produced by LAB, which specifically target bacterial membrane may be a viable therapeutic option for mitigation of gastrointestinal infections (Drider *et al.*, 2006; Riley, 2011; Chikindas *et al.* 2018). Further, unlike conventional antibiotics, which may possess a wider bactericidal spectrum and cause collateral damage (Cotter *et al.*, 2005; Cotter *et al.*, 2013; Cavera *et al.*, 2015; Fouhy *et al.*, 2012), LAB bacteriocins possess a narrow spectrum of activity against closely related gram-positive pathogens, such as *L. monocytogenes*, *E. faecalis* and *S. aureus* and are unlikely to impact the beneficial gut microbes. The fact that bacteriocins from LAB may play a critical role in facilitating pathogen clearance from GI tract provides impetus to the idea of developing bacteriocin-based therapeutics for targeted elimination of gastrointestinal pathogens (O'Shea *et al.*, 2012; Dobson *et al.*, 2012*).* However, bacteriocins, being proteinaceous in nature, are highly susceptible to proteolytic cleavage in the GI tract. To this end, in the present investigation, a milk protein extract (MPE) obtained from a decaseinated fraction of pasteurized milk was used to form a complex with pediocin, a bacteriocin produced by a native strain of *P. pentosaceus* CRA51. This bacteriocin was purified and characterized in an earlier study (Singh *et al.*, 2012a). The essential idea was to deploy MPE to impart protection of the bacteriocin against proteolytic cleavage, when subjected to the gastric milieu. Purified pediocin was initially incubated with MPE to generate the Ped-MPE complex and the antibacterial activity was tested in simulated gastric fluid (SGF). In a control experiment, pediocin was incubated with HSA, and the antibacterial activity was tested

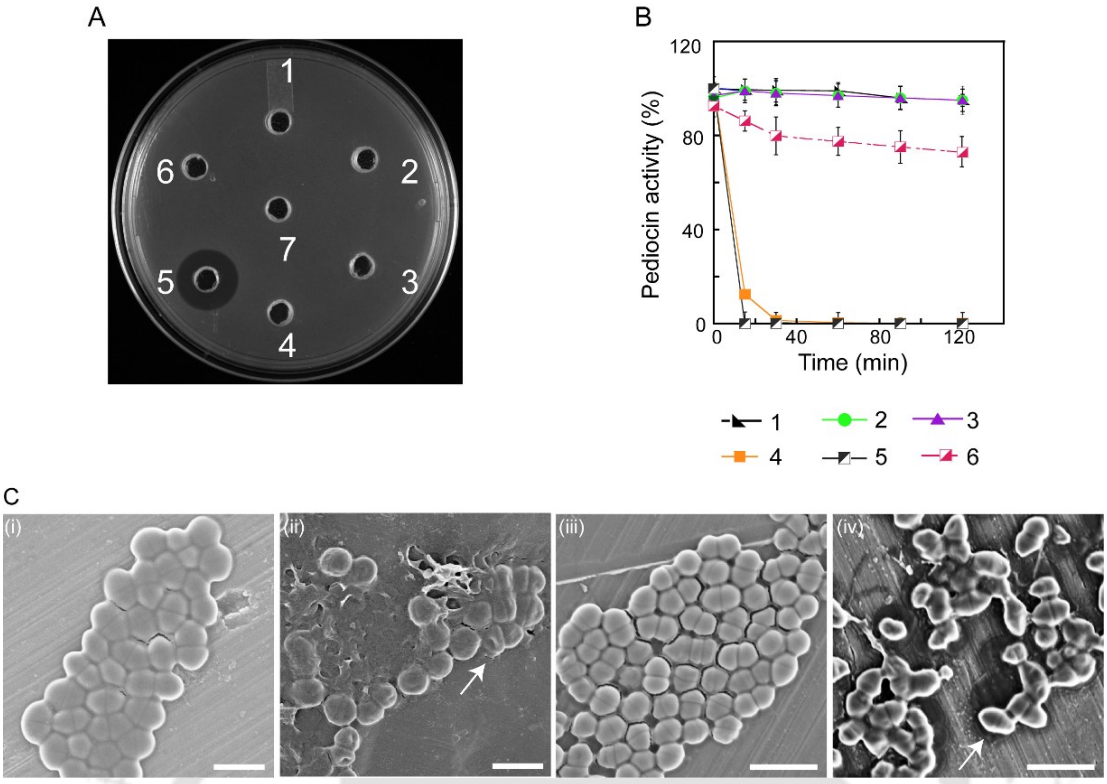

Figure 5.4. (A) Agar well diffusion assay performed on *L. monocytogenes* Scott A to ascertain pediocin activity. 1. SGF, 2. HSA in SGF, 3. Pediocin-HSA complex in SGF, 4. Pediocin in SGF, 5. Pediocin-MPE complex in SGF, 6. MPE in SGF, 7. MPE in PBS. (B) cFDA-SE leakage assay to ascertain pediocin activity 1. Pediocin (10 mM PBS), 2. Pediocin-HSA complex (10 mM PBS), 3. Pediocin-MPE complex (10 mM PBS), 4. Pediocin (SGF), 5. Pediocin-HSA complex (SGF), 6. Pediocin-MPE complex (SGF). (C) FESEM analysis to ascertain activity of pediocin-MPE complex on *S. aureus* MTCC 96 cells. (i) control cells (untreated), (ii) cells treated with pediocin, (iii) cells treated with pediocin incubated in SGF and (iv) cells treated with Pediocin-MPE complex (previously incubated in SGF). Arrows in panels (ii) and (iv) indicate damaged cells. Scale bar for the images is 2.0 µm.

in SGF. Incubation of purified pediocin in SGF led to a dramatic loss of activity as evidenced in the absence of a zone of inhibition against *L. monocytogenes* Scott A (Figure 5.4A, well no. 1). Pepsin is a major component of SGF (Charteris *et al.*, 1998) and is thus likely to inactivate pediocin, which is a proteinaceous bacteriocin. This fact is also supported by an earlier study, wherein pediocin was shown to lose its antibacterial activity in simulated gastric fluid (Kheadar *et al.*, 2010). Further, pediocin-HSA complex upon incubation in SGF failed to display a zone of inhibition, suggesting that the complexation with HSA could not hinder proteolytic inactivation of pediocin in

Table 5.1. Antibacterial activity of pediocin and pediocin-MPE complex against model gastrointestinal pathogen *L. monocytogenes* Scott A

Antibacterial Agent	Fluorescence Intensity (c.p.s.) [#]	Pediocin Activity (%) [*]
Pediocin in 10 mM PBS (pH 7.0)	825905	100
Pediocin in SGF (pH 2.0)	18995.815	2.26 ± 0.013
Pediocin-milk protein extract in 10 mM PBS (pH 7.4)	791216.99	95.8 ± 6.125
Pediocin-milk protein extract in SGF (pH 2.0)	588870.265	71.23 ± 4.83

[#] The fluorescence intensity was obtained in the cFDA-SE leakage assay as described in section 5.2.7.2.

***** Pediocin activity was obtained calculated based on the fluorescence intensity obtained in the cFDA-SE leakage assay as described in section 5.2.7.2.

SGF (Figure 5.4A, well no. 3). Interestingly, the pediocin-MPE complex on incubation in SGF displayed a clear zone of inhibition (Figure 5.4A, well no. 5), which strongly suggested that complexation of pediocin with MPE could protect pediocin against proteolytic cleavage in SGF. The results obtained in agar well diffusion assay was also validated by a cFDA-SE leakage assay, wherein the Ped-MPE complex incubated in SGF displayed significant retention of pediocin activity (Figure 5.4B). On quantification, the pediocin activity after incubation in SGF was found to be only 2.26 ± 0.013%, indicating virtually a complete loss in the antibacterial activity of pediocin upon incubation in SGF (Table 5.1). For instance, it was observed that complexation of pediocin with MPE resulted in the manifestation of 71.23% of pediocin activity, indicating significant retention of pediocin in Ped-MPE after gastric fluid challenge (Table 5.1). Retention of the antibacterial activity of pediocin-MPE complex was also captured in FESEM analysis, wherein considerable morphological perturbation of *S. aureus* MTCC 96 cells could be observed upon treatment with pediocin (in 10mM PBS) or Ped-MPE complex incubated in SGF, in contrast to the control cells as well as cells treated with pediocin incubated in SGF (Figure 5.4C, panels i-iv).

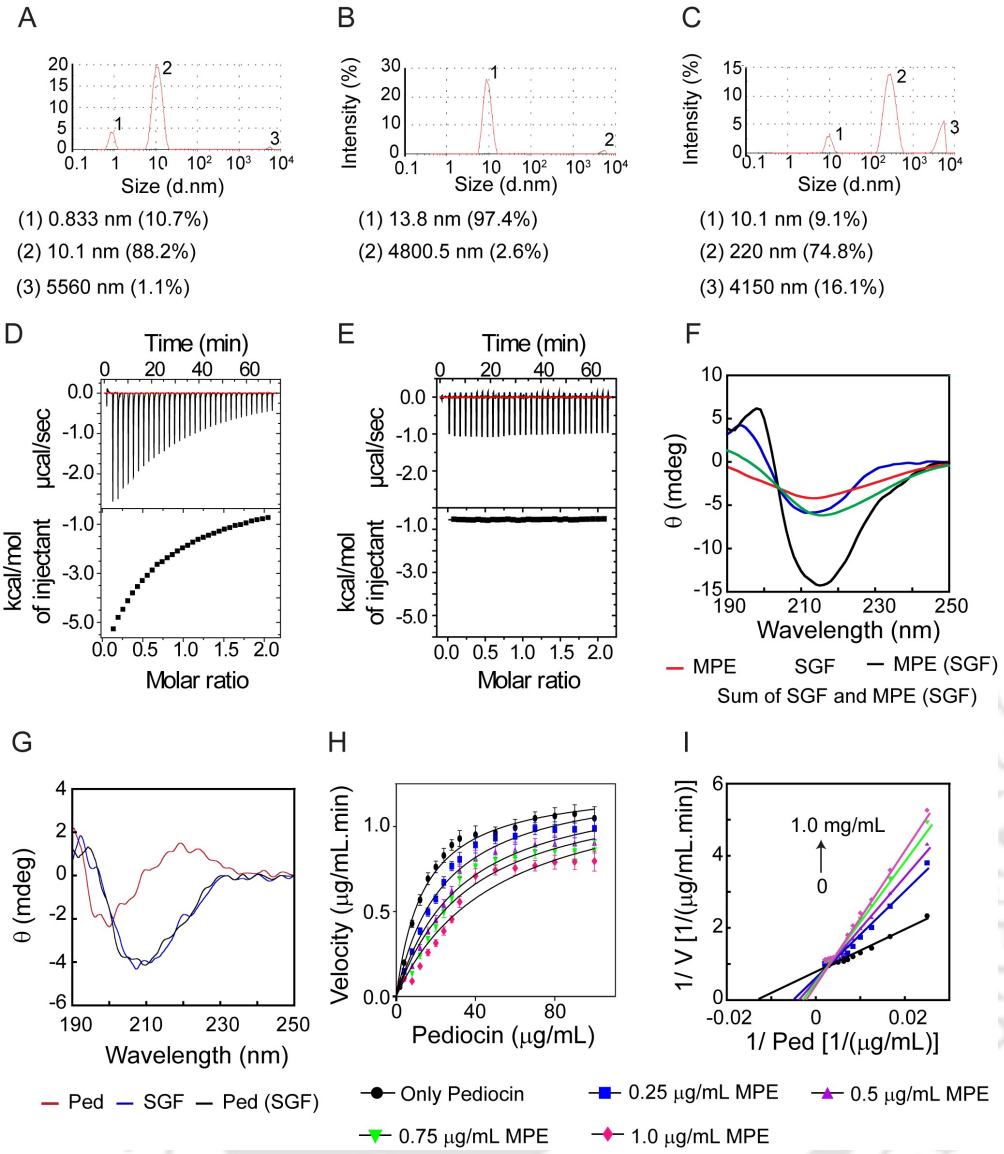

Figure 5.5. (A-C) Dynamic light scattering (DLS) based particle size analysis of MPE, SGF and MPE-SGF complex. The particle size and percentage of aggregated species of each sample (in parentheses) corresponding to peaks 1-3 are indicated below the plot. (D) Isothermal calorimetry (ITC) of MPE-SGF binding. (E) ITC of MPE-solvent interaction. (F) Circular dichroism (CD) spectra of MPE, SGF and MPE-SGF complex. (G) CD spectra of Ped, SGF and Ped-SGF complex. (H-I) Kinetics of pepsin-mediated digestion of pediocin in presence of MPE.

5.3.2. Interaction of MPE with SGF

Based on the encouraging results obtained from the antibacterial assays, which indicated that presence of MPE led to retention of pediocin activity in SGF (Figure

Table 5.2. Secondary structure analysis of pepsin in SGF, MPE, pediocin, MPE in SGF and pediocin in SGF.

Species	α-helix (%)	β-sheet (%)	Turns (%)	Random (%)
Pepsin (present in SGF)	2.4	74	0	23.5
MPE	0	22.1	16.8	61.2
Pediocin	0	47.3	24.7	28
MPE in SGF	15.7	45.8	11.2	27.2
Pediocin in SGF	1.3	73.6	0	25.1

5.4), it was considered pertinent to probe the mechanism behind the protective role of MPE. To this end, initial experiments using dynamic light scattering (DLS) were pursued to probe the complexation of MPE and SGF. It was found that in case of MPE, the principal aggregating species displayed a size of around 10 nm, whereas in case of SGF, the major aggregating species displayed a size of around 13 nm (Figure 5.5A-5.5B). On incubation of MPE in SGF, the principal species in solution (peak 2) was found to have a size of 220 nm, which suggested probable interaction between SGF and MPE (Figure 5.5C). In SGF, pepsin constitutes the proteinaceous component (Charteris *et al.*, 1998). Hence, it is plausible that pepsin present in SGF is likely to interact with MPE, leading to the formation of an aggregate. The interaction between SGF and MPE was further probed through isothermal calorimetry (ITC) wherein it was observed that at each injection, the binding was exothermic and the heat change gradually decreased to the basal dilution level (Figure 5.5D). The ITC pattern obtained for the control sample (titration of MPE against 0.5% saline, pH 2.0 without pepsin) indicated a lack of interaction between MPE and the solvent (Figure 5.5E). Further, the fitting of the isothermogram in a 1:1 stoichiometry yielded a hyperbolic curve (Figure 5.5D), indicating efficient binding between SGF and MPE, analogous to the strong binding reported previously for protein-ligand interactions (Sikora *et al.*, 2005; Zhou *et al.*, 2011). Subsequently, it was considered pertinent to probe the changes occurring in the secondary structure of pepsin, in SGF in presence of MPE. To this end, circular dichroism (CD) spectroscopy was pursued with SGF in presence of MPE. CD spectroscopy of SGF alone indicated a prominent ellipticity at 218 nm, indicating a high β-sheet content (Figure 5.5F and Table 5.2), which can perhaps be attributed to the presence of pepsin in SGF, as the enzyme is known to possess β-sheet rich region (Dunn, 2001, Ghosh *et al.*, 2015). Further, MPE was observed to display CD spectra

with a notable ellipticity at 220 nm, indicating the presence of a high α- helix content (Figure 5.5F). Interestingly, MPE-SGF complex displayed enhanced ellipticity and a reduced amount of β-sheet content (Figure 5.5F and Table 5.2). On analysis of the CD spectra of SGF in presence of MPE, it was found that the β-sheet content decreased considerably from 74% to 45.8% (Table 5.2). Further, there was also a concomitant increase in the amount of α-helix (2.4% to 15.7%) and turns (0 to 11.2%) measured for SGF in presence of MPE (Table 5.2). The significant decrease in the β-sheet content observed in case of MPE-SGF complex suggested the possibility of alterations in the secondary structure of pepsin present in SGF.

It may be mentioned here that CD spectroscopy of pediocin in SGF was also pursued, wherein the essential CD spectra observed earlier for SGF alone was conserved (Figure 5.5G and Table 5.2), which suggested that during the proteolytic digestion of pediocin in SGF, the secondary structure of pepsin present in SGF was essentially retained. Based on CD spectroscopy which indicated the possible perturbation of the secondary structure of pepsin (present in SGF) by MPE, it was pertinent to probe whether MPE could possibly inhibit the activity of pepsin present in SGF and thereby prevent proteolytic inactivation of pediocin in SGF. To this end, pepsin enzyme activity was ascertained in presence of MPE, using pediocin as a substrate. In the absence of MPE, pepsin present in SGF displayed significant activity against pediocin (Fig. 5.5H). Analysis of the kinetic parameters of pepsin activity on pediocin indicated that the K_m and V_{max} were 1.256 ± 0.037 µg/mL and 70.19 ± 7.3 [µg/mL]/min, respectively. However, presence of MPE, led to a significant increase in K_m (from 70.19 ± 7.3 µg/mL to 254.2 ± 19.5 µg/mL) with a minimal change in V_{max} (from 1.256 ± 0.037 [µg/mL]/min to 1.312 ± 0.15 [µg/mL]/min (Figure 5.5I). Based on the changes of the enzyme kinetics parameters, it can perhaps be construed that MPE may be functioning as competitive inhibitor of pepsin present in SGF, which presumably accounts for the retention of pediocin activity in SGF in presence of MPE.

5.3.3. Pediocin-loaded milk protein nanoparticle

Based on the favorable attributes of MPE with regard to its ability to retain pediocin activity in SGF, it was envisaged that MPE can perhaps be leveraged to develop a milk protein nanoparticle (MNP) that can facilitate encapsulation, retention of pediocin activity in the gastric milieu and delivery of the bacteriocin for alleviation of gastrointestinal pathogens. To this end, milk protein nanoparticle (MNP) was generated

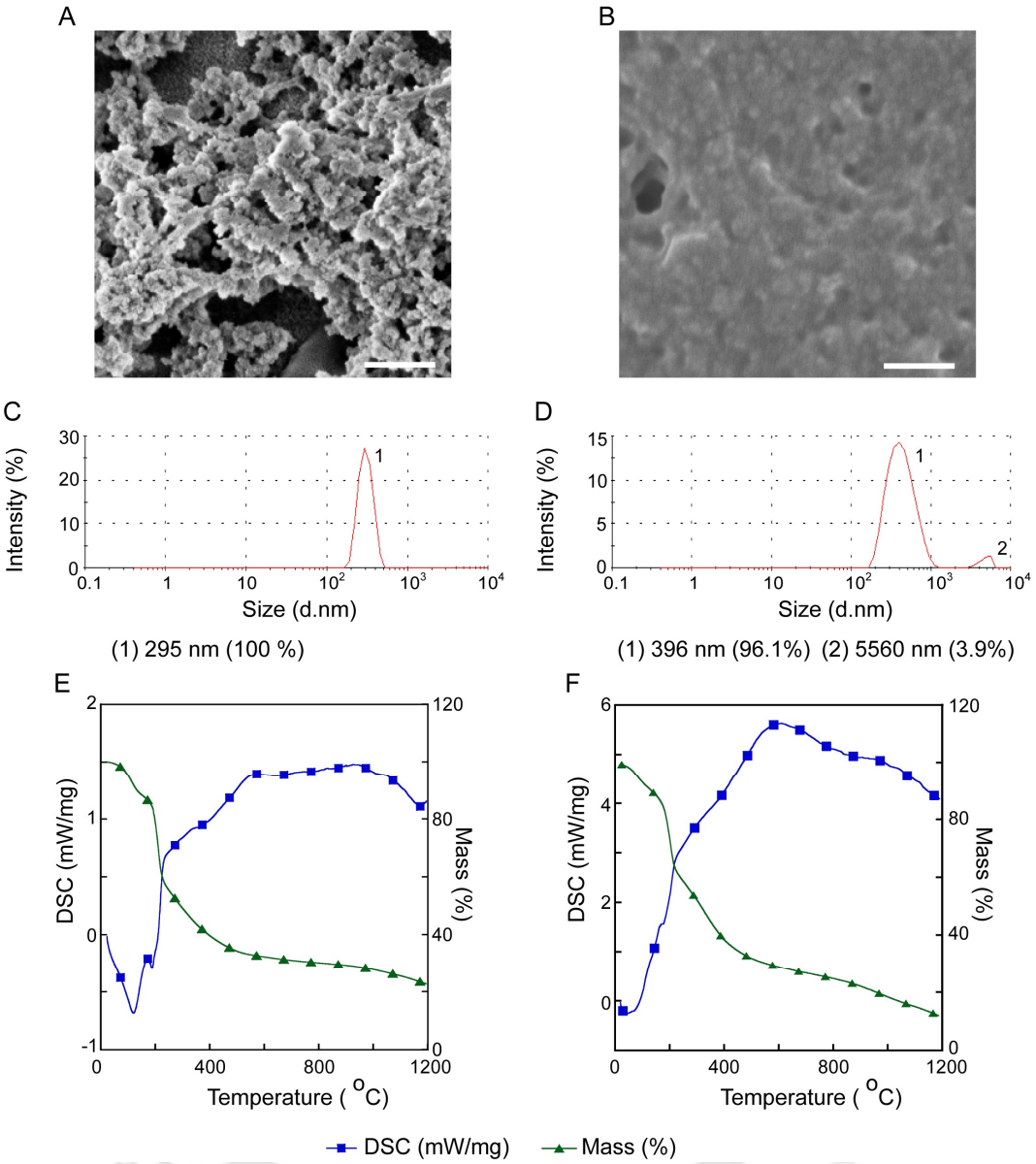

Figure 5.6. FESEM analysis of (A) MNP and (B) Ped-MNC. Scale bar for the images correspond to 200 nm. DLS-based particle size estimation of (C) MNP and (D) Ped-MNC. DSC and TGA of (E) MNP and (F) Ped-MNC.

from MPE using a standard desolvation technique (Langer *et al.*, 2003). The nanoparticles obtained after desolvation were essentially spherical in shape, with an average size of ~69.8 nm (Figure 5.6A). Following loading of pediocin onto MNPs, the pediocin-loaded milk protein nanocomposite (Ped-MNC) generated thereof were found to aggregate considerably, with a size of 97.6 nm (Figure 5.6B). DLS analysis indicated that the size of MNP was found to be nearly 295 nm (Figure 5.6C), whereas Ped-MNC

appeared to be highly aggregated in solution with a size of nearly 396 nm (Figure 5.6D). To assess the thermal stability of MNPs and Ped-MNC, thermogravimetric analysis (TGA) and differential scanning calorimetry (DSC) were performed. TGA revealed that the generated nanomaterials (MNP and Ped-MNC) were fairly stable up to ~100 °C with a three-step thermal decomposition (Figure 5.6E-5.6F). The loss of mass following increase in the temperature may be attributed to the proteinaceous nature of the developed nanomaterials (Figure 5.6E-5.6F). During the process of preparing MNP, glutaraldehyde was added as a cross-linking agent. It may be mentioned herein that glutaraldehyde may have toxic implications (Zeiger *et al.*, 2005; Takigawa and Endo, 2006). However, in the present study, glutaraldehyde was used at a final concentration of 0.08% (equivalent to 8.0 µM), which is lower than the concentration reported to be toxic to cultured human cells (Sun *et al.*, 1990; Vock *et al.*, 1999). Hence, it is anticipated that the prepared nanocomposite (Ped-MNC) is less likely to impart toxicological effects on human cells. However, in future, it would perhaps be worthwhile to explore the potential of food-grade crosslinkers such as glyceraldehyde, genipin and trans glutaminase (Caillard *et al.*, 2008; Manickam *et al.*, 2014; Tang *et al.*, 2006) in lieu of glutaraldehyde for preparation of MNPs suitable for therapeutic application.

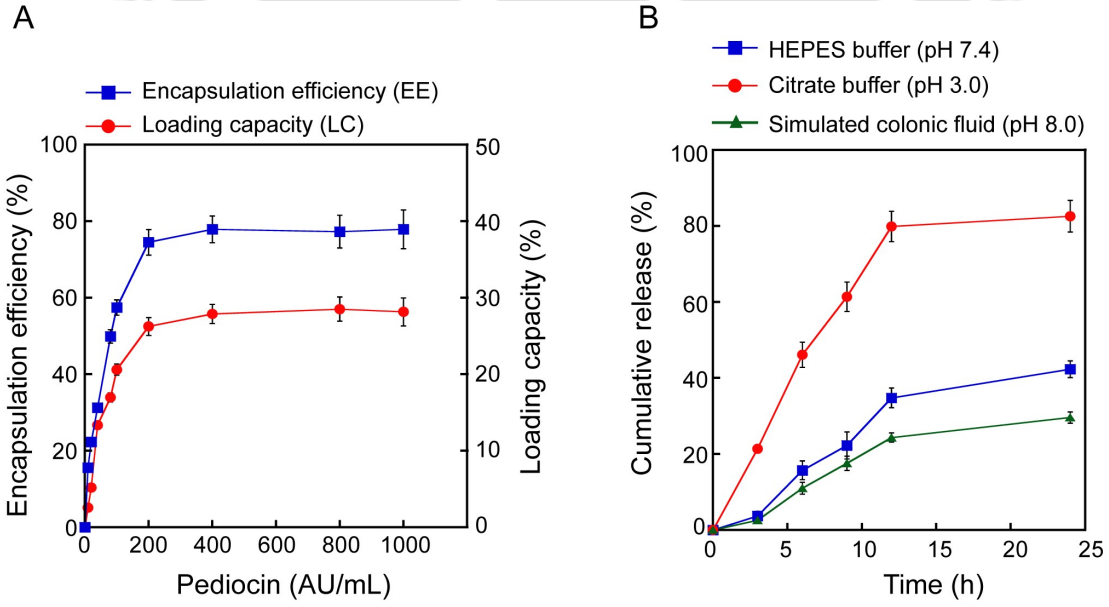

Figure 5.7. (A) Loading capacity (LC) and encapsulation efficiency (EE) of pediocin in MNP. (B) *In vitro* release kinetics of pediocin from Ped-MNC incubated in 10 mM HEPES buffer (pH 7.4), 10 mM citrate buffer (pH 3.0) and simulated colonic fluid (pH 8.0).

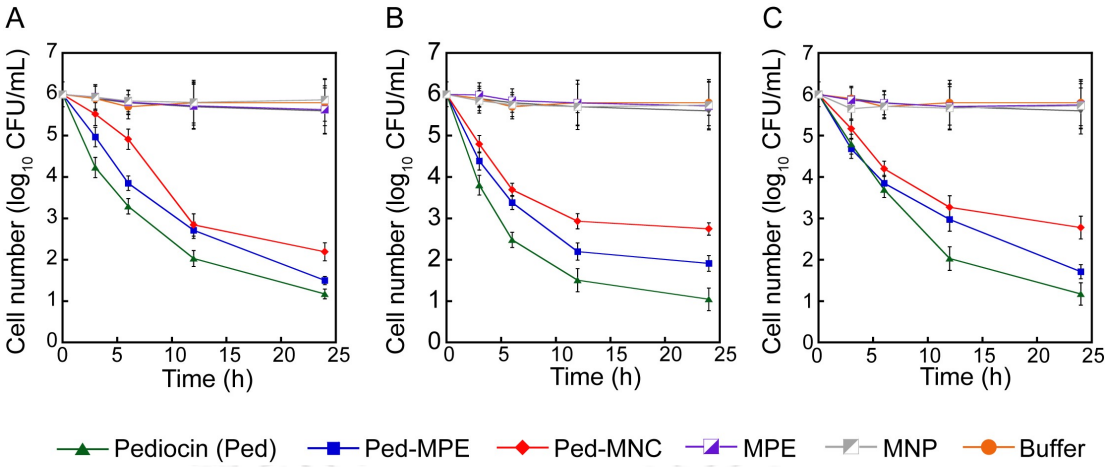

Figure 5.8. Time kill curve for target pathogens treated with pediocin-MPE complex and Ped-MNC in 10 mM phosphate buffer (pH 7.4). (A) *L. monocytogenes* Scott A, (B) *E. faecalis* MTCC 439 and (C) *S. aureus* MTCC 96.

The loading capacity (LC) and encapsulation efficiency (EE) of MNP was found to be 31 ± 4.2 % and 79.2 ± 6.9 % respectively (Figure 5.7A). The *in vitro* release kinetics of pediocin was studied with Ped-MNC loaded with a high concentration of pediocin (800 AU/mL). In HEPES buffer (pH 7.4) as well as in simulated colonic fluid (pH 8.0), a slow release of the bacteriocin from Ped-MNC was observed and the magnitude of the release from Ped-MNC in HEPES buffer and simulated colonic fluid was around 40% and 28%, respectively, following 24 h of incubation (Figure 5.7B). In acidic pH (pH 3.0), release of pediocin from Ped-MNC was rapid, as compared to the profile observed in HEPES buffer and simulated colonic fluid (Figure 5.7B). On performing a time-dependent assay in PBS (pH 7.4), it was found that both Ped-MPE and Ped-MNC could reduce the number of viable target cells of *L. monocytogenes* Scott A, *E. faecalis* MTCC 439 and *S. aureus* MTCC 96, with a comparatively slower killing kinetics as compared to pediocin alone (Figure 5.8). This phenomenon was anticipated as the killing efficiency of Ped-MPE and Ped-MNC would essentially depend on the dissociation of the bacteriocin from Ped-MPE complex or its release from Ped-MNC.

5.3.4. Bactericidal activity of pediocin-loaded milk protein nanocomposite (Ped-MNC)

In this study, HSA nanoparticle (HNP) was prepared and subsequently pediocin was loaded onto HNP to generate pediocin-loaded HSA nanoparticle (Ped-HNC). Subsequently, the activity of pediocin encapsulated in HNPs vis-à-vis MNPs was

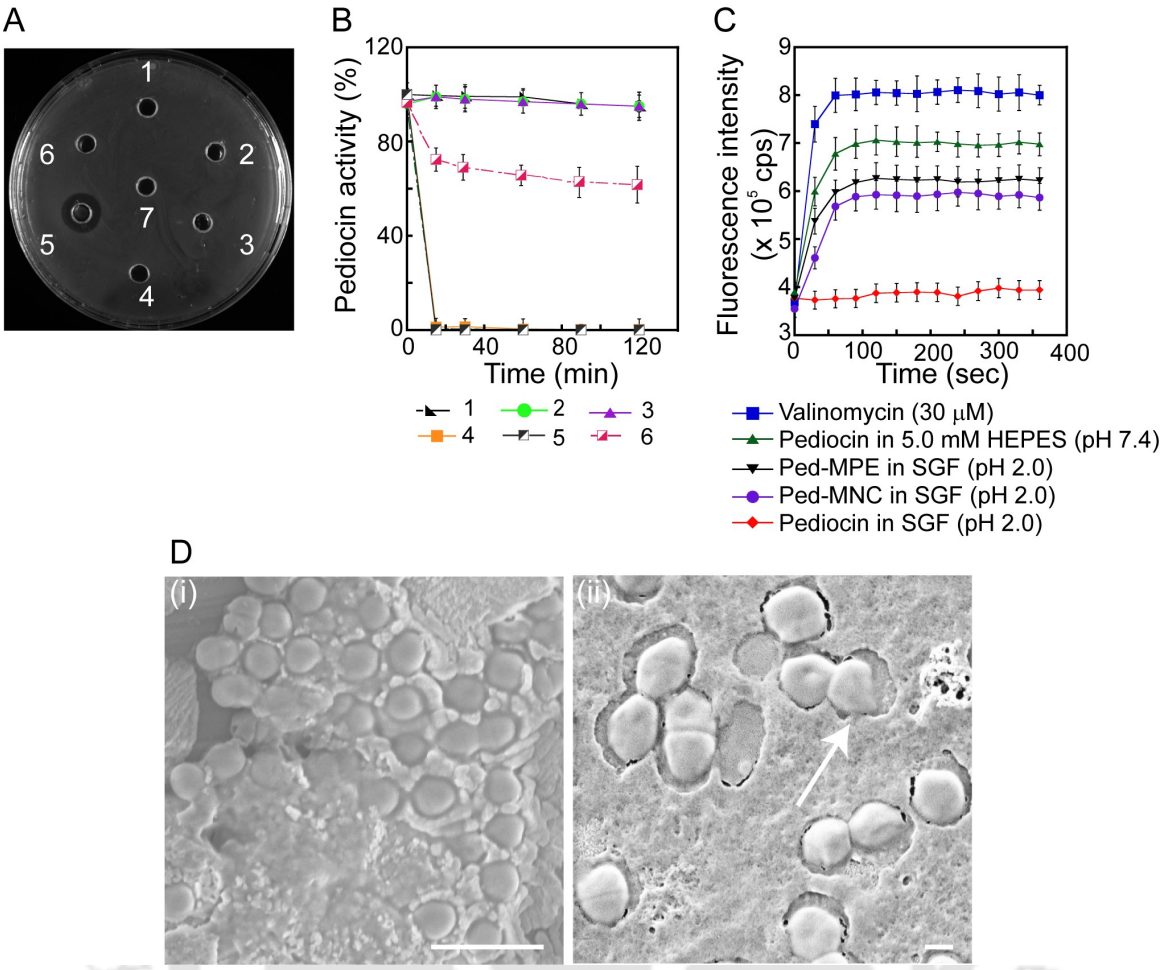

Figure 5.9. (A) Agar well diffusion assay performed on *L. monocytogenes* Scott A to ascertain pediocin activity. 1. SGF, 2. HNP in SGF, 3. Ped-HNC in SGF, 4. Pediocin in SGF, 5. Ped-MNC in SGF, 6. MNP in SGF, 7. MNP in PBS. (B) cFDA-SE-based pediocin activity assay. 1. Pediocin (in 10 mM PBS), 2. Ped-HNC (in 10 mM PBS), 3. Ped-MNC (in 10 mM PBS), 4. Pediocin (in SGF), 5. Ped-HNC (in SGF), 6. Ped-MNC (in SGF). (C) $DiSC_35$-based membrane potential assay to ascertain activity of Ped-MPE and Ped-MNC against *L. monocytogenes* Scott A. Valinomycin (30 µM) was used as a positive control. (D) FESEM analysis of *S. aureus* MTCC 96 treated with (i) MNP and (ii) Ped-MNC (previously incubated in SGF). Arrow in panel (ii) indicates damaged cell. Scale bar for the images corresponds to 1.0 µm.

compared following incubation in SGF. Encouragingly, the pediocin loaded milk protein nanocomposite (Ped-MNC) retained its bactericidal activity upon incubation in SGF as evident in the prominent zone of inhibition obtained in the agar well diffusion assay (Figure 5.9A, well no. 5), whilst HNP, Ped-HNC and pediocin failed to reveal any antibacterial activity upon incubation in SGF (Figure 5.9A, well nos. 2-4). Thus,

the ability of the milk protein extract (MPE) to protect pediocin from proteolytic inactivation in SGF could be leveraged as the milk protein nanoparticle derived from MPE could also demonstrate a similar attribute and retain the activity of the encapsulated pediocin in SGF. A cFDA-SE leakage assay also confirmed that the Ped-MNC incubated in SGF could demonstrate retention of pediocin activity against the pathogen *L. monocytogenes* Scott A (Figure 5.9B). The loss of antibacterial activity of Ped-HNC and pediocin in SGF was also captured in the cFDA-SE leakage assay (Figure 5.9B). In case of pediocin-loaded milk protein nanocomposite (Ped-MNC), it was interesting to observe that pediocin activity was conserved in SGF and upon quantitation by cFDA leakage assay, pediocin activity in Ped-MNC incubated in SGF amounted to 63.81 ± 4.12%, which clearly indicated considerable retention of pediocin activity in gastric fluid, in contrast to the complete loss of activity in case of pediocin incubated in SGF (Table 5.1). A membrane potential assay using $DiSC_35$ indicated that both Ped-MPE as well as Ped-MNC incubated in SGF could dissipate the transmembrane potential in target cells of *L. monocytogenes* Scott A (Figure 5.9C). Thus, the archetypal membrane depolarization activity associated with pediocin was largely retained in Ped-MPE and Ped-MNC even after incubation in SGF. However, pediocin incubated in SGF failed to render any change in the transmembrane potential of the target cells, corroborating the previous observed result wherein proteolytic degradation of pediocin leads to a loss in its antibacterial activity. The retention of the bactericidal activity of Ped-MNC incubated in SGF was also evidenced in FESEM analysis, wherein considerable target cell damage and morphological perturbation of the target cells of *S. aureus* MTCC 96 cells was manifested (Figure 5.9D, panel ii).

5.3.5. Interaction between MNP and SGF

The interaction between MNP and SGF was further probed through ITC. The primary observation was that at each injection, the binding was exothermic in nature and the heat change was found to gradually decrease to the basal dilution level (Figure 5.10A). The ITC pattern obtained for the control sample wherein MNP was added to 0.5% saline, pH 2.0 without pepsin indicated that there was a lack of binding between MNP and the solvent (Figure 5.10B). In case of the interaction between MNP and SGF, fitting of the isothermogram in a 1:1 stoichiometry yielded a hyperbolic curve (Figure 5.10A), which presumably indicates a strong binding between SGF and MNP. On subsequent CD analysis, the binding between MNP and pepsin present in SGF led to a

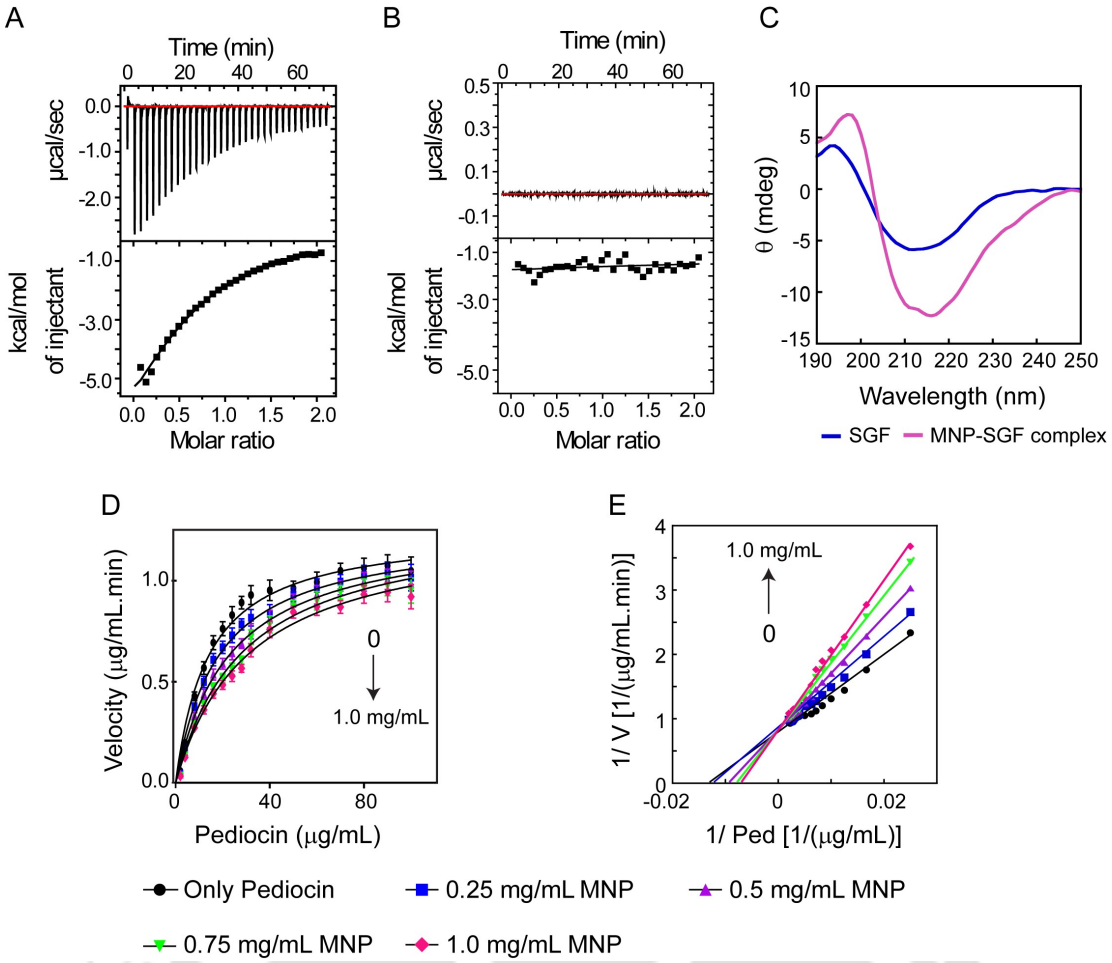

Figure 5.10. (A-B) ITC of MNP-SGF binding and MNP-solvent interaction. (C) CD spectra of SGF and MNP-SGF complex. (D-E) Kinetics of pepsin-mediated digestion of pediocin in Ped-MNC.

heightened ellipticity of the MNP-SGF complex as compared to SGF alone (Figure 5.10C). Further, it was found that the β-sheet content of SGF alone (74%) attributed to the presence of pepsin was reduced (57.2%) upon interaction of MNP and SGF (Table 5.2). Given that MNP could induce perturbation of the secondary structure of pepsin present in SGF, it was relevant to probe whether MNP could also inhibit the activity of pepsin present in SGF and thereby prevent proteolytic inactivation of pediocin in SGF. To this end, pepsin enzyme activity was ascertained in presence of MNP, using pediocin as a substrate. Interestingly, presence of MNP, led to an increase in K_m (from 70.19 ± 7.3 µg/mL to 121.9 ± 8.23 µg/mL) with a miniscule change in V_{max} (from 1.256 ± 0.037 [µg/mL]/min to 1.29 ± 0.2 [µg/mL]/min (Figure 5.10C-D). Based on the changes of the enzyme kinetics parameters, it can perhaps be interpreted that MNP may

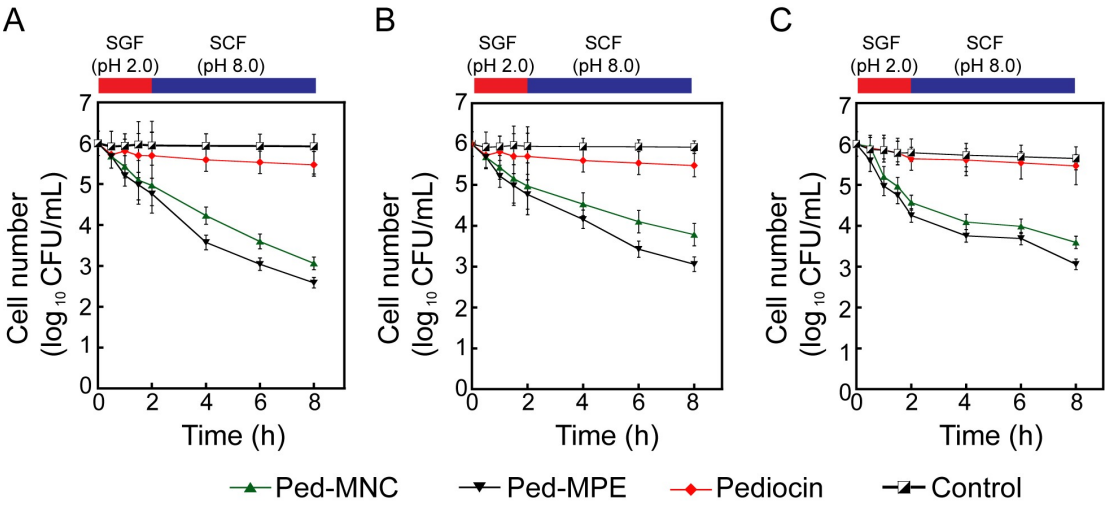

Figure 5.11. Loss of cell viability of model gastrointestinal pathogens upon treatment with Ped-MNC and Ped-MPE in a simulated gastric transit experiment. (A) *L. monocytogenes* Scott A, (B) *E. faecalis* MTCC 439 and (C) *S. aureus* MTCC 96.

be functioning as a competitive inhibitor of pepsin present in SGF, akin to MPE and presumably account for the retention of pediocin activity in Ped-MNC.

5.3.6. Bactericidal activity of pediocin-loaded milk protein nanocomposite (Ped-MNC) in a simulated gastric transit experiment

Subsequently, it was envisaged that it would be pertinent to probe the antibacterial efficacy of the developed Ped-MNC in fluids mimicking the environment during gastric transit. To this end, Ped-MNC was initially incubated in SGF (pH 2.0) and then transferred to SCF (pH 8.0). In the gastric transit experiment, only a nominal reduction in the number of viable cells from an initial 6.2 ± 0.29 $\log_{10}$ CFU/mL to 5.57 ± 0.37 $\log_{10}$ CFU/mL was evidenced, which amounted to only 11% decrease in cell viability (Figure 5.11A). Presumably the proteolytic digestion by pepsin in SGF leads to deactivation of pediocin in both SGF as well as in SCF. In case of Ped-MNC, there was a reduction in the cell number of *L. monocytogenes* Scott A in SGF by 1.2 $\log_{10}$ CFU/mL, indicating that retention of pediocin activity in Ped-MNC leads to loss of the target cell viability in SGF (Figure 5.11A). Further, incubation of Ped-MNC in SCF was found to reduce the viability of *L. monocytogenes* Scott A considerably and there was a reduction in the cell number of the target pathogen during gastric transit from an initial 6.2 ± 0.29 $\log_{10}$ CFU/mL to 3.17 ± 0.244 which amounted to 48.87% decrease in

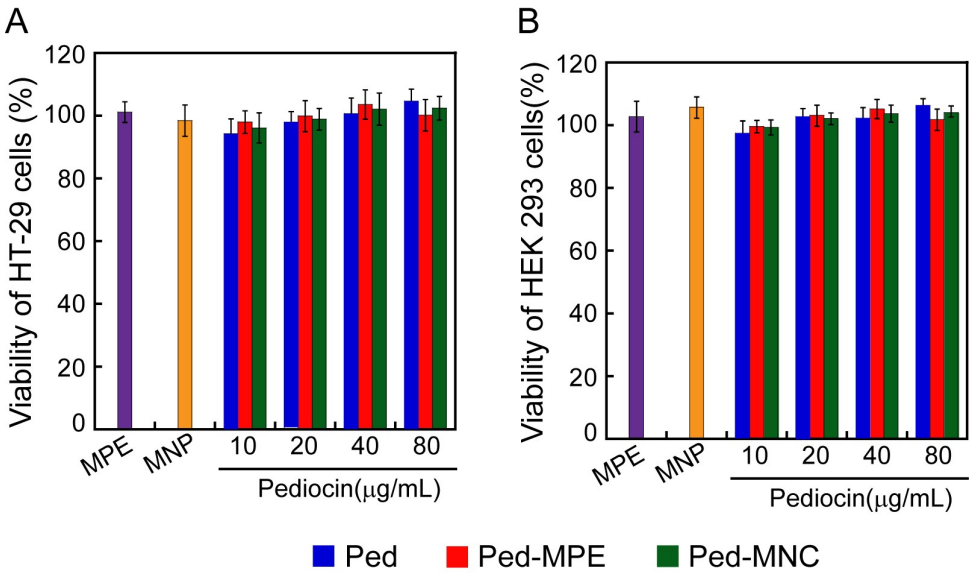

Figure 5.12. MTT assay to ascertain the *in vitro* cytotoxicity of Ped-MNC, MPE and MNP on (A) HT-29 and (B) HEK 293 cell lines, respectively. MTT assay was performed in six independent sets and each set consisted of three replicates.

bacterial viability (Figure 5.11A). These interesting observations indicated that the developed Ped-MNC was robust when subjected to the gastric transit experiments and was able to significantly retain the activity of the payload (pediocin) in a simulated gastrointestinal milieu. A similar loss in viability of target bacteria *E. faecalis* MTCC 439 and *S. aureus* MTCC 96 was also observed on incubation with Ped-MNC (Figure 5.11B-5.11C). For instance, upon treatment of *E. faecalis* MTCC 439 with Ped-MNC, the viable cell number reduced from 6.13 ± 0.19 $\log_{10}$ CFU/mL to 3.85 ± 0.6, which amounted to 37.19% decrease in bacterial viability (Figure 5.11B). In case of *S. aureus* MTCC 96, treatment with Ped-MNC in a simulated gastric transit experiment led to a decrease in the viable cell numbers from 6.1 ± 0.15 to 3.5 ± 0.2, with the decrease in viability being 42.63% (Figure 5.11C). Importantly, in an *in vitro* cytotoxicity assay conducted with HT-29 cells (colon adenocarcinoma cell line) and HEK 293 cells (human embryonic kidney cells), Ped-MNC was found to be non-toxic (Figure 5.12A-5.12B), indicating the biocompatibility and therapeutic potential of the developed proteinaceous nanocomposite for elimination of gastro-intestinal pathogens.

5.4. Significant Findings

The salient findings of this chapter are as follows:

1. LAB bacteriocins are promising antibacterials owing to their selective antibacterial activity towards gastrointestinal pathogens such as *L. monocytogenes*, *E. faecalis* and *S. aureus*. However, their therapeutic potential is limited due to their proteolytic inactivation by enzymes during gastric transit. The present investigation addresses this concern by deploying milk protein extract (MPE) and validating its potential in retention of antibacterial activity of pediocin in simulated gastric fluid (SGF).

2. Mechanistic studies revealed that MPE demonstrated a strong proclivity to interact with pepsin present in SGF and could render a competitive inhibition of the pepsin activity against pediocin.

3. The ability of MPE to hinder proteolytic cleavage of pediocin could be leveraged to develop milk protein nanoparticles (MNP) for the efficient delivery of pediocin in the gastric environment. Interestingly, pediocin-loaded milk protein nanocomposite (Ped-MNC) demonstrated retention of activity in SGF as well as in a simulated gastric transit experiment against the model gastrointestinal pathogens *L. monocytogenes*, *E. faecalis* and *S. aureus*.

4. *In vitro* cytotoxicity assays revealed that the developed nanocomposite was non-toxic to model human cell lines at the tested concentrations.

In recent times when the application of current therapeutic antibiotics is plagued with the associated cost of collateral damage to the gut microflora, the present study demonstrates the generation of a non-toxic LAB bacteriocin-loaded nanomaterial that can serve as a potent antibacterial agent for selective elimination of gastrointestinal pathogen. In this context, it would be pertinent to probe the possibility of deploying the antibacterial payload in conjunction with LAB with strong anti-adhesion capabilities to achieve significant abrogation of gastrointestinal pathogens on host cells. In line with this rational, the next chapter investigates the potential of pediocin-loaded milk protein nanocomposite in conjunction with native LAB to mitigate adhesion of model gastrointestinal pathogens in an *in vitro* extracellular matrix (ECM) and cell culture model.

Chapter 6

Combinatorial Effect of Bacteriocin-loaded Nanocomposite and Native LAB against Gastrointestinal Pathogenic Bacteria

This chapter illustrates the superior potency of the combinatorial effect of the native LAB strain and pediocin-loaded milk protein nanocomposite (Ped-MNC) in mitigation of gastrointestinal pathogen adhering onto ECM or HT-29 cells.

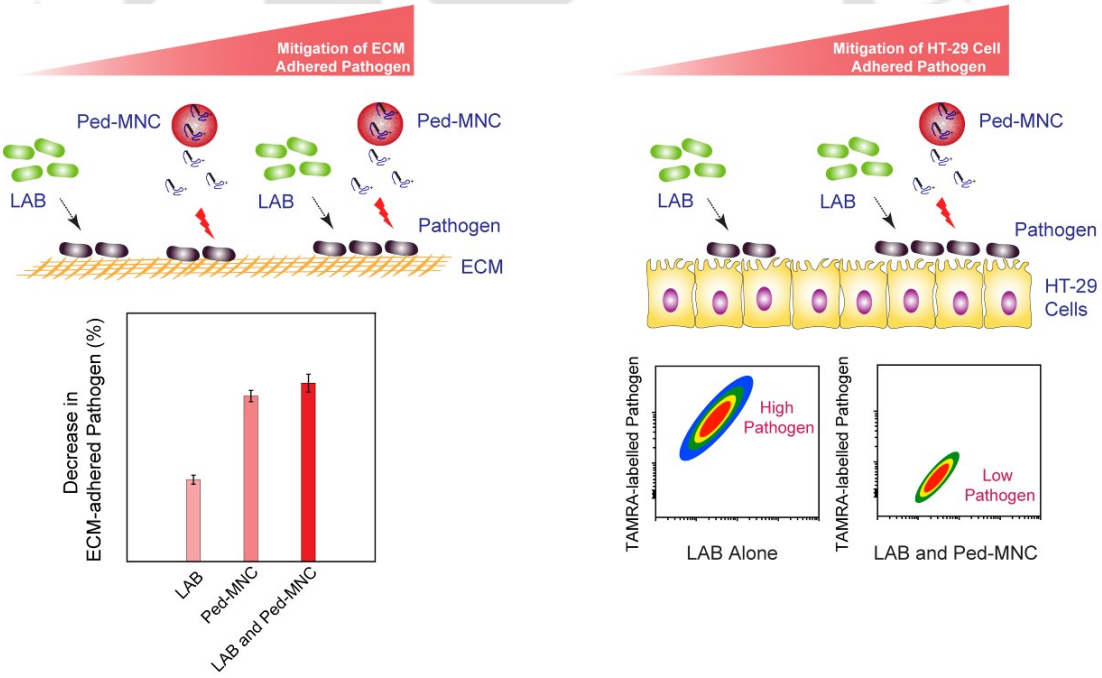

ABSTRACT

The increasing prevalence of gastrointestinal infections caused by pathogenic bacteria in conjunction with the loss of beneficial microbes due to the application of conventional therapeutic antibiotics has underscored the need for an alternate therapeutic approach. To this end, a combinatorial regimen of pediocin-loaded milk protein nanocomposite (Ped-MNC) and *L. plantarum* DF9 was explored in mitigating model gastrointestinal pathogens adhering onto extracellular matrix (ECM) or HT-29 cells in a cell culture model. A cFDA-SE based dye leakage assay indicated that Ped-MNC prior exposed to simulated gastric fluid (SGF) could demonstrate antibacterial activity on ECM-adhered pathogen, as manifested in 19.8% ± 3.07 leakage of the dye from that target *E. faecalis* cells adhering onto collagen-coated wells. Further, combinatorial deployment of Ped-MNC and *L. plantarum* DF9 led to 58.7% decrease in the number of pathogen adhering onto ECM as opposed to 38.2% decrease and 5.3% decrease in the number of ECM-adhered pathogen upon treatment with Ped-MNC or *L. plantarum* DF9, respectively. The superior activity of Ped-MNC and *L. plantarum* DF9 could be attributed to an increase in the dissociation constant (k_d) of *E. faecalis* cells adhering onto collagen from 15.8 $\log_{10}$ CFU per well to 29.5 $\log_{10}$ CFU per well and a decrease in maximum number of adhered bacterial cells (e_m) of *E. faecalis* cells on collagen from 9.29 $\log_{10}$ CFU per well to 5.1 $\log_{10}$ CFU per well. Combinatorial deployment of Ped-MNC and *L. plantarum* DF9 resulted in a substantially lower levels of *E. faecalis* MTCC 439 cells adhering onto HT-29 cells (25%) as compared to that observed when *L. plantarum* DF9 was used alone (61.1%). Estimation of the adhesion process parameters of *E. faecalis* MTCC 439 indicated that combination of Ped-MNC and *L. plantarum* DF9 led to an increase in k_d from 0.48×10^{-6} $\log_{10}$ CFU/mL to 8.3×10^{-6} $\log_{10}$ CFU/mL and a decline in e_m from 2.89 $\log_{10}$ CFU/mL per 10,000 HT-29 cells to 1.8 $\log_{10}$ CFU/mL per 10,000 HT-29 cells. This effect was also corroborated by a principal component analysis which indicated that the combinations of Ped-MNC or pediocin with either *L. plantarum* DF9 or the standard probiotic *L. rhamnosus* GG imparted a marked change in k_d and e_m of the adhesion of pathogen.

6.1. Introduction

Gastrointestinal infections due to pathogenic bacteria has been implicated in a rise in morbidity and mortality (Gibson and Barrett, 2010; Rodriguez *et al.*, 2011; Humphries *et al.*, 2015; Kirk *et al.*, 2015). In particular, gastrointestinal pathogens such as *Listeria monocytogenes*, *Enterococcus faecalis* and *Staphylococcus aureus* have been reported to be responsible for chronic intestinal infections (Cossart, 2011; Allen *et al.*, 2016; Barbuddhe and Chakraborty, 2009; Steck *et al.*, 2011; Shogan *et al.*, 2015; Kernbauer *et al.*, 2015). Further, the prevalence of antibiotic resistance genes in *E. faecalis* and their possible dissemination to other pathogens present in the gut (Werner *et al.*, 2012) is a cause of concern. Additionally, mitigation of pathogenic bacteria by conventional antibiotic has led to an extensive eradication of the beneficial microbes and consequent proliferation and invasion of gastric niche by opportunistic pathogenic bacteria (Ferrer *et al.*, 2014; Lin *et al.*, 2010; Schulfer and Blaser, 2015). Amongst the gut-colonizing pathogens, reports suggest that gastrointestinal infection by *E. faecalis* cells is associated with inflammation, ROS production and DNA damage to host cells (Strickertsson *et al.*, 2013). Further, gastric carriage of *E. faecalis* has been reported to cause bloodstream infections and mortality in healthcare settings (Maharshak *et al.*, 2015; Murray *et al.*, 2000). In the context of gastric colonization by *E. faecalis*, adhesion to extracellular matrix (ECM) and host intestinal cells is a critical step in its pathogenesis (Nallapareddy *et al.*, 2000; Gao *et al.*, 2013; Singh *et al.*, 2012b). Emerging literature reports have also elucidated the detrimental implications of colonization by *S. aureus* (Richards *et al.*, 2000; Acton *et al.*, 2009; Boyce and Havill, 2005; Yan *et al.*, 2014). *S. aureus* is known to be equipped with adhesins known as microbial surface component recognizing adhesive matrix molecules (MSCRAMMs) for binding to ECM molecule such as collagen (Foster *et al.*, 2014; Singh *et al.*, 2012b). On the other hand, reports also suggest that binding to mucin is critical for *S. aureus* pathogenesis and persistence in intestine (Gries *et al.*, 2005; Vesterlund *et al.*, 2006).

To mitigate the gastrointestinal infections caused by pathogenic bacteria, therapeutic interventions that demonstrate selective antibacterial activity towards gastrointestinal pathogens is needed. Bacteriocins, secreted by LAB, are ribosomally synthesized antimicrobial peptides (AMPs), displaying antibacterial activity against gastrointestinal pathogens such as *L. monocytogenes* Scott A, *E. faecalis*, *S. aureus* and *Clostridium difficile* (Drider *et al.*, 2006; Dobson *et al.*, 2012; Cotter *et al.*, 2013; Chikindas *et al.*, 2018). Encouragingly, LAB bacteriocins possess a narrow spectrum of

antibacterial activity (Drider *et al.*, 2006; Cotter *et al.*, 2013; Cavera *et al.*, 2015; Umu *et al.*, 2016) and are thus anticipated to have minimal effect on the beneficial microbes. However, application of LAB bacteriocin in the gastric niche demands retention of its activity during gastric transit, targeted delivery and sustained release kinetics in the vicinity of the pathogen. A way to overcome this issue, might be the encapsulation of LAB bacteriocin in a robust nanocarrier for protection in the presence of gastric enzymes and sustained release. In the previous chapter, this tenet has been demonstrated wherein the encapsulation of the LAB bacteriocin pediocin in a milk protein nanocomposite (Ped-MNC) resulted in significant retention of pediocin activity in a gastric transit experiment leading to mitigation of model intestinal pathogens.

Another interesting aspect of LAB is their propensity to adhere onto ECM molecules and host intestinal cells. Further, LAB can substantially influence the activity and composition of human intestinal microbiota (Priedis *et al.*, 2011; Shanahan, 2010; Patel and DuPont, 2015; Guandalini, 2011; Stecher *et al.*, 2010; O'Shea *et al.*, 2012). Thus, food isolates of LAB having probiotic virtues offer an exciting prospect of developing a safe LAB-based anti-bacterial regime, given their inherent propensity to survive in the harsh gastrointestinal niche and their ability to adhere onto ECM and host intestinal cells and thereby prevent pathogen adhesion. The LAB strain itself can be explored as an anti-adhesion agent, while the bacteriocin produced by the strain may serve as a safe therapeutic antibacterial. Based on this premise, this chapter describes the combinatorial application of pediocin-loaded milk protein nanocomposite and *L. plantarum* DF9 for the abrogation of gastrointestinal pathogens, *L. monocytogenes*, *E. faecalis* and *S. aureus* adhering onto ECM and HT-29 cell culture model.

6.2. Materials and Methods

6.2.1. Growth media and chemicals

Glutaraldehyde, 5 (and 6)-carboxyfluorescein diacetate succinimidyl ester (cFDA-SE), 5-carboxy-tetramethylrhodamine N-succinimidyl ester (TAMRA-SE), 2-(4-amidinophenyl)-6-indolecarbamidine dihydrochloride (DAPI), Triton X-100, pepsin, Dulbecco's modified Eagle's medium (DMEM) and penicillin-streptomycin were obtained from Sigma-Aldrich Chemicals, USA. Methanol was purchased from Merck, Mumbai, India. Brain-Heart Infusion (BHI) broth and deMan, Rogosa and Sharpe (MRS) broth were purchased from Himedia, Mumbai, India. Fetal bovine serum (FBS) was procured from Gibco, India.

6.2.2. Bacterial strain and growth conditions

The target pathogens used in the present investigation comprised of *Listeria monocytogenes* Scott A (*L. monocytogenes* Scott A), *Enterococcus faecalis* MTCC 439 (*E. faecalis* MTCC 439), *Staphylococcus aureus* MTCC 96 (*S. aureus* MTCC 96) and *Staphylococcus aureus* MTCC 740 (*S. aureus* MTCC 740). Prior to experiments, the bacterial strains were propagated in BHI broth at 37 °C and 180 rpm for 12 h. The standard LAB *L. rhamnosus* GG and the bacteriocinogenic native LAB *L. plantarum* DF9 were grown as per the conditions described previously in section 2.2.2. in Chapter 2. For production of pediocin, *Pediococcus pentosaceus* CRA51 was propagated in MRS broth at 37 °C in static condition for 18 h.

6.2.3. HT-29 cell culture

HT-29 cells were grown and maintained as previously described in Section 2.2.6. in Chapter 2. Prior to adhesion experiments, the HT-29 monolayer was washed twice with sterile phosphate buffered saline (PBS), trypsinized and transferred to a 24-well multi-dish plate (1×10^4 cells per well) having fresh DMEM medium and incubated at 37 °C in 5% CO_2. Subsequently, the monolayer of HT-29 cells was propagated for 7 days, with a change of medium every 2 days and used at late post-confluence stage for the adhesion assays.

6.2.4. Antibacterial activity of Ped-MNC on ECM-adhered pathogens

Purification of pediocin and generation of Ped-MNC was accomplished by following the methods described earlier in section 5.2.3. and section 5.2.9. respectively, in

Chapter 5. In separate sets, solution of either purified pediocin (800 AU/mL) or Ped-MNC (2.0 mg/mL MNP loaded with 800 AU/mL pediocin, pH adjusted to 2.0) were added to SGF and incubated for 2 h. Likewise, in separate sets, solution of either purified pediocin (800 AU/mL) or Ped-MNC (2.0 mg/mL MNP loaded with 800 AU/mL pediocin, pH adjusted to 7.4) were added to 10 mM phosphate buffer (pH 7.4) and incubated for 2 h. Following incubation, pediocin activity in all the samples was ascertained against ECM-adhered *E. faecalis* MTCC 439, *L. monocytogenes* Scott A and *S. aureus* MTCC 96 cells in separate sets. For the adhesion of the target pathogens onto ECM, cells of *E. faecalis* MTCC 439, *L. monocytogenes* Scott A and *S. aureus* MTCC 96 were labelled with cFDA-SE following the protocol described previously (Singh *et al*., 2012a) and fluorescence intensity was measured (F_T) using a multiplate reader (Infinite M200, Tecan, Switzerland). Subsequently, the cells were allowed to adhere onto collagen- or mucin-coated wells for 2 h followed by aspiration of non-adhered cells and washing to remove sparsely adhered cells. To each well, either purified pediocin (800 AU/mL pediocin pretreated with SGF or preincubated in 10 mM phosphate buffer) or Ped-MNC (loaded with 800 AU/mL pediocin and pretreated with SGF or preincubated in 10 mM phosphate buffer) was added followed by an incubation period of 2 h. Subsequently the supernatant was gently aspirated, centrifuged to remove any cells and the fluorescence intensity of the collected supernatant (F_S) was measured using a multiplate reader (Infinite M200, Tecan, Austria). The results were expressed as percentage leakage by comparing F_S to F_T in the experiments involving the test samples. Each experiment was performed in triplicate and the result was represented as mean ± standard deviation. The adhered cFDA-SE labelled pathogen following treatment with the test samples were also observed under fluorescence microscope (Eclipse Ti-U, Nikon, USA) with a filter that allowed blue light excitation for cFDA-SE.

6.2.5. Effect of Ped-MNC and LAB on ECM-adhered pathogens

The model pathogens *E. faecalis* MTCC 439, *L. monocytogenes* Scott A and *S. aureus* MTCC 96 were grown overnight, harvested by centrifugation, washed and resuspended in sterile PBS to OD_{600} of 1.0. Fluorescence labelling of the target pathogens with cFDA-SE was accomplished as described previously (Singh *et al.*, 2012a). The solution fluorescence of a 100 µL aliquot of the cFDA-SE-labelled pathogens was measured in a multiplate reader (Infinite M200, Tecan, Austria) and

considered as total fluorescence (F_T). Subsequently, 100 µL aliquot of cFDA-SE-labelled cells of the model pathogens was added to collagen or mucin-coated wells in separate sets and incubated for 2 h. Following incubation, non-adhered cells were aspirated and their fluorescence intensity was measured (F_{NA}). A quantitative measure of pathogen adhesion (F_A) to collagen and mucin was calculated from the following expression:

$$F_A = F_T - F_{NA} \quad .....6.1$$

Subsequently, to each well the following test samples were added: *L. plantarum* DF9 (7.0 $\log_{10}$ CFU added in 100 µL sterile PBS per well), *L. rhamnosus* GG (7.0 $\log_{10}$ CFU added in 100 µL sterile PBS per well), Ped-MNC (loaded with 800 AU/mL pediocin and added in 100 µL sterile PBS per well) or a combination of *L. plantarum* DF9 (7.0 $\log_{10}$ CFU added in 50 µL sterile PBS per well) and Ped-MNC (loaded with 800 AU/mL pediocin and added in 50 µL sterile PBS per well) or a combination of *L. rhamnosus* GG (7.0 $\log_{10}$ CFU added in 50 µL sterile PBS per well) and Ped-MNC (loaded with 800 AU/mL pediocin and added in 50 µL sterile PBS per well). The addition of test samples to ECM-adhered pathogen was followed by an incubation period of 2 h. Following incubation, the supernatant, which essentially consisted of non-adhered pathogen was gently aspirated, centrifuged and the fluorescence intensity of the collected supernatant (F_S) for each test sample was measured using a multiplate reader (Infinite M200, Tecan, Austria). The decrease in ECM-adhered pathogen (%) was estimated from the following expression:

$$\text{Decrease in ECM-adhered pathogen (\%)} = \frac{F_A - F_S}{F_A} \times 100 \quad .....6.2.$$

where F_A represents a quantitative measure of pathogen adhesion and F_S represents the quantitative measure of non-adhered cells of cFDA-labelled pathogens. All the experiments were performed in triplicates and the mean and standard deviation was calculated.

6.2.6. Determination of adhesion process parameters on ECM

E. faecalis MTCC 439 and *S. aureus* MTCC 96 were grown overnight, harvested and labelled with cFDA-SE as described earlier in section 3.2.5. in Chapter 3. The solution fluorescence of a 100 µl aliquot of the cFDA-SE-labelled LAB strains of varying cell

number (2.0–8.0 $\log_{10}$ CFU per well) was measured in a multiplate reader (Infinite M200, Tecan, Austria) and considered as total fluorescence (F_T). Subsequently, the cFDA-SE labelled bacterial cells (cell number ranging from 2.0–8.0 $\log_{10}$ CFU per well) were allowed to adhere onto ECM-coated wells for 2 h. Following the incubation, to separate wells the following test samples were also added: *L. plantarum* DF9 (7.0 $\log_{10}$ CFU added in 100 µL sterile PBS per well), *L. rhamnosus* GG (7.0 $\log_{10}$ CFU added in 100 µL sterile PBS per well), Ped-MNC (loaded with 800 AU/mL pediocin and added in 100 µL sterile PBS per well) or a combination of *L. plantarum* DF9 (7.0 $\log_{10}$ CFU added in 50 µL sterile PBS per well) and Ped-MNC (loaded with 800 AU/mL pediocin and added in 50 µL sterile PBS per well) or a combination of *L. rhamnosus* GG (7.0 $\log_{10}$ CFU added in 50 µL sterile PBS per well) and Ped-MNC (loaded with 800 AU/mL pediocin and added in 50 µL sterile PBS per well). Following 2 h of incubation, the dose-dependent adhesion onto collagen- or mucin-coated wells was quantified using the method described earlier in section 3.2.4. in Chapter 3. The maximum number of adhered bacteria (e_m) and the dissociation constant (k_d) for the adhesion process were ascertained by the method described earlier in section 3.2.4. in Chapter 3. All the experiments were performed in triplicates and mean ± SD was calculated using Microsoft excel (Microsoft Corporation, USA).

6.2.7. In vitro release kinetics of pediocin from Ped-MNC in DMEM medium

To study the *in vitro* release kinetics of pediocin in antibiotic-free DMEM, Ped-MNC loaded with 800 AU/mL of pediocin was dispersed in 1.0 mL of sterile antibiotic-free DMEM media. The samples were incubated in an orbital shaker at 180 rpm and 37 °C. At specific time intervals (3 h, 6 h, 9 h, 12 h and 24 h) the samples were withdrawn and centrifuged at 10,000 × g for 15 min. The supernatant from various samples was transferred into a fresh microcentrifuge tube and pediocin activity was ascertained based on cFDA-based leakage assay (section 5.2.10.4. in Chapter 5) and a previously generated calibration plot (section 5.2.10.5. in Chapter 5) was used to measure the quantity of pediocin released from Ped-MNC at specific time periods and expressed as % cumulative release.

6.2.8. Antibacterial activity of Ped-MNC on HT-29 cell-adhered pathogens

Initially a monolayer of HT-29 cells was prepared for the adhesion assay as outlined in section 2.2.6. in Chapter 2. Target cells of *E. faecalis* MTCC 439 (8.0 $\log_{10}$ CFU/mL)

and *S. aureus* MTCC 740 (8.0 $\log_{10}$ CFU/mL) were suspended in antibiotic-free DMEM medium and were added to the monolayer of HT-29 cells and incubated for 1 h. Following incubation, the non-adhered cells were aspirated and in separate sets, purified pediocin (800 AU/mL) or Ped-MNC (corresponding to pediocin levels of 800 AU/mL) were added and incubated for 1 h. At regular intervals (15 min, 30 min, 45 min and 60 min), the HT-29 cells were washed with PBS, followed by addition of 0.05% Triton-X to selectively lyse the HT-29 cells. For every sample the lysed cells were then serially diluted and plated on BHI agar plates to determine the viable cell numbers ($\log_{10}$ CFU/mL) of the adhered pathogen. All the experiments were performed in triplicate and data analysis and determination of standard deviation was performed with Microsoft Excel 2010 (Microsoft Corporation, USA).

6.2.9. Inhibition of pathogen adhesion onto HT-29 cells by LAB and pediocin-loaded nanocomposite

Initially the LAB cells (*L. plantarum* DF9 and *L. rhamnosus* GG) and model pathogens (*E. faecalis* MTCC 439 and *S. aureus* MTCC 740) were labelled with cFDA-SE and TAMRA-SE, respectively as described previously in section 4.2.4. of Chapter 4. Subsequently, the TAMRA-labelled pathogens were added to HT-29 cells in a 24-well multi-dish plates and incubated for 1 h. The wells were then washed with sterile PBS to remove the non-adherent bacteria and the following test samples were added in separate wells: *L. plantarum* DF9 (7.0 $\log_{10}$ CFU added in 500 µL sterile PBS per well), *L. rhamnosus* GG (7.0 $\log_{10}$ CFU added in 500 µL sterile PBS per well), Ped-MNC (loaded with 800 AU/mL pediocin and added in 500 µL sterile PBS per well) or a combination of *L. plantarum* DF9 (7.0 $\log_{10}$ CFU added in 250 µL sterile PBS per well) and Ped-MNC (loaded with 800 AU/mL pediocin and added in 250 µL sterile PBS per well) or a combination of *L. rhamnosus* GG (7.0 $\log_{10}$ CFU added in 250 µL sterile PBS per well) and Ped-MNC (loaded with 800 AU/mL pediocin and added in 250 µL sterile PBS per well). The addition of test samples to pathogens adhering onto HT-29 cells was followed by an incubation period of 1 h. Subsequently, HT-29 cells containing the adhered bacterial cells were treated with 0.05 % Triton X-100 to selectively lyse the mammalian cells and the suspension containing the bacterial cells were then subjected to FCM. Detection of fluorescence signal, data acquisition and data analysis were accomplished as described in section 4.2.4. in Chapter 4. All the

experiments were performed in triplicates and mean and standard deviation was calculated.

6.2.10. Estimation of process parameters for adhesion inhibition

Initially the LAB cells (*L. plantarum* DF9 and *L. rhamnosus* GG) and model pathogens (*E. faecalis* MTCC 439 and *S. aureus* MTCC 740) were labelled with cFDA-SE and TAMRA-SE, respectively as described previously in section 4.2.4. in Chapter 4. Subsequently, the TAMRA-SE labelled pathogen (cell numbers ranging from 4.0–8.0 $\log_{10}$ CFU per well) were allowed to adhere on HT-29 cells for 1 h. Following the incubation, to the following test samples were added in separate wells: *L. plantarum* DF9 (7.0 $\log_{10}$ CFU added in 500 µL sterile PBS per well), *L. rhamnosus* GG (7.0 $\log_{10}$ CFU added in 500 µL sterile PBS per well), Ped-MNC (loaded with 800 AU/mL pediocin and added in 500 µL sterile PBS per well) or a combination of *L. plantarum* DF9 (7.0 $\log_{10}$ CFU added in 250 µL sterile PBS per well) and Ped-MNC (loaded with 800 AU/mL pediocin and added in 250 µL sterile PBS per well) or a combination of *L. rhamnosus* GG (7.0 $\log_{10}$ CFU added in 250 µL sterile PBS per well) and Ped-MNC (loaded with 800 AU/mL pediocin and added in 250 µL sterile PBS per well). Following 1 h of incubation, HT-29 cells containing the adhered bacterial cells were treated with 0.05 % Triton X-100 to selectively lyse the mammalian cells. The suspension, which essentially consisted of the TAMRA-labelled pathogen and cFDA-labelled LAB were subjected to FCM and the results were acquired as quadrant plots as described previously in section 4.2.5. in Chapter 4. The quadrant plots were subjected to statistical analysis and the number of events obtained from upper left quadrant (for pathogens) and lower right quadrant (for LAB strains) was considered to assess the number of bacterial cells adhered onto HT-29 cells. Subsequently, the number of adhered pathogen was used to estimate the dissociation constant (k_d) and maximum number of adhered cells (e_m) as described in section 4.2.6. in Chapter 4. Each experiment was performed in triplicate and the result was represented as mean ± standard deviation. Principal component analysis (PCA) of the adhesion inhibition assays was performed using a standard method (Fernandes *et al*., 2014).

6.2.11. Imaging studies

Prior to cell imaging studies, HT-29 cells were seeded onto a 24-well multidish plate and grown in DMEM medium at 37 °C till 90% confluency under 5.0 % CO_2.

Subsequently, the cells were washed thrice with sterile PBS and incubated with 5.0 µM DAPI for 30 min. Following DAPI-labelling, HT-29 cells were washed with sterile PBS and incubated in separate sets with TAMRA-labelled *E. faecalis* MTCC 439 (8.0 $\log_{10}$ CFU/mL) for 1 h. Subsequently, the adhered pathogen was exposed to Ped-MNC (loaded with pediocin levels of 800 AU/mL) as described in section 6.2.8. Following incubation, HT-29 cells were gently washed with sterile PBS to remove any non-adherent or weakly adherent bacteria and observed under a fluorescence microscope (Eclipse Ti-U, Nikon, USA) using appropriate filters (UV filter for DAPI: Excitation: 360/20 nm, Emission: 460/25 nm; Green filter for TAMRA-SE: Excitation: 540/25 nm, Emission: 605/55 nm). To study adhesion inhibition of *E. faecalis* MTCC 439 by *L. plantarum* DF9 and Ped-MNC, the bacterial strains were labelled with TAMRA-SE and cFDA-SE, respectively, while HT-29 cells were labelled with DAPI. Subsequently, the experimental protocol for determining inhibition of pathogen adhesion onto HT-29 cells was followed as described previously in section 6.2.9. Subsequently, the cells were washed with sterile PBS and the images of the adhered cells was captured using appropriate filters (UV filter for DAPI: Excitation: 360/20 nm, Emission: 460/25 nm; Blue filter for cFDA-SE: Excitation: 480/15 nm, Emission: 535/20 nm; Green filter for TAMRA-SE: Excitation: 540/25 nm, Emission: 605/55 nm).

6.3. Results and Discussion

6.3.1. Antibacterial activity of Ped-MNC on ECM-adhered pathogens

The ability of *S. aureus* to adhere onto extracellular matrix (ECM) molecules and consequently colonize the intestine can be implicated in chronic infections (Foster *et al.*, 2014; Gries *et al.*, 2005; Hansen *et al.*, 2006). Further, the presence of microbial surface components recognizing adhesive matrix molecules (MSCRAMMs) in *E. faecalis* are known to mediate adhesion onto ECM and colonization on the host cells (Nallapareddy *et al.*, 2000; Gao *et al.*, 2013; McGuckin *et al.*, 2011). Given the strong antibacterial activity of pediocin against *L. monocytogenes*, *E. faecalis* and *S. aureus* (Singh *et al.*, 2012a), it was envisaged that the bacteriocin could perhaps curtail the ability of these pathogens to adhere and colonize ECM. To this end, Ped-MNC was initially incubated in simulated gastric fluid (SGF) as described in section 5.2.11. in Chapter 5. Incubation of Ped-MNC in SGF was pursued to simulate the gastric transit. Subsequently, Ped-MNC (treated with SGF) was deployed against ECM-adhered pathogens, *L. monocytogenes* Scott A, *E. faecalis* MTCC 439 and *S. aureus* MTCC 96.

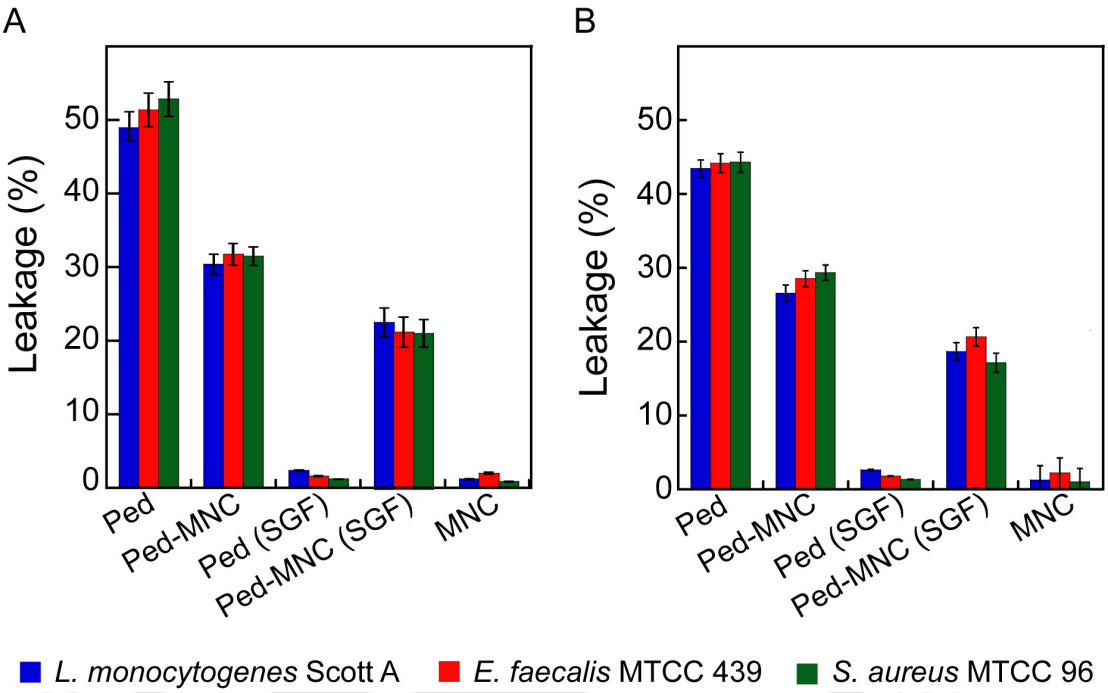

Figure 6.1. cFDA-SE leakage assay on (A) collagen- and (B) mucin-adhered target bacteria treated with test samples.

In executing these experiments, the model GI pathogens were initially labelled with the fluorescent dye cFDA-SE, which enabled us to perform a fluorescence-based cFDA leakage assay to determine the effect of Ped-MNC on ECM-adhered bacterial cells. It was interesting to note that exposure of collagen-adhering bacterial cells to Ped-MNC (incubated in 10 mM phosphate buffer) led to leakage of cFDA from target cells of *L. monocytogenes* Scott A (30.7% ± 2.5), *E. faecalis* MTCC 439 (31.3% ± 2.1) and *S. aureus* MTCC 96 (30.94% ± 2.4), indicating that Ped-MNC could exhibit the membrane-directed activity typically associated with pediocin, on the collagen-adhered pathogens (Figure 6.1A). Encouragingly, exposure of ECM-adhered pathogens to Ped-MNC which had been previously incubated in SGF, also led to cFDA leakage in the target cells of *L. monocytogenes* Scott A (22.5% ± 2.9), *E. faecalis* MTCC 439 (19.8 ± 3.07) and *S. aureus* MTCC 96 (19.5% ± 3.1). A similar trend of elimination of mucin-adhered pathogens was observed upon exposure to Ped-MNC (Figure 6.1B). Analysis of cFDA-SE labelled target bacterial cell under a fluorescence microscope indicated a reduction in the cell number subsequent to treatment with Ped-MNC (Figure 6.2A-6.2B) and these results were found to agree with the trend observed in the dye-leakage assays (Figure 6.1A-6.1B).

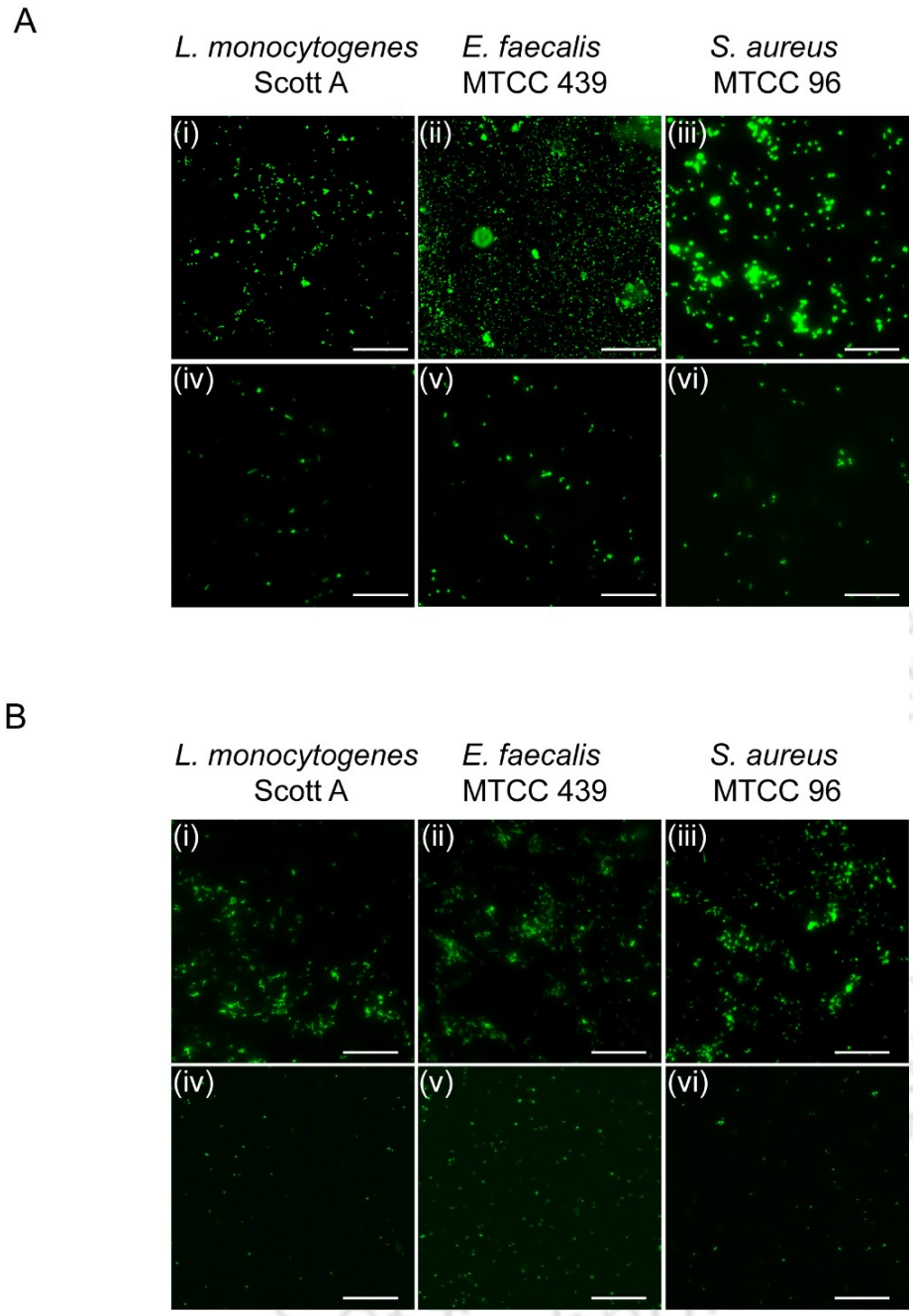

Figure 6.2. Fluorescence microscope analysis to study the effect of Ped-MNC (800 AU/mL pediocin) on (A) collagen- and (B) mucin-adhered target bacteria. Scale bar for the images is 200 µm. Panels: (i-iii) Images of untreated pathogen adhering onto collagen or mucin. (iv-vi) Images of pathogen treated with Ped-MNC (800 AU/mL pediocin).

6.3.2. Effect of Ped-MNC and LAB on ECM-adhered pathogens

Adhesion to ECM molecules is a critical step for pathogen colonization (Cossart *et al.* 2011; Foster *et al.* 2014). Thus, deploying therapeutic agents, which selectively target

the key step of bacterial adhesion onto ECM molecules may be a viable approach. In this context, it may be mentioned that the native *L. plantarum* DF9 strain demonstrated efficient adhesion onto the ECM molecule mucin. Further comparison of the adhesion process parameters suggested that the dissociation constant (k_d) was lower in case of *L. plantarum* DF9 (on collagen, k_d = 10.2 $\log_{10}$ CFU per well; on mucin, k_d = 8.0 $\log_{10}$ CFU per well) as compared to the model pathogens *L. monocytogenes* Scott A, *E. faecalis* MTCC 439 and *S. aureus* MTCC 96 (Table 3.2 in Chapter 3 and Table A3.1 in Appendix). This finding indicated that the native *L. plantarum* DF9 strain could perhaps be leveraged to render inhibition of the adhesion process of the pathogen onto ECM. Further, the abrogation of ECM-adhered pathogen by Ped-MNC was also demonstrated earlier (Figure 6.1 and Figure 6.2). Hence, the subsequent endeavor was to ascertain whether a higher level of abrogation of ECM-adhered pathogen could be achieved by deploying a combinatorial regimen of Ped-MNC and LAB strains. To this end, the model GI pathogens, *E. faecalis* MTCC 439 and *S. aureus* MTCC 96 were pre-labelled with cFDA-SE and incubated in collagen- or mucin-coated wells. Subsequently, the non-adhered cells were aspirated and either LAB cells or Ped-MNC or their combinations thereof was added to the ECM-adhered pathogens. In the adhesion assay, a primary observation was that the presence of Ped-MNC led to a comparatively higher elimination of the collagen-adhered *E. faecalis* MTCC 439 (38.2% ± 2.8) cells as compared to that observed for *L. plantarum* DF9 alone (5.3% ± 0.7) (Figure 6.3A). It can be construed that the released fraction of pediocin from Ped-MNC could perhaps directly target the adhered *E. faecalis* MTCC 439 and render membrane damage in the target cells. Consequently, it is anticipated that membrane damage in the target cells may compromise their ability to adhere onto ECM matrix. However, in case of deployment of *L. plantarum* DF9, hindrance to the adhesion of ECM-adhered *E. faecalis* is essentially dependent on a physical process wherein, the LAB cells must displace a large number of ECM-adhered target pathogen cells within a short period of assay (1 h in the present case). This tenet is manifested as a lower efficacy of *L. plantarum* DF9 cells in abrogating ECM-adhered *E. faecalis* MTCC 439 cells as compared to that observed for treatment with Ped-MNC (Figure 6.3A). Interestingly, application of a combinatorial regimen of *L. plantarum* DF9 and Ped-MNC led to a heightened elimination of collagen-adhered cells of *E. faecalis* MTCC 439 (58.7% ± 4.9) as compared to that observed for Ped-MNC or *L. plantarum* DF9 alone (Figure 6.3A). Presumably, the individual effects of Ped-MNC and *L. plantarum*

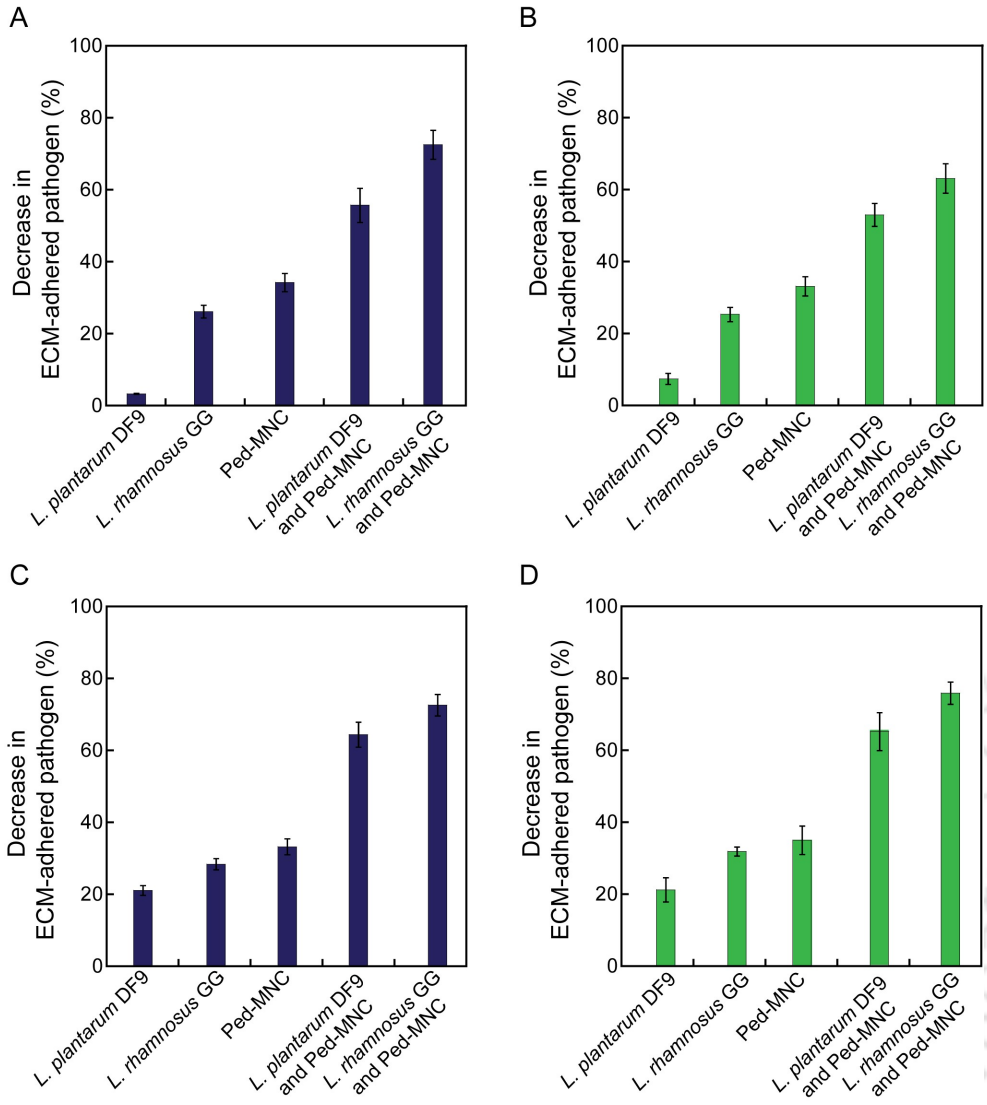

Figure 6.3. Adhesion inhibition on (A-B) collagen-coated or (C-D) mucin-coated wells by test samples. (A and C) represent adhesion inhibition of *E. faecalis* MTCC 439 and (B and D) represent adhesion inhibition of *S. aureus* MTCC 96.

DF9 are harnessed in tandem, which leads to superior abrogation of the ECM-adhered target pathogen in the combinatorial assay. The combination of Ped-MNC and *L. rhamnosus* GG led to a superior pathogen clearance as compared to Ped-MNC and *L. plantarum* DF9 (Figure 6.3A). This finding may be attributed to the higher adhesion of *L. rhamnosus* GG to collagen molecules as compared to that observed for *L. plantarum* DF9 (Figure 3.5A in Chapter 3). A similar trend of decrease in adhered cells of *S. aureus* MTCC 96 on collagen-coated wells was also observed with the combination of Ped-MNC and LAB cells (Figure 6.3B). The application of Ped-MNC

and *L. plantarum* DF9 in mucin-coated wells was observed to cause a superior elimination of *E. faecalis* MTCC 439 as compared to that observed in collagen-coated wells (Figure 6.3C). This result may be attributed to the comparatively higher adhesion potential of *L. plantarum* DF9 to mucin molecules as compared to collagen molecules (Figure 3.5A-3.5B in Chapter 3). An analogous trend of adhesion inhibition was also observed in case of *S. aureus* MTCC 96 on mucin-coated wells (Figure 6.3D). Notwithstanding the promising results obtained in the short period adhesion assay, the potential of the combination of Ped-MNC and *L. plantarum* DF9 strain to mitigate ECM-adhered target pathogen needs to be validated in future through more rigorous *in vivo* models.

6.3.3. Quantitative analysis of adhesion inhibition of pathogens on ECM

To acquire a nuanced understanding of the adhesion inhibition process by Ped-MNC and the LAB cells, varying cell numbers of *E. faecalis* MTCC 439 and *S. aureus* MTCC 96 were incubated in collagen-coated or mucin-coated wells in presence of the antibacterial agents. Subsequently, the dose dependent adhesion of the model pathogens was used to estimate the dissociation constant (k_d) and the maximum number of adhered cells (e_m) as mentioned previously in section 4.2.6. in chapter 4. In the absence of any intervention, cFDA-SE labelled cells of *E. faecalis* MTCC 439 demonstrated a systematic increase in adhesion to collagen-coated wells with increasing cell numbers (Figure 6.4A). At the highest tested cell concentration (8.0 $\log_{10}$ CFU/mL), a 57% of adhesion was recorded (Figure 6.4A). Further, addition of *L. plantarum* DF9 led to only a minor reduction in adhesion (44.3%) at the pathogen concentration of 8.0 $\log_{10}$ CFU/mL, which may be ascribed to the superior adhesion of *E. faecalis* cells to collagen as compared to *L. plantarum* DF9. Incubation of collagen-adhered *E. faecalis* MTCC 439 cells with Ped-MNC was found to lower the adhesion of the pathogen (26%), presumably due to the antibacterial activity of the bacteriocin loaded nanocomposite (Figure 6.4A). Interestingly, addition of Ped-MNC and *L. plantarum* DF9 led to a profound decline in the adhesion (12%) of *E. faecalis* MTCC 439 cells to collagen-coated wells (Figure 6.4A). At higher pathogen cell concentration (7.0 and 8.0 $\log_{10}$ CFU per well), the combination of Ped-MNC and *L. plantarum* DF9 failed to entirely prevent pathogen adhesion (Figure 6.4A). Presumably, the short period of assay leads to a low magnitude of pediocin release from Ped-MNC. Moreover, the physical displacement of pathogen by *L. plantarum* DF9 cells might be

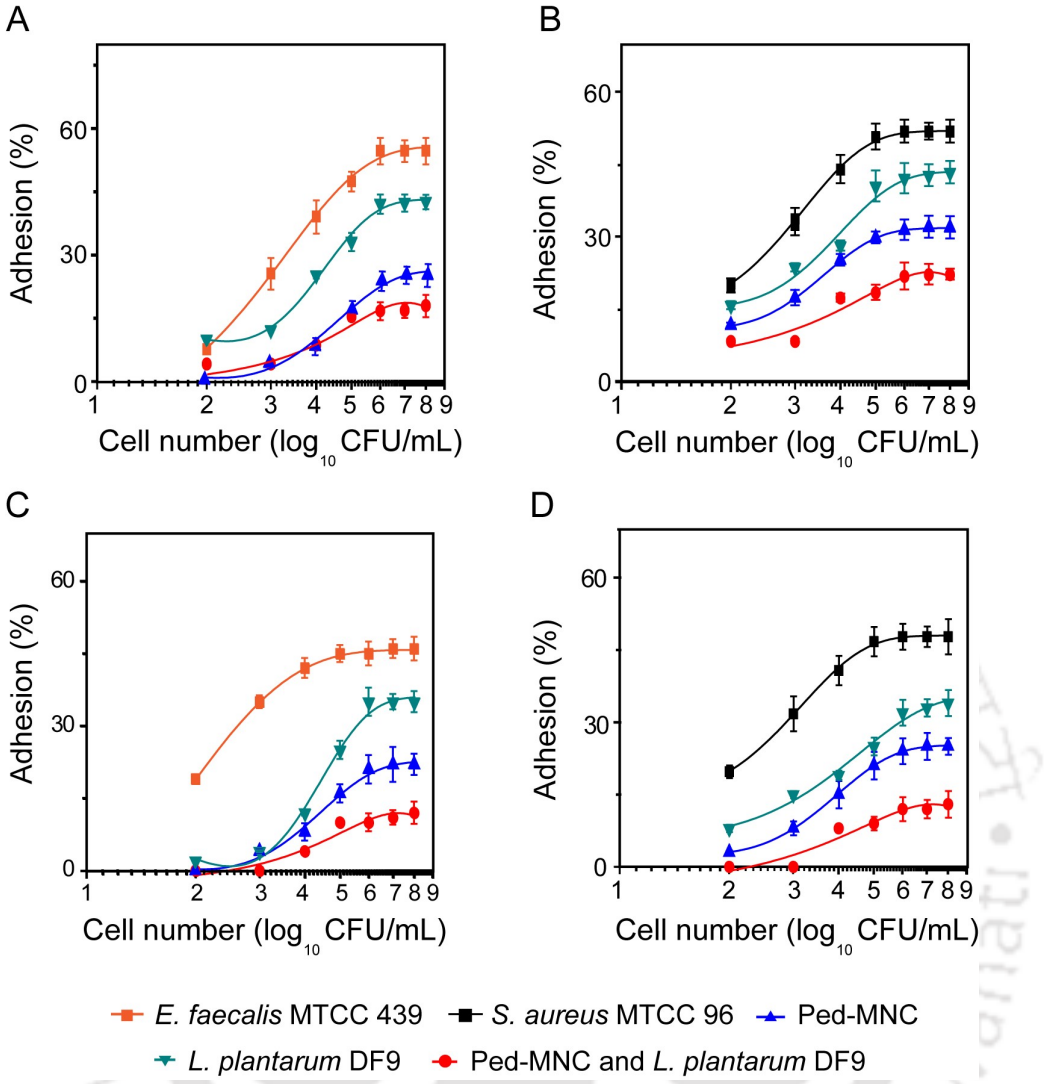

Figure 6.4. Concentration-dependent adhesion of pathogens on (A-B) collagen-coated and (C-D) mucin-coated wells. Target bacteria was (A and C) *E. faecalis* MTCC 439, (B and D) *S. aureus* MTCC 96.

hindered by the short time period of the assay. A similar trend of decrease in adhesion of *S. aureus* MTCC 96 was also observed on exposure to a combination of Ped-MNC and *L. plantarum* DF9 in collagen-coated wells (Figure 6.4B), albeit to a lesser extent. On performing the dose dependent experiment on mucin-coated wells, the primary observation was that the presence of *L. plantarum* DF9 led to a lower adhesion (22%) of *E. faecalis* MTCC 439 (Figure 6.4C). Further, on exposure of *E. faecalis* MTCC 439 cells to Ped-MNC and *L. plantarum* DF9, the adhesion was observed to reduce profoundly (10%) and this reduction was higher than that observed in case of collagen-coated wells (Figure 6.4C and Figure 6.4A). This may be attributed to the higher

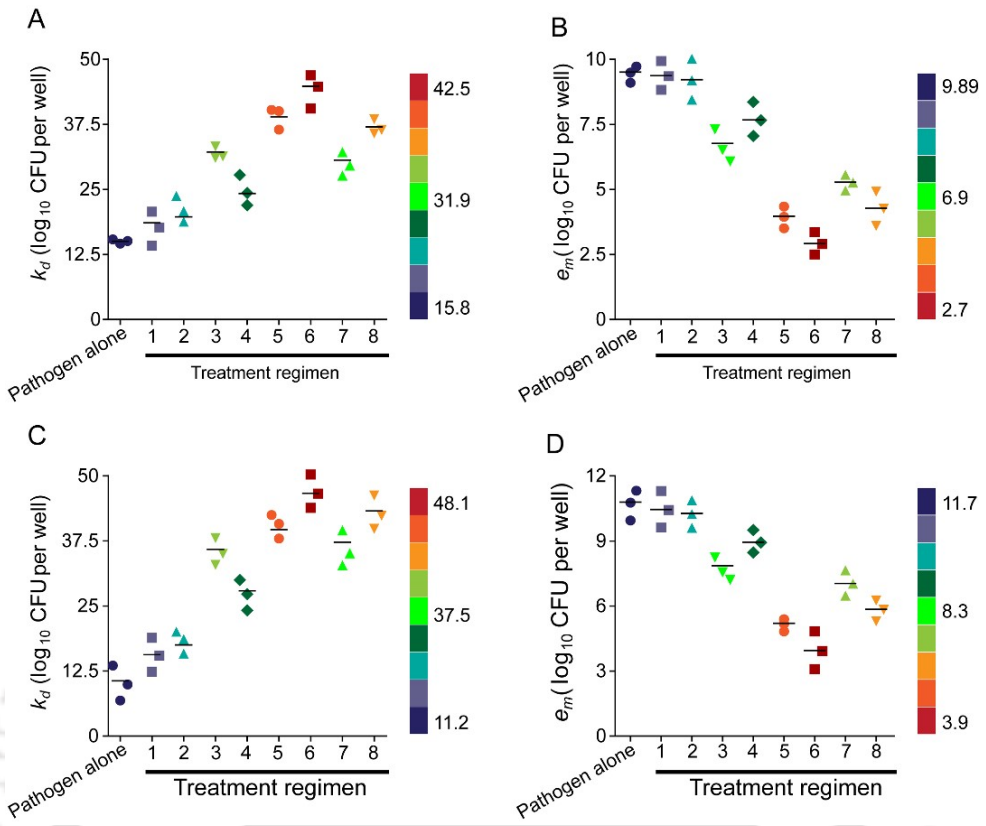

Figure 6.5. Change in adhesion process parameters of *E. faecalis* MTCC 439 in (A-B) collagen-coated wells and (C-D) mucin-coated wells respectively. 1. *L. plantarum* DF9, 2. *L. rhamnosus* GG, 3. Pediocin, 4. Ped-MNC, 5. *L. plantarum* DF9 and pediocin, 6. *L. rhamnosus* GG and pediocin, 7. *L. plantarum* DF9 and Ped-MNC, 8. *L. rhamnosus* GG and Ped-MNC.

adhesion of *L. plantarum* DF9 cells to mucin molecules as compared to collagen molecules as evidenced previously in section 3.3.1. (Figure 3.5) in chapter 3. An analogous reduction in adhesion was also observed in case *of S. aureus* MTCC 96 in presence of Ped-MNC and *L. plantarum* DF9 to mucin-coated wells (Figure 6.4D), although to a lesser extent.

Subsequently, the concentration-dependent adhesion of *E. faecalis* MTCC 439 and *S. aureus* MTCC 96 was used to probe the changes in the adhesion process parameters, (k_d and e_m) in presence of the test samples. The essential observation was that there was minimal change in k_d of *E. faecalis* MTCC 439 in presence of *L. plantarum* DF9 or *L. rhamnosus* GG (Figure 6.5A). This result may be attributed to the high surface coverage by *E. faecalis*, which leads to occlusion of binding sites for adhesion of LAB cells to collagen. Further, pediocin and Ped-MNC were found to

demonstrate significant increase in k_d of *E. faecalis* adhesion to collagen. Presumably, the membrane perturbation of *E. faecalis* cells by pediocin or Ped-MNC may reduce the strength of adhesion of the pathogen onto ECM molecules. Interestingly, the combination of Ped-MNC and *L. plantarum* DF9 against collagen-adhered *E. faecalis* MTCC 439 led to a substantial increase in k_d, indicating a considerable reduction in the binding efficiency of *E. faecalis* cells to collagen molecules. Further, the increase in k_d was observed to be higher than that observed for Ped-MNC or *L. plantarum* DF9 alone (Figure 6.5A). Perhaps, the individual abilities of Ped-MNC and *L. plantarum* DF9, to inhibit pathogen adhesion, could act in tandem to lead to a synergistic effect and cause reduction in collagen-adhered *E. faecalis* MTCC 439 cells. In case of e_m, the presence of *L. plantarum* DF9 was found to have minimal effect on the adhesion of *E. faecalis* MTCC 439 (Figure 6.5B). Further, there was a higher reduction in e_m of *E. faecalis* MTCC 439 upon exposure to Ped-MNC and *L. plantarum* DF9 (Figure 6.5B). Presumably, the antibacterial activity of Ped-MNC and the anti-adhesion potency of *L. plantarum* DF9 led to a substantial decline in the number of target pathogen cells adhering onto collagen, which is perhaps reflected as a decrease in e_m. An analogous result was also obtained in case of the adhesion process variables on mucin-coated wells (Figure 6.5C-6.5D). On performing the quantitative analysis of the change in adhesion process parameters of pre-adhered cells of *S. aureus* MTCC 96, a similar trend was recorded (Figure A6.1 in Appendix).

6.3.4. Antibacterial activity of Ped-MNC on pathogens adhering onto HT-29 cells

Considering the encouraging results obtained with Ped-MNC and *L. plantarum* DF9 against ECM-adhered pathogens, the subsequent aim was to probe the efficacy of this combinatorial regimen in abrogating pathogens adhering onto HT-29 cells. To this end, it was pertinent to initially probe the *in vitro* release kinetics of pediocin from Ped-MNC in antibiotic-free DMEM medium, which was used to propagate the HT-29 cells. A primary observation was that the release of pediocin from Ped-MNC in antibiotic-free DMEM media was observed to be slow and the magnitude was 26% after 24 h of incubation (Figure 6.6A). The low levels of pediocin release from Ped-MNC may be ascribed to the neutral pH of the DMEM medium as it has been previously demonstrated that the *in vitro* release kinetics from Ped-MNC in HEPES buffer (pH

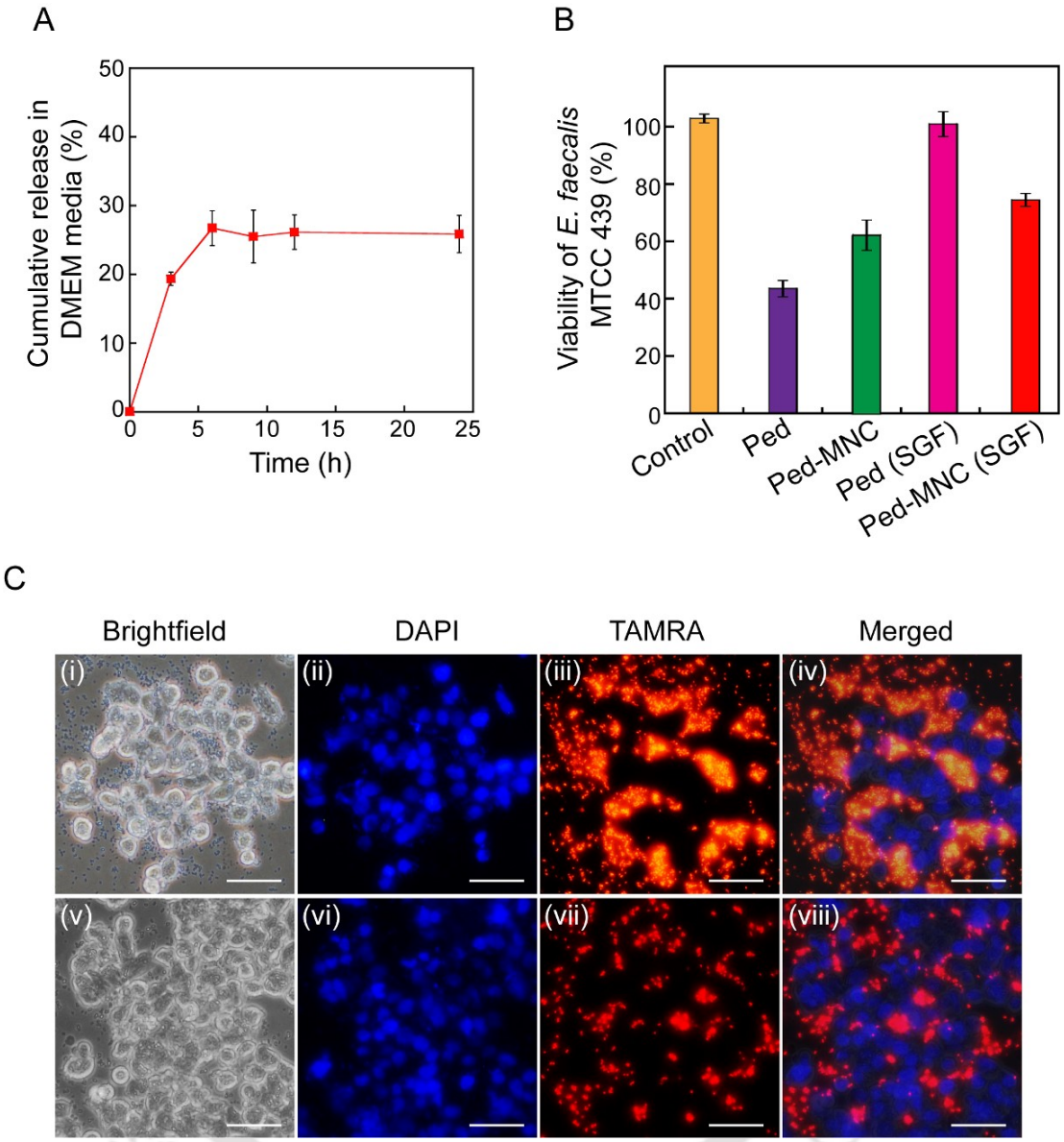

Figure 6.6. (A) *In vitro* release kinetics of pediocin from Ped-MNC incubated in antibiotic-free DMEM media. (B) Viability of *E. faecalis* MTCC 439 adhered onto HT-29 cells on exposure to test samples. (C) Fluorescence microscopic analysis to ascertain effect of Ped-MNC on adhered *E. faecalis* MTCC 439. (i-iv) and (v-viii) refer to untreated adhered cells and adhered cells treated with Ped-MNC, respectively. Scale bar for the images is 100 µm.

7.4) was also low (Figure 5.7 in Chapter 5). Exposure of HT-29 adhering *E. faecalis* MTCC 439 cells to Ped-MNC led to a viability of nearly 62% of the adhered pathogen (Figure 6.6B). However, the viability of adhered *E. faecalis* MTCC 439 cells was considerably higher than that observed for pure pediocin (40%) (Figure 6.6B). Release of pediocin from Ped-MNC is a prerequisite for its bactericidal activity, which may

account for the comparatively lower potency of Ped-MNC against ECM-adhered adhered pathogen as opposed to pediocin alone. However, pediocin exposed to SGF was observed to have minimal effect on the HT-29 adhered cells of *E. faecalis* MTCC 439 as evidenced by the high bacterial viability (99.2%) (Figure 6.6B). In contrast to pediocin incubated in SGF, Ped-MNC, which had been subjected to SGF treatment, was found to possess a higher bactericidal activity as evidenced by a lesser viability (75.9%) of the adhered *E. faecalis* cells, indicating that the retention of pediocin activity in Ped-MNC incubated in SGF was critical in order to mitigate the adhered pathogens (Figure 6.6B). This finding is encouraging considering that a therapeutic intervention directed against intestine-adhered pathogens must prevail in the harsh gastric environment. A similar trend in the loss of viability of *S. aureus* MTCC 740 cells was observed upon exposure to Ped-MNC (Figure A6.2 in Appendix). Fluorescence microscope analysis with TAMRA-SE labelled *E. faecalis* MTCC 439 cells also indicated a reduction in the adhered cells upon exposure to Ped-MNC (Figure 6.6C).

6.3.5. Effect of Ped-MNC and LAB on HT-29-adhered pathogens

Based on the encouraging results obtained with Ped-MNC against pathogens adhering onto HT-29 cells, it was envisaged that simultaneous deployment of *L. plantarum* DF9 and Ped-MNC in an adhesion assay can lead to superior elimination of the pathogens adhering onto the host cells. To this end, TAMRA-SE labelled model pathogens (8.0 $\log_{10}$ CFU/mL) were allowed to adhere onto HT-29 cells and subsequently exposed to a combination of Ped-MNC and cFDA-SE labelled *L. plantarum* DF9 cells. The presence of *L. plantarum* DF9 had minimal effect on adhered pathogen as evident from the significant levels of *E. faecalis* MTCC 439 cells adhering onto HT-29 cells (61.1%) (Figure 6.7A, upper left quadrant). The lack of a significant impact by *L. plantarum* DF9 cells in displacing pre-adhered *E. faecalis* MTCC 439 cells may be attributed to the high surface coverage of the HT-29 cells by the pathogen, which likely leads to occlusion of receptors for adhesion of *L. plantarum* DF9 cells. Interestingly, treatment of *E. faecalis* MTCC 439 cells adhered onto HT-29 cells with Ped-MNC and *L. plantarum* DF9 led to a notable decline in the population of adhered pathogenic cells (25.0%) (Figure 6.7B, upper left quadrant). Concomitantly, the decrease in the population of adhered *E. faecalis* MTCC 439 cells was associated with an increase

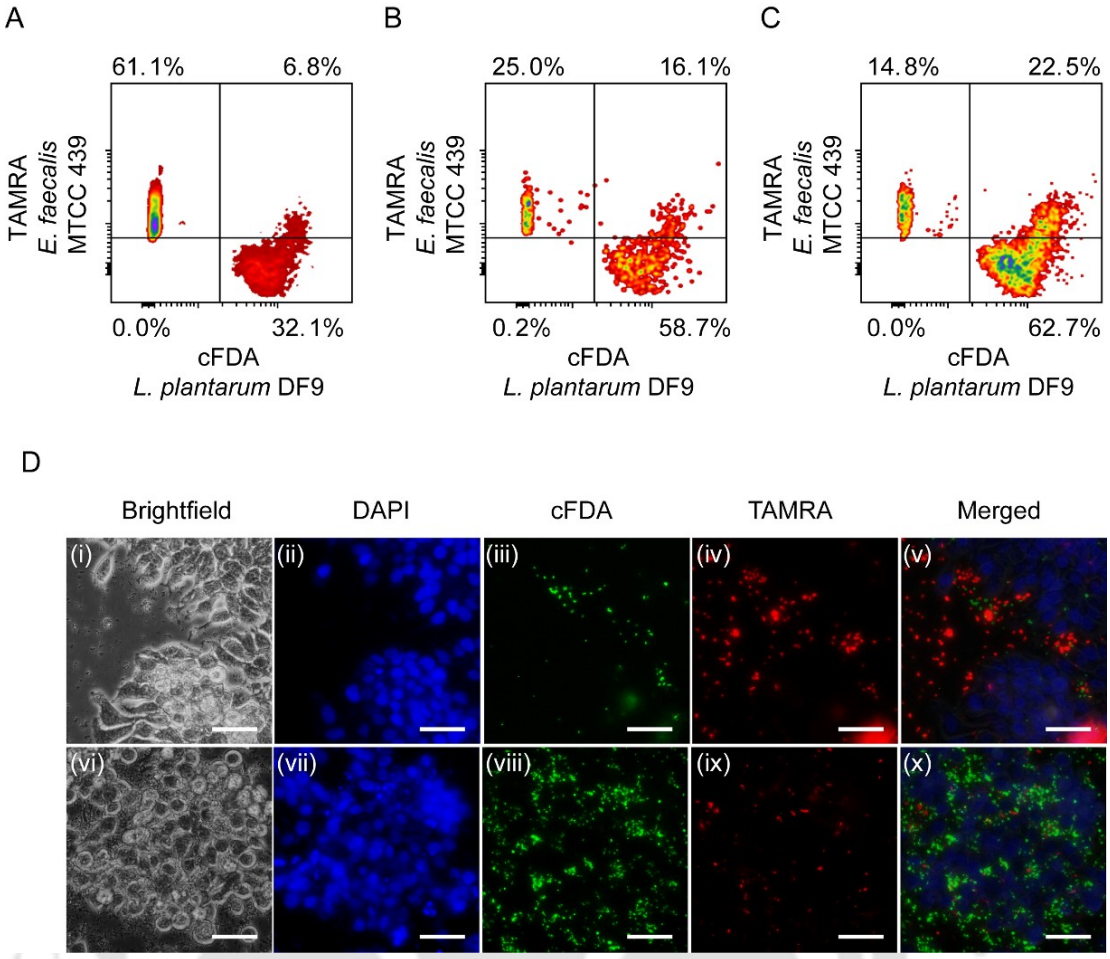

Figure 6.7. Dual color FCM-based adhesion assay to ascertain the effect of different test samples on adhesion of *E. faecalis* MTCC 439 onto HT-29 cells. (A) *L. plantarum* DF9, (B) *L. plantarum* DF9 and Ped-MNC, (C) *L. plantarum* DF9 and pediocin. (D) Fluorescence microscopic analysis to ascertain effect of different test samples on adhesion of *E. faecalis* MTCC 439 onto HT-29 cells. Panels (i-v) and (vi-x) refer to treatment with *L. plantarum* DF9 or a combination of *L. plantarum* DF9 and Ped-MNC, respectively. Scale bar for the images is 100 μm.

(from 32.1% to 58.7%) in the relative number of adhered *L. plantarum* DF9 cells (Figure 6.7A-6.7B, lower right quadrant). Presumably, the depletion of adhered *E.faecalis* cells on HT-29 monolayer was due to the combined effect of the antibacterial activity of Ped-MNC on the target pathogen as well as the propensity of *L. plantarum* DF9 to adhere onto HT-29 cells. Interestingly, the application of purified pediocin and *L. plantarum* DF9 led to a profound decrease in adhered population of *E. faecalis* MTCC 439 cells (14.8%), which may again be attributed to the availability of a high local concentration of the bacteriocin and *L. plantarum* cells for mitigation of

the adhered pathogen (Figure 6.7C). An analogous trend in decrease of adhered cells of *S. aureus* MTCC 740 on HT-29 monolayer was also recorded on exposure to Ped-MNC and *L. plantarum* DF9 cells (Figure A6.3 in Appendix). The observations of FCM analysis (Figure 6.7A-6.7C) was also validated through cell imaging studies, wherein higher abrogation of HT-29 cell adhered pathogen was recorded in combination with Ped-MNC and *L. plantarum* DF9, respectively, as opposed to treatment with *L. plantarum* DF9 alone (Figure 6.7D).

6.3.6. Quantitative analysis of adhesion inhibition of pathogens by native L. plantarum

To gain further insight, assessment of adhesion inhibition of varying concentrations (4.0 $\log_{10}$ CFU/mL, 6.0 $\log_{10}$ CFU/mL, 8.0 $\log_{10}$ CFU/mL) of *E. faecalis* MTCC 439 or *S. aureus* MTCC 740 by Ped-MNC and LAB strains was pursued using dual dye FCM analysis, and the adhesion process variables, such as dissociation constant (k_d) and the maximum number of adhered cells (e_m) of the pathogen were ascertained as mentioned previously in section 4.2.6 in Chapter 4. An essential observation was that there was an increase in k_d and decrease in e_m for *E. faecalis* MTCC 439, and this trend was unequivocally observed in presence of all of the test samples (Figure 6.8A-6.8B). The application of LAB strains, *L. plantarum* DF9 or *L. rhamnosus* GG led to miniscule change in k_d and e_m. The failure of *L. plantarum* DF9 or *L. rhamnosus* GG to cause a significant change in k_d and e_m may be attributed to the adhesion of *E. faecalis* to majority of host cells, leading to the availability of only weak binding sites on the host cells for adhesion of LAB. Pediocin and Ped-MNC were observed to cause significant increase in k_d and decrease in e_m (Figure 6.8A-6.8B). Presumably the membrane perturbation of *E. faecalis* MTCC 439 due to the antibacterial activity of pediocin hinders its binding efficiency to receptors present on the host cells, which is reflected as an increase in k_d. Further, *E. faecalis* MTCC 439 cells, which have undergone membrane damage will adhere in low numbers, leading to a decrease in e_m. Interestingly, the combination of Ped-MNC and *L. plantarum* DF9 led to a sharp increase in k_d and decrease in e_m, and this was superior to that observed for either Ped-MNC or *L. plantarum* DF9 alone (Figure 6.8A-6.8B). It may be construed that the antibacterial activity of the bacteriocin-loaded nanocomposite could have led to membrane-damage of *E. faecalis* MTCC 439, which in turn may compromise the adhesion propensity of the pathogen and thus enable *L. plantarum* DF9 cells in the vicinity to adhere efficiently onto the available binding sites in higher numbers. Given

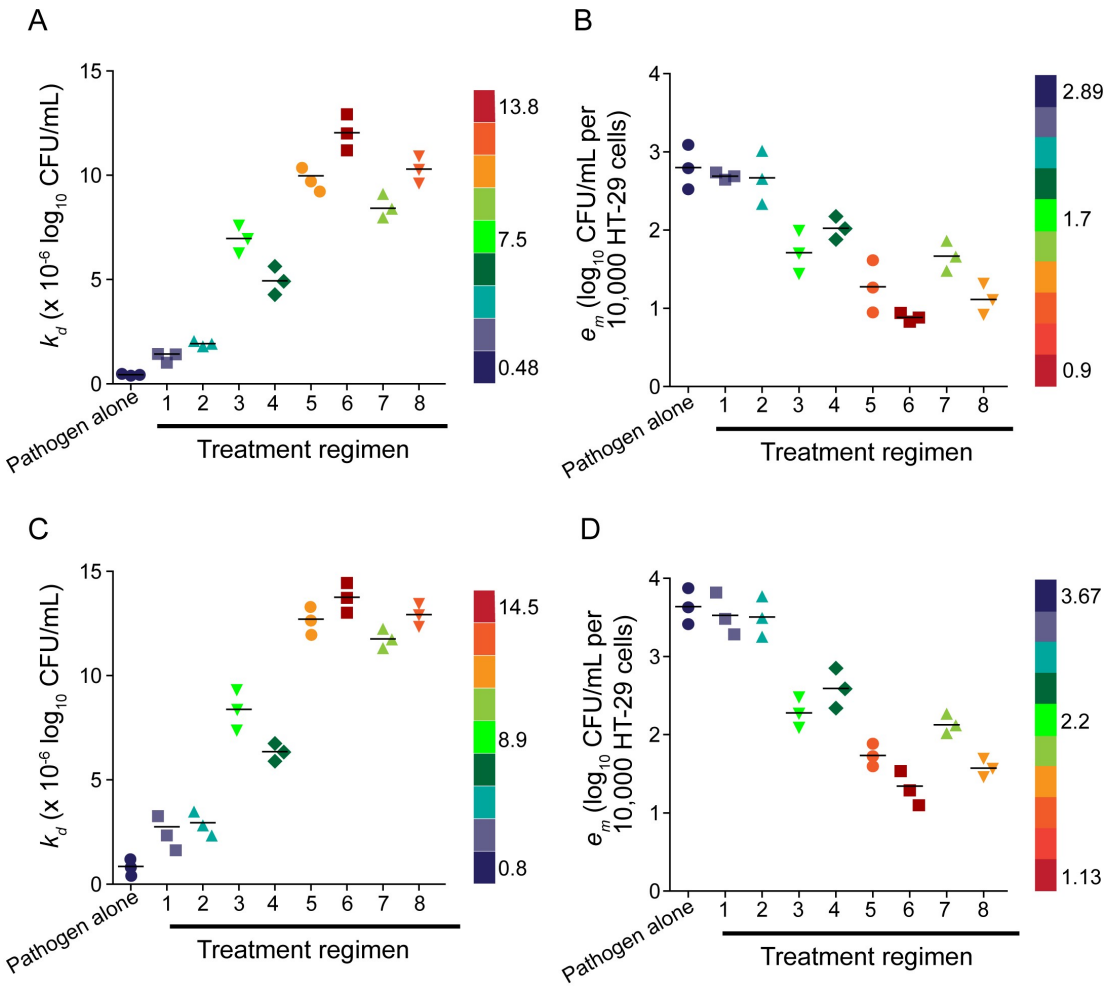

Figure 6.8. Change in adhesion process parameters of (A-B) *E. faecalis* MTCC 439 and (C-D) *S. aureus* MTCC 740 imparted by test samples. 1. *L. plantarum* DF9, 2. *L. rhamnosus* GG, 3. Pediocin, 4. Ped-MNC, 5. *L. plantarum* DF9 and pediocin, 6. *L. rhamnosus* GG and pediocin, 7. *L. plantarum* DF9 and Ped-MNC, 8. *L. rhamnosus* GG and Ped-MNC.

the potential of the combination of Ped-MNC and *L. plantarum* DF9 strain to mitigate host cell-adhered target pathogen, it would be interesting to validate the combination effect through more rigorous *in vivo* models. A similar trend in change of the adhesion process variables was also observed in case of *S. aureus* MTCC 740 (Figure 6.8C-6.8D).

6.3.7. Principal component analysis (PCA) for inhibition of pathogen adhesion

A holistic understanding of the change in adhesion process variables such as k_d and/or e_m of the pathogen in presence of either the antibacterial agents pediocin or Ped-MNC

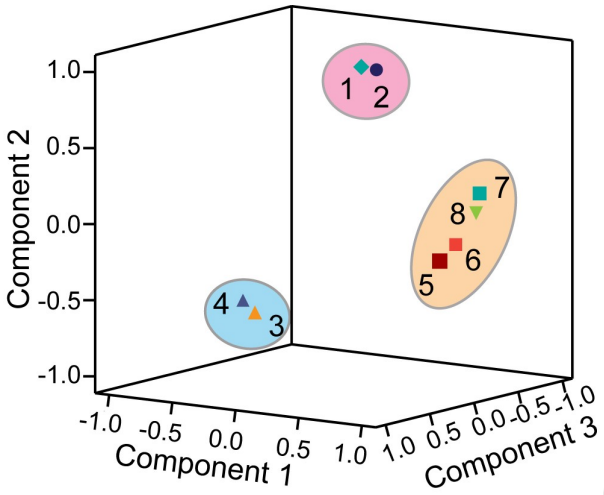

Figure 6.9. Principal component analysis to determine the relative influence of various LAB strains on the k_d and/or e_m of pathogen adhesion onto HT-29 cells. 1. *L. plantarum* DF9, 2. *L. rhamnosus* GG, 3. Pediocin, 4. Ped-MNC, 5. *L. plantarum* DF9 and pediocin, 6. *L. rhamnosus* GG and pediocin, 7. *L. plantarum* DF9 and Ped-MNC, 8. *L. rhamnosus* GG and Ped-MNC.

or anti-adhesion agents, *L. plantarum* DF9 or *L. rhamnosus* GG or combinations thereof could provide insights and foster development of efficient therapeutic intervention for selective elimination of GI pathogens. To this end, a principal component analysis (PCA) was performed based on the relative change in k_d and e_m of the pathogens in presence of various test samples. It may be mentioned that the PCA was performed on the change in k_d and/or e_m of pre-adhered pathogens. It was interesting to observe that *L. rhamnosus* GG and *L. plantarum* DF9 exhibited a high value for component 2 (Figure 6.9 and Table A6.1 in Appendix), reflecting that these strains imparted a larger change on k_d as compared to e_m of pathogen. Since these LAB strains possess superior binding affinity (k_d) to HT-29 cells as compared to the pathogens (Table 4.1 in Chapter 4), it may be construed that these strains were able to perhaps compete and displace some of the pre-adhered pathogen, which is captured as a change in the k_d of pathogen adhesion (Figure 6.9 and Table A6.1 in Appendix). However, it may be mentioned that the high surface coverage of HT-29 cells by pre-adhered pathogens perhaps limits the adhesion of a high number of LAB onto HT-29 cells. This is reflected as a minimal change in e_m of the model GI pathogen (Figure 6.9 and Table A6.1 in Appendix). Pediocin and Ped-MNC displayed a high value for component 3 (Figure 6.9 and Table A6.1 in Appendix), reflecting that these

agents exerted a pronounced effect on k_d and a lesser effect in e_m. Presumably, the antibacterial activity of pediocin causes membrane perforations in a fraction of the pathogens adhering onto HT-29 cells. This perhaps leads to loss of native state and function of cell surface proteins of the pathogens implicated in host cell adhesion. Consequently, there is a reduction in the strength of binding, which is in turn reflected as an increase in k_d and a minor decrease in e_m for adhesion of the pathogen (Figure 6.9 and Table A6.1 in Appendix). However, the combinations of Ped-MNC or pediocin with the LAB strains, *L. plantarum* DF9 and *L. rhamnosus* GG exhibited a high value for component 1 (Figure 6.9 and Table A6.1 in Appendix), indicating a marked change in k_d and e_m of pre-adhered pathogen. It may be construed that using an antibacterial agent and an anti-adhesion LAB strain perhaps magnifies the individual effects of the bacteriocin and LAB, which is manifested as a cumulative effect on the adhesion of the pathogen on HT-29 cells.

6.4. Significant Findings

The salient findings of this chapter are as follows:

1. Pediocin-loaded milk protein nanocomposite (Ped-MNC), which had been exposed to simulated gastric fluid (SGF), could abrogate ECM-adhered pathogens, in contrast to pediocin, which failed to be effective against ECM-adhered pathogens after incubation in SGF.

2. The combination of Ped-MNC and *L. plantarum* DF9 led to a considerable decrease in ECM-adhered pathogens. The remarkable activity of Ped-MNC and *L. plantarum* DF9 could be ascribed to a substantial change in the adhesion process parameters, such as dissociation constant (k_d) and the maximum number of adhered bacteria (e_m).

3. Ped-MNC, which had been pre-exposed to SGF, led to elimination of *E. faecalis* cells adhering onto HT-29. Further, the combination of Ped-MNC and *L. plantarum* DF9 led to a superior decline in the population of *E. faecalis* MTCC 439 adhering onto HT-29 cells, in contrast to that observed for *L. plantarum* DF9 alone.

4. The decline in the population of adhered *E. faecalis* MTCC 439 cells by a combination of Ped-MNC and *L. plantarum* DF9 was also associated with an increment in the relative number of *L. plantarum* DF9 cells adhering onto HT-29 cells, indicating the selective elimination of *E. faecalis* cells.

5. Assessment of the adhesion process parameters (k_d and e_m) in conjunction with a principal component analysis (PCA) provided an insight on the mechanistic aspect of the combinatorial activity of Ped-MNC and *L. plantarum* DF9.

In the constant endeavor to counter the menace of gastrointestinal infections caused by pathogenic bacteria, the present study, which describes a combinatorial approach comprising of a bacteriocin-loaded nanomaterial and a potentially probiotic LAB strain, presents a promising avenue for development of niche specific therapy for selective mitigation of intestinal pathogens. It will be interesting to validate the potential of the combinatorial activity of bacteriocin-loaded nanomaterial and LAB cells against a broader set of gastrointestinal pathogens and in *in vivo* models.

SUMMARY AND FUTURE PERSPECTIVE

SUMMARY AND FUTURE PERSPECTIVE

A critical challenge in modern healthcare regime is the rising incidence of gastrointestinal infections caused by pathogenic bacteria. The problem is further compounded due to the usage of therapeutic antibiotics, which leads to the abrogation of beneficial gut microflora, that are known to prevent colonization of the gastric niche by intestinal pathogens. In this context, the present investigation, which reports the potential of native isolates of probiotic LAB and its metabolite, namely bacteriocin, in mitigating gastrointestinal pathogenic bacteria, presents a prospective therapeutic approach for addressing a contemporary global healthcare problem. The salient advancements of the study and the future prospect is discussed in the following section:

(1) LAB strains isolated from indigenous sources, such as *dahi*, dried fish and salt-fermented cucumber were probed for their probiotic attributes using quantitative assays, that enabled the selection of potential strains. The revelation of the *in vitro* tests was interesting since native LAB isolates obtained from non-human source such as *dahi*, dried fish and fermented cucumber displayed functional traits, which are typically associated with potential probiotics. It is foreseen that some of the native bacteriocin-producing LAB isolates, which displayed potential probiotic attributes, may be subjected to *in vivo* studies, and in future, these strains may find application in the healthcare domain.

(2) The strong adhesion of bacteriocin-producing isolates of *L. plantarum* to ECM molecules collagen and mucin as well as HT-29 cells selected as model intestinal cells was captured through sensitive fluorescence-based assays. The ECM and HT-29 cell-adhering *L. plantarum* isolates were also bacteriocinogenic, which impart a competitive edge to these strains. Determination of the adhesion process parameters (k_d and e_m) and a principal component analysis provided an insight on the adhesion propensities of the LAB strains and the model pathogen and thereby provided a handle to select promising LAB strains that may hold potential in anti-adhesion therapy. In future, it would be important to validate this scope of the strains in *in vivo* models as a step towards the rational development of LAB-based safe antibacterial therapy.

(3) The collateral cost associated with therapeutic antibiotics underscores the need for therapeutic approaches with selective abrogation of gastrointestinal pathogenic bacteria. In this regard, LAB bacteriocins can be deployed considering their strong antibacterial activity towards intestinal pathogens and narrow antimicrobial spectrum. However, the possibility of proteolytic inactivation of LAB bacteriocins during gastric transit may limit their therapeutic potential. In the present investigation, this critical issue is addressed by presenting a robust milk protein based nanoparticle, for encapsulation and delivery of LAB bacteriocin. Interestingly, the developed nanoparticle could impart significant retention of the activity of encapsulated bacteriocin in a simulated gastric transit experiment. Mechanistic studies seem to suggest that the milk protein nanoparticle rendered a competitive inhibition of pepsin, a major proteolytic enzyme present in the gastric fluid. In the constant endeavor to mitigate gastrointestinal pathogenic bacteria, it will be interesting in future to validate the potential of the developed nanocomposite against a broader set of clinical gastrointestinal pathogenic bacteria and in *in vivo* infection models.

(4) The prospect of a combinatorial regimen of native *L. plantarum* strains and Ped-MNC in preventing adhesion of pathogenic bacteria on ECM and HT-29 cells has been evaluated. The ability of the combinatorial regimen to significantly change the adhesion process parameters of the pathogens adhering onto ECM or HT-29 cells is encouraging, considering the burden of gastrointestinal infections. It would be interesting to realize the potential of this treatment regimen in *in vivo* infection models.

The present investigation essentially encompasses a comprehensive effort towards the development of LAB-based therapeutic approaches that hold considerable promise in mitigating adhesion of pathogenic bacteria in the gastro-intestinal niche. A graphical representation of the significant findings emerging from the present investigation is indicated in in Scheme 1.

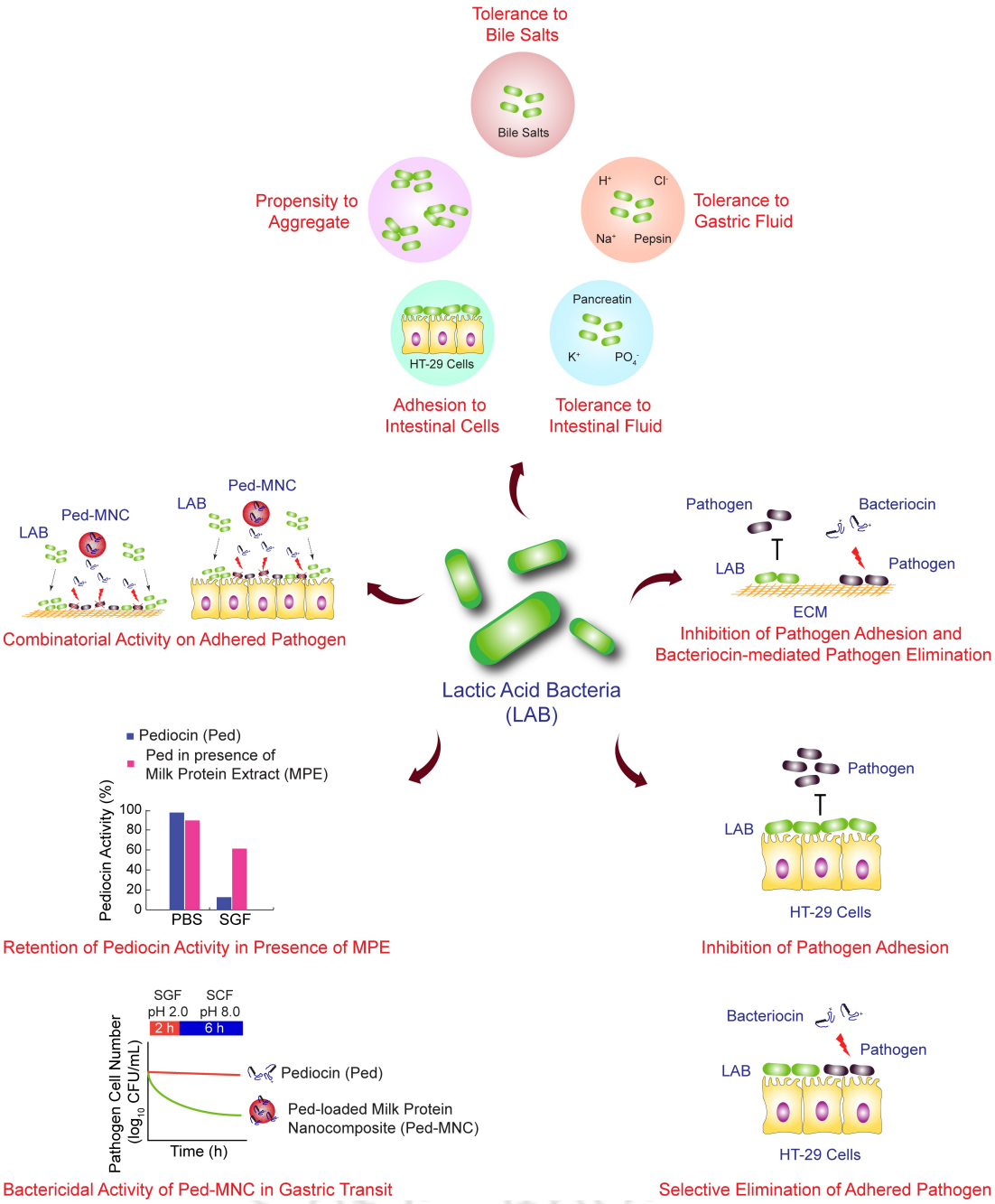

Scheme 1. Graphical representation of the significant findings of the present investigation.

BIBLIOGRAPHY

1. Abt, M.C.; Pamer, E.G. Commensal bacteria mediated defenses against pathogens. *Curr. Opin. Immun.* **2014**, *29*, 16-22.
2. Acton, D.S.; Plat-Sinnige, M.J.T.; Wamel, W.van.; Groot, N.de.; Belkum, A.Van. Intestinal carriage of *Staphylococcus aureus*: How does its frequency compare with that of nasal carriage and what is its clinical impact? *Eur. J. Clin. Microbiol. Infect. Dis.* **2009**, *28*, 115-127.
3. Alander, M.; Satokari, R.; Korpela, R.; Saxelin, M.; Vilpponen-Salmela, T.; Mattila-Sandholm, T. Persistence of colonization of human colonic mucosa by a probiotic strain, *Lactobacillus rhamnosus* GG, after oral consumption. *Appl. Environ. Microbiol.* **1999**, *65*, 351-354.
4. Alemka, A.; Clyne, M.; Shanahan, F.; Tompkins, T.; Corcionivoschi, N.; Bourke, B. Probiotic colonization of the adherent mucus layer of HT29MTXE12 cells attenuates *Campylobacter jejuni* virulence properties. *Infect. Immun.* **2010**, *78*, 2812-2822.
5. Allen, K.J.; Wałecka-Zacharska, E.; Chen, J.C.; Katarzyna, K.-P.; Devlieghere, F.; Van Meervenne, E.; Osek, J.; Wieczorek, K.; Bania, J. *Listeria monocytogenes* – An examination of food chain factors potentially contributing to antimicrobial resistance. *Food Microbiol.* **2016**, *54*, 178-189.
6. Alvarez-Sieiro, P.; Montalbán-López, M.; Mu, D.; Kuipers, O.P. Bacteriocins of lactic acid bacteria: Extending the family. *Appl. Microbiol. Biotechnol.* **2016**, *100*, 2939-2952.
7. Andermann, T.M.; Rezvani, A.; Bhatt Microbiota manipulation with prebiotics and probiotics in patients undergoing stem cell transplantation. *Curr. Hematol. Malig. Rep.* **2016**, *11*, 19–28.
8. Anderson, E.L.; Cole, J.N.; Olson, J.; Ryba, B.; Ghosh, P.; Nizet, V. The fibrinogen-binding M1 protein reduces pharyngeal cell adherence and colonization phenotypes of M1Y1 group A *Streptococcus*. *J. Biol. Chem.* **2014**, *289*, 3539-3546.
9. Angmo, K.; Kumari, A.; Savitri, B.T.C. Probiotic characterization of lactic acid bacteria isolated from fermented foods and beverage of Ladakh. *LWT - Food Sci. Technol.* **2016**, *66*, 428-435.
10. Arena, M.P.; Capozzi, V.; Spano, G.; Fiocco, D. The potential of lactic acid bacteria to colonize biotic and abiotic surfaces and the investigation of their

interactions and mechanisms. *Appl. Microbiol. Biotechnol.* **2017**, *101*, 2641–2657

11. Arnison, P.G.; Bibb, M.J.; Bierbaum, G.; Bowers, A.A.; Bugni, T.S.; Bulaj, G.; Camarero, J.A.; Campopiano, D.J.; Challis, G.L.; Clardy, J.; Cotter, P.D.; Craik, D.J.; Dawson, M.; Dittmann, E.; Donadio, S.; Dorrestein, P.C.; Entian, K-D.; Fischbach, M.A.; Garavelli, J.S.; Göransson, U.; Gruber, C.W.; Haft, D.H.; Hemscheidt, T.K.; Hertweck, C.; Hill, C.; Horswill, A.R.; Jaspars, M.; Kelly, W.L.; Klinman, J.P.; Kuipers, O.P.; Link, A.J.; Liu, W.; Marahiel, M.A.; Mitchell, D.A.; Moll, G.N.; Moore, B.S.; Müller, R.; Nair, S.K.; Nes, I.F.; Norris, G.E.; Olivera, B.M.; Onaka, H.; Patchett, M.L.; Piel, J.; Reaney, M.J.T.; Rebuffat, S.; Ross, R.P.; Sahl, H-G.; Schmidt, E.W.; Selsted, M.E.; Severinov, K.; Shen, B.; Sivonen, K.; Smith, L.; Stein, T.; Süssmuth, R.D.; Tagg, J.R.; Tang, G-L., Truman, A.W.; Vederas, J.C.; Walsh, C.T.; Walton, J.D.; Wenzel, S.C.; Willey, J.M.; van der Donk, W.A. Ribosomally synthesized and post-translationally modified peptide natural products: Overview and recommendations for a universal nomenclature. *Nat. Prod. Rep.* **2013**, *30*,108–160.
12. Balay, D.R.; Dangeti, R.V.; Kaur, K.; McMullen, L.M. Purification of leucocin A for use on wieners to inhibit *Listeria monocytogenes* in the presence of spoilage organisms. *Int. J. Food Microbiol.* **2017**, *255*, 25–31.
13. Barbosa, M.S.; Todorov, S.D.; Belguesmia, Y.; Choiset, Y.; Rabesona, H.; Ivanova, I. V.; Chobert, J-M.; Haertlé, T.; Franco, B.D.G.M. Purification and characterization of the bacteriocin produced by *Lactobacillus sakei* MBSa1 isolated from Brazilian salami. *J. Appl. Microbiol.* **2014**, *116*, 1195–1208.
14. Barbuddhe, S.B.; Chakraborty, T. *Listeria* as an enteroinvasive gastrointestinal pathogen. *Curr.Topics Microbiol. Immunol.***2009**, *337*, 173-195.
15. Baumler, A.J.; Sperandio, V. Interactions between the microbiota and pathogenic bacteria in the gut. *Nature* **2016**, *535*, 85-93.
16. Begley, M.; Gahan, C.G.M.; Hill, C. The interaction between bacteria and bile. *FEMS Microbiol. Rev.* **2005**, 29, 625-651.
17. Begley, M.; Hill, C.; Gahan, C.G.M. Bile salt hydrolase activity in probiotics. *Appl. Environ. Microbiol.* **2006**, *72*, 1729-1738.

18. Bendali, F.; Madi, N.; Sadoun, D. Beneficial effects of a strain of *Lactobacillus paracasei* subsp. *paracasei* in *Staphylococcus aureus*-induced intestinal and colonic injury. *Int. J. Infect. Dis.* **2011**, *15*, e787–e794.
19. Bermudez-Brito, M.; Plaza-Diaz, J.; Fontana, L.; Munoz-Quezada, S.; Gil, A. *In vitro* cell and tissue models for studying host–microbe interactions: A review. *Br. J. Nutr.* **2013**, *109*, S27-S34.
20. Bernbom, N.; Jelle, B.; Brogren, C.H.; Vogensen, F.K.; Norrung, B.; Licht, T.R. Pediocin PA-1 and a pediocin producing *Lactobacillus plantarum* strain do not change the HMA rat microbiota. *Int. J. Food Microbiol.* **2009**, *130*, 251-257.
21. Bhalla, A.; Aron, C.; D. Donskey, C.J. *Staphylococcus aureus* intestinal colonization is associated with increased frequency of *S. aureus* on skin of hospitalized patients. *BMC Infect. Dis.* **2007**, *7*, 105-112.
22. Bhunia, A. K.; Johnson, M.C.; Ray, B.; Kalchayanand, N. Mode of action of pediocin AcH from *Pediococcus acidilactici* H on sensitive bacterial strains. *J. Appl. Bact.* **1991**, *70*, 25-33.
23. Binachi, M.A.; Del Rio, D.; Pellegrini, N.; Sansebastiano, G.; Neviani, E.; Brighenti, F. A fluorescence-based method for the detection of adhesive properties of lactic acid bacteria to Caco-2 cells. *Lett. Appl. Microbiol.* **2004**, *39*, 301-305.
24. Bischoff, S.C.; Barbara, G.; Buurman, W.; Ockhuizen, T.; Schulzke, J.D.; Serino, M.; Tilg, H.; Watson, A.; Wells, J.M. Intestinal permeability - A new target for disease prevention and therapy. *BMC Gastroenterol.* **2014**, *14*, 189-205.
25. Biswas, S. R.; Ray, P.; Johnson, M.C.; Ray, B. Influence of growth conditions on the production of a bacteriocin, pediocin AcH, by *Pediococcus acidilactici* H. *Appl. Environ. Microbiol.* **1991**, *57*, 1265-1267.
26. Blaser, M. Antibiotic overuse: Stop the killing of beneficial bacteria. *Nature* **2011**, *476*, 393-394.
27. Blaser, M. J. Antibiotic use and its consequences for the normal microbiome. *Science* **2016**, *352*, 544-545.
28. Blay, G.L.; Fliss, I.; Lacroix, C. Comparative detection of bacterial adhesion to Caco-2 cells with ELISA, radioactivity and plate count method. *J. Microbiol. Meth.* **2004**, *59*, 211-221.

29. Blay, G.L.; Lacroix, C.; Zihler, A.; Fliss, I. *In vitro* inhibition activity of nisin A, nisin Z, pediocin PA-1 and antibiotics against common intestinal bacteria. *Lett. Appl. Microbiol.* **2007**, *45*, 252-257.
30. Botta, C.; Langerholc, T.; Cencič, A.; Cocolin, L. *In vitro* selection and characterization of new probiotic candidates from table olive microbiota *PLoS One* **2014**, *9*, e94457.
31. Boyce, J.M.; Havill, N.L. Nosocomial antibiotic-associated diarrhea associated with enterotoxin-producing strains of methicillin-resistant *Staphylococcus aureus*. *Am. J. Gastroenterol.* **2005**, *100*, 1828-1834.
32. Braïek, O.B.; Morandi, S.; Cremonesi, P.; Smaoui, S.; Hani, K.; Ghrairi, T. Biotechnological potential, probiotic and safety properties of newly isolated enterocin-producing *Enterococcus lactis* strains. *LWT - Food Sci. Tech.* **2018**, *92*, 361–370.
33. Brandl, K.; Plitas, G.; Mihu, C.N.; Ubeda, C.; Jia, T.; Fleisher, M.;Schnabl, B.; DeMatteo, R.P.; Pamer, E.G. Vancomycin-resistant enterococci exploit antibiotic-induced innate immune deficits. *Nature* **2008**, *455*, 804-807.
34. Brötz-Oesterhelt, H.; Brunner, N.A. How many modes of action should an antibiotic have? *Curr. Opin. Pharma.* **2008**, *8*, 564-573.
35. Browne, H. Antibiotics, gut bugs and the young. *Nat. Rev. Micro.* **2016**, *14*, 336-336.
36. Buffie, C.G.; Pamer, E.G. Microbiota-mediated colonization resistance against intestinal pathogens. *Nat. Rev. Immunol.* **2013**; 13: 790-801.
37. Bumann, D.; Valdivia, R.H. Identification of host-induced pathogen genes by differential fluorescence induction reporter systems. *Nat. Protoc.* **2007**, *2*, 770-777.
38. Buntin, N.; de Vos, WM.; Hongpattarakere, T. Variation of mucin adhesion, cell surface characteristics, and molecular mechanisms among *Lactobacillus plantarum* isolated from different habitats. *Appl. Microbiol. Biotechnol.* **2017**, *101*, 7663–7674.
39. Burns, P.; Vinderola, G.; Binetti, A.; Quiberoni, A.; de los Reyes-Gavilan, C.; Reinheimer, J. Bile-resistant derivatives obtained from non-intestinal dairy lactobacilli. *Int. Dairy J.* **2008**, *18*, 377-385.
40. Bush, K. Alarming β-lactamase-mediated resistance in multidrug-resistant Enterobacteriaceae. *Curr. Opin. Microbiol.* **2010**, *13*, 558-564.

41. Bustos, A.Y.; Raya, R.; de Valdez, G.F.; Taranto, M.P. Efflux of bile acids in *Lactobacillus reuteri* is mediated by ATP. *Biotechnol. Lett.* **2011**, *33*, 2265–2269.
42. Butler, M.S.; Robertson, A.A.B.; Cooper, M.A. Natural product and natural product derived drugs in clinical trials. *Nat. Prod. Rep.* **2014**, *31*, 1612-1661.
43. Calasso, M.; Di Cagno, R.; De Angelis, M.; Campanella, D.; Minervini, F.; Gobbetti, M. Effects of the peptide pheromone plantaricin A and cocultivation with *Lactobacillus sanfranciscensis* DPPMA174 on the exoproteome and the adhesion capacity of *Lactobacillus plantarum* DC400. *Appl. Environ. Microbiol.* **2013**, *79*, 2657-2669.
44. Caillard, R.; Remondetto, G.E.; Mateescu, M.A. Subirade, M. Characterization of amino cross-linked soy protein hydrogels. *J. Food Sci.*, **2008**, *73*, 283-291.
45. Campana, R.; Federici, S.; Ciandrini, E.; Baffone, W. Antagonistic activity of *Lactobacillus acidophilus* ATCC 4356 on the growth and adhesion/invasion characteristics of human *Campylobacter jejuni*. *Curr. Microbiol.* **2012**, *64*, 371–378.
46. Campana, R.; van Hemert, S.; Baffone, W. Strain-specific probiotic properties of lactic acid bacteria and their interference with human intestinal pathogens invasion. *Gut Pathog.* **2017**, *9*, 1-12
47. Cavera, V.L.; Arthur, T.D.; Kashtanov, D.; Chikindas, M.L. Bacteriocins and their position in the next wave of conventional antibiotics. *Int. J. Antimicrob. Agents* **2015**, *46*, 494-501.
48. Celebioglu, H.U.; Olesen, S.V.; Prehn, K.; Lahtinen, S.J.; Brix, S.; Hachem, M.A.; Svensson, B.; Mucin- and carbohydrate-stimulated adhesion and subproteome changes of the probiotic bacterium *Lactobacillus acidophilus* NCFM. *J. Proteom.* **2017**, *163*, 102-110.
49. Chagnot, C.; Anne, L.; Astruc, T.; Desvaux, M. Bacterial adhesion to animal tissues: Protein determinants for recognition of extracellular matrix components. *Cell. Microbiol.* **2012**, *14*, 1687-1696.
50. Chang, J.H.; Shim, Y.Y.; Cha, S.K.; Chee, K.M. Probiotic characteristics of lactic acid bacteria isolated from kimchi. *J. Appl. Microbiol.* **2010**, *109*, 220-230

51. Charalampopoulos, D.; Pandiella, S.S.; Webb, C. Evaluation of the effect of malt, wheat and barley extracts on the viability of potentially probiotic lactic acid bacteria under acidic conditions. *Int. J. Food Microbiol.* **2003**, *82*, 133-41.
52. Charteris, W.P.; Kelly, P.M.; Morelli, L.; Collins, J.K. Development and application of an *in vitro* methodology to determine the transit tolerance of potentially probiotic *Lactobacillus* and *Bifidobacterium* species in the upper human gastrointestinal tract. *J. Appl. Microbiol.* **1998**, *84*, 759-768.
53. Chatterjee, M.; Pushkaran, A.C.; Vasudevan A.K.; Menon, K.K.N.; Biswas, R.; Mohan, C.G. Understanding the adhesion mechanism of a mucin binding domain from *Lactobacillus fermentum* and its role in enteropathogen exclusion. *Int. J. Biol. Macromol.* **2018**, *110*, 598-607.
54. Chikindas, M. L.; García-Garcerá, M.J.; Driessen, A.J.; Ledeboer, A.M.; Nissen-Meyer, J.; Nes, I.F.; Abee, T.; Konings, W.N.; Venema, G. Pediocin PA-1, a bacteriocin from *Pediococcus acidilactici* PAC1.0, forms hydrophilic pores in the cytoplasmic membrane of target cells. *Appl. Environ. Microbiol.* **1993**, *59*, 3577-3584.
55. Chikindas, M.L.; Weeks, R.; Drider, D.; Chistyakov, V.A.; Dicks, L.M.T. Functions and emerging applications of bacteriocins. *Curr. Opinion Biotechnol.* **2018**, *49*, 23-28.
56. Cho, J.A.; Chinnapen, D.J.F.; Aamar, E.; te Welscher, Y.M.; Lencer, W.I.; Massol, R. Insights on the trafficking and retro-translocation of glycosphingolipid-binding bacterial toxins. *Front. Cell Infect. Microbiol.* **2012**, *2*, 51.
57. Choi, H.J.; Kim, J.Y.; Shin, M.S.; Lee, S.M.; Lee, W.K. Immuno-modulatory effects of bacteriocin-producing *Pediococcus pentosaceus* JWS 939 in mice. *Kor. J. Food Sci. Animal Res.* **2011**, *31*, 719-726.
58. Christensen, D.P.; Hutkins, R.W. Collapse of the proton motive force in *Listeria monocytogenes* caused by a bacteriocin produced by *Pediococcus acidilactici*. *Appl. Environ. Microbiol.* **1992**, *58*, 3312-3315.
59. Claesson, M.J.; O'Sullivan, O.; Wang, Q.; Nikkilä, J.; Marchesi, J.R.; Smidt, H.; de Vos, W.M.; Ross, R.P.; O'Toole, P.W. Comparative analysis of pyrosequencing and a phylogenetic microarray for exploring microbial community structures in the human distal intestine. *PLoS One* **2009**, *4*, e6669.

60. Claesson, M.J.; van Sinderen, D.; O'Toole, P.W. The genus *Lactobacillus* - A genomic basis for understanding its diversity. *FEMS Microbiol. Lett.* **2007**, *269*, 22–28.
61. Cleveland, J.; Montville, T.J.; Nes, I.F.; Chikindas, M.L. Bacteriocins: Safe, natural antimicrobials for food preservation. *Int. J. Food Microbiol.* **2001**, *71*, 1-20.
62. Collado, M.C.; Meriluoto, J.; Salminen, S. Role of commercial probiotic strains against human pathogen adhesion to intestinal mucus. *Lett. Appl. Microbiol.* **2007**, *45*, 454-460.
63. Coolbear, T.; Crow, V.; Harnett, J.; Harvey, S.; Holland, R.; Martley, F. Developments in cheese microbiology in New Zealand—Use of starter and non-starter lactic acid bacteria and their enzymes in determining flavour. *Int. Dairy J.* **2008**, *18*, 705-713.
64. Coombes, J.L.; Robey, E.A. Dynamic imaging of host-pathogen interactions *in vivo*. *Nat. Rev. Immunol.* **2010**, *10*, 353-64.
65. Corcoran, B.M.; Stanton, C.; Fitzgerald, G.F.; Ross, R.P. Survival of probiotic lactobacilli in acidic environments is enhanced in the presence of metabolizable sugars. *Appl. Environ. Microbiol.* **2005**, *71*, 3060-3067.
66. Corr, S.C.; Li, Y.; Riedel, C.U.; O'Toole, P.W.; Hill, C.; Gahan, C.G. Bacteriocin production as a mechanism for the anti-infective activity of *Lactobacillus salivarius* UCC118. *Proc. Natl. Acad. Sci. U.S.A.* **2007**, *104*, 7617-7621.
67. Cossart, P. Illuminating the landscape of host–pathogen interactions with the bacterium *Listeria monocytogenes*. *Proc. Nat. Acad. Sci.* **2011**, *108*, 19484-19491.
68. Costello, E. K.; Stagaman, K.; Dethlefsen, L.; Bohannan, B.J.M.; Relman, D. A. The application of ecological theory toward an understanding of the human microbiome. *Science* **2012**, *336*, 1255-1262.
69. Cotter, P.D.; Hill, C.; Ross, R.P. Bacteriocins: Developing innate immunity for food. *Nat. Rev. Micro.* **2005**, *3*, 777-788.
70. Cotter, P.D.; Ross, R.P.; Hill, C. Bacteriocins - A viable alternative to antibiotics? *Nat. Rev. Micro.* **2013**, *11*, 95-105.
71. Cotter, P.D.; Ross, R.P.; Hill, C. Flagging flora: Help from bacteriocins? *Nature* **2011**, *477*, 162-162.

72. Dabour, N.; Zihler, A.; Kheadr, E.; Lacroix, C.; Fliss, I. *In vivo* study on the effectiveness of pediocin PA-1 and *Pediococcus acidilactici* UL5 at inhibiting *Listeria monocytogenes*. *Int. J. Food Microbiol.* **2009**, *133*, 225-233.
73. De Vries, M.C.; Vaughan, E.E.; Kleerebezem, M.; De Vos, W.M. *Lactobacillus plantarum* - survival, functional and potential probiotic properties in the human intestinal tract. *Int. Dairy J.* **2006**, *16*, 1018-1028.
74. Deepika, G.; Green, R.J.; Frazier, R.A.; Charalampopoulos, D. Effect of growth time on the surface and adhesion properties of *Lactobacillus rhamnosus* GG. *J. Appl. Microbiol.* **2009**, *107*,1230–1240.
75. Deepika, G.; Karunakaran, E.; Hurley, C.R.; Biggs, C.A.; Charalampopoulos, D. Influence of fermentation conditions on the surface properties and adhesion of *Lactobacillus rhamnosus* GG. *Microb. Cell Fact.* **2012**, *11*, 116-128.
76. Defoirdt, T. Antivirulence therapy for animal production: Filling an arsenal with novel weapons for sustainable disease control. *PLoS Pathog*. **2013**, *9*, e1003603.
77. Delavenne, E.; Ismail, R.; Pawtowski, A.; Mounier, J.; Barbier, G.; Le Blay, G. Assessment of lactobacilli strains as yogurt bioprotective cultures. *Food Control* **2013**, *30*, 206–213.
78. Dhanani, A.S.; Bagchi, T. The expression of adhesin EF-Tu in response to mucin and its role in *Lactobacillus* adhesion and competitive inhibition of enteropathogens to mucin. *J. Appl. Microbiol.* **2013**, *115*, 546–554.
79. Dobson, A.; Cotter, P.D.; Ross, R.P.; Hill, C. Bacteriocin production: A probiotic trait? *Appl. Environ. Microbiol.* **2012**, *78*, 1-6.
80. Doron, S.; Snydman, D.R.; Gorbach, S.L. *Lactobacillus* GG: Bacteriology and clinical applications. *Gastroenterol. Clin. North Am.* **2005**, *34*, 483-498.
81. Drider, D.; Fimland, G.; Héchard, Y.; McMullen, L.M.; Prévost, H. The continuing story of class IIa bacteriocins. *Microbiol. Mol. Biol. Rev.* **2006**, *70*, 564-582.
82. Duary, R.K.; Batish, V.K.; Grover, S. Relative gene expression of bile salt hydrolase and surface proteins in two putative indigenous *Lactobacillus plantarum* strains under *in vitro* gut conditions. *Mol. Biol. Rep.* **2012**, *39*, 2541–2552.
83. Dunn, B.M. Overview of Pepsin-like Aspartic Peptidases. In Current Protocols in Protein Science. John Wiley & Sons, Inc. **2001.**

84. Dutra, V.; Silva, A.C.; Cabrita, P.; Peres, C.; Malcata, X.; Brito, L. *Lactobacillus plantarum* LB95 impairs the virulence potential of Gram-positive and Gram-negative food-borne pathogens in HT-29 and Vero cell cultures. *J. Med. Microbiol.* **2016**, *65*, 28–35.
85. Eckert, R.; He, J.; Yarbrough, D.K.; Qi, F.; Anderson, M.H.; Shi, W. Targeted killing of *Streptococcus mutans* by a pheromone-guided "smart" antimicrobial peptide. *Antimicrob. Agents Chemother.* **2006**, *50*, 3651-3657.
86. Elliott, S.N.; Buret, A.; McKnight, W.; Miller, M.J.S.; Wallace, J.L. Bacteria rapidly colonize and modulate healing of gastric ulcers in rats. *Am. J. Physiol. Gastrointest. Liver Physiol*. **1998**, *275*, 425-432.
87. Ennahar, S.; Sashihara, T.; Sonomoto, K.; Ishizaki, A. Class IIa bacteriocins: Biosynthesis, structure and activity. *FEMS Microbiol. Rev.* **2000**, *24*, 85-106.
88. FAO/WHO. Guidelines for the evaluation of probiotics in food. Food and Agriculture Organization of the United Nations/World Health Organization, London, Ontario. **2002**.
89. Fernandes, J.; Su, W.; Rahat-Rozenbloom, S.; Wolever, T.M.S.; Comelli, E.M.; Adiposity, gut microbiota and faecal short chain fatty acids are linked in adult humans. *Nutr. Diab.* **2014**. *4*, e121.
90. Fernebro, J. Fighting bacterial infections - Future treatment options. *Drug Res. Updates* **2011**, *14*, 125-139.
91. Ferrer, M.; dos Martins, S.; Vitor, A.P.; Ott, S.J.; Moya, A. Gut microbiota disturbance during antibiotic therapy. *Gut Microbes* **2014**, *5*, 64-70.
92. Fischbach, M.A., Bluestone, J.A.; Lim, W.A. Cell-based Therapeutics: The next pillar of medicine. *Sci. Trans. Med.* **2013**, *5*, 177-179.
93. Flemming, K.; Ackermann, G. Prevalence of enterotoxin producing *Staphylococcus aureus* in stools of patients with nosocomial diarrhoea. *Infection* **2007**, *35*, 356-358.
94. Forestier, C.; De Champs, C.; Vatoux, C.; Joly, B. Probiotic activities of *Lactobacillus casei rhamnosus*: *In vitro* adherence to intestinal cells and antimicrobial properties. *Res. Microbiol*. **2001**, *152*, 167-173.
95. Fosgerau, K.; Hoffmann, T. Peptide therapeutics: Current status and future directions. *Drug Disc. Today* **2015**, *20*, 122-128.

96. Foster, T.J.; Geoghegan, J.A.; Vannakambadi, K.G.; Hook, M. Adhesion, invasion and evasion: the many functions of the surface proteins of *Staphylococcus aureus*. *Nat. Rev. Microbiol.* **2014**, *12*, 49-62.
97. Fouhy, F.; Guinane, C.M.; Hussey, S.; Wall, R.; Ryan, C.A.; Dempsey, E.M.; Murphy, B.; Ross, R.P.; Fitzgerald, G.F.; Stanton, C.; Cotter, P.D. High-throughput sequencing reveals the incomplete, short-term recovery of infant gut microbiota following parenteral antibiotic treatment with ampicillin and gentamicin. *Antimicrob. Agents Chemother.* **2012**, *56*, 5811-5820.
98. Francino, M.P. Antibiotics and the human gut microbiome: dysbioses and accumulation of resistances. *Front. Microbiol.* **2015**, *6*, 1543-1560.
99. Fukuda, S.; Toh, H.; Hase, K.; Oshima, K.; Nakanishi, Y.; Yoshimura, K.; Tobe, T.; Clarke, J.M.; Topping, D.L.; Suzuki, T.; Taylor, T.D.; Itoh, K.; Kikuchi, J.; Morita, H.; Hattori, M.; Ohno, H. *Bifidobacteria* can protect from enteropathogenic infection through production of acetate. *Nature* **2011**, *469*, 543-547.
100. Fuller, M.E.; Streger, S.H.; Rothmel, R.K.; Mailoux, B.J.; Hall, J.A.; Onstott, T.C.; Fredrickson, J.K.; Balkwill, D.L.; DeFlaun, M.M. Development of a vital fluorescent staining method for monitoring bacterial transport in subsurface environments. *Appl. Environ. Microbiol.* **2000**, *66*, 10, 4486-4496.
101. Gaggia, F.; Di Gioia, D.; Baffoni, L.; Biavati, B. The role of protective and probiotic cultures in food and feed and their impact in food safety. *Trends Food Sci. Technol.* **2011**, *22*, S58–S66.
102. Gänzle, M.G. From gene to function: Metabolic traits of starter cultures for improved quality of cereal foods. *Int. J. Food Microbiol.* **2009**, *134*, 29–36.
103. Gao, P.; Pinkston, K.L.; Bourgogone, A.; Cruz, M.R.; Garsin, D.A.; Murray, B.E.; Harvey, B.R. Library screen identifies *Enterococcus faecalis* CcpA, the catabolite control protein a, as an effector of Ace, a collagen adhesion protein linked to virulence. *J. Bacteriol.* **2013**, *195*, 4761-4768.
104. Gao, Y.; Li, D.; Liu, X. Effects of *Lactobacillus sakei* C2 and sakacin C2 individually or in combination on the growth of *Listeria monocytogenes*, chemical and odor changes of vacuum-packed sliced cooked ham. *Food Control* **2015**, *47*, 27-31.
105. García-Cayuela, T.; Korany, A.M.; Bustos, I.; Gómez de Cadiñanos, L.; Requena, T.; Pelaez, C.; Martinez-Cuesta, M.C. Adhesion abilities of dairy

Lactobacillus plantarum strains showing an aggregation phenotype. *Food Res. Int.* **2014**, *57*, 44-50.

106. Ghosh, S.; Dolai, S.; Patra, T.; Dey, J. Solution behavior and interaction of pepsin with carnitine based cationic surfactant: Fluorescence, circular dichroism, and calorimetric studies. *J. Phy. Chem. B* **2015**, *119*, 12632-12643.
107. Ghoshal, U. C.; Gwee, K.-A.; Holtmann, G.; Li, Y.; Park, S. J.; Simadibrata, M.; Sugano, K.; Wu, K.; Quigley, E.M.M.; Cohen, H. The role of the microbiome and the use of probiotics in gastrointestinal disorders in adults in the Asia-Pacific region - Background and recommendations of a regional consensus meeting. *J. Gastroenterol. Hepat.* **2018**, *33*, 57–69.
108. Giavarina, D. Understanding Bland-Altman analysis. *Biochemia. Medica* **2015**, *25*, 141-151.
109. Gibson, P.R.; Barrett, J.S. The concept of small intestinal bacterial overgrowth in relation to functional gastrointestinal disorders. *Nutrition* **2010**, *26*, 1038-1043.
110. Goldstein, E.J.C.; Tyrrell, K.L.; Citron, D.M. *Lactobacillus* species: Taxonomic complexity and controversial susceptibilities. *Clin. Infect. Dis.* **2015**, *60*, 98–107.
111. González-Rodríguez, I.; Sánchez, B.; Ruiz, L.; Turroni, F.; Ventura, M.; Ruas-Madiedo, P.; Gueimonde, M.; Margolles, A. Role of extracellular transaldolase from *Bifidobacterium bifidum* in mucin adhesion and aggregation. *Appl. Environ. Microbiol.* **2012**, *78*, 3992–3998.
112. Gopal, P.K.; Prasad, J.; Smart, J.; Gill, H.S. *In vitro* adherence properties of *Lactobacillus rhamnosus* DR20 and *Bifidobactirium lactis* DR10 strains and their antagonistic activity against an enterotoxigenic *Escherichia coli*. *Int. J. Food Microbiol.* **2001**, *67*, 207-216.
113. Gotteland, M.; Andrews, M.; Toledo, M.; Muñoz, L.; Caceres, P.; Anziani, A.; Wittig, E.; Speisky, H.; Salazar, G. Modulation of *Helicobacter pylori* colonization with cranberry juice and *Lactobacillus johnsonii* La1 in children. *Nutrition* **2008**, *24*, 421–6.
114. Gries, D.M.; Pultz, N.J.; Donskey, C.J. Growth in cecal mucus facilitates colonization of the mouse intestinal tract by methicillin-resistant *Staphylococcus aureus*. *J. Infec. Dis.* **2005**, *192*, 1621-1627.

115. Grill, J.P.; Cayuela, C.; Antoine, J.M.; Schneider, F. Isolation and characterization of a *Lactobacillus amylovorus* mutant depleted in conjugated bile salt hydrolase activity: relation between activity and bile salt resistance. *J. Appl. Microbiol.* **2000**, *89*, 553-563.

116. Grimm, V.; Gleinser, M.; Neu, C.; Zhurina, D.; Riedel, C.U. Expression of fluorescent proteins in *Bifidobacteria* for analysis of host-microbe interactions. *Appl. Environ. Microbiol.* **2014**, *80*, 2842-2850.

117. Guandalini, S. Probiotics for prevention and treatment of diarrhea. *J. Clin. Gastroenterol*. **2011**, *45*, S149-S153.

118. Guarner, F.; Malagelada, J.R. Gut flora in health and disease. *Lancet* **2003**, *361*, 512-519.

119. Guinane, C.M.; Piper, C.; Draper, L.A.; O'Connor, P.M.; Hill, C.; Ross, R.P.; Cotter, P.D. Impact of environmental factors on bacteriocin promoter activity in gut-derived *Lactobacillus salivarius*. *Appl. Environ. Microbiol.* **2015**, *81*, 7851–9.

120. Gutierrez-Castrellon, P.; Lopez-Velazquez, G.; Diaz-Garcia, L.; Jimenez-Gutierrez, C.; Mancilla-Ramirez, J.; Estevez-Jimenez J, Parra M. Diarrhea in preschool children and *Lactobacillus reuteri*: A randomized controlled trial. *Pediatrics* **2014**, *133*, e904-e909.

121. Haleja, N.; Nair, G.B.; Abraham, P.; Ganguly, N.K. Health impact of probiotics - Vision and opportunities. *Gut Pathog.* **2012**, *4*, 1-6.

122. Hancock, R.E.W.; Nijnik, A.; Philpott, D.J. Modulating immunity as a therapy for bacterial infections. *Nat. Rev. Micro.* **2012**, *10*, 243-254.

123. Hansen, U.; Hussain, M.; Villone, D.; Herrmann, M.; Robenek, H.; Peters, G.; Sinha, B.; Bruckner, P. The anchorless adhesin Eap (extracellular adherence protein) from *Staphylococcus aureus* selectively recognizes extracellular matrix aggregates but binds promiscuously to monomeric matrix macromolecules. *Matrix Biol.* **2006**, *25*, 252-260.

124. Hartlova, A.; Cerveny, L.; Hubalek, M.; Krocova, Z.; Stulik, J. Membrane rafts: A potential gateway for bacterial entry into host cells. *Microbiol. Immunol.* **2010**, *54*, 237-245.

125. Hassan, M.; Kjos, M.; Nes, I.F.; Diep, D.B.; Lotfipour, F. Natural antimicrobial peptides from bacteria: Characteristics and potential applications to fight against antibiotic resistance. *J. Appl. Mircobiol.* **2012**, *113*, 723-736.

126. Hegarty, J.W.; Guinane, C.M.; Ross, R.P.; Hill, C.; Cotter, P.D. Bacteriocin production: A relatively unharnessed probiotic trait? *F1000Research* **2016**, *5*, 2587

127. Hill, C.; Guarner, F.; Reid, G.; Gibson, G.R.; Merenstein, D.J.; Pot, B.; Morelli, L.; Canani, R.B.; Flint, H.J.; Salminen, S.; Calder, P.C.; Sanders, M.E. The International Scientific Association for Probiotics and Prebiotics consensus statement on the scope and appropriate use of the term probiotic. *Nat. Rev. Gastroenterol. Hepatol.* **2014**, *11*, 506–514.

128. Hirano, S.; Yokota, Y.; Eda, M.; Kuda, T.; Shikano, A.; Takahashi, H.; Kimura, B. Effect of *Lactobacillus plantarum* Tennozu-SU2 on *Salmonella Typhimurium* infection in human enterocyte-like HT-29-Luc cells and BALB/c mice. *Prob. Antimicrob. Prot.* **2017**, *9*, 64-70.

129. Holzapfel, W.H.; Wood, B.J.B. Lactic acid bacteria: Biodiversity and taxonomy. **2014**. Wiley Online Library.

130. Huang, Y.; Adams, M.C. *In vitro* assessment of the upper gastrointestinal tolerance of potential probiotic dairy propionibacteria. *Int. J. Food Microbiol.* **2004**, *91*, 253-260.

131. Humphries, R.M.; Linscott, A.J. Laboratory Diagnosis of bacterial gastroenteritis. *Clin. Microbiol. Rev.* **2015**, *28*, 3-31.

132. Hungin, A. P. S.; Mulligan, C.; Pot, B.; Whorwell, P.; Agréus, L.; Fracasso, P.; Lionis, C.; Mendive, J.; Philippart de Foy, J. M.; Rubin, G.; Winchester, C.; Wit, N. Systematic review: Probiotics in the management of lower gastrointestinal symptoms in clinical practice – An evidence-based international guide. *Alim. Pharma. Ther.* **2013**, *38*, 864-886.

133. Huynh, H.Q.; deBruyn, J.; Guan, L.; Diaz, H.; Li, M.; Girgis, S.; Turner, J.; Fedorak, R.; Madsen, K. Probiotic preparation VSL#3 induces remission in children with mild to moderate acute ulcerative colitis: A pilot study. *Inflamm. Bowel Dis.* **2009**, *15*, 760-768.

134. Hwang, I. Y.; Koh, E.; Kim, H.R.; Yew, W.S.; Chang, M.W. Reprogrammable microbial cell-based therapeutics against antibiotic-resistant bacteria. *Drug Res. Updates* **2016**, *27*, 59-71.

135. Hytönen, J.; Haataja, S.; Finne, J. Use of flow cytometry for the adhesion analysis of *Streptococcus pyogenes* mutant strains to epithelial cells:

Investigation of the possible role of surface pullulanase and cysteine protease, and the transcriptional regulator Rgg. *BMC Microbiol.* **2006**, *6*, 18.

136. Indrio, F.; Di Mauro, A.; Riezzo, G.; Civardi, E.; Intini, C.; Corvaglia, L.; Ballardini, E.; Bisceglia, M.; Cinquetti, M.; Brazzoduro, E.; Del Vecchio, A.; Tafuri, S.; Francavilla, R. Prophylactic use of a probiotic in the prevention of colic, regurgitation, and functional constipation: A randomized clinical trial. *JAMA Pediatr.* **2014**, *168*, 228–233.
137. Ingrassia, I.; Leplingard, A.; Darfeuille-Michaud, A. *Lactobacillus casei* DN-114 001 inhibits the ability of adherent-invasive *Escherichia coli* isolated from Crohn's disease patients to adhere to and to invade intestinal epithelial cells. *Appl. Environ. Microbiol.* **2005**, *71*, 2880-2887.
138. Islam, K.B.; Fukiya, S.; Hagio, M.; Fujii, N.; Ishizuka, S.; Ooka,T.; Ogura, Y.; Hayashi, T.; Yokota, A. Bile acid is a host factor that regulates the composition of the cecal microbiota in rats. *Gastroenterol.* **2011**, *141*, 1773–1781.
139. Jariwala, R.; Mandal, H.; Bagchi, T. Indigenous lactobacilli strains of food and human sources reverse enteropathogenic *E. coli* O26:H11-induced damage in intestinal epithelial cell lines: Effect on redistribution of tight junction proteins. *Microbiol.* **2017**, *163*, 1263-1272.
140. Jensen, H.; Grimmer, S.; Naterstad, K.; Axelsson, L. *In vitro* testing of commercial and potential probiotic lactic acid bacteria. *Int. J. Food Microbiol.* **2012**, *153*, 216-222.
141. Jensen, H.; Roos, S.; Jonsson, H.; Rud, I.; Grimmer, S.; van Pijkeren, J-P.; Britton, R.A.; Axelsson, L. Role of *Lactobacillus reuteri* cell and mucus-binding protein A (CmbA) in adhesion to intestinal epithelial cells and mucus *in vitro*. *Microbiol.* **2014** *160*, 671-681.
142. Jiménez, J.J.; Borrero, J.; Diep, D.B.; Gútiez, L.; Nes, I.F.; Herranz, C.; Cintas, L.M.; Hernández, P.E. Cloning, production, and functional expression of the bacteriocin sakacin A (SakA) and two SakA-derived chimeras in lactic acid bacteria (LAB) and the yeasts *Pichia pastoris* and *Kluyveromyces lactis*. *J. Ind. Microbiol. Biotechnol.* **2013**, *40*, 977–993.
143. Jones, R.J.; Hussein, H.M.; Zagorec, M.; Brightwell, G.; Tagg, J.R. Isolation of lactic acid bacteria with inhibitory activity against pathogens and spoilage organisms associated with fresh meat. *Food Microbiol*. **2008**, *25*, 228-234.

144. Jones, R.M.; Desai, C.; Darby, T.M.; Luo, L.; Wolfarth, A.A.; Scharer, C.D.; Ardita, C.S.; Reedy, A.R.; Keebaugh, E.S.; Neish, A.S. Lactobacilli modulate epithelial cytoprotection through the Nrf2 pathway. *Cell Rep.* **2015**, *25*, 1217-25.

145. Józefiak, D.; Kieroñczyk, B.; Juoekiewicz, J.; Zduñczyk, Z.; Rawski, M.; Długosz, J.; Sip, A.; Hojberg, O. Dietary nisin modulates the gastrointestinal microbial ecology and enhances growth performance of the broiler chickens. *PLoS One* **2013**, *8*, e85347.

146. Kalan, L.; Wright, G.D. Antibiotic adjuvants: Multicomponent anti-infective strategies. *Exp. Rev. Mol. Med.* **2011**, *13*, E5.

147. Kaushik, J.K.; Kumar, A.; Duary, R.K.; Mohanty, A.K.; Grover, S.; Batish, V.K. Functional and probiotic attributes of an indigenous isolate of *Lactobacillus plantarum*. *PLoS One* **2009**, *4*, e8099.

148. Kernbauer, E.; Maurer, K.; Torres, V.J.; Shopsin, B.; Cadwell, K. Gastrointestinal dissemination and transmission of *Staphylococcus aureus* following bacteremia. *Infect. Immun.* **2015**, *83*, 372-378.

149. Kheadr, E.; Zihler, A.; Dabour, N.; Lacroix, C.; Le Blay, G.; Fliss, I. Study of the physicochemical and biological stability of pediocin PA-1 in the upper gastrointestinal tract conditions using a dynamic *in vitro* model. *J. Appl. Microbiol.* **2010**, *109*, 54-64.

150. Killeen, S.D.; Wang, J.H.; Andrews, E.J.; Redmond, H.P. Bacterial endotoxin enhances colorectal cancer cell adhesion and invasion through TLR-4 and NF-κb-dependent activation of the urokinase plasminogen activator system. *B. J. Cancer* **2009**, *100*, 1589-1602.

151. Kim, Y.; Mylonakis, E. *Caenorhabditis elegans* immune conditioning with the probiotic bacterium *Lactobacillus acidophilus* strain NCFM enhances Gram-positive immune responses. *Infect. Immun.* **2012**, *80*, 2500-2508.

152. Kirk, M.D.; Pires, S.M.; Black, R.E.; Caipo, M.; Crump, J.A.; Devleesschauwer, B.; Dopfer, D.; Fazil, A.; Fischer-Walker, C.L.; Hald, T.; Hall, A.J.; Keddy, K.H.; Lake, R.J.; Lanata, C.F.; Torgersen, P.R.; Havelaar, A.H.; Angulo, F.J. World Health Organization estimates of the global and regional disease burden of 22 foodborne bacterial, protozoal, and viral diseases, 2010: A Data Synthesis. *PLOS Med.* **2015**, *12*, e1001921.

153. Klaenhammer, T. R. Genetics of bacteriocins produced by lactic acid bacteria. *FEMS Microbiol. Rev.* **1993**, *12*, 39-85.

154. Kleerebezem, M.; Kuipers, O.P.; Smid, E.J.; Lactic acid bacteria - A continuing journey in science and application. *FEMS Microbiol. Rev.* **2017**, *41*, S1–S2.

155. Kommineni, S.; Bretl, D.J.; Lam, V.; Chakraborty, R.; Hayward, M.; Simpson, P.; Cao, Y.; Bousounis, P.; Kristich, C.J.; Salzman, N.H. Bacteriocin production augments niche competition by enterococci in the mammalian gastrointestinal tract. *Nature* **2015**, *526*, 719-22.

156. Korpela, K.; Salonen, A.; Virta, L.J.; Kekkonen, R.A.; Forslund, K.; Bork, P.; de Vos, W.M. Intestinal microbiome is related to lifetime antibiotic use in Finnish pre-school children. *Nat. Comm.* **2016**, *7*, 10410.

157. Kos, B.; Šuškovic, S.; Vukovic, S.; Šimpraga, M.; Frece, J.; Matošic, S. Adhesion and aggregation ability of probiotic strain *Lactobacillus acidophilus* M92. *J. Appl. Microbiol.* **2003**, *94*, 981-987.

158. Krachler, A.M.; Orth, K. Targeting the bacteria–host interface. *Virulence* **2013**, 4, 284-294.

159. Kumar, R.S.; Brannigan, J.A.; Prabhune, A.A.; Pundle, A.V.; Dodson,G.G.; Dodson, E.J.; Suresh, C.G. Structural and functional analysis of a conjugated bile salt hydrolase from *Bifidobacterium longum* reveals an evolutionary relationship with penicillin V acylase. *J. Biol.Chem.* **2006**, *281*, 32516–32525.

160. Kumar, R.S.; Kanmani, P.; Yuvaraj, N.; Paari, K.A.; Pattukumar, V.; Arul, V. *Lactobacillus plantarum* AS1 binds to cultured human intestinal cell line HT-29 and inhibits cell attachment by enterovirulent bacterium *Vibrio parahaemolyticus*. *Lett. Appl. Microbiol.* **2011**, *53*, 481-487.

161. Lambert, J.M.; Bongers, R.S.; de Vos, W.M.; Kleerebezem, M. Functional analysis of four bile salt hydrolase and penicillin acylase family members in *Lactobacillus plantarum* WCFS1. *Appl. Environ. Microbiol.* **2008**, *74*, 4719-4726

162. Langdon, A., Crook, N.; Dantas, G. The effects of antibiotics on the microbiome throughout development and alternative approaches for therapeutic modulation. *Genome Med.* **2016**, *8*, 39-49.

163. Langer, K.; Balthasar, S.; Vogel, V.; Dinauer, N.; von Briesen, H.; Schubert, D. Optimization of the preparation process for human serum albumin (HSA) nanoparticles. *Int. J. Pharm.* **2003**, *257*, 169-180.

164. Langerholc, T.; Maragkoudakis, P.A.; Wollgast, J.; Gradisnik, L.; Cencic, A. Novel and established cell line models – An indispensable tool in food science and nutrition. *Trends Food Sci. Technol.* **2011**, *22*, S11-S20

165. Lawley, T. D.; Clare, S.; Walker, A.W.; Stares, M.D.; Connor, T.R.; Raisen, C.; Goulding, D.; Rad, R.; Schreiber, F.; Brandt, C.; Deakin, L. J.; Pickard, D. J.; Duncan, S. H.; Flint, H. J.; Clark, T.G.; Parkhill, J.; Dougan, G. Targeted restoration of the intestinal microbiota with a simple, defined bacteriotherapy resolves relapsing *Clostridium difficile* disease in mice. *PLoS Pathog*. **2012**, *8*, e1002995.

166. Lebeer, S.; Claes, I.; Tytgat, H.L.P.; Verhoeven, T.L.A.; Marien, E.; von Ossoswski, I.; Reunaen, J.; Palva, A.; de Vos, W.M.; De Keersmaecker, S.C.J., Vanderleyden, J. Functional analysis of *Lactobacillus rhamnosus* GG pili in relation to adhesion and immunomodulatory interactions with intestinal epithelial cells. *Appl. Environ. Microbiol.* **2012**, *78*, 185-193.

167. Lebeer, S.; Vanderleyden, J.; De Keersmaecker, S.C. Genes and molecules of Lactobacilli supporting probiotic action. *Microbiol. Mol. Biol. Rev.* **2008**, *72*, 728-764

168. Lebeer, S.; Vanderleyden, J.; De Keersmaecker, S.C.J. Host interactions of probiotic bacterial surface molecules: Comparison with commensals and pathogens. *Nat. Rev. Micro.* **2010**, *8*, 171-184.

169. Lee, Y. K.; Lim, C.M.; Teng, W.L.; Ouwehand, A. C.; Tuomola, E.M.; Salminen, S. Quantitative approach in the study of adhesion of lactic acid bacteria to intestinal cells and their competition with enterobacteria. *Appl. Environ. Microbiol.* **2000**, *66*, 3692-3697.

170. Lee, Y.K.; Ho, P.S.; Low, C.S.; Arvilommi, H.; Salminen S. Permanent colonization by *Lactobacillus casei* is hindered by the low rate of cell division in mouse gut. *Appl. Environ. Microbiol.* **2004**, *70*, 670-674.

171. Lee, Y.K.; Puong, K.Y.; Ouwehand, A.C.; Salminen, S. Displacement of bacterial pathogens from mucus and Caco-2 cell surface by Lactobacilli. *J. Med. Microbiol.* **2003**, *52*, 925-930.

172. Lee, Y-K. Mathematical modeling of intestinal bacteria–host interactions. Lactic acid bacteria, 3rd edition, **2004**, Marcel Dekker.

173. Lemon, K.P.; Armitage, G.C.; Relman, D.A.; Fischbach, M.A. Microbiota-targeted therapies: An ecological perspective. *Sci. Trans. Med.* **2012**, *4*, 137-135.

174. Leroy, F.; De Vuyst, L. Lactic acid bacteria as functional starter cultures for the food fermentation industry. *Trends Food Sci. Technol.* **2004**, *15*, 67-78

175. Liévin-Le Moal, V.; Servin, A.L. Anti-infective activities of *Lactobacillus* strains in the human intestinal microbiota: From probiotics to gastrointestinal anti-infectious biotherapeutic agents. *Clin. Microbiol. Rev.* **2014**, *27*,167-99.

176. Lin, P. W.; Nasr, T.R.; Berardinelli, A.J.; Kumar, A.; Neish, A.S. The probiotic *Lactobacillus* GG may augment intestinal host defense by regulating apoptosis and promoting cytoprotective responses in the developing murine gut. *Ped. Res.* **2008**, *64*, 511-516.

177. Lin, Z.; Kotler, D.P.; Schlievert, P.M.; Sordillo, E.M. Staphylococcal enterocolitis: Forgotten but not gone? *Diges. Dis. Sci.* **2010**, *55*, 1200-1207.

178. Liong, M.; Shah, N. Acid and bile tolerance and cholesterol removal ability of lactobacilli strains. *J. Dairy Sci.* **2005**, *88*, 55-66.

179. Liu, H.-Y.; Roos, S.; Jonsson, H.; Ahl, D.; Dicksved, J.; Lindberg, J.E.; Lundh, T. Effects of *Lactobacillus johnsonii* and *Lactobacillus reuteri* on gut barrier function and heat shock proteins in intestinal porcine epithelial cells. *Physiol. Rep.* **2015**, *3*, e12355,

180. Lonnermark, E.; Friman, V.; Lappas, G.; Sandberg, T.; Berggren, A.; Adlerberth, I. Intake of *Lactobacillus plantarum* reduces certain gastrointestinal symptoms during treatment with antibiotics. *J. Clin. Gastro.* **2010**, *44*, 106-112.

181. Looft, T.; Allen, H.K. Collateral effects of antibiotics on mammalian gut microbiomes. *Gut Microbes* **2012**, *3*, 463-467.

182. Lorca, G.; Torino, M. I.; Font de Valdez, G.; Ljungh, A. A. Lactobacilli express cell surface proteins which mediate binding of immobilized collagen and fibronectin. *FEMS Microbiol. Lett.* **2002**, *206*, 31-37.

183. Lukic, J.; Strahinic, I.; Jovcic, B.; Filipic, B.; Topisirovic, L.; Kojic, M.; Begovic, J. Different roles for lactococcal aggregation factor and mucin binding protein in adhesion to gastrointestinal mucosa. *Appl. Environ. Microbiol.* **2012**, *78*, 7993–8000.

184. MacKenzie, D.A.; Jeffers, F.; Parker, M.L.; Vibert-Vallet, A.; Bongaerts, R.J.; Roos, S.; Walter, J.; Juge, N. Strain-specific diversity of mucus-binding proteins in the adhesion and aggregation properties of *Lactobacillus reuteri*. *Microbiol.* **2010**, *156*, 3368-3378.

185. Maharshak, N.; Huh, E.Y.; Paiboonrungruang, C.; Shanahan, M.; Thurlow, L.; Herzog, J.; Djukic, Z.; Orlando, R.; Pawlinksi, R.; Ellermann, M.; Borst, L.; Patel, S.; Dotan, I.; Sartor, R.B.; Carroll, I.M. *Enterococcus faecalis* gelatinase mediates intestinal permeability via protease-activated receptor 2. *Infect.Immun.* **2015**, *83*, 2762-2770.

186. Manley, K.J.; Fraenkel, M.B.; Mayall, B.C.; Power, D.A. Probiotic treatment of vancomycin-resistant enterococci: A randomised controlled trial. *Med. J. Aust.* **2007**, *186*, 454-457.

187. Manickam, B.; Sreedharan, R.; Elumalai, M. 'Genipin' - The natural water-soluble cross-linking agent and its importance in the modified drug delivery systems: An overview. *Curr. Drug Delivery*, **2014**, *11*, 139-145.

188. Marchant, M.; Moreno, M.A. Dynamics and diversity of *Escherichia coli* in animals and system management of the manure on a commercial farrow-to-finish pig farm. *Appl. Environ. Microbiol.* **2013**, *79*, 853-859

189. Margolles, A.; García, L.; Sánchez, B.; Gueimonde, M.; de los Reyes-Gavilán, C.G. Characterisation of a *Bifidobacterium* strain with acquired resistance to cholate - A preliminary study. *Int. J. Food Microbiol.* **2003**, *82*, 191–198.

190. Marques, M.R.; Loebenberg, R.; Almukainzi, M. Simulated biological fluids with possible application in dissolution testing. *Dissolut. Technol.* **2011**, *18*, 15-28.

191. Martin Bland, J.; Altman, D. Statistical methods for assessing agreement between two methods of clinical measurement. *Lancet* **1986**, *327*, 307-310.

192. Maudsotter, L.; Jonsson, H.; Roos, S.; Jonsson, A-B. *Lactobacilli* reduce cell cytotoxicity caused by *Streptococcus pyogenes* by producing lactic acid that degrades the toxic component lipoteichoic acid. *Antimicrob. Agents Chemother.* **2011**, *55*, 1622-1628.

193. Maxson, T.; Mitchell, D.A. Targeted treatment for bacterial infections: Prospects for pathogen-specific antibiotics coupled with rapid diagnostics. *Tetrahedron* **2016**, *72*, 3609-3624.

194. McGuckin, M.A.; Lindén, S.K.; Sutton, P.; Florin, T.H. Mucin dynamics and enteric pathogens. *Nat. Rev. Microbiol.* **2011**, *9*, 265-278.

195. Medellin-Peña, M.J.; Griffiths, M.W. Effect of molecules secreted by *Lactobacillus acidophilus* strain La-5 on *Escherichia coli* O157:H7 colonization. *Appl. Environ. Microbiol.* **2009**, *75*, 1165-1172.

196. Meijerink, M.; van Hemert, S.; Taverne, N.; Wels, M.; de Vos, P.; Bron, P.A.; Savelkoul, H.F.; van Bilsen, J.; Kleerebezem, M.; Wells, J.M. Identification of genetic loci in *Lactobacillus plantarum* that modulate the immune response of dendritic cells using comparative genome hybridization. *PLoS One* **2010**, *5*, e10632.

197. Miele, E.; Pascarella, F.; Giannetti, E.; Quaglietta, L.; Baldassano, R.N.; Staiano, A. Effect of a probiotic preparation (VSL#3) on induction and maintenance of remission in children with ulcerative colitis. *Am. J. Gastro.* **2009**, *104*, 437-443.

198. Miljkovic, M.; Strahinic, I.; Tolinacki, M.; Zivkovic, M.; Kojic, S.; Golic, N.; Kojic, M. AggLb is the largest cell-aggregation factor from *Lactobacillus paracasei* subsp. *paracasei* BGNJ1-64, functions in collagen adhesion, and pathogen exclusion *in vitro*. *PLoS One* **2015**, *10*, e0126387.

199. Millette, M.; Cornut, G.; Dupont, C.; Shareck, F.; Archambault, D.; Lacroix, M. Capacity of human nisin- and pediocin-producing lactic acid bacteria to reduce intestinal colonization by vancomycin-resistant enterococci. *Appl. Environ. Microbiol.* **2008**, *74*, 1997-2003.

200. Miyoshi, Y.; Okada, S.; Uchimura, T.; Satoh, E.A. Mucus adhesion promoting protein, MAPa, mediates the adhesion of *Lactobacillus reuteri* to Caco-2 human intestinal epithelial cells. *Biosci. Biotech. Biochem.* **2006**, *70*, 1622-1628.

201. Mujagic, Z.; de Vos, P.; Boekschoten, M.V.; Govers, C.; Pieters, Harm-J.H. M.; de Wit, N. J. W.; Bron, P.A.; Masclee, Ad. A. M.; Troost, F.J. The effects of *Lactobacillus plantarum* on small intestinal barrier function and mucosal gene transcription; a randomized double-blind placebo controlled trial. *Sci. Rep.* **2017**, *7*, 40128-40136.

202. Muñoz-Provencio, D.; Llopis, M.; Antolín, M.; Torres, I.D.; Guarner, F.; Martínez, G.P.; Monedero, V. Adhesion properties of *Lactobacillus casei* strains to resected intestinal fragments and components of the extracellular matrix. *Arch. Microbiol.* **2009**, *191*, 153-161.

203. Murray, B.E. Vancomycin-resistant enterococcal infections. *N. Engl. J. Med.* **2000**, *342*, 710-721.

204. Nader-Macias, M.E.; Otero, M.C.; Espeche, M.C.; Maldonado, N.C. Advances in the design of probiotic products for the prevention of major diseases in dairy cattle. *J. Ind. Microbiol. Biotechnol.* **2008**, *35*, 1387-1395.

205. Nallapareddy, S.R.; Qin, X.; Weinstock, G.M.; Hook, M.; Murray, B.E. *Enterococcus faecalis* adhesin, Ace, mediates attachment to extracellular matrix proteins collagen type IV and laminin as well as collagen type I. *Infect. Immun.* **2000**, *68*, 5218-5224.

206. Natividad, J. M. M.; Petit, V.; Huang, X.; de Palma, G.; Jury, J.; Sanz, Y.; Philpott, D.; Garcia Rodenas, C.L.; McCoy, K.D.; Verdu, E.F. Commensal and probiotic bacteria influence intestinal barrier function and susceptibility to colitis in Nod1−/−;Nod2−/− Mice. *Inflam. Bowel Dis.* **2012**, *18*, 1434-1446.

207. Nieto Lozano, J.C.; Meyer, J. N.; Sletten, K.; Pelaz, C.; Nes, I.F. Purification and amino acid sequence of a bacteriocin produced by *Pediococcus acidilactici*. *J. Gen. Microbiol.* **1992**, *138*, 1985-1990.

208. Nikaido, H. Multidrug resistance in bacteria. *Ann. Rev. Biochem.* **2009**, *78*, 119-146.

209. Nishiyama, K.; NAkamata, K.; Ueno, S.; Terao, A.; Aryantini, N.P.D.; Sujaya, I.N.; Fukuda, K.; Urashima, T.; Yamamoto, Y.; Mukai, T. Adhesion properties of *Lactobacillus rhamnosus* mucus binding factor to mucin and extracellular matrix. *Biosci. Biotech. Biochem.* **2016**, *79*, 271-279.

210. Nishiyama, K.; Sugiyama, M.; Mukai, T. Adhesion properties of lactic acid bacteria on intestinal mucin. *Microorg.* **2016**, *4*, 34-52.

211. Nueno-Palop, C.; Narbad, A. Probiotic assessment of *Enterococcus faecalis* CP58 isolated from human gut. *Int. J. Food Microbiol.* **2011**, *145*, 390-394.

212. O'Callaghan, J.; Butto, L.F.; MacSharry, J.; Nally, K.; O'Toole, P.W. Influence of adhesion and bacteriocin production by *Lactobacillus salivarius* on the intestinal epithelial cell transcriptional response. *Appl. Environ. Microbiol.* **2012**, *78*, 5196-5203.

213. O'Connor, P.M.; Ross, R.P.; Hill, C.; Cotter, P.D. Antimicrobial antagonists against food pathogens: A bacteriocin perspective. *Curr. Opin. Food Sci.* **2015**, *2*, 51–57.

214. O'Shea, E.F.; Cotter, P.D.; Stanton, C.; Ross, R.P.; Hill, C. Production of bioactive substances by intestinal bacteria as a basis for explaining probiotic mechanisms: bacteriocins and conjugated linoleic acid. *Int. J. Food Microbiol.* **2012**, *152*, 189-205.

215. O'Toole, P.W.; Cooney, J.C. Probiotic bacteria influence the composition and function of the intestinal microbiota. *Interdisci. Perspec. Infect. Dis.* **2008**, Article ID 175285, 9 pages.

216. Oguntoyinbo, F.A.; Narbad, A. Multifunctional properties of *Lactobacillus plantarum* strains isolated from fermented cereal foods. *J. Func. Foods* **2015**, *17*, 621-631.

217. Ohland, C.L.; MacNaughton, W.K. Probiotic bacteria and intestinal epithelial barrier function. *Am. J. Physiol. Gastrointest. Liver Physiol.* **2010**, *298*, 807-810.

218. Ossowski, I.; Reunanen, J.; Satokari, R.; Vesterlund, S.; Kankainen, M.; Huhtinen, H.; Tynkkynen, S.; Salminen, S.; De Vos, W.M.; Palva, A. Mucosal adhesion properties of the probiotic *Lactobacillus rhamnosus* GG SpaCBA and SpaFED pilin subunits. *Appl. Environ. Microbiol.* **2010**, *76*, 2049-2057.

219. Ouwehand, A.C.; Salminen, S. *In vitro* adhesion assays for probiotics and their *in vivo* relevance: A review. *Micro. Eco. Health Dis.* **2003**, *15*, 175-184.

220. Ouwehand, A.C.; Salminen, S.; Isolauri, E. Probiotics: An overview of beneficial effects. *Antonie van Leeuwenhoek* **2002**, *82*, 279-289.

221. Ouwehand, A.C.; Tuomola, E.M.; Tolkko, S.; Salminen, S. Assessment of adhesion properties of novel probiotic strains to human intestinal mucus. *Int. J. Food Microbiol.* **2001**, *64*, 119-126.

222. Pagnini, C.; Saeed, R.; Bamias, G.; Aresneau, K.O.; Pizarro, T.T.; Cominelli, F. Probiotics promote gut health through stimulation of epithelial innate immunity. *Proc. Nat. Acad. Sci.* **2010**, *107*, 454-459.

223. Pamer, E.G. Resurrecting the intestinal microbiota to combat antibiotic-resistant pathogens. *Science* **2016**, *352*, 535-540

224. Patel, A.K.; Singhania, R.R.; Pandey, A.; Chincholkar, S.B. Probiotic bile salt hydrolase: Current developments and perspectives. *Appl. Biochem. Biotechnol.* **2010**, *162*, 166-180.

225. Patel, R.; DuPont, H.L. New Approaches for bacteriotherapy: Prebiotics, new-generation probiotics, and synbiotics. *Clin. Infect. Dis.* **2015**, *60*, S108-S121.

226. Paton, A.W.; Morona, R.; Paton, J.C. Designer probiotics for prevention of enteric infections. *Nat. Rev. Microbiol.* **2006**, *4*, 193-200.

227. Perez, R.H.; Zendo, T.; Sonomoto, K. Novel bacteriocins from lactic acid bacteria (LAB): Various structures and applications. *Microb. Cell Fact.* **2014**, *13*, S3-S16.

228. Petersson, J.; Schreiber, O.; Hansson, G.C.; Gendler, S.J.; Velcich, A.; Lundberg, J.O.; Roos, S.; Holm, L.; Phillipson, M. Importance and regulation of the colonic mucus barrier in a mouse model of colitis *Am. J. Phys. Gastro. Liver Phys.* **2011**, *300*, G327-G333.

229. Pham, T.A.N.; Lawley, T.D. Emerging insights on intestinal dysbiosis during bacterial infections. *Curr. Opin. Microbiol.* **2014**, *17*, 67-74.

230. Porto, M.C.W.; Kuniyoshi, T.M.; Azevedo, P.O.S.; Vitolo, M.; Oliveira, R.P.S. *Pediococcus* spp.: An important genus of lactic acid bacteria and pediocin producers. *Biotechnol. Adv.* **2017**, *35*, 361-374.

231. Priedis, G.A.; Hill, C.; Guerrant, R.L.; Ramakrishna, B.S.; Tannock, G.W.; Versalovic, J. Probiotics, enteric and diarrheal diseases, and global health. *Gastroent.* **2011**, *140*, 8-14.

232. Prince, T.; McBain, A.J.; O'Neill, C.A. *Lactobacillus reuteri* protects epidermal keratinocytes from *Staphylococcus aureus*-induced cell death by competitive exclusion. *Appl. Environ. Microbiol.* **2012**, *78*, 5119-5126.

233. Quigley, E.M.M. Prebiotics and probiotics: Their role in the management of gastrointestinal disorders in adults. *Nutr. Clin. Prac.* **2012**, *27*, 195-200.

234. Ramiah, K.; van Reenen, C.A.; Dicks, L.M.T. Surface-bound proteins of *Lactobacillus plantarum* 423 that contribute to adhesion of Caco-2 cells and their role in competitive exclusion and displacement of *Clostridium sporogenes* and *Enterococcus faecalis*. *Res. Microbiol.* **2008**, *159*, 470-475.

235. Rastall, R.A.; Gibson, G.R.; Gill, H.S.; Guarner, F.; Klaenhammer, T.R.; Pot, B.; Reid, G.; Rowland, I.R.; Sanders, M.E. Modulation of the microbial ecology of the human colon by probiotics, prebiotics and synbiotics to enhance human health: An overview of enabling science and potential applications. *FEMS Microb. Eco.* **2005**, *52*, 145-152.

236. Rautava, S.; Salminen, S.; Isolauri, E. Specific probiotics in reducing the risk of acute infections in infancy- A randomised, double-blind, placebo-controlled study. *B. J. Nutr.* **2009**, *101*, 1722-1726.

237. Reid, G.; Burton, J. Use of *Lactobacillus* to prevent infection by pathogenic bacteria. *Microbes. Infect.* **2002**, *4*, 319-324.

238. Reid, G.; Younes, J.A.; Van der Mei, H.C.; Gloor, G.B.; Knight, R.; Busscher, H.J. Microbiota restoration: Natural and supplemented recovery of human microbial communities. *Nat. Rev. Microbiol.* **2011**, *9*, 27-38.

239. Reller, L.B.; Weinstein, M.; Jorgensen, J.H.; Ferraro, M.J. Antimicrobial susceptibility testing: A review of general principles and contemporary practices. *Clin. Infect. Dis.* **2009**, *49*, 1749-1755.

240. Rendueles, O.; Ferrières, L.; Frétaud, M.; Begaud, E.; Herbomel, P.; Levraud, J-P.; Ghigo, J-M. A new zebrafish model of oro-intestinal pathogen colonization reveals a key role for adhesion in protection by probiotic bacteria. *PLoS Path.* **2012**, *8*, e1002815.

241. Rhee, S.J.; Lee, J-E; Lee, C-H. Importance of lactic acid bacteria in Asian fermented foods. *Microb. Cell Fact.* **2011**, *10*, S5-S10.

242. Ribeiro, S.C.; O'Connor, P.M.; Ross, R.P.; Stanton, C.; Silva, C.C.G. An anti-listerial *Lactococcus lactis* strain isolated from Azorean Pico cheese produces lacticin 481. *Int. Dairy J.* **2016**, *63*, 18-28.

243. Ribet, D.; Cossart, P. How bacterial pathogens colonize their hosts and invade deeper tissues. *Microbes Infect.* **2015**, *17*, 173-183.

244. Richards, M.J.; Edwards, J.R.; Culver, D.H.; Gaynes, R.P. Nosocomial infections in combined medical-surgical intensive care units in the United States. *Infect. Contr.Hosp. Epidemiol.* **2000**, *21*, 510-515.

245. Rieu, A.; Aoudia, N.; Jego, G.; Chluba, J.; Yousfi, N.; Briandet, R.; Deschamps, J.; Gasquet, B.; Monedero, V.; Garrido, C.; Guzzo, J. The biofilm mode of life boosts the anti-inflammatory properties of *Lactobacillus*. *Cell Microbiol*. **2014**, *16*, 1836–1853.

246. Riley, M.A. Bacteriocin-mediated competitive interactions of bacterial populations and communities. In *Prokaryotic Antimicrobial Peptides: From Genes to Applications*, D. Drider, S. Rebuffat (eds.). New York, NY, Springer New York, **2011**, 13-26.

247. Ringner, M. What is principal component analysis? *Nat. Biotechnol.* **2008**, *26*, 303-304.

248. Ritchie, M.L.; Romanuk, T.N. A meta-analysis of probiotic efficacy for gastrointestinal diseases. *PLoS One* **2012**, *7*, e34938.

249. Rivera-Espinoza, Y.; Gallardo-Navarro, Y. Non-dairy probiotic products. *Food Microbiol.* **2010**, *27*, 1-11

250. Rodríguez, J.M.; Martínez, M.I.; Kok, J. Pediocin PA-1, a wide-spectrum bacteriocin from lactic acid bacteria. *Crit. Rev. Food Sci. Nutr.* **2002**, *42*, 91-121.

251. Rodríguez, L.; Cervantes, E.; Ortiz, R. Malnutrition and gastrointestinal and respiratory infections in children: A public health problem. *Int. J. Environ. Res. Pub. Heal.* **2011**, *8*, 1174-1205.

252. Rubenstein, E.; Keynan, Y. Vancomycin-resistant Enterococci. *Crit. Care Clin.* **2013**, *4*, 841-852.

253. Ruggiero P. Use of probiotics in the fight against *Helicobacter pylori*. *W. J. Gastrointest. Pathophysiol.* **2014**; *5*, 384-391

254. Ruiz, L.; O'Connell-Motherway, M.; Zomer, A.; de los Reyes-Gavilán, C.G.; Margolles, A.; van Sinderen, D. A bile-inducible membrane protein mediates bifidobacterial bile resistance. *Microb. Biotechnol.* **2012**, *5*, 523–535.

255. Ruiz, L.; Sánchez, B.; Ruas-Madiedo, P.; de los Reyes-Gavilán, C.G.; Margolles, A. Cell envelope changes in *Bifidobacterium animalis* ssp. *Lactis* as a response to bile. *FEMS Microbiol. Lett.* **2007**, *274*, 316–322.

256. Ruszczyński, M.; Radzikowski, A.; Szajewska, H. Clinical trial: Effectiveness of *Lactobacillus rhamnosus* (strains E/N, Oxy and Pen) in the prevention of antibiotic-associated diarrhoea in children. *Alimen. Pharmacol. Therap.* **2008**, *28*, 154-161.

257. Saint-Cyr, M.J.; Haddad, N.; Taminiau, B.; Poezevara, T.; Quesne, S.; Amelot, M.; Daube, G.; Chemaly, M.; Dousset, X.; Guyard-Nicodème, Muriel. Use of the potential probiotic strain *Lactobacillus salivarius* SMXD51 to control *Campylobacter jejuni* in broilers. *Int. J. Food Microbiol.* **2017**, *247*, 9-17.

258. Salminen, S.; Nyborn, S.; Meriluoto, J.; Collado, M.C.; Vesterlund, S.; El-Nezami, H. Interaction of probiotics and pathogens - Benefits to human health. *Curr. Opin. Biotechnol.* **2010**, *21*, 157-167.

259. Salvetti, E.; Torriani, S.; Felis, G.E.; The genus *Lactobacillus*: A taxonomic update. *Prob. Antimicrob. Prot.* **2012**, *4*, 217–226.

260. Sambuy, Y.; De Angelis, I.; Ranaldi, G.; Scarino, M.L.; Stammati, A.; Zucco, F. The Caco-2 cell line as a model of the intestinal barrier: Influence of cell and

culture-related factors on Caco-2 cell functional characteristics. *Cell Biol. Toxicol.* **2005**, *21*, 1-26

261. Sańchez, B.; Urdaci, M.C.; Margolles, A. Extracellular proteins secreted by probiotic bacteria as mediators of effects that promote mucosa - bacteria interactions. *Microbiol.* **2010**, *156*, 3232–3242.
262. Saxelin, M.; Tynkkynen, S.; Sandholm, T.M.; de Vos, W.M. Probiotic and other functional microbes: from markets to mechanisms. *Curr. Opin. Biotech.* **2005**, *16*, 204-211.
263. Schillinger, U. Bacteriocins of lactic acid bacteria. *Biotechnology and Food Safety: Proceedings of the Second International Symposium* **2014**, *55.*
264. Schlee, M.; Harder, J.; Köten, B.; Stange, E.F.; Wehkamp, J.; Fellermann, K. Probiotic lactobacilli and VSL#3 induce enterocyte β-defensin 2. *Clin. Exp. Immunol.* **2008**, *151*, 528-535.
265. Schulfer, A.; Blaser M.J. Risks of antibiotic exposure early in life on the developing microbiome. *PLoS Pathog.* **2015**, *11*,e1004903.
266. Senn, L.; Clerc, O.; Zanetti, G.; Basset, P.; Prod'hom, G.; Gordon, N.C.; Sheppard, A.E.; Crook, D.W.; James, R.; Thorpe, H.A.; Feil, E.J.; Blan, D.S. The stealthy superbug: The role of asymptomatic enteric carriage in maintaining a long-term hospital outbreak of ST228 methicillin-resistant *Staphylococcus aureus*. *mBio* **2016**, *7*, 1.
267. Shanahan, F. Probiotics in perspective. *Gastroent.* **2010**, *139*, 1808-1812.
268. Shanahan, F.; Dinan, T.G.; Ross, P.; Hill, C. Probiotics in transition. *Clin. Gastro. Hepat.* **2012**, *10*, 1220-1224.
269. Shapiro, H.M.; Perlmutter, N.G. Killer applications: Toward affordable rapid cell-based diagnostics for malaria and tuberculosis. *Cyt. Part B: Clin. Cyt.* **2008**, *74B*, S152-S164.
270. Shogan, B.D.; Belogortseva, N.; Luong, P.M.; Zaborin, A.; Lax, S.; Bethel, C.; Ward, M.; Muldoon, J.P.; Singer, M.; An, G.; Umanskiy, K.; Konda, V.; Shakhsheer, B.; Luo, J.; Klabbers, R.; Hancock, L.E.; Gilbert, J.; Zaborina, O.; Alverdy, J.C. Collagen degradation and MMP9 activation by *Enterococcus faecalis* contributes to intestinal anastomotic leak. *Sci. Transl. Med.* **2015**, *7*, 286-313.

271. Sikora, C.W.; Turner, R.J. Investigation of ligand binding to the multidrug resistance protein emre by isothermal titration calorimetry. *Biophy. J.* **2005**, *88*, 475-482.

272. Singh, A.K.; Ramesh, A. Succession of dominant and antagonistic lactic acid bacteria in fermented cucumber: Insights from a PCR-based approach. *Food Microbiol.* **2008**, *25*, 278-287.

273. Singh, A.K.; Ramesh, A. Evaluation of a facile method of template DNA preparation for PCR-based detection and typing of lactic acid bacteria. *Food Microbiol.* **2009**, *26*, 540-513.

274. a. Singh, A.; Mukherjee, S.; Adhikari, M.; Ramesh, A. Fluorescence-based comparative evaluation of bactericidal potency and food application potential of anti-listerial bacteriocin produced by lactic acid bacteria isolated from indigenous samples. *Probiotics Antimicrob. Prot.* **2012**, *4*, 122-132.

275. b. Singh, B.; Fleury, C.; Jalalvand, F.; Riesbeck, K. Human pathogens utilize host extracellular matrix proteins laminin and collagen for adhesion and invasion of the host. *FEMS Microbiol. Rev.* **2012**, *36*, 1122-1180.

276. Singh, A.P.; Prabha, V.; Rishi, P. Value addition in the efficacy of conventional antibiotics by nisin against *Salmonella*. *PLoS One* **2013**, *8*, e76844.

277. Singh, A.P., Preet, S., Rishi, P. Nisin/ β-lactam adjunct therapy against *Salmonella enterica* serovar *Typhimurium*: A mechanistic approach. *J. Antimicrob. Chemother.* **2014**, *69*, 1877–1887.

278. Sivaraman, D.; Yeh, H-Y.; Mulchandani, A.; Yates, M.V.; Chen, W. Use of flow cytometry for rapid, quantitative detection of poliovirus-infected cells via tat peptide-delivered molecular beacons. *Appl. Environ. Microbiol.* **2013**, *79*, 696-700.

279. Stecher, B.; Chaffron, S.; Kappeli, R.; Hapfelmeier, S.; Freedrich, S.; Weber, T.C.; Kirundi, J.; Suar, M.; McCoy, K.; von Mering, C.; Macpherson, A.J.; Hardt, W-D. Like will to like: Abundances of closely related species can predict susceptibility to intestinal colonization by pathogenic and commensal bacteria. *PLoS Pathog*. **2010**, *6*, e1000711.

280. Steck, N.; Hoffmann, M.; Sava, I.G.; Kim, S.C.; Hahne, H.; Tonkonogy, S.L.; Mair, K.; Krueger, D.; Pruteanu, M.; Shanahan, F.; Vogelmann, R.; Schemann, M.; Kuster, B.; Sartor, R.B.; Haller, D. *Enterococcus faecalis* metalloprotease

compromises epithelial barrier and contributes to intestinal inflammation. *Gastroenterol.* **2011**, *141*, 959-971.

281. Stern, N.J.; Svetoch, E.A.; Eruslanov, B.V.; Perelygin, V.V.; Mitsevich, E.V.; Mitsevich, I.P.; Pokhilenko, V.D.; Levchuk, V.P.; Svetoch, O.E.; Seal, B.S. Isolation of a *Lactobacillus salivarius* strain and purification of its bacteriocin, which is inhibitory to *Campylobacter jejuni* in the chicken gastrointestinal system. *Antimicrob. Agents Chemother.* **2006**, *50*, 3111–3116.
282. Stiles, M.E. Biopreservation by lactic acid bacteria. *Antonie Van Leeuwenhoek*, **1996**, *70*, 331–345.
283. Strickertsson, J.A.B.; Rasmussen, L.J.; Friis-Hansen, L. *Enterococcus faecalis* infection and reactive oxygen species down-regulates the miR-17-92 cluster in gastric adenocarcinoma cell culture. *Genes*. **2014**, *5*, 726-738.
284. Sun, H.W.; Feigal, R.J.; Messer, H.H. Cytotoxicity of glutaraldehyde and formaldehyde in relation to time of exposure and concentration. *Ped. Dent.*, **1990**, *12*, 303-307.
285. Sur, D.; Manna, B.; Niyogi, S.K.; Ramamurthy, T.; Palit, A.; Nomoto, K.; Takahashi, T.; Shima, T.; Tsuji, H.; Kurakawa, T.; Takeda, Y.; Nair, G.B.; Bhattacharya, S.K. Role of probiotic in preventing acute diarrhoea in children: A community-based, randomized, double-blind placebo-controlled field trial in an urban slum. *Epidemiol. Infect.* **2011**, *139*, 919-926.
286. Svensson, M.; Platt, F.M.; Svanborg, C. Glycolipid receptor depletion as an approach to specific antimicrobial therapy. *FEMS Microbiol. Lett.* **2006**, *258*, 1-8.
287. Tabasco, R.; de Palencia, P.F.; Fontecha, J.; Pelaez, C.; Requena, T. Competition mechanisms of lactic acid bacteria and bifidobacteria: Fermentative metabolism and colonization. *LWT - Food Sci. Tech.* **2014**, *55*, 680-684.
288. Tallon, R.; Arias, S.; Bressollier, P.; Urdaci, M.C. Strain- and matrix-dependent adhesion of *Lactobacillus plantarum* is mediated by proteinaceous bacterial compounds. *J. Appl. Microbiol.* **2007**, *102*, 442-451.
289. Takigawa, T.; Endo, Y. Effect of glutaraldehyde exposure on human health. *J. Occup. Health*, **2006**, *48*, 75-87.

290. Tang, C-H.; Chen, Z.; Li, L.; Yang, X-Q. Effects of transglutaminase treatment on the thermal properties of soy protein isolates. *Food Res. Int.*, **2006**, *39*, 704–11.

291. Tuomola. E.M.; Salminen, S.J. Adhesion of some probiotic and dairy *Lactobacillus* strains to Caco-2 cell cultures. *Int. J. Food Microbiol.* **1998**, *5*, 45-51.

292. Turpin, W.; Humblot, C.; Noordine, M-L.; Thomas M., Guyot J-P. *Lactobacillaceae* and cell adhesion: Genomic and functional screening. *PLoS One* **2012**, *7*, e38034.

293. Tytgat, H.L.P.; Douillard, F.P.; Reunanen, J.; Rasinkangas, P.; Hendrickx, A.P.A; Laine, P.K.; Paulin, L.; Satokari, R.; de Vos, W.M. *Lactobacillus rhamnosus* GG outcompetes *Enterococcus faecium* via mucus-binding pili: Evidence for a novel and heterospecific probiotic mechanism. *Appl. Environ. Microbiol.* **2016**, *82*, 5756 –5762.

294. Ubeda, C.; Pamer, E.G. Antibiotics, microbiota, and immune defense. *Trends Immunol.* **2012**, *33*, 459-466.

295. Ubeda, C.; Taur, Y.; Jenq, R.R.; Equinda, M.J.; Son, T.; Samstein, M.; Viale, A.; Socci, N.D.; van der Brink, M.R.M.; Kamboj, Mini; Pamer, E.G. Vancomycin-resistant *Enterococcus* domination of intestinal microbiota is enabled by antibiotic treatment in mice and precedes bloodstream invasion in humans. *J. Clin. Invest.* **2010**, *120*, 4332-4341.

296. Umu, Ö.C.O.; Bäuerl, C.; Oostindjer, M.; Pope, P.B.; Hernández, P.E.; Pérez-Martínez, G.; Diep, D.B. The potential of class II bacteriocins to modify gut microbiota to improve host health. *PLoS One* **2016**, *11*, e0164036.

297. Valeriano, V.D.; Parungao-Balolong, M.M.; Kang, D.-K. *In vitro* evaluation of the mucin-adhesion ability and probiotic potential of *Lactobacillus mucosae* LM1. *J. Appl. Microbiol.* **2014**, *117*, 485–497.

298. van Baarlen, P.; Wells, J.M.; Kleerebezem, M. Regulation of intestinal homeostasis and immunity with probiotic lactobacilli. *Tends Immunol.* **2013**, *34*, 208-215.

299. van Beek, A.A.; Sovran, B.; Hugenholtz, F.; Meijer, M.; Hoogerland, J.A.; Mihailova, V.; van der Ploeg, C.; Belzer, C.; Boekschoten, M.V.; Hoeijimekers, J.H.J.; Vermeij, W.P.; de Vos, P.; Wells, J.M.; Leenen, P.J.M.; Nicoletti, C.;

Hendriks, R.W.; Savelkoul, H.F.J. Supplementation with *Lactobacillus plantarum* WCFS1 prevents decline of mucus barrier in colon of accelerated aging Ercc1−/Δ7 mice. *Front. Immunol.* **2016**, *7*, 408-420.

300. van de Guchte, M.; Serror, P.; Chervaux, C.; Smokvina, T.; Ehrlich, S.D.; Maguin, E. Stress responses in lactic acid bacteria. *Antonie van Leeuwenhoek* **2002**, *82*, 187–216.
301. van Harten, R.M.; Willems, R.J.L.; Martin, N.I.; Hendrickx, A.P.A. Multidrug-resistant enterococcal infections: New compounds, novel antimicrobial therapies? *Trends Microbiol.* **2017**, *25*, 467-479.
302. van Hemert, S.; Meijerink, M.; Molenaar, D.; Bron, PA; de Vos, P.; Kleerebezem, M.; Wells, JM; Marco, ML. Identification of *Lactobacillus plantarum* genes modulating the cytokine response of human peripheral blood mononuclear cells. *BMC Microbiol.* **2010**, *10*, 293-306.
303. van Pijkeren, J-P.; Canchaya, C.; Ryan, KA.; Li, Y.; Claesson, M.J.; Sheil, B.; Steidler, L.; O'Mohany, L.; Fitzgerald, G.F.; van Sinderen, D.; O'Toole, PW. Comparative and functional analysis of sortase-dependent proteins in the predicted secretome of *Lactobacillus salivarius* UCC118. *Appl. Environ. Microbiol.* **2006**, *72*, 4143–4153.
304. Van Tassell, M.L.; Miller, M.J. *Lactobacillus* adhesion to mucus. *Nutrients* **2011**, *3*, 613-636.
305. Vélez, M.P.; Keersmaecker, S.C.J.; Vanderleyden, J. Adherence factors of *Lactobacillus* in the human gastrointestinal tract. *FEMS Microbiol. Lett.* **2007**, *276*, 140-148.
306. Verdu, E.F.; Bercik, P.; Collins, S.M. Effect of probiotics on gastrointestinal function: Evidence from animal models. *Ther. Adv. Gastroenterol.* **2009**, *2*, S31-S35.
307. Verdu, E.F.; Bercik, P.; Verma-Gandhu, M.; Huang, X.X.; Blennerhassett, P.; Jackson, W.; Mao, Y.; Wang, L.; Rochat, F.; Collins, S.M. Specific probiotic therapy attenuates antibiotic induced visceral hypersensitivity in mice. *Gut* **2006**, *55*, 182-190.
308. Verma, S.K.; Sood, S.K.; Saini, R.K.; Saini, N. Pediocin PA-1 containing fermented cheese whey reduces total viable count of raw buffalo (Bubalis bubalus) milk. *LWT - Food Sci. Tech.* **2017**, *83*, 193-200.

309. Vesterlund, S.; Karp, M.; Salminen, S.; Ouwehand, A.C. *Staphylococcus aureus* adheres to human intestinal mucus but can be displaced by certain lactic acid bacteria. *Microbiol.* **2006**, *152*, 1819-1826.

310. Vesterlund, S.; Paltta, J.; Karp, M.; Ouwehand, A.C. Adhesion of bacteria to resected human colonic tissue: Quantitative analysis of bacterial adhesion and viability. *Res. Microbiol.* **2005**, *156*, 238-244.

311. Vesterlund, S.; Paltta, J.; Karp, M.; Ouwehand, A.C. Measurement of bacterial adhesion - *In vitro* evaluation of different methods. *J. Microbiol. Meth.* **2005**, *60*, 225-233.

312. Vitali, B.; Minervini, G.; Rizzello, C.G.; Spisni, E.; Maccaferri, S.; Brigidi, P.; Gobbetti, M.; Di Cagno, R. Novel probiotic candidates for humans isolated from raw fruits and vegetables. *Food Microbiol.* **2012**, *31*, 116-125.

313. Vitetta, L.; Briskey, D.; Alford, H.; Hall, S.; Coulson, S. Probiotics, prebiotics and the gastrointestinal tract in health and disease. *Inflammopharm*. **2014**, *22*,135–154.

314. Vock, E.H.; Lutz, W.K.; Ilinskaya, O.; Vamvakas, S. Discrimination between genotoxicity and cytotoxicity for the induction of DNA double-strand breaks in cells treated with aldehydes and diepoxides. *Mutation Res.*, **1999**, *441*, 85–93.

315. von Ossowski, I.; Reunanen, J.; Satokari, R.; Vesterlund, S.; Kankainen, M.; Huhtinen, H.; Tynkkynen, S.; Salminen, S.; de Vos, W.M.; Palva, A. Mucosal adhesion properties of the probiotic *Lactobacillus rhamnosus* GG SpaCBA and SpaFED pilin subunits. *Appl. Environ. Microbiol.* **2010**, *76*, 2049–2057.

316. Walsh, M.C.; Gardiner, G.E.; Hart, O.M.; Lawlor, P.G.; Daly, M.; Lynch, B.; Richert, B.T.; Radcliffe, S.; Giblin, L.; Hill, C.; Fitzgerald, G.F.; Stanton, C.; Ross, P. Predominance of a bacteriocin-producing *Lactobacillus salivarius* component of a five-strain probiotic in the porcine ileum and effects on host immune phenotype. *FEMS Microbiol. Eco.* **2008**, *64*, 317-327.

317. Walsham, A.D.S.; MacKenzie, D.A.; Cook, V.; Wemyss-Holden, S.; Hews, C.L.; Juge, N.; Schüller, S. *Lactobacillus reuteri* inhibition of enteropathogenic *Escherichia coli* adherence to human intestinal epithelium. *Front Microbiol.* **2016**, *7*, 244-250.

318. Walter, J. Ecological role of Lactobacilli in the gastrointestinal tract: Implications for fundamental and biomedical research. *Appl. Environ. Microbiol.* **2008**, *74*, 4985-4996.

319. Weisser, M.; Oostdijk, E.A.; Willems, R.J.; Bonten, M.J.,;Frei, R., Elzi, L.; Halter, J.; Widmer, A.F.; Top, J. Dynamics of ampicillin-resistant *Enterococcus faecium* clones colonizing hospitalized patients: data from a prospective observational study. *BMC Infect. Dis.* **2012**, *12*, 68.

320. Werner, G.; Klare, I.; Fleige, C.; Geringer, U.; Witte, W.; Just, H.-M.; Ziegler, R. Vancomycin-resistant vanB-type *Enterococcus faecium* isolates expressing varying levels of vancomycin resistance and being highly prevalent among neonatal patients in a single ICU. *Antimicrob. Resis. Infect. Contr.* **2012**, *1*, 21.

321. Woo, J.; Ahn, J. Probiotic-mediated competition, exclusion and displacement in biofilm formation by food-borne pathogens. *Lett. Appl. Microbiol.* **2013**, *56*, 307–313.

322. Wood, B.J.; Holzapfel, W.H. The genera of lactic acid bacteria. **2009**, Springer-Science.

323. Yadav, A.K.; Tyagi, A.; Kaushik, J.K.; Saklani, A.C.; Grover, S.; Batisha, V.K. Role of surface layer collagen binding protein from indigenous *Lactobacillus plantarum* 91 in adhesion and its anti-adhesion potential against gut pathogen. *Micro. Res.* **2013**, *168*, 639-645.

324. Yadav, A.K.; Tyagi, A.; Kumar, A.; Saklani, A.C.; Grover, S.; Batish, V.K. Adhesion of indigenous *Lactobacillus plantarum* to gut extracellular matrix and its physicochemical characterization. *Arch. Microbiol.* **2015**, *197*, 155–164

325. Yan H.; Haitao, Y.; Xia, L.; Zhan, Z.; He, W.; Cao, J.; Yang, P-C.; Liu, Z. Staphylococcal enterotoxin B suppresses Alix and compromises intestinal epithelial barrier functions. *J. Biomed. Sci.* **2014**, *21*, 29-35.

326. Yan, F.; Polk, D.B. Probiotics: progress toward novel therapies for intestinal diseases. *Curr. Opin. Gastroenterol.* **2010**, *26*, 95-101

327. Younes, J.A.; van der Mei, H.C.; van den Heuvel, E.; Busscher, H.J.; Reid, G. Adhesion forces and coaggregation between vaginal *Staphylococci* and *Lactobacilli*. *PLos One* **2012**, *7*, e36917.

328. Yu, X.; Åvall-Jääskeläinen, S.; Koort, J.; Lindholm, A.; Rintahaka, J.; von Ossowski, I.; Palva, A.; Hynönen, U. A comparative characterization of different host-sourced *Lactobacillus ruminis* strains and their adhesive, inhibitory, and immunomodulating functions. *Front. Microbiol.* **2017**, *8*, 657.

329. Zeiger, E.; Gollapudi, B.; Spencer, P. Genetic toxicity and carcinogenicity studies of glutaraldehyde - A review. *Mutation Res.*, **2005**, *589*, 136–151.

330. Zhang, W.; Wang, H.; Liu, J.; Zhao, Y.; Gao, K.; Zhang, J. Adhesive ability means inhibition activities for *Lactobacillus* against pathogens and S-layer protein plays an important role in adhesion. *Anaerobe* **2013**, *22*, 97-103.

331. Zheng, J.; Gänzle, M.G.; Lin, X.B.; Ruan, L.; Sun, M. Diversity and dynamics of bacteriocins from human microbiome. *Environ. Microbiol.* **2015**, *17*, 2133–43.

332. Zhou, J.S.; Gill, H.S. Immunostimulatory probiotic *Lactobacillus rhamnosus* HN001 and *Bifidobacterium lactis* HN019 do not induce pathological inflammation in mouse model of experimental autoimmune thyroiditis. *Int. J. Food Microbiol.* **2005**, *103*, 97-104.

333. Zhou, X.; Kini, R.M.; Sivaraman, J. Application of isothermal titration calorimetry and column chromatography for identification of biomolecular targets. *Nat. Prot.* **2011**, *6*, 158-165.

334. Zhu, X.; Zhao, Y.; Sun, Y.; Gu, Q. Purification and characterisation of plantaricin ZJ008, a novel bacteriocin against *Staphylococcus* spp. from *Lactobacillus plantarum* ZJ008. *Food Chem.* **2014**, *165*, 216-223.

335. Zivkovic, M.; Hidalgo-Cantabrana, C.; Kojic, M.; Gueimonde, M.; Golic, N.; Ruas-Madiedo, P. Capability of exopolysaccharide-producing *Lactobacillus paraplantarum* BGCG11 and its non-producing isogenic strain NB1, to counteract the effect of enteropathogens upon the epithelial cell line HT29-MTX. *Food Res. Int.* **2015**, *74*, 199-207.


भारतीय प्रौद्योगिकी संस्थान गुवाहाटी
Indian Institute of Technology Guwahati

APPENDIX

APPENDIX

Table A2.1. Viability of standard LAB in presence of oxgall bile salts

Strain	[a] Viable count (log_{10} CFU/mL) ± SD			
	0 h	**6 h**	**12 h**	**24 h**
L. acidophilus NRRL B4495	6.1 ± 0.03	6.7 ± 0.01	7.01 ± 0.02	9.96 ± 0.02
L. gasseri NRRL B4240	6.12 ± 0.05	6.80 ± 0.02	7.07 ± 0.02	9.0 ± 0.01
L. helveticus NCIM 2126	6.11 ± 0.01	6.90 ± 0.03	7.06 ± 0.1	9.0 ± 0.5
L. johnsonii NRRL B2178	6.0 ± 0.02	6.80 ± 0.01	7.09 ± 0.04	8.92 ± 0.07
L. plantarum MTCC 1325	6.11 ± 0.02	6.51 ± 0.05	7.06 ± 0.01	9.04 ± 0.04
L. plantarum MTCC 1407	6.1 ± 0.01	6.7 ± 0.02	7.05 ± 0.01	9.04 ± 0.03
L. plantarum MTCC 1746	6.0 ± 0.04	6.6 ± 0.03	7.0 ± 0.09	9.0 ± 0.3
L. plantarum NCIM 2083	6.1 ± 0.03	6.61 ± 0.02	7.0 ± 0.07	8.96 ± 0.01
L. plantarum NCIM 2592	6.06 ± 0.01	6.6 ± 0.08	7.04 ± 0.05	9.0 ± 0.04

[a] Viable cell numbers are expressed as mean cell count (log_{10} CFU/mL) followed by standard deviation (SD) value.

Table A2.2. BLAST analysis for *L. plantarum* CRA38 *bsh* gene

Description	Max Score	Total score	Query cover	E-value	Identity	Accession number
L. plantarum strain K259 chromosome, complete genome	544	544	100%	7×10^{-151}	99%	CP025590.1
L. plantarum strain KC3 chromosome, complete genome	544	544	100%	7×10^{-151}	99%	CP025586.1
L. plantarum strain ATCC 8014 chromosome, complete genome	544	544	100%	7×10^{-151}	99%	CP024413.1
L. plantarum strain GBLP1, complete genome	544	544	100%	7×10^{-151}	99%	CP020564.1
L. plantarum strain TMW 1.1623, complete genome	544	544	100%	7×10^{-151}	99%	CP017379.1

Table A2.3. BLAST analysis for *L. plantarum* CRA38 *cnbp* gene

Description	Max Score	Total score	Query cover	E-value	Identity	Accession number
L. plantarum strain ATCC 8014 chromosome, complete genome	850	850	100%	0.0	100%	CP024413.1
L. plantarum strain B21, complete genome	850	850	100%	0.0	100%	CP010528.1
L. plantarum DOMLa, complete genome	850	850	100%	0.0	100%	CP004406.1
L. plantarum JDM1, complete genome	850	850	100%	0.0	100%	CP001617.1
L. plantarum PC520 chromosome, complete genome	845	845	100%	0.0	99%	CP023772.1

Table A2.4. BLAST analysis for *L. plantarum* CRA38 *fbp* gene

Description	Max Score	Total score	Query cover	E-value	Identity	Accession number
L. plantarum strain ATCC 8014 chromosome, complete genome	843	843	100%	0.0	100%	CP024413.1
L. plantarum strain B21, complete genome	843	843	100%	0.0	100%	CP010528.1
L. plantarum DOMLa, complete genome	843	843	100%	0.0	100%	CP004406.1
L. plantarum JDM1, complete genome	843	843	100%	0.0	100%	CP001617.1
L. plantarum PC520 chromosome, complete genome	837	837	100%	0.0	99%	CP023772.1

Table A2.5. Viability of standard LAB in simulated gastric fluid (SGF)

Strain	[a] Viable count (log_{10} CFU/mL) ± SD			
	0 min	**40 min**	**80 min**	**120 min**
L. acidophilus NRRL B4495	6.09 ± 0.01	6.03 ± 0.06	5.96 ± 0.1	5.24 ± 0.04*
L. gasseri NRRL B4240	6.1 ± 0.03	5.57 ± 0.05*	5.1 ± 0.1*	5.04 ± 0.04*
L. helveticus NCIM 2126	6.07 ± 0.02	6.01 ± 0.01	5.94 ± 0.02	5.31 ± 0.07*
L. johnsonii NRRL B2178	6.07 ± 0.05	6.02 ± 0.01	5.91 ± 0.06	5.26 ± 0.11*
L. plantarum MTCC 1325	6.11 ± 0.02	6.01 ± 0.1	5.5 ± 0.09*	5.04 ± 0.2*
L. plantarum MTCC 1407	6.1 ± 0.01	5.97 ± 0. 2	5.1 ± 0.2*	4.95 ± 0.01*
L. plantarum MTCC 1746	6.0 ± 0.04	5.5 ± 0.07*	5.0 ± 0.02*	4.5 ± 0.1*
L. plantarum NCIM 2083	6.1 ± 0.03	6.01 ± 0.2	5.7 ± 0.27	5.16 ± 0.04*
L. plantarum NCIM 2592	6.06 ± 0.01	5.96 ± 0.04	5.34 ± 0.1*	5.0 ± 0.05*

[a] Viable cell numbers are expressed as mean cell count (log_{10} CFU/mL) followed by standard deviation (SD) value. * indicates p value < 0.05 obtained in a one-way ANOVA.

Table A2.6. Viability of standard LAB in simulated intestinal fluid (SIF)

Strain	[a] Viable count (log_{10} CFU/mL) ± SD			
	0 min	**2 h**	**4 h**	**6 h**
L. acidophilus NRRL B4495	6.09 ± 0.01	6.05 ± 0.04	6.00 ± 0.07	6.00 ± 0.09
L. gasseri NRRL B4240	6.1 ± 0.03	6.00 ± 0.08	5.97 ± 0.09	5.96 ± 0.08
L. helveticus NCIM 2126	6.07 ± 0.02	6.00 ± 0.05	5.96 ± 0.12	5.96 ± 0.05
L. johnsonii NRRL B2178	6.07 ± 0.05	6.03 ± 0.06	5.97 ± 0.14	5.97 ± 0.1
L. plantarum MTCC 1325	6.11 ± 0.02	6.1 ± 0.01	6.0 ± 0.2	5.99 ± 0.01
L. plantarum MTCC 1407	6.1 ± 0.01	6.1 ± 0.02	6.0 ± 0.03	6.0 ± 0.3
L. plantarum MTCC 1746	6.0 ± 0.04	6.0 ± 0.27	5.97 ± 0.02	5.95 ± 0.1
L. plantarum NCIM 2083	6.1 ± 0.03	6.08 ± 0.05	6.01 ± 0.1	6.0 ± 0.4
L. plantarum NCIM 2592	6.06 ± 0.01	6.01 ± 0.1	5.94 ± 0.05	5.93 ± 0.01

[a] Viable cell numbers are expressed as mean cell count (log_{10} CFU/mL) followed by standard deviation (SD) value.

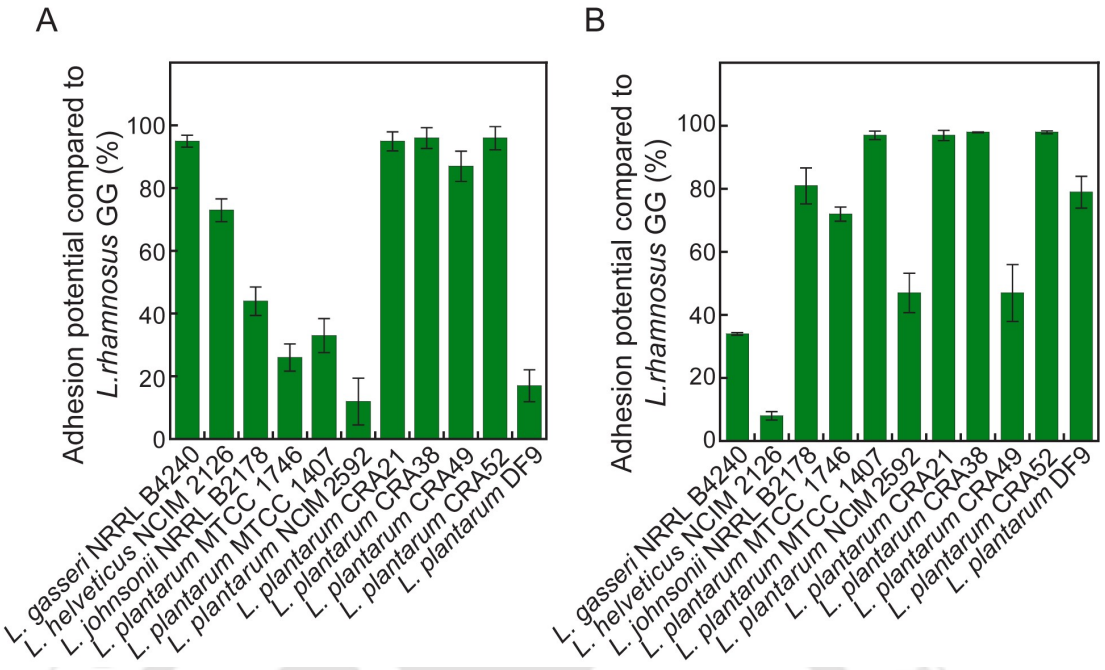

Figure A3.1. Crystal violet-based adhesion assay of *L. plantarum* strains onto (A) collagen and (B) mucin.

Table A3.1. Quantitative parameters for the adhesion process of model pathogens on collagen and mucin

Strains	**Adhesion on collagen**		**Adhesion on mucin**	
	Maximum number of adhered bacteria (e_m) $\log_{10}$ CFU per well	Dissociation constant (k_d) $\log_{10}$ CFU per well	Maximum number of adhered bacteria (e_m) $\log_{10}$ CFU per well	Dissociation constant (k_d) $\log_{10}$ CFU per well
S. aureus MTCC 96	6.78	12.7	12.0	18.25
E. faecalis MTCC 439	9.29	15.8	11.7	11.2
L. monocytogenes Scott A	4.1	20.7	3.2	22.7

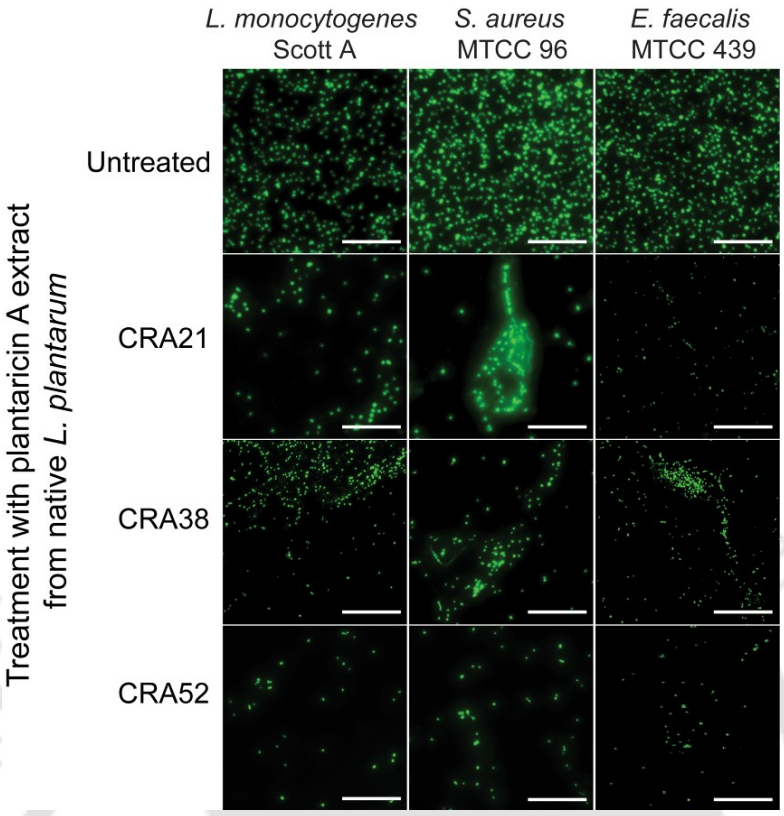

Figure A3.2. Fluorescence microscope analysis to study the effect of plantaricin A extract (400 AU/mL) from *L. plantarum* strains on mucin-adhered target bacteria. Scale bar for the images is 200 µm.

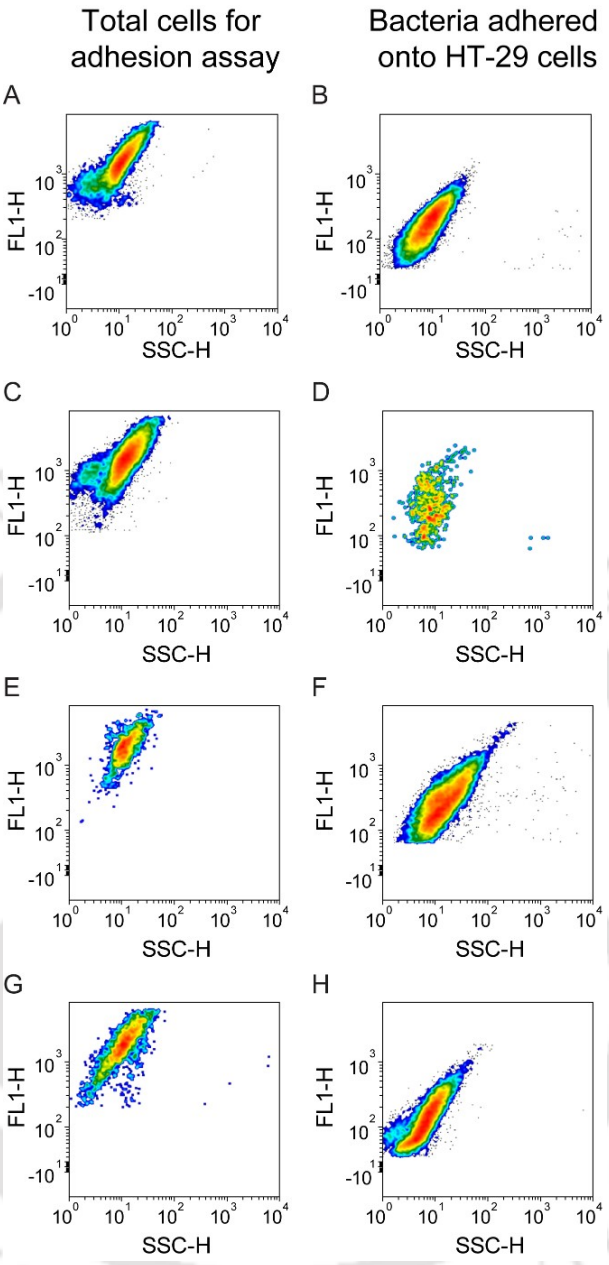

Figure A4.1. Dot plots from FCM analysis to study adhesion of native *L. plantarum* strains onto HT-29 cells. (A) and (B) *L. plantarum* CRA21, (C) and (D) *L. plantarum* CRA38, (E) and (F) *L. plantarum* CRA49, (G) and (H) *L. plantarum* CRA52.

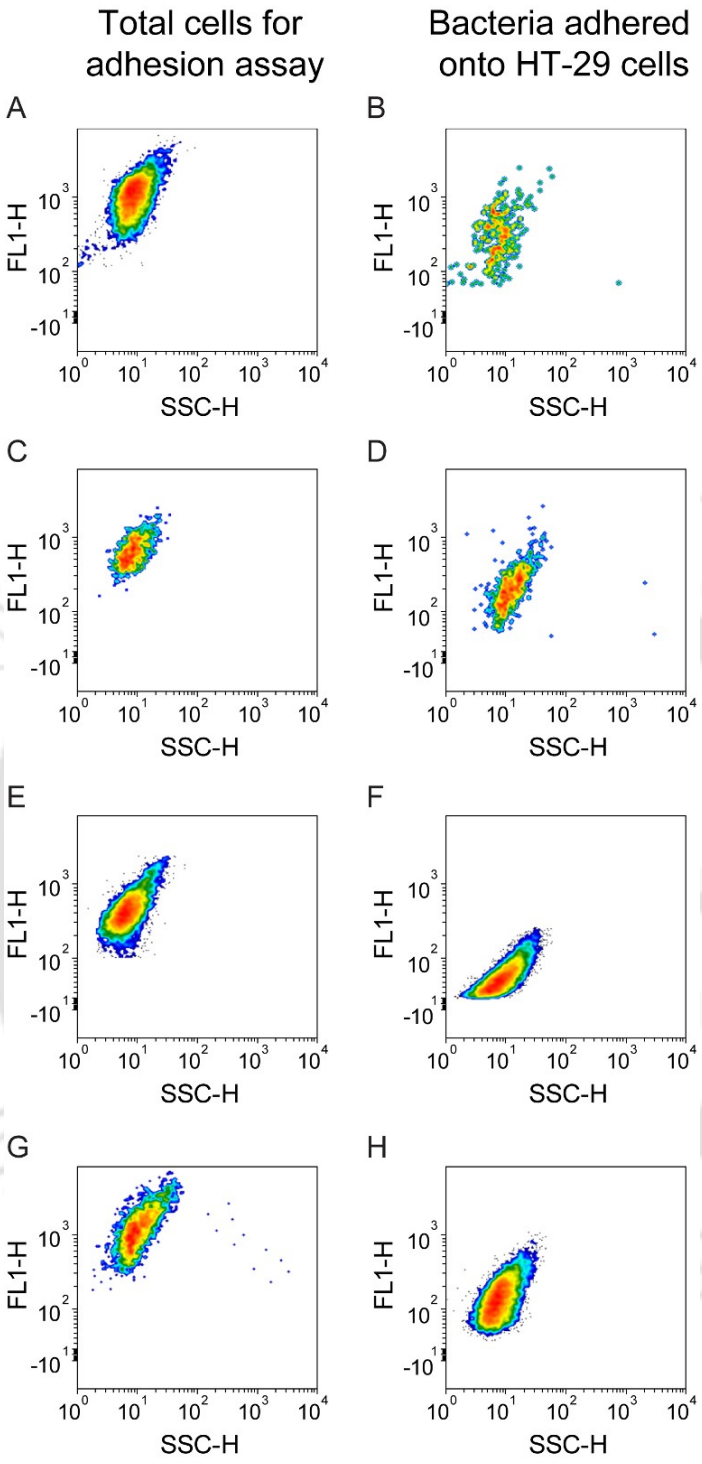

Figure A4.2. Dot plots from FCM analysis to study adhesion of standard *L. plantarum* strains onto HT-29 cells. (A) and (B) *L. plantarum* MTCC 1325, (C) and (D) *L. plantarum* MTCC 1407, (E) and (F) *L. plantarum* MTCC 1746, (G) and (H) *L. plantarum* NCIM 2592.

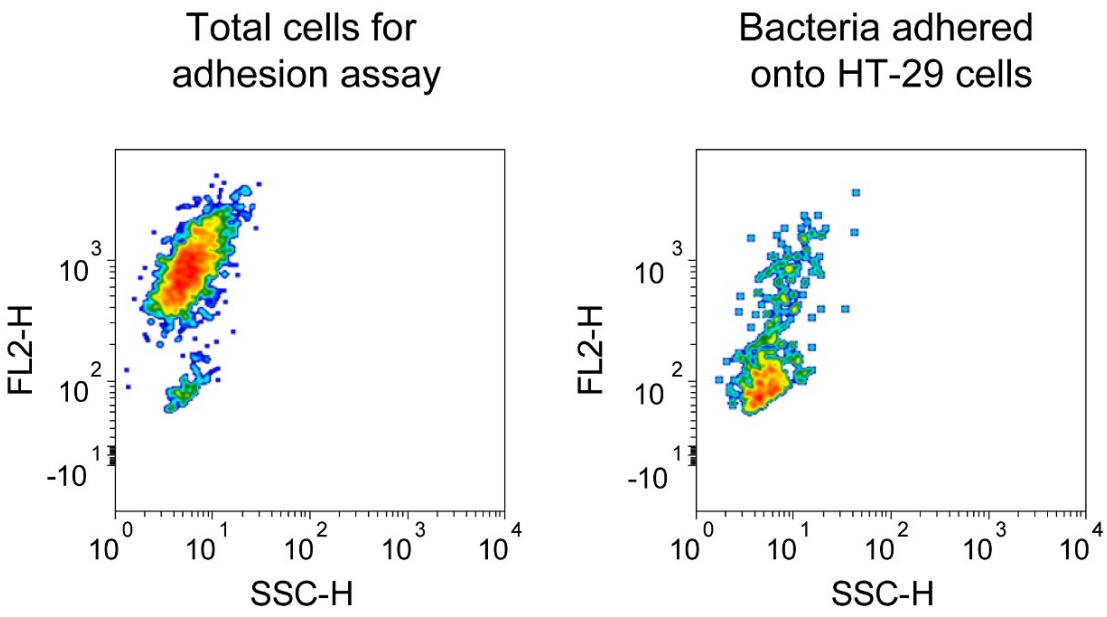

Figure A4.3. Dot plots from FCM analysis to study adhesion of *L. monocytogenes* Scott A.

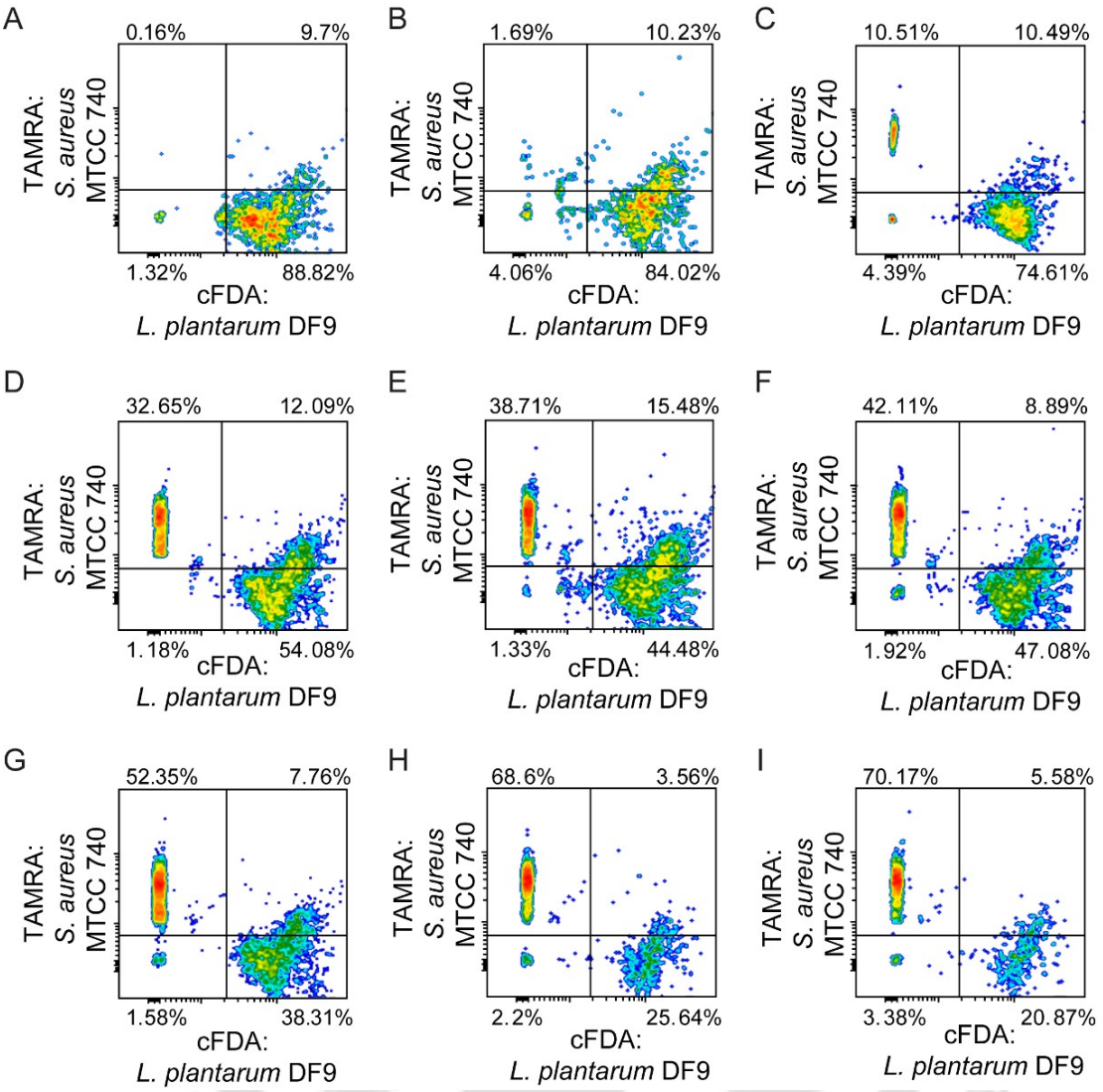

Figure A4.4. Quadrant plots for dual-color FCM based adhesion assay on HT-29 cells. (A), (B) and (C) represents exclusion mode of adhesion inhibition, and (D), (E) and (F) represents competition mode of adhesion inhibition and (G), (H) and (I) represent displacement mode of adhesion inhibition of 4.0 $\log_{10}$ CFU/mL, 6.0 $\log_{10}$ CFU/mL, and 8.0 $\log_{10}$ CFU/mL of *S. aureus* MTCC 740, respectively, by *L. plantarum* DF9.

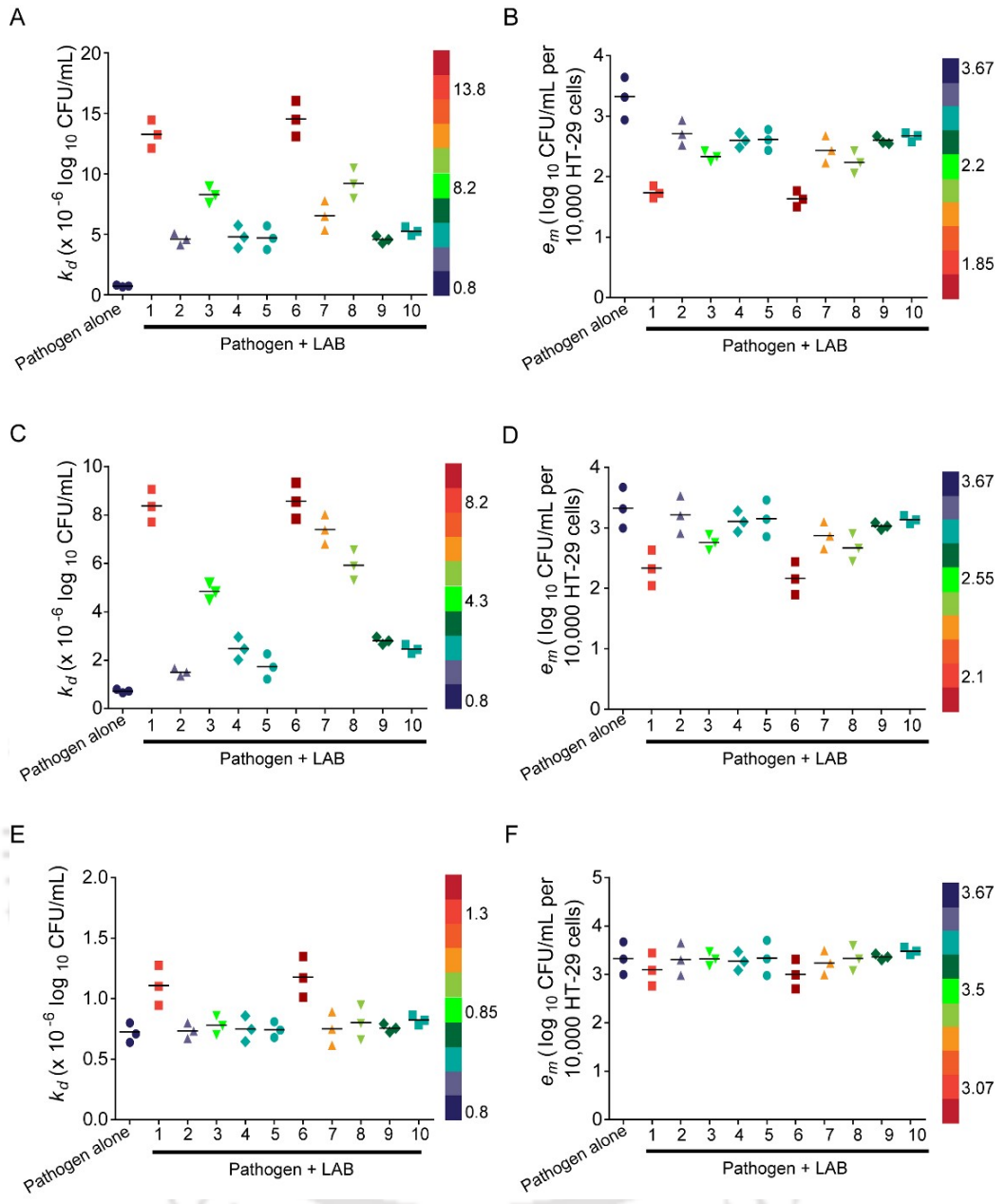

Figure A4.5. Change in adhesion process parameters of *S. aureus* MTCC 740 imparted by LAB strains. (A) and (B) exclusion mode of adhesion inhibition, (C) and (D) competition mode of adhesion inhibition and (E) and (F) displacement mode of adhesion inhibition. 1. *L. plantarum* DF9, 2. *L. plantarum* CRA21, 3. *L. plantarum* CRA38, 4. *L. plantarum* CRA49, 5. *L. plantarum* CRA52, 6. *L. rhamnosus* GG, 7. *L. plantarum* MTCC 1325, 8. *L. plantarum* MTCC 1407, 9. *L. plantarum* MTCC 1746, 10. *L. plantarum* NCIM 2592.

Table A4.1. Factors derived from principal component analysis for changes in parameters of adhesion inhibition process of *E. faecalis* MTCC 439 and *S. aureus* MTCC 740.

Strain	Component		
	1	2	3
L. plantarum DF9	0.956	0.087	0.021
L. plantarum CRA21	0.027	0.070	0.967
L. plantarum CRA38	0.878	-0.025	0.176
L. plantarum CRA49	0.309	0.720	0.564
L. plantarum CRA52	0.067	0.962	-0.087
L. rhamnosus GG	0.919	0.223	0.050
L. plantarum MTCC 1325	0.150	0.905	0.361
L. plantarum MTCC 1407	0.725	0.326	0.398
L. plantarum MTCC 1746	0.367	0.308	0.751
L. plantarum NCIM 2592	0.100	0.099	0.954

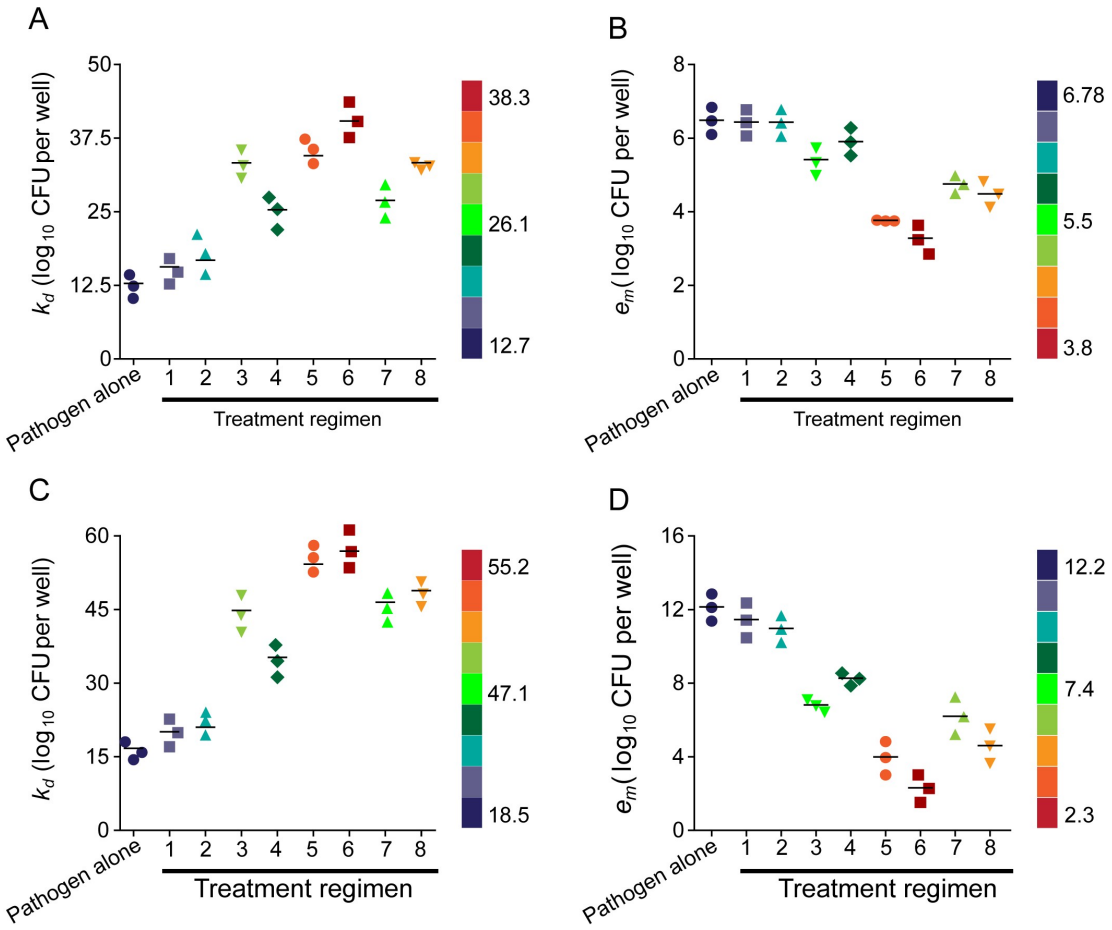

Figure A6.1. Change in adhesion process parameters of *S. aureus* MTCC 96 in (A-B) collagen-coated wells and (C-D) mucin-coated wells respectively. 1. *L. plantarum* DF9, 2. *L. rhamnosus* GG, 3. Pediocin, 4. Ped-MNC, 5. *L. plantarum* DF9 and pediocin, 6. *L. rhamnosus* GG and pediocin, 7. *L. plantarum* DF9 and Ped-MNC, 8. *L. rhamnosus* GG and Ped-MNC.

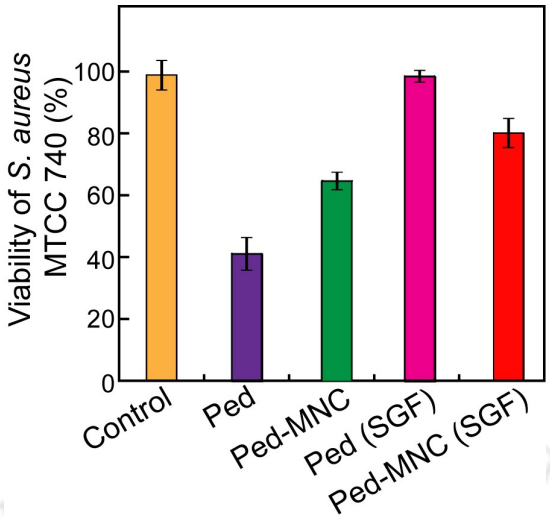

Figure A6.2. Viability of *S. aureus* MTCC 740 adhered onto HT-29 cells.

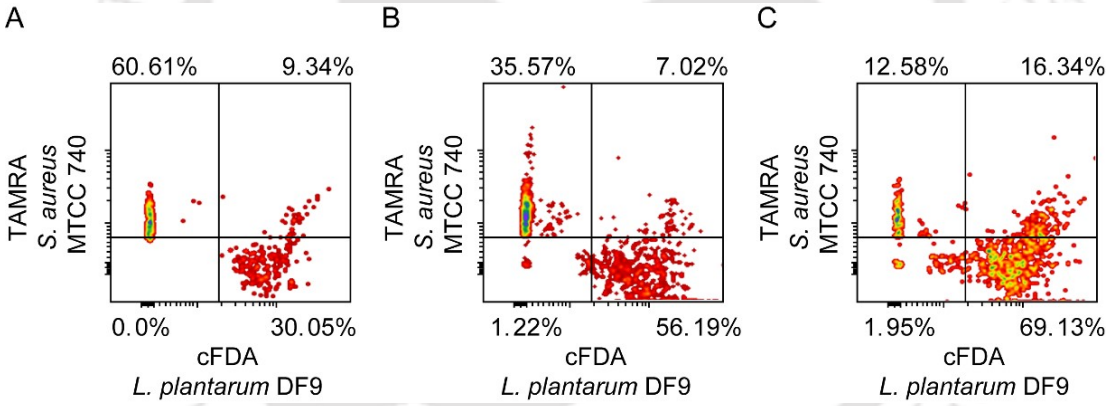

Figure A6.3. Dual color FCM-based adhesion assay to ascertain the effect of different test samples on adhesion of *S. aureus* MTCC 740 onto HT-29 cells. (A) *L. plantarum* DF9, (B) *L. plantarum* DF9 and Ped-MNC, (C) *L. plantarum* DF9 and pediocin.

Table A6.1. Factors derived from principal component analysis for changes in parameters of adhesion inhibition process of pre-adhered cells of *E. faecalis* MTCC 439 and *S. aureus* MTCC 740.

Test sample	Component		
	1	2	3
L. plantarum DF9	-0.023	0.932	-0.359
L. rhamnosus GG	0.028	0.906	-0.418
Pediocin	-0.042	-0.504	0.859
Ped-MNC	-0.113	-0.458	0.873
L. plantarum DF9 and pediocin	0.973	-0.137	0.166
L. rhamnosus GG and pediocin	0.996	-0.060	0.050
L. plantarum DF9 and Ped-MNC	0.975	0.101	-0.193
L. rhamnosus GG and Ped-MNC	0.934	0.174	0.300

LIST OF PUBLICATIONS

List of Publications

Publications from Ph.D. Thesis Work:

(A) Journal Publications:

1. **Mukherjee, S.**, Singh, A.K., Adhikari, M. D., and Ramesh, A. (2013). Quantitative appraisal of the probiotic attributes and *in vitro* adhesion potential of anti-listerial bacteriocin-producing lactic acid bacteria. *Probiotics and Antimicrobial Proteins* **5**, 99-109.
2. **Mukherjee, S.** and Ramesh, A. (2015). Bacteriocin-producing strains of *Lactobacillus plantarum* inhibit adhesion of *Staphylococcus aureus* to extracellular matrix: Quantitative insight and implications in antibacterial therapy. *Journal of Medical Microbiology* **64**, 1514-1526.
3. **Mukherjee, S.** and Ramesh, A. (2017). Dual-label flow cytometry-based host cell adhesion assay to ascertain the prospect of probiotic *Lactobacillus plantarum* in niche-specific antibacterial therapy. *Microbiology* **163**, 1822-1834.
4. **Mukherjee, S.**, Das, G, and Ramesh, A. (2018). A biocompatible nanocomposite tailored to endure the gastric niche and render effective elimination of intestinal pathogenic bacteria **(Manuscript under preparation)**.

(B) Patent:

1. **Mukherjee, S.**, Das, G, and Ramesh, A. (2018). Gastric fluid-resistant proteinaceous nanocomposite for mitigation of gastrointestinal pathogenic bacteria. **Indian Patent Application No. 201831001543**.

(C) Publications from Other Research Projects:

1. Singh, A. K., **Mukherjee, S.**, Adhikari, M. D. and Ramesh, A. (2012). Fluorescence-based comparative evaluation of bactericidal potency and food application potential of anti-listerial bacteriocin produced by lactic acid bacteria isolated from indigenous samples. *Probiotic and Antimicrobial Proteins* **4**, 122-132.
2. Datta, B. K., **Mukherjee, S.**, Kar, C., Ramesh, A. and Das, G. (2013). Zn^{2+} and pyrophosphate sensing: Selective detection in physiological conditions and application in DNA-based estimation of bacterial cell numbers. *Analytical Chemistry* **85**, 8369-8375.
3. Adhikari, M. D., **Mukherjee, S.**, Saikia, J., Das, G., and Ramesh, A. (2014). Magnetic nanoparticles for selective capture and purification of an antimicrobial peptide secreted by food-grade lactic acid bacteria. *Journal of Materials Chemistry B* **2**, 1432-1438.
4. Kar, C., Samanta, S., **Mukherjee, S.**, Dutta, B. K., Ramesh, A. and Das, G. (2014). A simple and efficient fluorophoric probe for dual sensing of Fe^{3+} and F^{-}: Application to bioimaging in native cellular iron pools and live cells. *New Journal of Chemistry* **38**, 2660-2669.
5. Gogoi, A., **Mukherjee, S.**, Ramesh, A. and Das, G. (2015). Nanomolar Zn (II) sensing and subsequent PPi detection in physiological medium and live cells with a benzothiazole functionalized chemosensor. *RSC Advances* **5**, 63634-63640.
6. Gogoi, A., **Mukherjee, S.**, Ramesh, A. and Das, G. (2015). Aggregation-induced emission active metal-free chemosensing platform for highly selective turn-on sensing and bioimaging of pyrophosphate anion. *Analytical Chemistry* **87**, 6974-6979.
7. Kapoor, V., Rai, R., Thiyagarajan, D., **Mukherjee, S.,** Das, G., Ramesh, A. (2017). A nonbactericidal zinc-complexing ligand as a biofilm inhibitor: Structure-guided contrasting effects on *Staphylococcus aureus* biofilm. *ChemBioChem* **18**, 1502-1508.
8. Chauhan, P., Dey, P., **Mukherjee, S.**, Manna, U., Das, G., Ramesh, A. (2018). A cytocompatible zinc oxide nanocomposite loaded with an amphiphilic arsenal for alleviation of *Staphylococcus* biofilm. *ChemistrySelect* **3**, 2492-2497.

9. Dey, P., **Mukherjee, S.**, Das, G., Ramesh, A. (2018). Micellar chemotherapeutic platform based on a bifunctional salicaldehyde amphiphile delivers a "combo-effect" for heightened killing of MRSA. *Journal of Materials Chemistry B* **6**, 2116-2125.
10. Sahareen, T.; Dey, P.; **Mukherjee, S.**; Das, G.; Ramesh, A. (2018). Potential of pyridine amphiphiles as staphylococcal nuclease inhibitor. *ChemBioChem* **19**, 1400-1408.